AD_____

Award Number: DAMD17-02-1-0680

TITLE: Posttranscriptional Regulation of the Neurofibromatosis 2 Gene

PRINCIPAL INVESTIGATOR: Long-Sheng Chang, Ph.D.

CONTRACTING ORGANIZATION: Children's Hospital, Columbus
Columbus, OH 43205-2696

REPORT DATE: July 2006

TYPE OF REPORT: Final

PREPARED FOR: U.S. Army Medical Research and Materiel Command
Fort Detrick, Maryland 21702-5012

REPORT DOCUMENTATION PAGE

Form Approved
OMB No. 0704-0188

1. REPORT DATE *(DD-MM-YYYY)*	**2. REPORT TYPE**	**3. DATES COVERED** *(From - To)*
01-07-2006	Final	1 AUG 2002 - 14 JUN 2006

4. TITLE AND SUBTITLE
Posttranscriptional Regulation of the Neurofibromatosis 2 Gene

5a. CONTRACT NUMBER

5b. GRANT NUMBER
DAMD17-02-1-0680

5c. PROGRAM ELEMENT NUMBER

6. AUTHOR(S)
Long-Sheng Chang, Ph.D.

E-Mail: lchang@chi.osu.edu

5d. PROJECT NUMBER

5e. TASK NUMBER

5f. WORK UNIT NUMBER

7. PERFORMING ORGANIZATION NAME(S) AND ADDRESS(ES)

Children's Hospital, Columbus
Columbus, OH 43205-2696

8. PERFORMING ORGANIZATION REPORT NUMBER

9. SPONSORING / MONITORING AGENCY NAME(S) AND ADDRESS(ES)
U.S. Army Medical Research and Materiel Command
Fort Detrick, Maryland 21702-5012

10. SPONSOR/MONITOR'S ACRONYM(S)

11. SPONSOR/MONITOR'S REPORT NUMBER(S)

12. DISTRIBUTION / AVAILABILITY STATEMENT
Approved for Public Release; Distribution Unlimited

13. SUPPLEMENTARY NOTES

14. ABSTRACT: Neurofibromatosis type 2 (NF2) is associated with a homozygous inactivation of the neurofibromatosis 2 (NF2) gene. Despite intense study of the NF2 gene, the mechanism by which the NF2 tumor suppressor acts to prevent tumor formation is not well understood. The goal of this research is to examine the role of posttranscriptional regulation of the NF2 gene. With this grant support, we have confirmed that vestibular schwannomas express a distinct pattern of alternatively spliced NF2 transcripts lacking specific exons. Analysis of NF2 expression during embryonic development reveals that NF2 is an early expression marker. Strong NF2 promoter activity was seen in the embryonic ectoderm and in all NF2-affected tissues examined. Importantly, we observed strong NF2 promoter activity in the developing brain and in sites containing migrating cells including the neural tube closure and branchial arches. Furthermore, we noted a transient change of NF2 promoter activity during neural crest cell migration. The NF2 promoter expression pattern during embryogenesis suggests a specific regulation of the NF2 gene during neural crest cell migration and further support the role of merlin in cell adhesion, motility, and proliferation during development. By using the conditional gene targeting approach, we have generated an Nf2flox8 allele. Transgenic and conditional knockout mice have been generated to address whether the alternative splicing NF2 isoform with exon 8 deletion preferentially expressed in schwannomas possess any additional properties conducive to tumor formation in vivo. Also, we show that the 3' UT sequence of the NF2 gene does not affect the stability of NF2 RNA or the efficiency of protein translation in vitro. Utilizing the vestibular schwannoma samples procured from this study, we have established a quantifiable human vestibular schwannoma xenograft model in SCID mice and identified cyclin D3 as a growth-promoting factor for vestibular schwannomas. The vestibular schwannoma xenografts represent a model complimentary to Nf2 transgenic and knockout mice for translational vestibular schwannoma research.

15. SUBJECT TERMS Neurofibromatosis 2 (NF2), NF2 Gene, merlin, ezrin-radixin-moesin (ERM), vestibular schwannoma, Schwann cells, posttranscriptional regulation, alternative splicing, transcript, RNA, cDNA isoform, transgenic mice, gene targeting, neural tube closure, neural crest cell migration, xenograft, severe combined immunodeficiency (SCID) mice, and differential polyadenylation

16. SECURITY CLASSIFICATION OF:			**17. LIMITATION OF ABSTRACT**	**18. NUMBER OF PAGES**	**19a. NAME OF RESPONSIBLE PERSON**
a. REPORT	**b. ABSTRACT**	**c. THIS PAGE**			USAMRMC
U	U	U	UU	122	**19b. TELEPHONE NUMBER** *(include area code)*

TABLE OF CONTENTS

INTRODUCTION:

Neurofibromatosis type 2 (NF2) is a hereditary disorder characterized by the development of bilateral vestibular schwannomas (reviewed in Baser et al., 2003; Chang et al., 2005). NF2 is associated with a homozygous inactivation of the neurofibromatosis 2 gene (*NF2*), which encodes a protein named 'merlin' for moesin-ezrin-radixin like protein (Trofatter et al., 1993). Despite intense study of the *NF2* tumor-suppressor, the mechanism by which merlin acts to prevent tumor formation is not well understood. The *NF2* transcripts undergo alternative splicing, generating a series of mRNA isoforms lacking one or more exons. Presently, the role of alternative splicing of *NF2* mRNAs is not understood. *NF2* isoform 1 (without exon 16) but not isoform 2 (containing all 17 exons) possess growth inhibitory properties (Gutmann et al., 1999). Also, transgenic mice over-expressing the *NF2* isoform with a deletion of exons 2 and 3 in Schwann cell lineage showed a high prevalence of Schwann cell hyperplasia and tumors (Giovannini et al., 1999). These results raise the possibility that functional contribution of the *Nf2* tumor suppressor may require a balanced expression of various isoform proteins in Schwann cells and/or other cell types. In addition, we found that differential usage of multiple polyadenylation sites also contributes to the complexity of human *NF2* transcripts (Chang et al., 2002). Presently, the role of differential polyadenylation of *NF2* transcripts is not known. The goal of the proposed research is to examine the role of posttranscriptional regulation (alternative splicing and differentiation polyadenylation) of the *NF2* gene. Ultimately we hope to provide a better understanding of the mechanisms of NF2 tumorigenesis.

BODY:

Aim 1: Analysis of the Expression Pattern of Alternatively Sliced *NF2* Transcripts in Schwann Cells and Vestibular Schwannomas.

Task 1: Three Human Subjects Protocols were prepared according to the Army's Compliance of Human Subjects Protocols and were approved by the Institutional Review Boards (IRB) of The Ohio State University. Vestibular schwannomas and normal vestibular nerves were procured throughout the entire study period. Written informed consent for tumors and nerves was obtained from all patients prior to surgical removal of their tumors. RNAs from the vestibular schwannomas and vestibular nerves were isolated.

Task 2: Schwann cells were also prepared from procured nerves according to Ratner et al. (1986) and used for RNA isolation.

Task 3: We have conducted reverse transcription-polymerase chain reaction (RT-PCR) analysis on *NF2* RNA isoform expression in vestibular schwannomas, vestibular nerves, and several other normal human tissues. By cloning and sequencing we have examined the complete exon structures and relative frequency of alternatively spliced *Nf2* isoforms.

Task 4: Genomic DNA was isolated from the blood sample of the patient with a sporadic schwannoma that only expresses *NF2* mRNAs lacking at least exon 8. By PCR, cloning and sequencing, we conducted *NF2* mutational analysis on the patient's DNA.

Research Findings:

This Aim was accomplished, yielding three major reportable outcomes. First, by analyzing *NF2* RNAs expressed in vestibular schwannomas, normal vestibular nerves, and various normal human tissues, we found that the expression pattern and relative frequency of the alternatively spliced *NF2* transcripts in vestibular schwannomas were different from those detected in other human tissues or cell lines. In particular, we found that vestibular schwannomas expressed a high percentage of the *NF2* mRNA isoform lacking exons 15 and 16. These findings were published in Otology and Neurotology (Neff et al., 2005; see Appendices). In addition, we identified a sporadic schwannoma, which predominantly expressed *NF2* transcripts lacking exons 8, 15 and 16. Other cDNAs missing exon 8, exons 8 and 16, and exons 2, 8, 15, and 16 were also detected. Sequence comparison revealed that all of

the cDNAs from this schwannoma completely matched the wild-type *NF2* sequence with the exception of the spliced exons. Taken together, these results indicate that vestibular schwannomas express a distinct pattern of alternatively spliced *NF2* transcripts lacking specific exons

Second, utilizing the vestibular schwannoma samples procured from this study, we have established a quantifiable human vestibular schwannoma xenograft model in severe combined immunodeficiency (SCID) mice. We implanted vestibular schwannoma specimens near the sciatic nerve in the thigh of SCID mice. We used a 4.7-tesla MRI to monitor tumor growth over one year period. Three-dimensional tumor volumes were calculated from MRI images. We found that vestibular schwannoma xenografts demonstrated variability in their growth rates similar to human vestibular schwannoma *in situ*. The majority of vestibular schwannoma xenografts did not grow but persisted throughout the study, while two of 15 xenografts grew significantly. Histopathological examination and immunohistochemistry confirmed that vestibular schwannoma xenografts retained their original microscopic and immunohistochemical characteristics after prolonged implantation. The vestibular schwannoma xenografts represent a model complimentary to *Nf2* transgenic and knockout mice for translational vestibular schwannoma research. These findings have been accepted for publication in The Laryngoscope (Chang et al., 2006; see Appendices). We are now examining whether the vestibular schwannomas that showed growth over time expressed specific *NF2* isoforms.

Third, utilizing the vestibular schwannoma samples procured from this study we have also sought factors that could affect vestibular schwannoma growth. By immunostaining analysis, we found that while none of the 15 vestibular schwannomas examined showed detectable cyclin D_1 staining, seven of them stained positive for the cyclin D_3 protein. Cyclin D_3 staining was taken up in the nucleus of schwannoma tumor cells in greater proportion than Schwann cells of adjacent vestibular nerve. These results suggest that the cyclin D_3 protein may have a growth-promoting role in vestibular schwannomas. The paper described these findings was published in The Laryngoscope (Neff et al., 2006; see Appendix). An attempt to correlate cyclin D_3 expression with the *NF2* isoform expression pattern is presently under investigation.

Aim 2: Functional Analysis of the *NF2* Isoforms Commonly Expressed in Vestibular Schwannomas.

Task 5: We have cloned the *NF*2 cDNA isoforms commonly expressed in vestibular schwannomas and placed them under the control of a 2.4-kb human *NF2* promoter for *in vivo* expression. To better understand *NF2* expression *in vivo*, we generated transgenic mice carrying a 2.4-kb *NF2* promoter driving β-galactosidase (β-gal) with a nuclear localization signal and examined the β-gal expression pattern during embryonic development. To confirm that 2.4-kb *NF2* promoter recapitulates the endogenous *Nf2* expression pattern, *in situ* hybridization and immunostaining with an anti-merlin antibody were performed.

Task 6: To test the biochemical and biological activities of the *NF2* cDNA isoforms *in vitro*, we employed the pIND inducible expression system (Invitrogen). Hemagglutinin (HA) epitope-tagged *NF2* cDNA isoforms were constructed and inserted into the pIND vector. These inducible constructs carrying the HA-tagged *NF2* cDNA were co-transfected with the pVgRXR expression plasmid carrying an insect steroid hormone receptor into human adenovirus-transformed embryonic kidney 293 cells and rat RT4 schwannoma cells.

Task 7: We first analyzed 293 cells co-transfected with the HA-tagged *NF2* cDNA expression vector and the pVgRXR plasmid. Upon induction with an insect steroid hormone ponasterone, expression of the HA-tagged *NF2* isoform protein was detected using an anti-HA antibody. However, little or no growth inhibitory or promoting effects on the 293 cells expressing either one of the two schwannoma-expressed *NF2* isoform proteins were detected. We also performed a similar experiment using rat RT-4 schwannoma cells. RT4 were co-transfected with the *NF2* cDNA expression vector and pVgRXR. Upon hormone induction, expression of the

schwannoma-expressed *NF2* isoforms also did not give rise to any effect on the growth properties of RT4 cells.

Task 8: To determine the ability of the schwannoma-expressed *NF2* isoform proteins to form inter- and intra-molecular interactions, we fused the carboxyl terminus of the *NF2* coding region from these *NF2* cDNA isoforms with the glutathione-S-transferase (GST) protein. Because we did not detect any biological activities from the two schwannoma-expressed *NF2* cDNA isoforms (lacking exons 15 and 16 and exons 8 and 16, respectively) in both 293 kidney and RT4 schwannoma cells, we reasoned that deletion of exon 15 would result in a frame-shift of the 3' *NF2* coding region, consequently inactivating the function of the encoded protein. This hypothesis was supported by the previous findings that the C-terminal end of merlin is important for its intramolecular interaction with the N-terminal region (Gutmann et al., 1999) and that no mutations have ever been found in exon 16 in vestibular schwannomas (Baser et al., 2003; Neff et al., 2006). Deletion of exon 8, however, is in-frame, resulting in a protein isoform missing the amino acid encoded by the exon. Previously, Gutmann et al. (1999) identified two sites in the N-terminal region required for merlin's intramolecular interaction; the very N-terminal site of merlin can interact with the middle N-terminal site, and the C-terminal region folds back to interact with the N-terminal region (see diagram below). Such interactions result in a closed conformation of merlin which possesses the growth suppressor function. Since exon 8-encoded amino acid residues are located at the middle N-terminal binding site, deletion of exon 8 in merlin may abolish its ability to form intramolecular interaction or may only allow forming a partially closed conformation. Thus, we have focused on the role of the *NF2* isoform with the exon 8 deletion. We have taken the approach of generating a conditional exon 8 deletion. Two loxP sites flanking the exon 8 sequence were successfully introduced into the germline *Nf2* allele by homologous recombination. The embryonic stem (ES) cell clones carrying the $Nf2^{flox8}$ allele were isolated and used to generate transgenic mice. To conditionally delete the exon 8 sequence, we have produced transgenic mice carrying the Cre recombinase expression unit driven under the control of the *NF2* promoter. As an alternative, we have also obtained transgenic mice carrying the Cre recombinase expression unit driven under the control of the myelin protein *P0* promoter. The $Nf2^{flox8}$ mice are being mated with the Cre mice. It is likely that mice with conditional exon 8-deletion mice in Schwann cells will give rise to interesting phenotype since mice with over-expression of *NF2* isoform lacking exon 2 or with the deletion of exon 2 in Schwann cells displayed schwannoma formation 10 months or later (Giovannini et al., 1999, 2000).

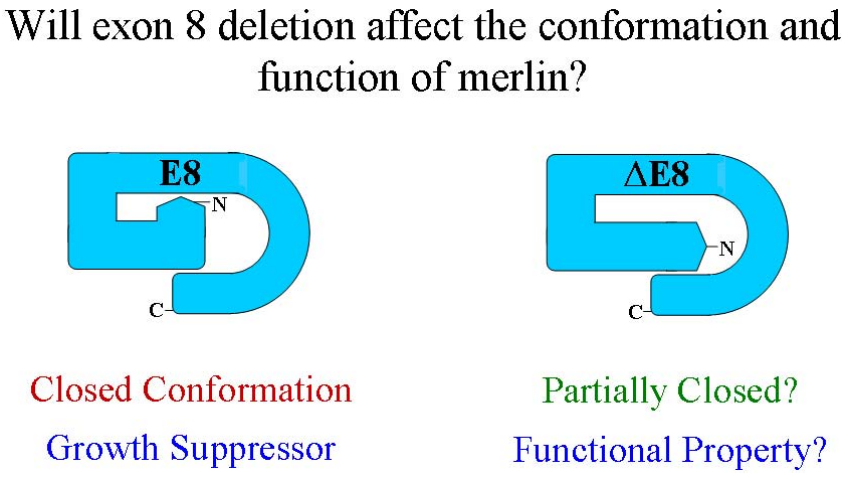

Research Findings:

The major accomplishment from this aim is two-fold. First, we have cloned the *NF*2 cDNA isoforms commonly expressed in vestibular schwannomas and placed them under the control of a 2.4-kb human *NF2* promoter for *in vivo* expression. To better understand *NF2* expression *in vivo*, we generated

transgenic mice carrying a 2.4-kb *NF2* promoter driving β-galactosidase (β-gal) with a nuclear localization signal. Whole-mount embryo staining revealed that the *NF2* promoter directed β-gal expression as early as embryonic day E5.5. Strong expression was detected at E6.5 in the embryonic ectoderm containing many mitotic cells. β-gal staining was also found in parts of embryonic endoderm and mesoderm. The β-gal staining pattern in the embryonic tissues was corroborated by *in situ* hybridization analysis of endogenous *Nf2* RNA expression. Importantly, we observed strong *NF2* promoter activity in the developing brain and in sites containing migrating cells including the neural tube closure, branchial arches, dorsal aorta, and paraaortic splanchnopleura. Furthermore, we noted a transient change of *NF2* promoter activity during neural crest cell migration. While little β-gal activity was detected in premigratory neural crest cells at the dorsal ridge region of the neural fold, significant activity was seen in the neural crest cells already migrating away from the dorsal neural tube. In addition, we detected considerable *NF2* promoter activity in various NF2-affected tissues such as acoustic ganglion, trigeminal ganglion, spinal ganglia, optic chiasma, the ependymal cell-containing tela choroidea, and the pigmented epithelium of the retina. The *NF2* promoter expression pattern during embryogenesis suggests a specific regulation of the *NF2* gene during neural crest cell migration and further support the role of merlin in cell adhesion, motility, and proliferation during development. A paper describing these findings has been accepted for publication in Developmental Dynamics (Akhmametyeva et al., 2005; see Appendices). An important implication from our study is that the *NF2* promoter will be useful to study *NF2* function during embryonic development. It will also be useful for the expression of schwannoma-expressed *NF2* cDNA isoforms in various NF2-affected tissues during development.

Second, to examine the effect of expression of the schwannoma-expressed *NF2* isoforms lacking exon 8 *in vivo*, we have used the embryonic stem (ES) cell-gene targeting strategy to delete the exon 8 of the germline *Nf2* allele. A conditional gene targeting vector containing the exon 8 sequence flanked by two *loxP* recombination sites was generated. The vector also contained a PGK-neo expression cassette for positive selection of recombinant clones. By screening more than 400 G418 (neo)-resistant clones, we have successfully introduced two *loxP* recombination sites flanking exon 8 into the endogenous *Nf2* allele. We obtained at least three ES clones that contain a flox allele of *Nf2* ($Nf2^{flox8}$). Southern blot analysis of EcoRV-digested genomic DNA using the sequence from the exon 7 region as the probe confirmed the identity of these recombinant clones. These targeted ES clones have been used to generate an $Nf2^{flox8}$ mouse. In addition, we have produced transgenic mice carrying the Cre recombinase expression unit driven under the control of the *NF2* promoter. As an alternative, the P0-Cre mice have also been obtained. The $Nf2^{flox8}$ mice are being mated with the Cre mice in order to generate a conditional deletion of exon 8 in Schwann cells. Note that Giovannini et al. (2000) previously showed that mice with a deletion of exon 2 in Schwann cells displayed schwannoma formation 10 months or later (Giovannini et al., 1999, 2000). It will be interesting to see whether mice with a deletion of exon 8 that we are generating will also result in schwannoma formation. Should it be the case, it would imply that the exon 8-encoded amino acid residues play an important role in merlin's conformation and tumor suppressor function.

Aim 3: Examination of the Potential Role of Differential Polyadenylation of *NF2* Transcripts.

Task 9: We have constructed expression plasmids for the three human *NF2* cDNAs of 6.1, 3.1, and 2.7 kb in length. These cDNAs carrying different polyadenylation signal sequences. We have also inserted a hemagglutinin (HA) epitope to the N-terminus of the *NF2*-coding region to facilitate protein detection. These *NF2* cDNA expression plasmids were transfected into various human cell lines and the half life of the expressed *NF2* RNA was compared.

Task 10: A series of 3' unidirectional deletion derivatives from the 6.1-kb *NF2* cDNA expression plasmid has been generated for the identification of any regulatory sequence.

Task 11: The 6.1-, 3.1- and 2.7-kb *NF2* cDNA expression plasmids carrying different lengths of the

3' UT sequences were transfected into RT4 schwannoma, SK-N-AS neuroblastoma, and 293 kidney cells. Western blot analysis was performed to compare the efficiency of protein translation.

Task 12: We have presented our research findings to national and local meetings every year during the funding period. Also, we have published five papers in peer-reviewed journal.

Research Findings:

This Aim was accomplished. We transfected the 6.1-, 3.1- and 2.7-kb *NF2* cDNA expression plasmids carrying different lengths of the 3' untranslated (UT) region into RT4 schwannoma, SK-N-AS neuroblastoma, and 293 kidney cells. 48 hrs later, transfected cells were treated with actinomycin D to block transcription. At various times after actinomycin D treatment, cells were harvested for RNA isolation. RNase protection experiment using a riboprobe derived from the 5' region of the *NF2* sequence as the probe revealed that the half-life of the *NF2* RNA was about 12 hours; however, the *NF2* RNA expressed from the 6.1-, 3.1- and 2.7-kb *NF2* cDNA expression plasmids did not show any difference in their half-life. These results indicate that the 3' UT sequence of the *NF2* gene does not affect the stability of *NF2* RNA *in vitro*.

To examine whether the 3' UT sequence affected the efficiency of protein translation, we transfected the *NF2* cDNA expression plasmids with different lengths of the 3' untranslated (UT) region into RT4 schwannoma cells. At 48 hrs after transfection, cells were harvested and cell lysates prepared for Western Blot analysis. No difference in the amount of merlin protein expression from the three *NF2* cDNA expression plasmids was found. These results indicate that the 3' UT sequence of the *NF2* gene does not play a role in the efficiency of protein translation *in vitro*.

We have published a paper (Chang et al., 2005; see appendices) summarizing transcriptional and posttranscriptional regulation of the NF2 gene that we have found. Since the experiments conducted above utilizing transfected cells, we plan in the future to examine whether the 3' UT sequence play any role in transgene expression in transgenic mice.

KEY RESEARCH ACCOMPLISHMENTS:

(1) We have confirmed that vestibular schwannomas express a distinct pattern of alternatively spliced *NF2* transcripts lacking specific exons. The findings were reported in the paper by Neff et al. (2005)

(2) A key accomplishment during this funding period is the characterization of the *NF2* promoter expression pattern during embryonic development. By a combination of approaches, transgenic analysis, *in situ* hybridization, and antibody staining, we show that *NF2* is an early expression marker. Strong *NF2* promoter activity was detected in the embryonic ectoderm and continued to be actively expressed in the neural ectoderm and its derived neural tissues throughout mid-embryogenesis. Importantly, we observed robust *NF2* promoter activity in the developing brain and in sites containing migrating cells including the neural tube closure. Furthermore, we noted a transient change of *NF2* promoter activity during neural crest cell migration. In addition, we detected considerable *NF2* promoter activity in various NF2-affected tissues such as acoustic ganglion, spinal ganglia, and the pigmented epithelium of the retina. The *NF2* promoter expression pattern during embryogenesis suggests a specific regulation of the *NF2* gene during neural crest cell migration and further support the role of merlin in cell adhesion, motility, and proliferation during development. A manuscript describing these findings has been prepared for publication (Akhmametyeva et al., 2005).

(3) Another key effort was devoted to the generation of a conditional targeting allele of the mouse *Nf2* gene. By using the Cre:*loxP* approach, we constructed a conditional gene targeting vector containing the exon 8 sequence of the *Nf2* gene flanked by two *loxP* recombination sites. By homologous recombination in mouse embryonic stem cells, we have successfully identified several ES clones carrying the $Nf2^{flox8}$ allele. In addition, we have produced transgenic mice carrying the Cre recombinase expression unit driven under the control of the *NF2* promoter. As an alternative, the P0-Cre mice have also been obtained. The $Nf2^{flox8}$ mice are being mated with the Cre mice in order to

generate a conditional deletion of exon 8 in Schwann cells. This experiment should allow us to examine the functional importance of exon 8 which was alternatively spliced in vestibular schwannoma.

(4) Utilizing the vestibular schwannoma samples procured from this study, we have established a quantifiable human vestibular schwannoma xenograft model in SCID mice. We found that vestibular schwannoma xenografts demonstrated variability in their growth rates similar to human vestibular schwannoma *in situ*. The majority of vestibular schwannoma xenografts did not grow but persisted throughout the study, while two of 15 xenografts grew significantly. Histopathological examination and immunohistochemistry confirmed that vestibular schwannoma xenografts retained their original characteristics after prolonged implantation. The vestibular schwannoma xenografts represent a model complimentary to *Nf2* transgenic and knockout mice for translational vestibular schwannoma research (Chang et al., 2006).

(5) Utilizing the vestibular schwannoma samples procured from this study, we have also sought factors that could affect vestibular schwannoma growth. We have found that while none of the 15 vestibular schwannomas examined showed detectable cyclin D_1 staining, seven of them stained positive for the cyclin D_3 protein. Cyclin D_3 staining was taken up in the nucleus of schwannoma tumor cells in greater proportion than Schwann cells of adjacent vestibular nerve. These results suggest that the cyclin D_3 protein may have a growth-promoting role in vestibular schwannomas. These findings were published in The Laryngoscope (Neff et al., 2006).

(6) In transfection studies, we found that the 3' UT sequence of the *NF2* gene does not affect the stability of *NF2* RNA or the efficiency of protein translation *in vitro*. A paper a paper summarizing transcriptional and posttranscriptional regulation of the NF2 gene was reported (Chang et al., 2005).

REPORTABLE OUTCOMES:

12 research abstracts were presented to national meetings and seven research abstracts were presented at local meetings during the entire funding period. Also, five research papers were published during the entire funding period. The research abstracts and publications are listed below.

Abstracts Presented to National and Local Meetings

(1) Chang, L.-S., E.M. Akhmametyeva, Y. Wu, and D.B. Welling. 2003. Transcriptional Regulation of the Human Neurofibromatosis 2 (*NF2*) Gene. Pediatric Academic Societies' Meeting, Seattle, WA.
(2) Akhmametyeva, E., S. Yao, Y. Wu, D.B. Welling, and L.-S. Chang. 2003. Novel Alternatively Spliced *NF2* Transcripts In Vestibular Schwannomas. Pediatric Academic Societies' Meeting, Seattle, WA.
(3) Welling, D.B., J.M. Lasak, E.M. Akhmametyeva, B.A. Neff, and L.-S. Chang. 2003. Analysis of Genes and Pathways Deregulated in Vestibular Schwannomas. The NNFF International Consortium for Molecular Biology of NF1 And NF2, Aspen, CO.
(4) Lebedeva, L., S.A. Trunova, N.A. Bulgakova, L.V. Omelyanchuk, E.M. Akhmametyeva, L.-S. Chang. 2003. The Role of *Drosophila* merlin in the Control of Mitosis Exit and Development. The NNFF International Consortium for Molecular Biology of NF1 and NF2, Aspen, CO.
(5) Welling, D.B., J.M. Lasak, E.M. Akhmametyeva, B.A. Neff, and L.-S. Chang. 2003. Analysis of Genes and Pathways Deregulated in Vestibular Schwannomas. 4th International Symposium on Vestibular Schwannomas and Other Cerebellum Pontine Angle Tumors, Cambridge, England.
(6) Akhmametyeva, E.M., D.B. Welling, and Chang, L.-S. 2004. Expression of the Neurofibromatosis 2 Gene during Early Development. Pediatric Academic Societies' Meeting, San Francisco, CA.
(7) Welling, D.B., BA. Neff, Brenda Hall, John M. Lasak, and L.-S. Chang. 2004. Long-Term Hearing Rehabilitation in NF2 Patients With Cochlear Implants. The NNFF International Consortium for Molecular Biology of NF1 And NF2, Aspen, CO.
(8) Lorenz, M., B.A. Neff, E.M. Akhmametyeva, J. Rock, J. Shoreman, S. Tae, P. Schmalbrock, D.B. Welling, and L.-S. Chang. 2004. Vestibular Schwannomas Xenografted in SCID Mice and Expression of Cyclin D1,

D3, and Telomerase. The NNFF International Consortium for Molecular Biology of NF1 And NF2, Aspen, CO.

(9) Chang, L.-S., E.M. Akhmametyeva, L. Lebedeva, N.A. Bulgakova, and L.V. Omelyanchuk. 2004. Developmental Expression of the *NF2* Gene and Genetic Analysis of Merlin Function. The NNFF International Consortium for Molecular Biology of NF1 And NF2, Aspen, CO.

(10) Akhmametyeva, E.M., H. Luo, M. Mihaylova, D.B. Welling, and L.-S. Chang. 2005. The Neurofibromatosis Type 2 Gene Is Strongly Expressed in Neural Ectoderm and Pigmented Epithelium of the Retina During Early Development. The CTF International Consortium for Molecular Biology of NF1 And NF2, Aspen, CO.

(11) Akhmametyeva, E.M., H. Luo, M. Mihaylova, and L.-S. Chang. 2005. Developmental Expression of the Neurofibromatosis 2 Gene Promoter in Transgenic Mice. Pediatric Academic Societies' Annual Meeting, Washington, D.C.

(12) Akhmametyeva, E.M., M. Mihaylova, H. Luo, S. Kharzai, D.B. Welling, and L.-S. Chang. 2006. Regulation of the *Neurofibromatosis 2* Gene Promoter Expression during Embryonic Development. The CTF International Consortium for Molecular Biology of NF1 And NF2, Aspen, CO.

Abstracts Presented at Local Meetings

(1) Akhmametyeva, E.M., Y. Wu, D.B. Welling, and L.-S. Chang. 2003. Analysis of Novel Alternatively Spliced *NF2* Transcripts in Vestibular Schwannomas. The Annual OSU Comprehensive Cancer Center Scientific Meeting, Columbus, OH.

(2) Chang, L.-S., E.M. Akhmametyeva, Y. Wu, and D.B. Welling. 2003. Transcriptional Regulation of the Human Neurofibromatosis 2 (*NF2*) Gene. Columbus Children's Research Institute Annual Research Conference, Columbus, OH.

(3) Akhmametyeva, E., Y. Wu, D.B. Welling, and L.-S. Chang. 2003. Novel Alternatively Spliced *NF2* Transcripts In Vestibular Schwannomas. Columbus Children's Research Institute Annual Research Conference, Columbus, OH.

(4) Yao, S. E.M. Akhmametyeva, D.B. Welling, And L.-S. Chang. 2003. Expression of Novel Alternatively Spliced *NF2* cDNA isoforms in Vestibular Schwannomas. Eleventh Annual Department of Otolaryngology Alumni Symposium, Longaberger Alumni House, Columbus, OH.

(5) Chang, L.-S., E.M. Akhmametyeva, D.B. Welling,L. Lebedeva, N.A. Bulgakova, and L.V. Omelyanchuk. 2003. Expression and Function of the Neurofibromatosis 2 Gene During Early Development. Molecular Biology and Cancer Genetics Group Retreat, The Ohio State University Comprehensive Cancer Center, Deer Creek Park, OH.

(6) Akhmametyeva, E,M., L. Lebedeva, S.A. Trunova, N.A. Bulgakova, L.V. Omelyanchuk, and L.-S. Chang. 2004. Developmental Expression of the *NF2* Gene and Genetic Analysis of Merlin Function. Columbus Children's Research Institute Annual Research Conference, Columbus, OH.

(7) Akhmametyeva, E.M., L. Lebedeva, S.A. Trunova, N.A. Bulgakova, L.V. Omelyanchuk, and Long-Sheng Chang. 2004. Developmental Expression of the *NF2* Gene and Genetic Analysis of Merlin Function. The 6th Annual Comprehensive Cancer Center Scientific Meeting, Columbus, OH

Publications

(1) Neff, B.A., D.B. Welling, E.M. Akhmametyeva, and L.-S. Chang. 2006. The Molecular Biology of Vestibular Schwannomas: Dissecting the Pathogenic Process at the Molecular Level. Otol. Neurotol. 27:197-208.

In this paper, we reviewed the clinical characteristics of vestibular schwannomas and neurofibromatosis type 2 (NF2) syndromes and related to alterations in the NF2 gene. Additionally, we discussed potential functions of the NF2 gene product and its alternatively spliced isoforms in vestibular schwannomas and other cell types. The discovery of how merlin interacts with other proteins may lead to a better understanding of NF2 function. Understanding merlin's interactions with other proteins, signaling pathways, and regulation of the NF2 gene will lead to the development of novel treatments for vestibular schwannomas. By using recently developed cDNA microarray technology, genes or pathways that are deregulated in vestibular schwannomas have been identified. Ultimately, drug therapies will be designed to stop schwannoma progression. This

will offer alternatives to the current options of untreated observation of tumor growth, stereotactic radiation, or surgical removal. Furthermore, it may also be possible to develop targeted therapy that may shrink or altogether eradicate preexisting tumors.

(2) Chang, L.-S., A. Jacob, M. Lorenz, J. Rock, E.M. Akhmametyeva, G. Mihai, P. Schmalbrock, A.R. Chaudhury, R. Lopez, J. Yamate, M.R. John, H. Wickert, B.A. Neff, E. Dodson, and D.B. Welling. 2006. Magnetic Resonance Imaging Noninvasively Quantifies Schwannoma Xenografts in SCID Mice. Laryngoscope 116: In Press.

Models for the development of new treatment options in vestibular schwannoma treatment are lacking. The purpose of this study is to establish a quantifiable human vestibular schwannoma xenograft model in severe combined immunodeficiency (SCID) mice. We implanted vestibular schwannoma specimens near the sciatic nerve in the thigh of SCID mice. We used a 4.7-tesla MRI to monitor tumor growth over one year period. Three-dimensional tumor volumes were calculated from MRI images. We found that vestibular schwannoma xenografts demonstrated variability in their growth rates similar to human vestibular schwannoma in situ. The majority of vestibular schwannoma xenografts did not grow but persisted throughout the study, while two of 15 xenografts grew significantly. Histopathological examination and immunohistochemistry confirmed that vestibular schwannoma xenografts retained their original microscopic and immunohistochemical characteristics after prolonged implantation. The vestibular schwannoma xenografts represent a model complimentary to Nf2 transgenic and knockout mice for translational vestibular schwannoma research.

(3) Neff, B.A., E. Oberstein, M. Lorenz,, A. Chadhury, D.B. Welling, and L.-S. Chang. 2006. Cyclin D_1 and D_3 Expression in Vestibular Schwannomas. Laryngoscope 116:423-426.

The G_1 regulators of the cell cycle, cyclin D_1 and D_3, have been implicated in the regulation of Schwann cell proliferation and differentiation. The purpose of this study is to evaluate cyclin D_1 and D_3 protein expression and the corresponding clinical characteristics of vestibular schwannomas. Tissue sections of 15 sporadic vestibular schwannomas were prepared. Immunohistochemical analysis of the vestibular schwannomas was performed with anti-cyclin D_1 and anti-cyclin D_3 antibodies. The immunoreactivity was evaluated in comparison with adjacent vestibular nerves. Tissue sections of breast carcinoma and prostate carcinoma were used as positive controls for cyclin D_1 and D_3 staining, respectively. Patient demographics, tumor characteristics, and cyclin D expression were reviewed, and statistical analysis was performed. While the breast carcinoma control expressed abundant cyclin D_1 protein, none of the 15 vestibular schwannomas showed detectable cyclin D_1 staining. In contrast, seven of 15 vestibular schwannomas stained positive for the cyclin D_3 protein. Cyclin D_3 staining was taken up in the nucleus of schwannoma tumor cells in greater proportion than Schwann cells of adjacent vestibular nerve. Although sample size was small, no significant difference in the average age of presentation, tumor size, and male to female ratios for the cyclin D_3+ or cyclin D_3- groups was found. In conclusion, the cyclin D_1 protein does not appear to play a prominent role in promoting cell cycle progression in vestibular schwannomas. In contrast, cyclin D_3 expression was seen in nearly half of the tumors examined, suggesting that it may have a growth-promoting role in some schwannomas.

(4) Akhmametyeva, E.M., M. Mihaylova, H. Luo, Sadeq Kharzai, D.B. Welling, and L.-S. Chang. 2006. Regulation of the *Neurofibromatosis 2* Gene Promoter Expression during Embryonic Development. Dev. Dyn. 235, In Press.

To better understand NF2 expression in vivo, we generated transgenic mice carrying a 2.4-kb NF2 promoter driving β-galactosidase (β-gal) with a nuclear localization signal. Whole-mount embryo staining revealed that the NF2 promoter directed β-gal expression as early as embryonic day E5.5. Strong expression was detected at E6.5 in the embryonic ectoderm containing many mitotic cells. β-gal staining was also found in parts of embryonic endoderm and mesoderm. The β-gal staining pattern in the embryonic tissues was corroborated by in situ hybridization analysis of

endogenous Nf2 RNA expression. Importantly, we observed strong NF2 promoter activity in the developing brain and in sites containing migrating cells including the neural tube closure, branchial arches, dorsal aorta, and paraaortic splanchnopleura. Furthermore, we noted a transient change of NF2 promoter activity during neural crest cell migration. While little β-gal activity was detected in premigratory neural crest cells at the dorsal ridge region of the neural fold, significant activity was seen in the neural crest cells already migrating away from the dorsal neural tube. In addition, we detected considerable NF2 promoter activity in various NF2-affected tissues such as acoustic ganglion, trigeminal ganglion, spinal ganglia, optic chiasma, the ependymal cell-containing tela choroidea, and the pigmented epithelium of the retina. The NF2 promoter expression pattern during embryogenesis suggests a specific regulation of the NF2 gene during neural crest cell migration and further support the role of merlin in cell adhesion, motility, and proliferation during development.

(5) Chang, L.-S., E.M. Akhmametyeva, M. Mihaylova, H. Luo, S. Tae, B. Neff, and D.B. Welling. 2005. Dissecting the Molecular Pathways in Vestibular Schwannoma Tumorigenesis. Recent Research Development in Genes & Genomes 1: 1-33.

The NF2 tumor suppressor gene is frequently mutated in all three types of vestibular schwannomas. Analysis of NF2 function and regulation has provided the first step toward the better understanding of the molecular mechanism of schwannoma tumorigenesis. In this review, we summarized our findings on the regulation of expression of the NF2 gene at the transcriptional and post-transcriptional level. We also described our transgenic study to examine NF2 promoter expression during early embryonic development. The NF2 gene encodes a protein termed merlin/schwannomin, which shares a high degree of homology with the ezrin, radixin, and moesin (ERM) proteins. Genetic knockout experiments have shown that the NF2 gene product is a tumor suppressor for Schwann cell and meningeal cells. By using cDNA microarray analysis, we identified genes and pathways that were deregulated in vestibular schwannomas. Furthermore, we have revealed potential underlying molecular differences among the types of vestibular schwannomas. It is anticipated that further analysis of the information will lead to the development of novel pharmaco-therapeutics, offering alternatives to the current options of untreated observation of tumor growth, stereotactic radiation, or surgical removal.

LIST OF PERSONNEL

Long-Sheng Chang, Ph.D., Principal Investigator
D. Bradley Welling, M.D., Ph.D., Co-Investigator
Elena M. Akhmametyeva, M.D., Ph.D., Postdoctoral Research Associate
Huijun Luo, Ph.D., Postdoctoral Fellow
Maria M. Mihaylova, B.S., Research Assistant
Sarah Burns, B.S. (Expected), Research Aide

CONCLUSIONS:

Vestibular schwannomas express a distinct pattern of alternatively spliced *NF2* transcripts lacking specific exons, suggesting that these alternatively spliced exons may be important for *NF2* function. The results from the analysis of the *NF2* promoter expression pattern during embryogenesis suggest a specific regulation of the *NF2* gene during neural crest cell migration and further support the role of merlin in cell adhesion, motility, and proliferation during development. Transgenic and conditional knockout mice have been generated to address whether the alternative splicing *NF2* isoforms preferentially expressed in schwannomas possess any additional properties conducive to tumor formation *in* vivo. Also, we show that the 3' UT sequence of the *NF2* gene does not affect the stability of *NF2* RNA or the efficiency of protein translation *in vitro*. Utilizing the vestibular schwannoma

samples procured from this study, we have established a quantifiable human vestibular schwannoma xenograft model in SCID mice and identified cyclin D_3 as a growth-promoting factor for vestibular schwannomas.

REFERENCES:

Akhmametyeva, E.M., M.M. Mihaylova, H. Luo, S. Kharzai, D.B. Welling, and L.-S. Chang. 2006. Regulation of the *NF2* Gene Promoter Expression During Embryonic Development. Dev. Dyn. 235: In Press.

Baser, M.E., Evans, D.G.R., and Gutmann, D.H. 2003. Neurofibromatosis 2. Curr. Opin. Neurol. 16:27-33.

Chang, L.-S., Akhmametyeva, E.M., Mihaylova, M., Luo, H., Tae, S., Neff, B., Jacob, A., and Welling, D.B. 2005. Dissecting the molecular pathways in vestibular schwannoma tumorigenesis. Recent Res. Devel. Genes & Genomes 1:1-33.

Chang, L.-S., Akhmametyeva, E.M., Wu, Y., and Welling, D.B. 2002. Multiple transcription initiation sites, alternative splicing, and differential polyadenylation contribute to the complexity of human neurofibromatosis 2 transcripts. Genomics 79:63-76.

Chang, L.-S., A. Jacob, M. Lorenz, J. Rock, E.M. Akhmametyeva, G. Mihai, P. Schmalbrock, A.R. Chaudhury, R. Lopez, J. Yamate, M.R. John, H. Wickert, B.A. Neff, E. Dodson, and D.B. Welling. 2006. Magnetic Resonance Imaging Noninvasively Quantifies Schwannoma Xenografts in SCID Mice. Laryngoscope 116: In Press.

Giovannini M, Robanus-Maandag E, Niwa-Kawakita M, van der Valk M, Woodruff JM, Goutebroze L, Merel P, Berns A, Thomas G. 1999. Schwann cell hyperplasia and tumors in transgenic mice expressing a naturally occurring mutant NF2 protein. Genes Dev. 13:978-986.

Giovannini, M., Robanus-Maandag, E., van der Valk, M., Niwa-Kawakita, M., Abramowski, V., Goutebroze, L., Woodruff, J.M., Berns, A., and Thomas, G. 2000. Conditional biallelic *Nf2* mutation in the mouse promotes manifestations of human neurofibromatosis type 2. Genes Dev. 14:1617-1630.

Gutmann, D.H., Haipek, C.A., and Hoang Lu, K. 1999. Neurofibromatosis 2 tumor suppressor protein, merlin, forms two functionally important intramolecular associations. J. Neurosci. Res. 58:706-716.

Gutmann DH,Sherman L, Seftor L, Haipek C, Hoang Lu K, Hendrix M. 1999. Increased expression of the NF2 tumor suppressor gene product, merlin, impairs cell motility, adhesion and spreading. Hum. Mol. Genet. 8:267-275.

Neff, B.A., E. Oberstein, M. Lorenz,, A. Chadhury, D.B. Welling, and L.-S. Chang. 2006. Cyclin D_1 and D_3 Expression in Vestibular Schwannomas. Laryngoscope 116:423-426.

Neff, B.A., D.B. Welling, E.M. Akhmametyeva, and L.-S. Chang. 2006. The Molecular Biology of Vestibular Schwannomas: Dissecting the Pathogenic Process at the Molecular Level. Otol. Neurotol. 27:197-208.

Ratner, N., Bunge, R.P., Glaser, L. 1986. Schwann cell proliferation in vitro. An overview. Ann N Y Acad Sci.486:170-181.

Trofatter, J.A., MacCollin, M.M., Rutter, J.L., Murrell, J.R., Duyao, M.P., Parry, D.M., Eldridge, R., Kley, N., Menon, A.G., Pulaski, K., Haase, V.H., Ambrose, C.M., Munroe, D., Bove, C., Haines, J.L., Martuza, R.L., MacDonald, M.E., Seizinger, B.R., Short, M.P., Buckler, A.L., Gusella, J.F. 1993. A novel Moesin-, Exrin-, Radixin-like gene is a candidate for the neurofibromatosis 2 tumor-suppressor. Cell 72:791-800.

ABSTRACT

Neurofibromatosis type 2 (NF2) is associated with a homozygous inactivation of the neurofibromatosis 2 gene (*NF2*). Despite intense study of the *NF2* gene, the mechanism by which the *NF2* tumor suppressor acts to prevent tumor formation is not well understood. The *NF2* transcripts undergo alternative splicing, generating a series of mRNA isoforms lacking one or more exons. Presently, the role of alternative splicing of *NF2* mRNAs is not understood. The *NF2* transcripts are also terminated at different polyadenylation sites. The role of this differential polyadenylation is not known. The goal of this research is to examine the role of alternative splicing and differentiation polyadenylation of the *NF2* gene. With this grant support, we have confirmed that vestibular schwannomas express a distinct pattern of alternatively spliced *NF2* transcripts lacking specific exons. Analysis of *NF2* expression during embryonic development reveals that *NF2* is an early expression marker. Strong *NF2* promoter activity was seen in the embryonic ectoderm and in all NF2-affected tissues examined. Importantly, we observed strong *NF2* promoter activity in the developing brain and in sites containing migrating cells including the neural tube closure and branchial arches. Furthermore, we noted a transient change of *NF2* promoter activity during neural crest cell migration. The *NF2* promoter expression pattern during embryogenesis suggests a specific regulation of the *NF2* gene during neural crest cell migration and further support the role of merlin in cell adhesion, motility, and proliferation during development. By using the conditional gene targeting approach, we have also generated an $Nf2^{flox8}$ allele. Transgenic and conditional knockout mice have been generated to address whether the alternative splicing *NF2* isoforms preferentially expressed in schwannomas possess any additional properties conducive to tumor formation *in* vivo. Also, we show that the 3' UT sequence of the *NF2* gene does not affect the stability of *NF2* RNA or the efficiency of protein translation *in vitro* Utilizing the vestibular schwannoma samples procured from this study, we have established a quantifiable human vestibular schwannoma xenograft model in SCID mice and identified cyclin D_3 as a growth-promoting factor for vestibular schwannomas. The vestibular schwannoma xenografts represent a model complimentary to *Nf2* transgenic and knockout mice for translational vestibular schwannoma research.

APPENDICES:

Publications and Papers In Press

(1) Neff, B.A., D.B. Welling, E.M. Akhmametyeva, and L.-S. Chang. 2006. The Molecular Biology of Vestibular Schwannomas: Dissecting the Pathogenic Process at the Molecular Level. Otol. Neurotol. 27:197-208.
(2) Chang, L.-S., A. Jacob, M. Lorenz, J. Rock, E.M. Akhmametyeva, G. Mihai, P. Schmalbrock, A.R. Chaudhury, R. Lopez, J. Yamate, M.R. John, H. Wickert, B.A. Neff, E. Dodson, and D.B. Welling. 2006. Magnetic Resonance Imaging Noninvasively Quantifies Schwannoma Xenografts in SCID Mice. Laryngoscope 116: In Press.
(3) Neff, B.A., E. Oberstein, M. Lorenz,, A. Chadhury, D.B. Welling, and L.-S. Chang. 2006. Cyclin D_1 and D_3 Expression in Vestibular Schwannomas. Laryngoscope 116:423-426.
(4) Akhmametyeva, E.M., M. Mihaylova, H. Luo, D.B. Welling, and L.-S. Chang. 2006. Regulation of the *Neurofibromatosis 2* (*NF2*) Promoter Expression during Early Embryonic Development. Dev. Dyn. 235: In Press.
(5) Chang, L.-S., E.M. Akhmametyeva, M. Mihaylova, H. Luo, S. Tae, B. Neff, and D.B. Welling. 2005. Dissecting the Molecular Pathways in Vestibular Schwannoma Tumorigenesis. Recent Research Development in Genes & Genomes 1: 1-33.

Otology & Neurotology
27:197–208 © 2006, Otology & Neurotology, Inc.

The Molecular Biology of Vestibular Schwannomas: Dissecting the Pathogenic Process at the Molecular Level

*Brian A. Neff, *D. Bradley Welling, †Elena Akhmametyeva, and *†‡§¶Long-Sheng Chang

*Departments of *Otolaryngology, †Pathology, ‡Pediatrics, §Molecular Cellular Biochemistry, and ¶Veterinary Biosciences, The Ohio State University College of Medicine and Children's Hospital, Columbus, Ohio*

Objective: The goal of this article was to review concisely what is currently known about the tumorigenesis of vestibular schwannomas.
Background: Recent advances in molecular biology have led to a better understanding of the cause of vestibular schwannomas. Mutations in the neurofibromatosis type 2 tumor suppressor gene (*NF2*) have been identified in these tumors. In addition, the interactions of merlin, the protein product of the *NF2* gene, and other cellular proteins are beginning to give us a better idea of *NF2* function and the pathogenesis of vestibular schwannomas.
Methods: Review of the relevant basic science studies at our institution as well as the basic science and clinical literature.
Results: The clinical characteristics of vestibular schwannomas and neurofibromatosis type 2 syndromes are reviewed and related to alterations in the *NF2* gene. Studies demonstrating our current understanding of tumor developmental pathways are highlighted. In addition, methods of clinical and genetic screening for neurofibromatosis type 2 disease are outlined. Avenues for the development of potential future research and therapies are discussed.
Conclusion: Great strides have been made to identify why vestibular schwannomas develop at the molecular level. Continued research is needed to find targeted therapies with which to treat these tumors. **Key Words:** Acoustic neuroma—*NF2* gene—Merlin—Neurofibromatosis type 2—Vestibular schwannoma.

Otol Neurotol **27:**197–208, 2006.

Vestibular schwannomas are histologically benign tumors of the neural sheath that originate on the superior or inferior vestibular branches of Cranial Nerve VIII. The term "vestibular schwannoma" is preferred over the more commonly used term "acoustic neuroma" because these tumors are not neuromas, nor do they arise from the acoustic (cochlear) nerve. They occur either as sporadic unilateral tumors or bilateral tumors; the development of bilateral vestibular schwannomas is the hallmark of neurofibromatosis type 2 (NF2). Various types of vestibular schwannomas can be loosely grouped into unilateral sporadic vestibular schwannomas, bilateral or NF2-associated schwannomas, and cystic schwannomas.

This study was supported by the National Institutes of Health and the Department of Defense Neurofibromatosis Research Program.

Address correspondence and reprint requests to Bradley Welling, M.D., Ph.D., 456 West 10th Avenue, Columbus, OH 43210, U.S.A.; E-mail: welling.1@osu.edu

Unilateral schwannomas are the most common presentation, and they constitute 95% of all vestibular schwannomas. Sporadic vestibular schwannomas occur in approximately 10 per 1 million persons per year (1). However, the true incidence may be higher, as highlighted by Anderson et al., who demonstrated an incidence of 7 unsuspected schwannomas per 10,000 brain magnetic resonance imaging (MRI) studies (0.07%) (2). Sporadic tumors usually occur in the fourth and fifth decades, with a mean presentation of 50 years of age. Although histologically benign, schwannomas can, if large enough, cause hydrocephalus, brainstem compression, herniation, and death. Most commonly, however, they are associated with hearing loss, tinnitus, imbalance, and other symptoms related to compression of adjacent cranial nerves.

NF2 is clinically an autosomal dominant disease that is highly penetrant (3). NF2-associated tumors account for approximately 5% of all vestibular schwannomas. Patients who inherit an abnormal copy of the *NF2* tumor suppressor gene have a 95% chance of

developing bilateral vestibular schwannomas. However, approximately one-half of the cases have no family history of NF2, and thus they represent new germline mutations that were not inherited. Other disease features of NF2 include intracranial meningiomas, ependymomas, spinal schwannomas, and presenile lens opacities (4,5). Of the four different sets of diagnostic criteria for NF2, the Manchester criteria are the most sensitive, and they are summarized in Table 1 (6). NF2 is now recognized as a disease that is distinctly different from neurofibromatosis type 1 (NF1) or von Recklinghausen's disease. NF1, which is associated with multiple peripheral neuromas, is caused by a mutation in the *NF1* tumor suppressor gene on chromosome 17.

NF2 is currently subdivided into three groups on the basis of clinical presentation and severity of disease (7). The Wishart type has a more severe clinical presentation. In addition to bilateral vestibular schwannomas, patients often suffer from associated spinal tumors, with a typical onset in the late teens or early 20s (8). The Gardner type has a later onset and a less severe presentation. Although patients present with bilateral schwannomas, the incidence of associated intracranial tumors is less common (9). A more recently recognized third category of NF2 has been termed mosaic NF2, where a mutation occurs in embryogenesis rather than in the germline DNA; therefore, only a portion of the patients' cells carry the mutation (10,11). This is different from those patients with traditional NF2 who inherit the mutation from their parent. Kluwe et al. recently estimated that mosaicism may account for 24.8% (58 of 233) of NF2 cases of any subtype among patients whose parents did not display the disease (11). Patients with somatic mosaicism can display bilateral vestibular schwannomas if the postzygotic mutation occurred early in embryogenesis. However, they may also display an atypical presentation, or segmental NF2, in which the patient has a unilateral vestibular schwannoma and an ipsilateral, additional intracranial tumor, such as a meningioma, if the postzygotic mutation occurred late in development (10). Unlike the traditional forms of NF2, the risk of passing NF2 caused by mosaicism to future offspring is very low (12); however, in the unlikely event that NF2 is inherited from a mosaic parent, the offspring will carry the mutation in all their cells, and the clinical presentation would be severe and consistent with the conventional form of NF2.

TABLE 1. *Manchester criteria for the diagnosis of NF2*[a,b]

A. Bilateral vestibular schwannomas
B. First-degree relative with NF2 and unilateral vestibular schwannoma or any two of the following: meningioma, schwannoma, glioma, neurofibroma, juvenile posterior subcapsular lens opacity
C. Unilateral vestibular schwannoma and any two of the following: meningioma, schwannoma, glioma, neurofibroma, posterior subcapsular lenticular opacities
D. Multiple meningiomas (two or more) and unilateral vestibular schwannoma or any two of the following: schwannoma, glioma, neurofibroma, cataract

[a]Data from Baser et al. (6).

[b]Note: "any two of" refers to two individual tumors or cataract. For example, a unilateral schwannoma and two gliomas would meet the criteria.

Schwannomatosis, a recently defined form of neurofibromatosis, is characterized by multiple schwannomas without any NF2-associated vestibular schwannomas. Patients with schwannomatosis frequently present with intractable pain rather than cranial nerve deficits. They do not develop other intracranial tumors or malignancies. MacCollin et al. noted that approximately one-third of patients with schwannomatosis had tumors in an anatomically limited distribution, such as a single limb, several contiguous segments of the spine, or one side of the body (13). Sporadic cases of schwannomatosis are as common as NF2, but few cases of familial schwannomatosis have been identified. This is in contradistinction to NF1 and NF2, which are autosomal dominant, highly penetrant syndromes that are frequently found clustered in families. The underlying molecular disruption in schwannomatosis is a pattern of somatic *NF2* gene inactivation incompatible with NF1 or NF2, but this has not been completely defined.

Cystic vestibular schwannomas are a particularly aggressive group of unilateral, sporadic schwannomas that invade the surrounding cranial nerves, splaying them throughout the tumors. Cystic vestibular schwannomas are associated with either intratumoral or extratumoral cysts that develop in the loosely organized Antoni B tissues. In addition, a higher degree of nuclear atypia is seen in cystic tumors (14). Careful distinction must be drawn between the truly cystic schwannomas and the very common heterogeneous schwannomas, which are not as aggressive in their clinical behavior. MRI clearly distinguishes between the solid and cystic vestibular schwannomas. Cystic regions of the tumors are hyperintense on T2-weighted images, and the cysts do not enhance with gadolinium administration. The noncystic component of the cystic tumors enhances with gadolinium in a manner similar to the unilateral and NF2-associated schwannomas (Fig. 1). Cystic tumors may grow rapidly, and they are very difficult to manage because of the high rate of hearing loss and facial nerve paralysis that occurs after surgical removal (15). When compared with solid tumors of a similar size, the rate of complete facial nerve paralysis (House-Brackmann Grade VI) with surgical removal of cystic tumors was 41%, as compared with 27% for that of solid unilateral schwannomas (16). Cystic tumors are also more likely to have continued growth and facial nerve paralysis even with stereotactic radiation treatments than either the unilateral

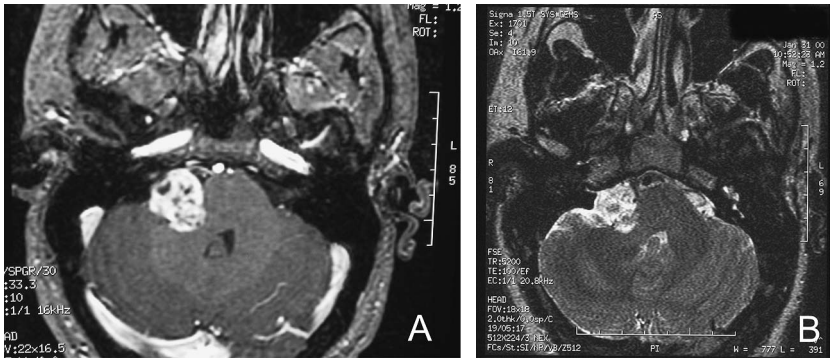

FIG. 1. MRI scans of vestibular schwannomas. (*A*) Axial T1-weighted MRI scan with gadolinium contrast. There is an enhancing right-sided cerebellopontine angle tumor with areas of central low intensity that correspond with cysts within this pathologically confirmed vestibular schwannoma. (*B*) Axial T2-weighted MRI scan. The tumor is more hyperintense than the typical T2 signal characteristics of a vestibular schwannoma. In addition, there are focal areas of increased signal intensity that correspond with the intratumoral cysts.

spontaneous or NF2-associated schwannomas (17,18). To date, some differences in the gene expression profiles of cystic tumors have been identified, compared with those of sporadic and NF2-associated tumors (19,20); however, there has not been a clear tumorigenic pathway demonstrated to definitively explain the aggressive growth seen with cystic schwannomas, and this is an area of current investigation.

Although the effectiveness of treatment with current surgical and radiation treatments for vestibular schwannomas are generally good, treatment-related morbidity continues to be problematic. The field of molecular biology is proposed as the discipline to advance the level of diagnosis and to improve the treatment of vestibular schwannomas. When applied to various neurotologic abnormalities, "molecular neurotology" may soon develop as a medical discipline in a manner similar to the advent of surgical neurotology in the 1960s. A brief review of the recent discoveries and advances in the molecular biology of vestibular schwannomas follows.

THE *NF2* GENE

The *NF2* gene was localized to chromosome 22 through a genetic linkage analysis (21). Subsequently, 23 patients from a large NF2 kindred were studied, and the *NF2* locus was further mapped close to the center of the long arm of chromosome 22 (22q12) (22). After genetic and physical mapping, positional cloning studies led to the discovery of the *NF2* gene. In 1993, Trofatter et al. and Rouleau et al. independently identified the *NF2* gene, which is frequently mutated in NF2-related vestibular schwannomas (23, 24). Since that time, mutations in the *NF2* gene have been found not only in NF2 tumors but also in sporadic unilateral schwannomas and cystic schwannomas (Table 2) (25–39). In addition, mutations within the *NF2* gene have been frequently identified in meningiomas and occasionally identified in other tumor types such as mesotheliomas (26,39–42).

NF2 MUTATIONS AND THEIR CLINICAL CORRELATION

Several groups have attempted to correlate clinical expression of tumors with specific *NF2* mutations in vestibular schwannomas and other NF2-associated tumors. A number of somatic mutations and their specific clinical behavior in vestibular schwannomas have been characterized in sporadic unilateral tumors and NF2 tumors (25–31,38–40,43–47). We previously studied a series of patients who had vestibular schwannomas and found that the frequency, type, and distribution of *NF2* mutations were shown to be different between the sporadic and familial NF2 tumors (25). Mutations were identified in 66% of the sporadic cases but in only 33% of the NF2 cases; therefore, the rate of detection of a mutation in unilateral schwannomas was significantly higher than that in familial schwannomas. Point mutations accounted for the majority of mutations identified in NF2 patients, whereas small deletions accounted for the majority of mutations found in the sporadic unilateral tumors (28,30,43).

Studies were also conducted to determine whether the genotype could be a predictor of disease severity. The clinical phenotypes of NF2, Wishart and Gardner, were further examined, as was a potential third phenotype, mosaic or segmental NF2. Deletion mutations that cause truncation of the NF2 protein have been reported to cause a more severe phenotype in NF2 pedigrees (28,30,43), whereas missense mutations or small in-frame insertions in the *NF2*-coding region have been reported to associate with a mild phenotype (25,26,31,39,46). However, this has not held true in other studies, which showed that some missense mutations associated with a severe phenotype. In addition, missense mutations within the α-helical domain of the NF2 protein appear to associate with a less severe phenotype than those within the conserved FERM domain (48). This lack of genotype-phenotype correlation was also seen for large deletions, which could give rise to mild phenotypes and the previously reported severe disease expression (49).

TABLE 2. *Summary of NF2 mutation detection*

Reference	No. of NF2 patients	No. of non-NF2 patients	% Detected	Methods*
Jacoby[28] 1994	8	30	53	SSCP
MacCollin[27] 1994	33		64	SSCP
Merel[26] 1995	91		35	DGGE
Welling[25] 1996	32	29	54	HA, DS
Ruttledge[31] 1996	111		54	SSCP
Mautner[32] 1996	9	3	75	SSCP
Parry[30] 1996	32		66	SSCP
Kluwe[29] 1996	59		34	SSCP
Evans[34] 1998	125		43	DS
Zucman-Rossi[33] 1998	19		84	DGGE, DS
Antinheimo[35] 2000	8	12	70	CGH
Hung[36] 2000	20		80	NIRCA

*HA, heteroduplex analysis; DS, direct sequencing; DGGE, denaturing gradient gel electrophoresis; SSCP, single-stranded conformation polymorphism analysis; CGH, comparative genomic hybridization; NIRCA, nonisotopic RNAase cleavage assay.

Given the heterogeneity of clinical response to various types of mutations, no clear genotype-to-phenotype correlation has been established, and this is further evidenced by the fact that phenotypic variability within the NF2 families with the same mutation has been seen (32). By extensive screening of the *NF2* gene, Zucman-Rossi et al. reported an 84% mutation detection rate in vestibular schwannomas; thus, additional mechanisms for inactivation of the *NF2* gene in some patients may exist (33). The possibility of a modifier gene has been suggested (50). Also, mutation or methylation in the regulatory region of the *NF2* gene has been suggested as a possible mechanism of gene inactivation (51,52). The complexity of *NF2* transcripts generated by posttranscriptional alternative splicing and differential polyadenylation may also be considered as possible means of inactivating the *NF2* gene (52).

ALTERNATIVELY SPLICED *NF2* MRNA ISOFORMS IN VESTIBULAR SCHWANNOMAS

DNA consists of regions called exons and introns. The exons are the segments of DNA that are transcribed and brought together as a mature mRNA product. The introns represent the sections of DNA that are transcribed but are spliced out during RNA processing. Alternative splicing is the mechanism by which different exon combinations are brought together to produce multiple mRNA transcripts from the same gene. These alternatively spliced transcripts can include all of the gene's exons or can be missing one or multiple exons. The different RNA transcripts produced from this process are termed mRNA isoforms.

The coding region of the *NF2* gene consists of 17 exons, and the *NF2* gene undergoes alternative splicing of these coding exons. An example of *NF2* mRNA isoforms is shown in Figure 2. Multiple alternatively spliced *NF2* transcripts have been identified in various human cells. The most common isoforms in these cells were isoforms II (containing all 17 exons) and I (without exon 16) (26,52–54).

We have also examined the expression of alternatively spliced *NF2* mRNA isoforms in vestibular schwannomas (one NF2 schwannoma, seven sporadic schwannomas, and two cystic schwannomas). Cloning and sequencing analysis showed that the expression pattern and relative frequency of the alternatively spliced *NF2* transcripts appeared to be different from those detected in other human cell types described above. Particularly, in addition to isoforms I and II, these schwannomas expressed a high percentage of the *NF2* mRNA isoform lacking exons 15 and 16 (Fig. 2). These alternatively spliced *NF2* transcripts could encode different protein products (Please provide name and initials of source of unpublished dataunpublished data).

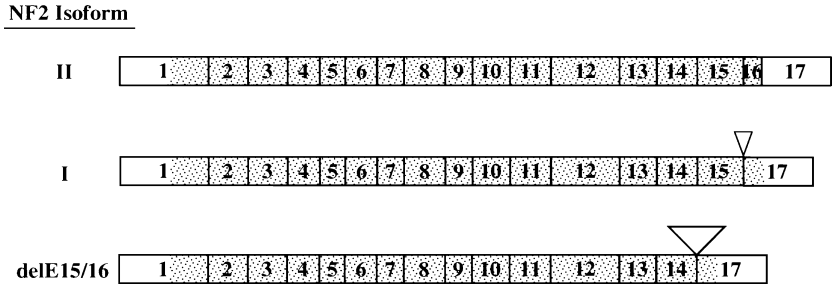

FIG. 2. The *NF2* gene is transcribed into mRNA; however, alternative splicing can produce different mRNA transcripts or isoforms. Different exon combinations can be brought together to produce multiple mRNAs from the same gene. Our studies showed that isoform I, II, and delE15/16 were the most common isoforms found in vestibular schwannomas examined.

Presently, the role of alternative splicing of *NF2* mRNA is not well understood. It is possible that the functional contribution of the *NF2* tumor suppressor may require a balanced expression of various isoform proteins in Schwann cells and/or other cell lineages (52,55). Alternative splicing may be another mechanism for Schwann cells to inactivate merlin function and/or to generate isoforms that have additional properties conducive to tumor formation. We are presently conducting experiments to test these possibilities.

THE *NF2* GENE PROMOTER

The upstream and downstream untranslated regions of the *NF2* gene have been characterized so that these regions could be screened for mutations in both sporadic and familial tumors in which no mutation was found in the *NF2*-coding region. Our laboratory has mapped the major transcription initiation site of the *NF2* gene and found that multiple regions in the *NF2* promoter are required for full *NF2* promoter activity (52,56). Both positive and negative *cis*-acting regulatory elements required for transcription of the *NF2* gene have been found in the 5′ flanking region of the promoter. A G/C-rich sequence located in the proximal promoter region, which can be bound by the Sp1 transcription factor, serves as a positive regulatory element. Both the 5′ and 3′ flanking regions of the human *NF2* locus are G/C rich and could serve as targets for gene methylation and inactivation (52).

THE NF2 PROTEIN: STRUCTURE AND FUNCTION

The *NF2*-coding region encompasses 90 kb of DNA on chromosome 22 (23,24,33). It encodes a 595–amino acid protein product which has been named merlin (for *m*oesin-*e*zrin-*r*adixin *l*ike prote*in*) or *schwannomin* (derived from schwannoma) (23,24). For simplicity, the *NF2* protein will be referred to as merlin in this article.

Merlin shares a high degree of homology to the erythrocyte protein 4.1–related superfamily of proteins, which act to link the actin cytoskeleton to the plasma membrane. In particular, three proteins, ezrin, radixin, and moesin, referred to as the ERM family, share a great deal of structural similarity with merlin (24). The proteins belonging to this family all have a similar N-terminal globular domain, also known as the FERM domain, followed by an α-helical stretch, and finally a charged C-terminus (57). The key functional domains of merlin may lie within the highly conserved FERM domains and the unique C-terminus of the protein. The ERM proteins have been shown to be involved in cellular remodeling involving the actin cytoskeleton (58). These proteins bind actin filaments in the cytoskeleton via a conserved C-terminal domain and possibly via a second actin-binding site in the N-terminal half of the protein (59,60).

Like the ERM proteins, merlin is expressed in a variety of cell types, where it localizes to the areas of membrane remodeling, particularly membrane ruffles, although its precise distribution may differ from the ERM proteins expressed in the same cell (61). Interestingly, schwannoma cells from NF2 tumors show dramatic alterations in the actin cytoskeleton and display abnormalities in cell spreading (62). These results suggest that merlin may play an important role in regulating both the actin cytoskeleton-mediated processes and cell proliferation (63). However, it should be noted that merlin has a growth suppression role, whereas other ERM-family members seem to facilitate cell growth.

MERLIN ACTS AS A TUMOR SUPPRESSOR

Overexpression of the *NF2* gene in mouse fibroblasts or rat schwannoma cells can limit cell growth (46,64) and suppress cell transformation by the ras oncogene (65). The growth control of certain Schwann cells and meningeal cells is lost in the absence of *NF2* function, suggesting that *NF2* mutations and merlin deficiency disrupt some aspect of intracellular signaling that leads to cellular transformation. Together with animals, these findings demonstrate merlin's ability to act as a tumor suppressor.

Mouse Models

Scientists have developed *Nf2* knockout mice that were designed to be missing one or both copies of the *Nf2* gene in the germline. Intriguingly, heterozygous *Nf2* knockout mice go on to develop osteosarcomas and, less often, fibrosarcomas or hepatocellular carcinomas (66). Genetic analysis of these tumors shows that nearly all of them are missing both *Nf2* alleles because of a mutation causing a loss of the second *Nf2* allele. The fact that tumor growth occurs in the absence of both *Nf2* alleles indicates that the *Nf2* gene possesses a classical tumor suppressor function. However, none of the heterozygous *Nf2* mice develop tumors or clinical manifestations associated with human NF2.

Homozygous *Nf2* mutant mice, which are designed to be missing both *Nf2* alleles, also do not demonstrate clinical characteristics of human NF2, and the mutant embryos die at approximately seven days of gestation, indicating that a homozygous *Nf2* mutation is embryonic lethal (67). Together with our preliminary data showing that the *Nf2* gene is expressed early in embryogenesis (Akhmametyeva EM, et al. Data unpublished.), these results indicate that the *Nf2* gene product plays an important role during early embryonic development.

By engineering mice whose Schwann cells have exon 2 excised and removed from both *Nf2* alleles,

conditional homozygous *Nf2* knockout mice have been produced that display some characteristics of NF2 including schwannomas, Schwann cell hyperplasia, cataracts, and osseous metaplasia (68). Although these results argue that loss of merlin is sufficient for schwannoma formation in vivo, none of the tumors observed in these conditional knockout mice were found on the vestibular nerve. This is in contrast to those vestibular schwannomas commonly found in patients with NF2. Although these mouse models are a valuable tool with which to study potential therapeutic interventions for NF2, further work is needed to develop a mouse model that phenotypically displays schwannomas originating from the VIIIth cranial nerve.

MERLIN CELL SIGNALING AND REGULATION

In addition to the actin cytoskeleton, merlin has been shown to associate with cell membrane domains, which are highly enriched in signaling molecules that regulate cellular responses to proliferative and antiproliferative stimuli (69). To date, several proteins that are likely to interact with merlin have been identified. These include the ERM proteins, hyalurin receptor CD44, F-actin, paxillin, microtubules, βII-spectrin, β1-integrin, β-fodrin, the regulatory cofactor of Na^+-H^+ exchanger, SCHIP-1, hepatocyte growth factor-regulated tyrosine kinase substrate, p21-activated kinase 1 and 2 (Pak1 and Pak2), Rac1, RalGDS, N–WASP, Erbin, and RIB subunit of protein kinase A (70–83, 112–114).

Presently, how these protein–protein interactions relate to the tumor suppressor activity of merlin is largely not understood. The association of merlin with CD44 and β1-integrin raises the possibility that merlin might function as a molecular switch in the signaling pathways. CD44 is a transmembrane hyaluronic acid receptor implicated in cell–cell adhesion, cell–matrix adhesion, cell motility, and metastasis (82,83). Recent evidence suggests that merlin mediates contact inhibition of cell growth through signals from the extracellular matrix. At high cell density, merlin becomes hypophosphorylated and inhibits cell growth in response to hyaluronate, a mucopolysaccharide that surrounds cells. Merlin's growth-inhibitory activity depends on specific interaction with the cytoplasmic tail of CD44. At low cell density, merlin is phosphorylated; growth permissive; and exists in a complex with ezrin, moesin, and CD44. These data indicate that merlin and CD44 form a molecular switch that specifies cell growth arrest or proliferation (84). Also, merlin colocalizes and interacts with adherens components in confluent cells. Mouse fibroblasts lacking *Nf2* function do not undergo contact–dependent growth and can not form stable cadherin–containing cell:cell junctions. These results indicate that merlin functions as a tumor and metastasis suppressor by controlling cadherin–mediated cell:cell contact (111). Rac1, a member of the RhoGTPase family, has recently been demonstrated to promote phosphorylation of merlin, thereby inactivating its growth suppressor mechanism. In addition, among the Rac/Cdc42 effectors, p21-activated kinase 2 (Pak2) has been shown to phosphorylate merlin at serine 518 and inactivates its function (69,85,86). Kissil et al. also recently reported an interaction between merlin and Pak1. Merlin inhibits the activation dynamic of Pak1. Loss of merlin expression leads to the inappropriate activation of Pak1, whereas overexpression of merlin results in the inhibition of Pak1 activity (72) (Fig. 3).

MERLIN'S GROWTH REGULATORY FUNCTION IS RELATED TO ITS CONFORMATION AND PROTEIN–PROTEIN INTERACTIONS

The activities of the ERM proteins are controlled by self-association of the proteins' N-terminal and C-terminal regions (87). The ERM proteins can exist in the ''closed'' conformation, where the N- and C-terminal regions undergo an intramolecular interaction, thus folding the protein to mask the conserved actin-binding site (Fig. 3). The molecule can be converted to the open conformation in which the intramolecular interaction is disrupted by signals such as phosphorylation or treatment with phosphoinositides (46,72,86,88).

Merlin's ability to function as a growth regulator is also related to its ability to form such intramolecular associations. Two such interactions have been identified. The first interaction is between residues that fold the N-terminal end of the protein onto itself, whereas the second interaction folds the entire protein so that there is contact between N- and C-terminal

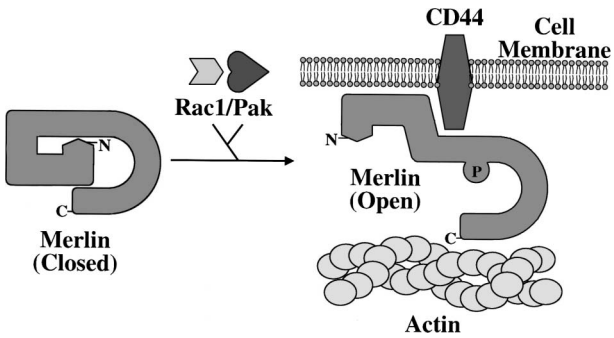

FIG. 3. Schematic diagram of merlin action. This diagram shows how Rac1 and Pak help convert the merlin protein from a closed conformation to an open conformation by phosphorylation of the protein. Consequently, merlin, in its open conformation, can interact with CD44 and facilitate linking the actin cytoskeleton to the cell membrane.

ends of the protein (46,89,90) (Fig. 3). In a fashion similar to the ERM proteins, merlin may cycle between the open and 'closed' conformations that differentially determine whether it binds with the ERM proteins or other molecules to transduce merlin's growth inhibition signal (91). In addition, the association between merlin and hepatocyte growth factor-regulated tyrosine kinase substrate, a substrate implicated in the signaling pathway initiated by hepatocyte growth factor binding to the c-met receptor (92), appears to be regulated by merlin folding, suggesting that the ability of merlin to cycle between the open and closed conformations may integrate CD44 and hepatocyte growth factor signaling pathways relevant to growth regulation (90).

IMMUNOHISTOCHEMICAL MARKERS OF GROWTH IN VESTIBULAR SCHWANNOMAS: CLINICAL CORRELATION

Attempts to correlate clinical parameters with immunohistologic evaluation of protein expression in vestibular schwannomas have been performed. An increase in Ki-67, which is an index of nuclear proliferation, was shown to correlate with the growth of solid schwannomas on MRI (93). Higher rates of tumor recurrence have also been suggested in tumors with an increased rate of nuclear proliferation and mitotic indexes, although the supporting data for this claim are not conclusive (94). Positron emission tomography scanning has been conducted to assess the metabolic activity of vestibular schwannomas preoperatively and to correlate the metabolic activity with the proliferation index, Ki-67. No correlation was found between the large and recurrent tumors and the uptake of 18-fluorodeoxyglucose as a radionucleotide tracer to measure glucose metabolism by positron emission tomography scanning. In additiion, there was no correlation between 18-fluorodeoxyglucose uptake and Ki-67 expression measured by immunostaining (95). A possible reason for this is that vestibular schwannomas are slow-growing tumors with only a small proportion of the tumor cells being in S-phase (active division) (96). Cystic schwannomas are associated with a 36-fold decrease in nuclear proliferation as measured with Ki-67 staining when compared with solid tumors. This suggests that the rapid clinical growth seen in cystic schwannomas is related to the accumulation of fluid during cyst formation and not by an actual increase in the growth rate of tumor cells (97). However, before this can be stated as fact, the cellular mechanism leading to the development of cystic schwannomas needs to be better understood. Lastly, *NF2*-associated schwannomas have been shown to have an increased proliferation index by Ki-67 and proliferating cell nuclear antigen immunostaining when compared with unilateral solid schwannomas (98).

Another possible marker for tumor growth is the transforming growth factor-β1. Immunostaining for transforming growth factor-β1 was positive in 96% of blood vessels within schwannomas and in 84% of schwannoma tissue samples; however, again, no clinical correlation with tumor types or tumor growth was found (99). Immunohistochemical association of β1-integrin with merlin has been demonstrated but has not been related directly to tumor phenotypes (77).

Considered together, these studies demonstrate a degree of correlation between clinical growth as assessed by MRI scans and historical data, and nuclear growth indexes in solid unilateral and *NF2*-associated schwannomas. However, cystic tumor growth appears to occur via a different mechanism. Although the defective *NF2* gene is the underlying common denominator in tumor formation of unilateral sporadic, *NF2*-associated, and cystic schwannomas, other differences at the molecular level likely account for the variable clinical presentations of these tumors.

CLINICAL SCREENING FOR NF2

Routine clinical and radiographic examinations are required for at-risk patients including patients with a first-degree relative with NF2. In addition, patients younger than 30 years with a unilateral vestibular schwannoma, or any patient with multiple intracranial or spinal tumors or other stigmata associated with NF2, should have a surveillance plan initiated. Any offspring of patients with NF2 should have annual ocular examinations starting soon after birth and annual neurologic examinations starting at 7 years of age. Biannual audiography and annual MRI evaluations should be conducted beginning at age 7. Others have recommended starting a similar screening process at 10 years of age, with an MRI every other year and annually if a vestibular schwannoma is found (100). We do not perform screening spinal imaging in undiagnosed, at-risk patients because nonsurgical management is usually recommended in cases of asymptomatic spinal tumors (101). The only time we would recommend spinal imaging in an at-risk patient is if they presented with complaints suggesting a symptomatic spinal tumor. Once a diagnosis of NF2 is made secondary to intracranial schwannomas and/or other tumors, we suggest obtaining a baseline spinal MRI scan, but the spinal scans should only be repeated if symptoms or physical examination findings suggest a new or progressive spinal tumor. The important point in this discussion is to begin some form of screening at an early age to pick up tumors while hearing preservation surgery is still possible.

GENETIC SCREENING FOR NF2

There are three scenarios worth considering in reference to genetic screening for NF2. Each instance

deals with an asymptomatic, undiagnosed child that is at-risk for developing NF2 disease. The first scenario pertains to an NF2 parent who has already had their specific mutation detected in the DNA of peripheral blood cells and/or a previously excised vestibular schwannoma. Another possibility is that the parent has a mosaic form of NF2 in which a mutation is often not detectable in the peripheral blood cells because only a portion of their cells carries the mutation. In these mosaic individuals, the mutation can often only be found when testing an excised vestibular schwannoma. In either case, if a mutation had been previously characterized in a parent, the sensitivity of genetic testing in this circumstance is nearly 100%, because the DNA being screened can be directly compared with the known mutation in the parent. Therefore, if the screening test was negative, then the child would not be at any higher risk for developing NF2 than the normal population and could avoid annual MRI screenings.

The second scenario is when multiple family members have been diagnosed with NF2 and none of them have had mutational analysis performed. In this case, we feel that it would be prudent to perform mutational screening on the affected family members to find a specific mutation that can be used to screen their children. Again, this would have a sensitivity of nearly 100%, and frequent testing could thus be avoided. If a specific mutation cannot be identified in any of the family members, linkage analysis of multiple NF2 family members may be used to screen children for NF2 (102).

The last scenario involves whether to screen children whose NF2 parent has not previously had a mutation identified or a previous attempt to find a mutation was unsuccessful. Several physicians feel that genetic screening is a useful tool in directing surveillance in this scenario; however, currently, this is a controversial position. We do not perform routine genetic screening in this specific instance, and the following discussion highlights the reasons why. It is important to note that this scenario is quite common because testing has only been available in the last decade; therefore, it is not uncommon to have 30- and 40-year-old NF2 patients who have not undergone mutational analysis. Furthermore, it is not unusual to have only one family member affected with NF2 because new mutations account for up to 50% of NF2 cases (7). In this instance, when screening a child whose NF2 mutation is unknown in their parent, probing the *NF2* gene for a specific known mutation is not possible, but rather a general probe for an unknown mutation is performed. In other words, instead of looking at a child's DNA to see whether it matches a known parental mutation that is located in a specific stretch of DNA within the *NF2* coding region, one is searching the entire *NF2* coding region for an unknown mutation, and consequently, in this instance, the sensitivity of genetic screening drops from nearly 100% to between 34 and 84%. Obviously, this leaves a significant number of patients whose NF2 mutation is not detected by this screening process and makes it difficult to predict those patients who will develop NF2 (25–36). Taking this fact into consideration, those children who had a negative screening test would still need annual MRI scans and biannual audiometric testing. In addition, if a mutation was detected during DNA sequencing, we would still recommend annual MRI scans and biannual audiometric testing to detect the development of vestibular schwannomas at the earliest possible stage. Early detection in NF2 does make a significant difference in the ability to successfully treat vestibular schwannomas. Therefore, because a positive or a negative NF2 mutation screen does not alter the recommended clinical follow-up of these at-risk children, when a mutation has not already been identified in a parent, we do not recommend routine genetic screening. Our current position may need to be reconsidered as the sensitivity of screening increases and the cost of mutation detection decreases.

IDENTIFYING DEREGULATED GENES IN VESTIBULAR SCHWANNOMAS

With 69,227 mRNA sequences representing unique human genes and more than 3 million expressed sequence tags in the UniGene database, the success of the Human Genome Project is evident. However, the expression, function, and regulation of the majority of genes are not yet known (103). The study of large-scale gene expression profiles using cDNA microarrays allows examination of the so-called transcriptome of a tissue, and gives a means of exploring a broad view of the basic biology of tumors (104). Data from the human genome project makes the expression profiles more readily searchable, and organization of the genes into functional groupings allows examination of distinct pathways. For example, cell cycle control, DNA damage repair, or signal transduction and transcription factors can be organized and reviewed for various tumors (105). Biochips that contain thousands of oligonucleotides representing genes from the human genome have been created and are used to perform cDNA microarrays.

To evaluate the gene expression profile in a tumor, RNA is isolated from the tumor and converted into cDNA or cRNA. This cDNA or cRNA is then labeled with a fluorescent dye and hybridized to the oligonucleotides on the biochip. The same process can be used to evaluate RNA expressed in a normal tissue and then to compare gene expression differences between the affected and normal tissues. Consequently, deregulated genes in the affected tissues can be identified. Microarray gene expression analysis has been successfully used in recent years to evaluate a number of solid tumors including breast carcinoma, colon

carcinoma, prostate carcinoma, ovarian carcinoma, and vestibular schwannomas (19,20,106–109).

Gene expression analysis has revealed differences among tumors that are not distinguishable histologically. Molecular classification, rather than histologic classification, may also better predict the response of certain tumor types to specific therapies (110). This genomic scale approach has helped to identify subclasses of colon carcinoma, breast carcinoma, melanoma, leukemias, and lymphomas (108,109). In several instances, cDNA microarray analysis has identified genes that appear to be useful for predicting clinical behavior.

Vestibular schwannoma characteristics cannot be explained by the current understanding of the mutation types alone. Investigating intertumor variability of gene expression profiles shows promise in helping to unravel the clinical differences among subtypes of vestibular schwannomas. To better understand the pathways leading to schwannoma formation, we have used cDNA microarray analysis to evaluate gene expression profiles of vestibular schwannomas (19,20). Three sporadic vestibular schwannomas, two NF2-associated schwannomas, and three cystic schwannomas were compared with a normal vestibular nerve from a patient with a sporadic schwannoma. The goal was to seek patterns of gene expression consistently elevated or decreased across all tumors. Of 25,920 genes or expressed sequence tags screened, 42 genes were significantly upregulated (by a factor of three or more) consistently across at least six of the eight tumors examined. In addition, multiple genes were found to be significantly downregulated in the majority of vestibular schwannomas examined. Of these genes, eight genes involved with cell signaling and division were downregulated, including an apoptosis-related, putative tumor suppressor gene, *LUCA-15*, which was downregulated in seven of eight schwannomas studied. Two mediators of angiogenesis, endoglin and osteonectin, were highly elevated in most of the tumors examined. Osteonectin is a secreted glycoprotein that interacts with extracellular matrix proteins to decrease adhesion of cells from the matrix, thereby inducing a biological state conducive to cell migration, and endoglin is a transforming growth factor-α receptor that is known to be an endothelial marker for angiogenesis in solid tumors. Osteonectin was elevated in all of the tumors studied, and endoglin was found to be significantly upregulated in all of the solid tumors but not in any of the cystic tumors examined. The difference in endoglin gene expression may be a future avenue of investigation into why some schwannomas develop the aggressive cystic phenotype (19). An example of a deregulated signaling pathway suggested by the microarray data is the retinoblastoma protein-cyclin-dependent kinase (CDK) pathway. Among genes involved in G_1 to S progression, CDK2 was found to be downregulated in seven of eight tumors, and every tumor examined had multiple genes deregulated in this pathway (20). To further validate the microarray results, quantitative real-time polymerase chain reaction and immunohistochemistry have been used to confirm RNA and protein expression levels, respectively, but the significance of these findings in the role of tumorigenesis is still under investigation (19,20).

CONCLUSION

The discovery of molecular mechanisms underlying vestibular schwannoma formation is rapidly moving forward. Understanding merlin's interactions with other proteins, signaling pathways, and regulation of the *NF2* gene will possibly lead to the development of novel drug therapies for vestibular schwannomas. In the future, it may also be possible to develop a targeted molecular therapy that will stop tumor progression or altogether eradicate preexisting tumors. It is hoped that these new avenues of treatment will offer improved alternatives to the current options of untreated observation of tumor growth, stereotactic radiation, or surgical removal. These are the challenges facing the "molecular neurotologist" of the future.

REFERENCES

1. Howitz MF, Johansen C, Tos M, et al. Incidence of vestibular schwannoma in Denmark, 1977–1995. *Am J Otol* 2000;21: 690–4.
2. Anderson TD, Loevner LA, Bigelow DC, et al. Prevalence of unsuspected acoustic neuroma found by magnetic resonance imaging. *Otolaryngol Head Neck Surg* 2000;122:643–6.
3. Bull. World Health Org. Prevention and control of neurofibromatosis: Memorandum from a joint WHO/NNFF meeting. *Bull World Health Org* 1992;70:173–82.
4. Kanter WR, Eldridge R, Fabricant R, et al. Central neurofibromatosis with bilateral acoustic neuroma: genetic, clinical and biochemical distinctions from peripheral neurofibromatosis. *Neurology* 1980;30:851–9.
5. Martuza RL, Eldridge R. Neurofibromatosis 2 (bilateral acoustic neurofibromatosis). *N Engl J Med* 1988;318:684–8.
6. Baser ME, Friedman JM, Wallace AJ, et al. Evaluation of clinical diagnostic criteria for neurofibromatosis 2. *Neurology* 2002;59:1759–65.
7. Evans DGR, Huson SM, Donnai D, et al. A genetic study of type 2 neurofibromatosis in the United Kingdom: I. Prevalence, mutation rate, fitness, and confirmation of maternal transmission effect on severity. *J Med Genet* 1992;29:841–6.
8. Wishart JH. Case of tumors in the skull, dura mater, and brain. *Edinburgh Med Surg J* 1822;18:393–7.
9. Gardner WJ, Frazier CH. Bilateral acoustic neurofibromatosis: a clinical study and field survey of a family of five generations with bilateral deafness in thirty-eight members. *Arch Neurol Psychiatry* 1930;23:266–302.
10. Ruggieri M, Huson SM. The clinical and diagnostic implications of mosaicism in neurofibromatosis. *Neurology* 2001;56:1433–43.
11. Kluwe L, Mautner V, Heinrich B. Molecular study of frequency of mosaicism in neurofibromatosis 2 patients with bilateral vestibular schwannomas. *J Med Genet* 2003;40:109–14.
12. Moyhuddin A, Baser MG, Watson C. Somatic mosaicism in neurofibromatosis 2: prevalence and risk of disease transmission to offspring. *J Med Genet* 2003;40:459–63.

13. MacCollin M, Willett C, Heinrich B, et al. Familial schwannomatosis: exclusion of the NF2 locus as the germline event. *Neurology* 2003;60:1968–74.
14. Charabi S, Tos M, Thomsen J, et al. Cystic vestibular schwannoma: clinical and experimental studies. *Acta Otolaryngol* 2000;543(Suppl):11–3.
15. Charabi S, Tos M, Borgesen SE, et al. Cystic acoustic neuromas: results of translabyrinthine surgery. *Arch Otolaryngol Head Neck Surg* 1994;120:1333–8.
16. Fundova P, Charabi S, Tos M, et al. Cystic vestibular schwannoma: surgical outcome. *J Laryngol Otol* 2000;114: 935–9.
17. Pendl G, Ganz JC, Kitz K, et al. Acoustic neurinomas with macrocysts treated with gamma knife radiosurgery. *Stereotact Funct Neurosurg* 1995;66(Suppl):103–11.
18. Shirato H, Sakamoto T, Takeichi N, et al. Fractionated stereotactic radiotherapy for vestibular schwannoma (VS): comparison between cystic-type and solid-type VS. *Int J Radiat Oncol Biol Phys* 2000;48:1395–401.
19. Welling DB, Lasak JM, Akhmametyeva EM, et al. cDNA microarray analysis of vestibular schwannomas. *Otol Neurotol* 2002;23:736–48.
20. Lasak JM, Welling DB, Salloum M, et al. Deregulation of the pRb-CDK pathway in vestibular schwannomas. *Laryngoscope* 2001;112:1555–61.
21. Rouleau GA, Wertelecki W, Haines JL, et al. Genetic linkage of bilateral acoustic neurofibromatosis to a DNA marker on chromosome 22. *Nature* 1987;329:246–8.
22. Wertelecki W, Rouleau GA, Superneau DW, et al. Neurofibromatosis 2: clinical and DNA linkage studies of a larger kindred. *N Engl J Med* 1988;319:278–83.
23. Rouleau GA, Merel P, Lutchman M, et al. Alteration in a new gene encoding a putative membrane-organizing protein causes neurofibromatosis type 2. *Nature* 1993;363:515–21.
24. Trofatter JA, MacCollin MM, Rutter JL, et al. A novel Moesin-, Exrin-, Radixin-like gene is a candidate for the neurofibromatosis 2 tumor-suppressor. *Cell* 1993;72:791–800.
25. Welling DB, Guida M, Goll F, et al. Mutational spectrums in the neurofibromatosis type 2 gene in sporadic and familial schwannomas. *Hum Genet* 1996;98:189–93.
26. Merel P, Khe HX, Sanson M, et al. Screening for germ-line mutations in the NF2 gene. *Genes Chromosome Cancer* 1995; 12:117–2.
27. MacCollin M, Ramesh V, Jacoby LB, et al. Mutational analysis of patients with neurofibromatosis 2. *Am J Hum Genet* 1994;55:314–20.
28. Jacoby LB, MacCollin M, Louis DN, et al. Exon scanning for mutation of the NF2 gene in schwannomas. *Hum Mol Genet* 1994;3:413–9.
29. Kluwe L, Bayer S, Baser ME, et al. Identification of NF2 germ-line mutations and comparison with neurofibromatosis 2 phenotypes. *Hum Genet* 1996;98:534–8.
30. Parry DM, MacCollin MM, Kaiser-Kupfer MI, et al. Germline mutations in the neurofibromatosis 2 gene: correlation with disease severity and retinal abnormalities. *Am J Hum Genet* 1996;59:529–3.
31. Ruttledge MH, Andermann AA, Phelan CM, et al. Type of mutation in the neurofibromatosis type 2 gene (NF2) frequently determines severity of disease. *Am J Hum Genet* 1996;59:331–42.
32. Mautner VF, Baser ME, Kluwe L. Phenotypic variability in two families with novel splice-site and frameshift NF2 mutations. *Hum Genet* 1996;98:203–6.
33. Zucman-Rossi J, Legoix P, Der Sarkissian H, et al. NF2 gene in neurofibromatosis type 2 patients. *Hum Mol Genet* 1998; 7:2095–101.
34. Evans DG, Trueman L, Wallace A, et al. Genotype/phenotype correlations in type 2 neurofibromatosis (NF2): evidence for more severe disease associated with truncating mutations. *J Med Genet* 1998;35:450–5.
35. Antinheimo J, Sallinen SL, Sallinen P, et al. Genetic aberrations in sporadic and neurofibromatosis 2 (NF2)-associated schwannomas studied by comparative genomic hybridization (CGH). *Acta Neurochir (Wien)* 2000;142:1099–104.
36. Hung G, Faudoa R, Baser ME, et al. Neurofibromatosis 2 phenotypes and germ-line NF2 mutations determined by an RNA mismatch method and loss of heterozygosity analysis in NF2 schwannomas. *Cancer Genet Cytogenet* 2000;118:167–8.
37. Welling DB. Clinical manifestations of mutations in the neurofibromatosis type 2 gene in vestibular schwannomas (acoustic neuromas). *Laryngoscope* 1998;108:178–89.
38. Jacoby LB, MacCollin M, Barone R, et al. Frequency and distribution of NF2 mutations in schwannomas. *Genes Chromosomes Cancer* 1996;17:45–55.
39. Merel P, Hoang-Xuan K, Sanson M, et al. Predominant occurrence of somatic mutations of the NF2 gene in meningiomas and schwannomas. *Genes Chromosomes Cancer* 1995;13:1211–6.
40. Bianchi AB, Hara T, Ramesh V, et al. Mutations in transcript isoforms of the neurofibromatosis 2 gene in multiple human tumour types. *Nat Genet* 1994;6:185–92.
41. Ruttledge MH, Sarrazin J, Rangaratnam S, et al. Evidence for the complete inactivation of the NF2 gene in the majority of sporadic meningiomas. *Nat Genet* 1994;6:180–4.
42. Deguen B, Goutebroze L, Giovannini M, et al. Heterogeneity of mesothelioma cell lines as defined by altered genomic structure and expression of the NF2 gene. *Int J Cancer* 1998; 77:554–60.
43. Irving RM, Moffat DA, Hardy DG, et al. Somatic NF2 gene mutations in familial and non-familial vestibular schwannoma. *Hum Mol Genet* 1994;3:347–50.
44. Sainz J, Figueroa K, Baser ME, et al. High frequency of nonsense mutations in the NF2 gene caused by C to T transitions in five CGA codons. *Hum Genet* 1995;4:137–9.
45. Sainz J, Huynh DP, Figueroa K, et al. Mutations of the neurofibromatosis type 2 gene and lack of the gene product in vestibular schwannomas. *Hum Mol Genet* 1994;3:885–91.
46. Gutmann DH, Geist RT, Xu H, et al. Defects in neurofibromatosis 2 protein function can arise at multiple levels. *Hum Mol Genet* 1998;7:335–4.
47. Stokowski RP, Cox DR. Functional analysis of the neurofibromatosis type 2 protein by means of disease-causing point mutations. *Am J Hum Genet* 2000;66:873–91.
48. Gutmann DH, Hirbe AC, Haipek CA. Functional analysis of neurofibromatosis 2 (NF2) missense mutations. *Hum Mol Genet* 2001;10:1519–2.
49. Bruder DEG, Kirvela C, Tapia-Paez I, et al. High resolution deletion analysis of constitutional DNA from neurofibromatosis type 2 (NF2) patients using microarray-CGH. *Hum Mol Genet* 2001;10:271–82.
50. Bruder CE, Ichimura K, Blennow E, et al. Severe phenotype of neurofibromatosis type 2 in a patient with a 7.4-MB constitutional deletion on chromosome 22: possible localization of a neurofibromatosis type 2 modifier gene? *Genes Chromosomes Cancer* 1999;25:184–90.
51. Kino T, Takeshima H, Nakao M, et al. Identification of the cis-acting region in the NF2 gene promoter as a potential target for mutation and methylation-dependent silencing in schwannoma. *Genes Cells* 2001;6:441–54.
52. Chang LS, Akhmametyeva EM, Wu Y, et al. Multiple transcription initiation sites, alternative splicing, and differential polyadenylation contribute to the complexity of human neurofibromatosis 2 transcripts. *Genomics* 2002;79:63–76.
53. Hitotsumatsu T, Kitamoto T, Iwaki T, et al. An exon 8-spliced out transcript of neurofibromatosis 2 gene is constitutively expressed in various human tissues. *J Biochem* 1994;116: 1205–7.
54. Pykett MJ, Murphy M, Harnish PR, et al. The neurofibromatosis type 2 tumor suppressor gene encodes multiple alternatively spliced transcripts. *Hum Mol Genet* 1994;3: 559–64.
55. Giovannini M, Robanus-Maandag E, Niwa-Kawakita M, et al. Schwann cell hyperplasia and tumors in transgenic mice

expressing a naturally occurring mutant NF2 protein. *Genes Dev* 1999;13:978–86.
56. Welling DB, Akhmametyeva EM, Daniels RL, et al. Analysis of the human neurofibromatosis type 2 gene promoter and its expression. *Otolaryngol Head Neck Surg* 2000;123:413–8.
57. Chishti AH, Kim AC, Marfatia SM, et al. The FERM domain: a unique module involved in the linkage of cytoplasmic proteins to the membrane. *Trends Biochem Sci* 1998;23:281–2.
58. Bretscher A, Chambers D, Nguyen R, et al. ERM-Merlin and EBP50 protein families in plasma membrane organization and function. *Annu Rev Cell Dev Biol* 2000;16:113–43.
59. Turunen O, Wahlstrom T, Vaheri A. Ezrin has a COOH-terminal actin-binding site that is conserved in the ezrin protein family. *J Cell Biol* 1994;126:1445–53.
60. Roy C, Martin M, Mangeat P. A dual involvement of the amino-terminal domain of ezrin in F- and G-actin binding. *J Biol Chem* 1997;272:20088–95.
61. Gonzalez-Agosti C, Xu L, Pinney D, et al. The merlin tumor suppressor localizes preferentially in membrane ruffles. *Oncogene* 1996;13:1239–47.
62. Pelton PD, Sherman LS, Rizvi TA, et al. Ruffling membrane, stress fiber, cell spreading, and proliferation abnormalities in human schwannoma cells. *Oncogene* 1998;17:2195–209.
63. Deguen B, Merel P, Goutebroze L, et al. Impaired interaction of naturally occurring mutant NF2 protein with actin-based cytoskeleton and membrane. *Hum Mol Genet* 1998;7: 217–26.
64. Lutchman M, Rouleau GA. The neurofibromatosis type 2 gene product, schwannomin, suppresses growth of NIH 3T3 cells. *Cancer Res* 1995;55:2270–4.
65. Tikoo A, Varga M, Ramesh V, et al. An anti-Ras function of neurofibromatosis type 2 gene product (NF2/Merlin). *J Biol Chem* 1994;269:23387–90.
66. McClatchey AI, Saotome I, Mercer K, et al. Mice heterozygous for a mutation at the NF2 tumor suppressor locus develop a range of highly metastatic tumors. *Genes Dev* 1998; 12:1121–33.
67. McClatchey AI, Saotome I, Ramesh V, et al. The NF2 tumor suppressor gene product is essential for extraembryonic development immediately prior to gastrulation. *Genes Dev* 1997;11:1253–65.
68. Giovannini M, Robanus-Maandag E, van der Valk M, et al. Conditional biallelic *Nf2* mutation in the mouse promotes manifestations of human neurofibromatosis type 2. *Genes Dev* 2000;14:1617–30.
69. Shaw RJ, Paez JG, Curto M, et al. The NF2 tumor suppressor, merlin, functions in Rac-dependent signaling. *Dev Cell* 2001;1:63–72.
70. Fernandez-Valle C, Tang Y, Ricard J, et al. Paxillin binds schwannomin and regulates its density-dependent localization and effect on cell morphology. *Nat Genet* 2000;31:354–62.
71. Gronholm M, Vossebein L, Carlson CR, et al. Merlin links to the cAMP neuronal signaling pathway by anchoring the R1 beta subunit of protein kinase A. *J Biol Chem* 2003;278: 41167–72.
72. Kissil JL, Wilker EW, Johnson KC, et al. Merlin, the product of the NF2 tumor suppressor gene, is an inhibitor of the p21-activated kinase, PAK1. *Mol Cell* 2003;12:841–9.
73. Takeshima H, Izawa I, Lee PS, et al. Detection of cellular proteins that interact with the NF2 tumor suppressor gene product. *Oncogene* 1994;9:2135–44.
74. Sainio M, Zhao F, Heiska L, et al. Neurofibromatosis 2 tumor suppressor protein co-localizes with ezrin and CD44 and associates with actin-containing cytoskeleton. *J Cell Sci* 1997;110:2249–60.
75. Huang L, Ichimaru E, Pestonjamasp K, et al. Merlin differs from moesin in binding to F-actin and in its intra- and intermolecular interactions. *Biochim Biophys Res Commun* 1998;248:548–53.
76. Murthy A, Gonzalez-Agosti C, Cordero E, et al. NHE-RF, a regulatory cofactor for Na(+)-H+ exchange, is a common interactor for merlin and ERM (MERM) proteins. *J Biol Chem* 1998;273:1273–6.
77. Obremski VJ, Hall AM, Fernandez-Valle C. Merlin, the neurofibromatosis type 2 gene product, and β1 integrin associate in isolated and differentiating Schwann cells. *J Neurobiol* 1998;37:487–501.
78. Scoles DR, Huynh DP, Morcos PA, et al. Neurofibromatosis 2 tumor suppressor schwannomin interacts with βII-spectrin. *Nat Genet* 1998;18:354–9.
79. Scoles DR, Huynh DP, Chen MS, et al. The neurofibromatosis 2 tumor suppressor protein interacts with hepatocyte growth factor-regulated tyrosine kinase substrate. *Hum Mol Genet* 2000;9:1567–74.
80. Xu HM, Gutmann DH. Merlin differentially associates with the microtubule and actin cytoskeleton. *J Neurosci Res* 1998; 51:403–15.
81. Goutebroze L, Brault E, Muchardt C, et al. Cloning and characterization of SCHIP-1, a novel protein interacting specifically with spliced isoforms and naturally occurring mutant NF2 proteins. *Mol Cell Biol* 2000;20:1699–712.
82. Herrlich P, Morrison H, Sleeman J, et al. CD44 acts both as a growth and invasiveness-promoting molecule and as a tumor-suppressing cofactor. *Ann N Y Acad Sci* 2000;910: 106–18.
83. Sherman L, Sleeman J, Herrlich P, et al. Hyaluronate receptors: key players in growth, differentiation, migration, and tumor progression. *Curr Opin Cell Biol* 1994;6:726–33.
84. Morrison H, Sherman LS, Legg J, et al. The NF2 tumor suppressor gene product, merlin, mediates contact inhibition of growth through interactions with CD44. *Genes Dev* 2001; 15:968–80.
85. Xiao GH, Beeser A, Chernoff J, et al. P21-activated kinase links Rac/Cdc42 signaling to merlin. *J Biol Chem* 2002;277: 883–6.
86. Kissil JL, Johnson KC, Eckman MS, et al. Merlin phosphorylation by p21-activated kinase 2 and effects of phosphorylation on merlin localization. *J Biol Chem* 2002;277: 10394–9.
87. Bretscher A, Reczek D, Berryman M. Ezrin: a protein requiring conformational activation to link microfilaments to the plasma membrane in the assembly of cell surface structures. *J Cell Sci* 1997;110:3011–8.
88. Hirao M, Sato N, Kondo T, et al. Regulation mechanism of ERM (ezrin/radixin/moesin) protein/plasma membrane association: possible involvement of phosphatidylinositol turnover and Rho-dependent signaling pathway. *J Cell Biol* 1996;135: 37–51.
89. Gutmann DH, Sherman L, Seftor L, et al. Increased expression of the NF2 tumor suppressor gene product, merlin, impairs cell motility, adhesion and spreading. *Hum Mol Genet* 1999;8:267–75.
90. Gutmann DH, Haipek CA, Burke SP, et al. The *NF2* interactor, hepatocyte growth factor-regulated tyrosine kinase substrate (HRS), associates with merlin in the 'open' conformation and suppresses cell growth and motility. *Hum Mol Genet* 2001;10:825–34.
91. Pearson MA, Reczek D, Bretscher A, et al. Structure of the ERM protein moesin reveals the FERM domain fold masked by an extended actin binding tail domain. *Cell* 2000;101:259–70.
92. Komada M, Kitamura N. Growth factor-induced tyrosine phosphorylation of HRS, a novel 115- kilodalton protein with a structurally conserved putative zinc finger domain. *Mol Cell Biol* 1995;15:6213–21.
93. Niemczyk K, Vaneecloo FN, Lecomte MH, et al. Correlation between Ki-67 index and some clinical aspects of acoustic neuromas (vestibular schwannomas). *Otolaryngol Head Neck Surg* 2000;123:779–83.
94. Light JP, Roland JT Jr, Fishman A, et al. Atypical and low-grade malignant vestibular schwannomas: clinical implications of proliferative activity. *Otol Neurotol* 2001; 22:922–7.

95. Chen JM, Houle S, Ang LC, et al. A study of vestibular schwannomas using positron emission tomography and monoclonal antibody Ki-67. *Am J Otol* 1998;19:840–5.
96. Kesterson L, Shelton C, Dressler L, et al. Clinical behavior of acoustic tumors: a flow cytometric analysis. *Arch Otolaryngol Head Neck Surg* 1993;119:269–71.
97. Charabi S, Klinken L, Tos M, et al. Histopathology and growth pattern of cystic acoustic neuromas. *Laryngoscope* 1994;104:1348–52.
98. Antinheimo J, Haapasalo H, Seppala M, et al. Proliferative potential of sporadic and neurofibromatosis 2-associated schwannomas as studied by MIB-1 (Ki-67) and PCNA labeling. *J Neuropathol Exp Neurol* 1995;54:776–82.
99. Cardillo MR, Filipo R, Monini S, et al. Transforming growth factor-beta1 expression in human acoustic neuroma. *Am J Otol* 1999;20:65–8.
100. Evans DGR, Sainio M, Baser ME. Neurofibromatosis type 2. *J Med Genet* 2000;37:897–904.
101. Mautner VF, Lindenau M, Baser ME, et al. The neuroimaging and clinical spectrum of neurofibromatosis 2. *Neurosurgery* 1996;38:880–85.
102. Sainio M, Strachan T, Blomstedt G, et al. Presymptomatic DNA and MRI diagnosis of neurofibromatosis 2 with mild clinical course in an extended pedigree. *Neurology* 1995;45: 1314–22.
103. Lander ES, Lenton LM, Birren B, et al. Initial sequencing and analysis of the human genome. *Nature* 2001;409:860–921.
104. Lockhart DJ, Winzeler EA. Genomics, gene expression, and DNA arrays. *Nature* 2000;405:827–36.
105. DeRisi JL, Iyer VR, Brown PO. Exploring the metabolic and genetic control of gene expression on a genomic scale. *Science* 1997;278:680–6.
106. Zhang DH, Salto-Tellez M, Chiu LL, et al. Tissue microarray study for classification of breast tumors. *Life Sci* 2003;73: 3189–99.
107. Nishizuku S, Chen ST, Gwadry FG, et al. Diagnostic markers that distinguish colon and ovarian adenocarcinomas: identification, genomic, proteomic, and tissue array profiling. *Cancer Res* 2003;63:5243–50.
108. Alizadeh AA, Ross DT, Perou CM, et al. Towards a novel classification of human malignancies based on gene expression patterns. *J Pathol* 2001;195:41–52.
109. Jordan CT. Unique molecular and cellular features of acute myelogenous leukemia stem cells. *Leukemia* 2002;16: 559–62.
110. Klausner RD. Cancer, genomics, and the National Cancer Institute. *J Clin Invest* 1999;104:S15–7.
111. Lallemand D, Curto M, Saotome I, Giovannini M, McClatchey AI. NF2 deficiency promotes tumorigenesis and metastasis by destabilizing adherens junction. *Genes Dev* 2003;17:1090–1100.
112. Ryu CH, Kim SW, Lee KH, et al. The merlin tumor suppressor interacts with Ral guanine nucleotide dissociation stimulator and inhibits its activity. *Oncogene* 2005;24: 5355–64.
113. Manchanda N, Lyubimova A, Ho HY, et al. The NF2 tumor suppressor Merlin and ERM proteins interact with N–WASP and regulate its actin polymerization function. *J Biol Chem* 2005;280:12517–22.
114. Rangwala R, Banine F, Borg JP, Sherman LS. Erbin regulates mitogen–activated protein (MAP) kinase activation and MAP kinase–dependent interactions between Merlin and adherens junction protein complexes in Schwann cells. *J Biol Chem* 2005;280:11790–7.

Editorial Manager(tm) for The Laryngoscope
Manuscript Draft

Manuscript Number: LS3808R1

Title: Growth of Benign and Malignant Schwannoma Xenografts in SCID Mice

Article Type: Original Study

Section/Category: Otology

Keywords: Vestibular schwannoma, Neurofibromatosis type 2 (NF2), xenograft, severe combined immunodeficiency (SCID) mice, magnetic resonance imaging (MRI), cystic, malignant, gadolinium

Corresponding Author: Dr. Long-Sheng Chang, Ph.D.

Corresponding Author's Institution: The Ohio State University, and The Children's Research Institute, Columbus Children's Hospital

First Author: Long-Sheng Chang, PhD

Order of Authors: Long-Sheng Chang, PhD; Abraham Jacob, MD; Mark Lorenz, MD; Jonathan Rock, BS; Elena M Akhmametyeva, MD PhD; Georgeta Mihai, MS; Petra Schmalbrock, PhD; Abhik R Chaudhury, MD; Raul Lopez, BS; Jyoji Yamate, PhD; Markus R John, PhD; Hannes Wickert, PhD; Brian A Neff, MD; Edward Dodson, MD; D Bradley Welling, MD PhD

Manuscript Region of Origin:

View Letter

Close

Date: Oct 28, 2005
To: "Long-Sheng Chang" lchang@chi.osu.edu
From: "The Laryngoscope" lynchjj@upmc.edu
Subject: Your Submission

Ref.: Ms. No. LS2765R1
Cyclin D1 and D3 Expression in Vestibular Schwannomas
The Laryngoscope

Dear Dr. Chang,

I am pleased to tell you that your work has now been accepted for publication in The Laryngoscope.

Before we can continue the publishing process, we need you to submit a "Copyright Transfer Form." This can be found on our website at http://lscope.edmgr.com.

Thank you for submitting your work to this journal.

With kind regards

Jonas T. Johnson, M.D.
Editor
The Laryngoscope

Close

*** Response to Reviewers**

Dear Dr. Johnson,

We sincerely thank you for your consideration of our manuscript. We greatly appreciate the comments of reviewers and have revised our manuscript according your and reviewers' suggestions.

We wish to reply to the comments in order of yours and reviewer number.

Editor's Comments:

1. "Please make the paper more concise - reduce length by 20%" – We have made the paper as concise as we could and reduced the total number of pages from 24 to 19. Specifically we have greatly shortened the Abstract and Introduction. We also trimmed down the Materials and Methods and the Discussion. **The sections with major deletion are indicated in bold letters**.

2. "Please reduce the number of references" – We have trimmed the number of references from 44 to 21.

Reviewer #1:

We sincerely thank the reviewer's positive comment on our data presentation and writing. According to reviewer's comments, we provide the following responses.

1. "The abstract is not well structured or clear…" – We have reformatted to highlight the experimental technique and results. We also removed all unnecessary words and sentences.

2. "The background chapter should be shortened…" – We have substantially shortened the Introduction by removing the well-known data about VS and other distally related information.

3. "The figures legends are also too long-please reduce." – Accordingly, we have also reduced the figure legends by about one page (down from three pages to two).

Reviewer: 2

We also thank the reviewer's positive comment on our manuscript. We provide the following response to the reviewer's comment.

(1) "Very nice piece of basic science research, but too lengthy…" – As indicated above, we have substantially shortened our manuscript.

In summary, we have reduced the page number of our manuscript by more than 20% as suggested. We hope that this revision will be favorably considered for acceptance by the journal. Thank you very much for your time and consideration.

Sincerely,

Long-Sheng Chang, Ph.D.

cc. Abraham Jacob, Mark Lorenz, Jonathan Rock, Elena M. Akhmametyeva, Georgeta Mihai, Petra Schmalbrock, Abhik R. Chaudhury, Raul Lopez, Jyoji Yamate, Markus R. John, Hannes Wickert, Brian A. Neff, Edward Dodson, D. Bradley Welling.

Abstract

Objectives: Models for the development of new treatment options in vestibular schwannoma (VS) treatment are lacking. The purpose of this study is to establish a quantifiable human VS xenograft model in mice. ***Study Design and Methods:*** Both rat malignant schwannoma cells (KE-F11 and RT4) and human malignant schwannoma (HMS-97) cells were implanted near the sciatic nerve in the thigh of severe combined immunodeficiency (SCID) mice. Additionally, human benign VS specimens were implanted in another set of SCID mice. Three-dimensional tumor volumes were calculated from MRI images over the next six months. ***Results:*** Mice implanted with malignant schwannoma cells developed visible tumors within two weeks. Imaging using a 4.7-tesla MRI and immuno-histopathological examination identified solid tumors in all KE-F11 and HMS-97 xenografts while RT4 xenografts consistently developed cystic schwannomas. VS xenografts demonstrated variability in their growth rates similar to human VS. The majority of VS xenografts did not grow but persisted throughout the study, while two of 15 xenografts grew significantly. Histopathological examination and immunohistochemistry confirmed that VS xenografts retained their original microscopic and immunohistochemical characteristics after prolonged implantation. ***Conclusions:*** This study describes the first animal model for cystic schwannomas. Also, we demonstrate the use of high-field MRI to quantify VS xenograft growth over time. The VS xenografts represent a model complimentary to *Nf2* transgenic and knockout mice for translational VS research.

Growth of Benign and Malignant Schwannoma Xenografts in SCID Mice

Chang, Long-Sheng[1,2,3,5,6,*], Abraham Jacob[2], Mark Lorenz[5], Jonathan Rock[5], Elena M. Akhmametyeva[1,6], Georgeta Mihai[4], Petra Schmalbrock[4,5], Abhik R. Chaudhury[3,5], Raul Lopez[5], Jyoji Yamate[7], Markus R. John[8], Hannes Wickert[9], Brian A. Neff[2,♠], Edward Dodson[2,5], and D. Bradley Welling[2,5]

Departments of [1]Pediatrics, [2]Otolaryngology, [3]Pathology, and [4]Radiology, The Ohio State University [5]College of Medicine, Columbus, Ohio 43210, USA; [6]Center for Childhood Cancer, Children's Research Institute, Columbus, Ohio 43205, USA; [7]Laboratory of Veterinary Pathology, Osaka Prefecture University, Osaka, Japan; [8]Musculoskeletal Diseases Exploratory Clinical Development Unit, Novartis Pharma AG, WSJ-103.4.26, CH-4002 Basel, Switzerland; [9]Hygiene Institut, Abteilung Parasitologie, Universitätsklinikum Heidelberg, Im Neuenheimer Feld 324, 69120 Heidelberg, Germany

Running title: Schwannoma xenografts

Keywords: Vestibular schwannoma, Neurofibromatosis type 2 (NF2), xenograft, severe combined immunodeficiency (SCID) mice, magnetic resonance imaging (MRI), cystic, malignant, gadolinium

[*]Corresponding author: Dr. Long-Sheng Chang, Children's Hospital and Department of Pediatrics, The Ohio State University, 700 Children's Drive, Columbus, Ohio 43205; Phone: 614-355-2658; Fax: 614-722-5895; E-mail: lchang@chi.osu.edu

[♠]Current address: Department of Otolaryngology Head and Neck Surgery, The Mayo Clinic, Rochester, MN

Abstract

Objectives: **Models for the development of new treatment options in vestibular schwannoma (VS) treatment are lacking. The purpose of this study is to establish a quantifiable human VS xenograft model in mice.** ***Study Design and Methods:*** **Both rat malignant schwannoma cells (KE-F11 and RT4) and human malignant schwannoma (HMS-97)** cells were implanted near the sciatic nerve in the thigh of severe combined immunodeficiency (SCID) mice. **Additionally, human benign VS specimens were implanted in another set of SCID mice. Three-dimensional tumor volumes were calculated from MRI images over the next six months.** ***Results:*** **Mice implanted with malignant schwannoma cells** developed visible tumors within two weeks. Imaging using a 4.7-tesla MRI and immuno-histopathological examination identified solid tumors in all KE-F11 and HMS-97 xenografts while RT4 xenografts consistently developed cystic schwannomas. **VS xenografts demonstrated variability in their growth rates similar to human VS. The** majority of VS xenografts did not grow but persisted throughout the study, while two of 15 xenografts grew significantly. Histopathological examination and immunohistochemistry confirmed that VS xenografts retained their original microscopic and immunohistochemical characteristics after prolonged implantation. ***Conclusions:*** **This study describes the first animal model for cystic schwannomas. Also, we** demonstrate the use of high-field MRI to quantify VS xenograft growth over time. The VS xenografts represent a model complimentary to *Nf2* transgenic and knockout mice for translational VS research.

Background

Vestibular schwannomas (VS) have no known medical therapies available. However, significant morbidity including hearing loss and facial weakness remain major concerns. VS

can be divided into four general categories including unilateral sporadic VS, neurofibromatosis type 2 (NF2)-associated VS, cystic, and malignant schwannomas (1). Among VS, sporadic unilateral solid tumors are by far the most common, occurring in 10-13 persons per million per year. The development of bilateral VS is the hallmark of NF2, an autosomal dominant disease caused by mutations in the *Neurofibromatosis type 2 (NF2)* gene on chromosome 22q12 (2,3). Most of these solid tumors, either sporadic or NF2-associated, grow at a slow rate of about 1-2 mm per year (1). Cystic schwannomas are a particularly aggressive group of unilateral schwannomas. They invade the surrounding cranial nerves, splaying them throughout the tumor (4). Cystic tumors may grow rapidly and are typically more difficult to manage, often resulting in hearing loss and facial nerve paralysis upon their removal (5). In addition to NF2-associated tumors, mutations in the *NF2* gene have been detected in sporadic VS and cystic schwannomas (6). The most aggressive and rare variant is the malignant VS or triton tumor. These malignant tumors occur either sporadically or following radiation, and are uniformly fatal (7).

MRI distinguishes clearly among the various types of VS. Cystic regions within cystic schwannomas are signal intense on T2-weighted images, while non-cystic components of these tumors enhance on T1-weighted images with gadolinium (Gd) in a manner similar to those seen in sporadic and NF2-associated VS (1). These represent a unique tumor type clinically and histologically, and should not be confused with degenerative regions of larger tumors. The irregular appearance of some heterogeneous tumors on contrast enhanced T1-weighted images may be accounted for by hemosiderin deposits, which correlates with increasing tumor size (8) but these tumors do not contain fluid as demonstrated on T2 imaging. Although distinct clinically and by MRI, the underlying molecular differences among the three benign types of VS are not understood. Malignant schwannomas invade surrounding tissues locally and progress rapidly (7). Most appear solid and enhance on T1-

weighted images but lack the capsule of the more common benign VS. Additionally, the optimal treatment regimen for each subtype of VS is not known because of a lack of understanding of fundamental tumor biology and a lack of rigorous clinical outcome studies.

Several studies previously attempted to implant human VS tissues in immunodeficient mice. Lee et al. (9) implanted human schwannomas in nude mice and showed that the tumors grew most consistently when placed in the sciatic nerve region. Charabi et al. (10) and Stidham et al. (11) confirmed that VS tissues could be successfully implanted and maintained in a subcutaneous pocket of nude mice. Although these studies demonstrated macroscopic growth in some of the transplanted VS tissues, an effective means of assessing the survival, growth, and blood supply of tumor xenografts was lacking. In addition, no study to date has compared the growth potential of various types of schwannoma tissues in mice.

Herein, we evaluated the growth characteristics of rodent and human malignant schwannoma cells as well as benign human VS xenografts in severe combined immunodeficiency (SCID) mice using a 4.7-tesla MRI. Our results demonstrated the feasibility of using MRI to quantify VS xenografts in mice. Interestingly, MRI also distinguished two different schwannoma types, which were confirmed by **immuno- and** histopathological analysis.

Materials and Methods

Experimental Design. The Institutional Animal Care and Use Committee of The Ohio State University approved the animal protocols utilized in this study. **Healthy female SCID mice (Harlan Co. Indianapolis, IN) were housed according to approved procedures. The** first series of experiments involved injecting three groups of SCID mice subcutaneously in the thigh with rat malignant schwannoma cells KE-F11 (12) and RT4 (13) as well as

human malignant schwannoma HMS-97 cells (14). Tumor growth was observed over four weeks and measured using a 4.7-tesla small-animal MRI scanner (Bruker, Billerica, MA). After euthanizing the animals, specimens were harvested for histopathological analysis. A second set of experiments was performed using human VS specimens. SCID mice were implanted with VS tissues obtained directly from patients undergoing surgical resection. All VS implants were placed in the proximal thigh of the left leg near the sciatic nerve. Tumor growth, if any, was accessed serially by MRI over the subsequent months after xenotransplantation. Histopathological examination and immunohistochemical analysis were also performed on selected mice in order to confirm the imaged regions contain viable tumor rather than scar tissues.

Tissue Procurement. A Human Subject protocol for the acquisition and analysis of human vestibular schwannomas was approved **by our Institutional Reviewed Board. Patient consents were obtained prior to surgery. Each tumor specimen was confirmed by a pathologist as schwannoma.** For implantation of human VS tissues into SCID mice, freshly removed specimen was placed in a sterile tube containing Dulbecco's modified minimum essential (DME) medium (Invitrogen, Carlsbad, CA) and transported immediately to the animal research facility. Also, a portion of tumor was snap-frozen in liquid nitrogen for future molecular studies.

Growth of Schwannoma Cells. **Rat malignant schwannoma KE-F11 and RT4 cells, and human malignant schwannoma HMS-97 cells** were grown in DME medium supplemented with 10% fetal bovine serum (Invitrogen, Carlsbad, CA). For inoculation of rat KE-F11 or RT4 cells into each SCID mouse, 2.5 X 10^5 cells were washed with phosphate-buffered saline and suspended in 0.2 ml of Matrigel® (BD Biosciences, San Jose, CA). For inoculation of human HMS-97 cells into each SCID mouse, 5 X 10^5 cells were used.

Injection Technique. SCID mice were anesthetized by intraperitoneal injection of

Avertin® (2,2,2-tribromoethanol + tert-amyl alcohol; Sigma-Aldrich, St. Louis, MO) or by isofluorane inhalation. Under anesthesia, the left flank of mouse was shaved and prepped using aseptic technique. An 18-gauge needle was used to inject 0.2 ml of schwannoma cells 3 mm inferior to the greater trochanter of femur. The thigh was selected for ease of implantation and the ability to grossly observe tumor growth. Additionally, previous studies indicated that proximity to a peripheral nerve **might affect growth** (9-11). Injected mice were revived on a warming blanket until recovery and were watched daily for tumor growth.

Surgical Implantation Technique. **An incision was made along the long axis of the proximal thigh. The contralateral leg was not dissected and used as a control for imaging. Soft tissues were dissected bluntly in order to identify the biceps femoris muscle and the sciatic nerve. A piece of VS tumor specimen (1 ~ 5 mm in diameter) was implanted en bloc near the nerve and the skin was closed using a single layer of interrupted suture.**

MRI. Mice were anesthetized with Avertin®, immobilized on an animal holder, and placed prone in a 4.7 Tesla/cm MRI system with a 120-mm inner diameter gradient coil (max. 400 mT/m), a 72-mm inner diameter proton volume RF coil for transmit, and a 4-cm surface receive coil. For T1-weighted axial and coronal images, a spin echo sequence with TR of 550-600 ms and TE of 10.5 ms was used. For T2-weighted images, a Rapid Acquisition with Refocusing Echoes (RARE) sequence with TR of 2500-2600 ms, an effective TE of 47-54 ms, and a RARE-factor of 4 was employed. In-plane resolution was 156 μm on the axial and 195 μm on the coronal images, and the slice thickness was 0.8 mm with a 0.2-mm gap between slices. Scan time was 5-6 minutes per scan.

In addition, contrast enhanced T1 axial and coronal images were acquired after a bolus injection with Gadodiamine (Omniscan™, GE Healthcare, Piscataway, NJ; 0.1 ml bolus of 10 mM). The contrast agent was injected through a tail vein catheter using a thin polyethylene

tubing that reached outside the magnet and allowed quick delivery of the contrast agent without changing the position of the mouse inside the magnet. Mice with rat schwannoma cell implants were imaged within 2 weeks of implantation and those with human schwannoma cell implants were imaged about 4 week after inoculation. Mice with human VS implants were imaged at indicated times over the course of a year post-procedure.

Multi-planar tumor volumes were determined from T1- and T2-weighted images. For these measurements, tumor areas were manually traced on axial and coronal T1 and T2 images. Post contrast images were also used when available. Tumor volumes were calculated by adding the traced areas from all slices depicting the tumor and multiplying with the distance between slice (i.e., 0.8-mm slice thickness + 0.2-mm gap = 1 mm). Tumor volumes measured from axial and coronal or T1 and T2 images were in fair agreement. All volume measurements were referenced to the first MR images taken one month after implantation.

Immuno-histopathological analysis. Tumors grown in mice with schwannoma xenografts were dissected, fixed in 10% buffered formalin, and embedded in paraffin. Five-micron tissue sections **were mounted, deparaffinized** and processed for standard hematoxylin-eosin staining or immunostaining with antibodies against S100 protein (1:200 dilution of anti-S100 from Dako, Carpinteria, CA), myelin basic protein (MBP) (prediluted anti-MBP from Zymed, San Francisco, CA), and NGF-receptor ($p75^{NGFR}$)/neurotrophin receptor (1:100 dilution of anti- $p75^{NGFR}$ from LabVision/NeoMarker, Fremont, CA) according to previously described procedures **(6). A hematoxylin counterstain was then applied and the stained tissue visualized by light microscopy.** Negative controls were treated with the same immunostaining procedure except without the primary antibody.

Results

KE-F11 and HMS-97 schwannoma xenografts developed solid tumor phenotypes while

RT4 xenografts produced cystic tumors. SCID mice injected with either the KE-F11 or RT4 rat malignant schwannoma cells produced visible tumors within one week after inoculation. On the MRI obtained within 2 weeks of xenotransplantation, the two sets of mice demonstrated significantly different imaging characteristics. All mice implanted with KE-F11 cells developed solid tumors, and the presence of tumor created significant asymmetry in the implanted thigh (Figure 1A). Coronal and axial T2-weighted RARE images showed that the tumor mass appeared homogenous but was hyperintense or brighter to the surrounding musculature. On T1-weighted images, the tumor-containing region was near isointense to muscle and enhanced on post-contrast T1 images (arrows) as is characteristics of human VS tissues *in situ*. In contrast, all mice injected with RT4 cells demonstrated a distinctive cystic phenotype (Figure 1B). Within the tumor mass, blood filled cavities appeared darkest on both T1- and T2-weighted images while the cysts displayed high signal intensity on T2 images but were dark on T1 images. Similar to the KE-F11 xenografts, MR images revealed that all mice with human malignant schwannoma HMS-97 implants developed large, homogenous, solid tumors by four weeks post implantation as seen on coronal and axial T1- and T2-weighted images (Figure 1C). There were no cystic changes.

To confirm that the xenografts retained their schwannoma phenotype, histopathological examination was performed on tumor-bearing mice. No metastatic lesions were found. Macroscopic and microscopic analysis confirmed the solid phenotype for both the KE-F11 and HMS-97 tumors and the cystic phenotype for the RT4 xenografts (Figure 2). The KE-F11 cell line was derived from a spontaneous malignant schwannoma found in an aged male F344 rat (12). The KE-F11 xenograft was a grayish, creamy globoid mass, which histologically consisted of actively growing, heterochromatic, oval- or spindle-shaped cells with large pleomorphic nuclei (Figure 2A). RT4 is a clonal schwannoma cell line derived from a peripheral nervous system tumor induced by ethylnitrosourea injection in a newborn

BDIX rat (13). The xenograft generated by RT4 cells contained multiple cysts; some of the cysts contained dark, viscous blood products, while others were filled with serous fluid. Histologically, the RT-4 tumor contained compact spindle cells with a high nucleus to cytoplasm ratio and had increased perivascular cellularity (Figure 2B). The HMS-97 cell line was established from a malignant schwannoma from an adult patient with oncogenic osteomalacia (14). Similar to KE-F11, the HMS-97 tumor was a large globoid mass comprised of heterochromatic ovoid cells with multiple mitotic figures (Figure 2C). The HMS-97 xenograft was transplantable. When a small piece of the tumor was transplanted to another SCID mouse, tumor growth was readily seen within two weeks (data not shown).

Because Schwann cells originate from the neuroectodermal neural crest, Schwann cell-derived tumors often show immunoreactions to S-100 protein, MBP, and $p75^{NGFR}$ (15-18). Immunostaining with an anti-S100 antibody showed that tumor cells from the HMS-97 xenograft strongly and diffusely expressed S-100 protein (Figure 3A). Similarly, HMS-97 tumor cells also stained robustly for MBP expression (Figure 3B). The staining for $p75^{NGFR}$ expression was weak but detectable (Figure 3C).

Collectively, these results are consistent with previous reports that malignant schwannomas are transplantable and their Schwann cell characteristics were maintained after xenotransplantation (12-13). Our study further demonstrates the feasibility of using MRI to detect the phenotype and growth characteristics of schwannomas in SCID mice. The KE-F11 and HMS-97 xenografts engender malignant solid schwannomas while the RT4 cells produce distinct cystic tumors.

Human VS xenografts persisted for a long period of time and some showed growth in SCID mice. **To evaluate potential growth characteristics of human VS, freshly removed tumors were implanted in the thigh of SCID mice.** High-field MRI was used to visualize

and quantify all VS xenografts in mice as described above. Analysis of images obtained from each animal at various times after xenotransplantation revealed that the majority of VS xenografts persisted but did not show significant growth (Figure 4). Most tumor volumes were either unchanged or reduced over the study period. The tumor with the most reduction diminished to about half its original tumor volume over six months. It is important to note that even without growth the xenograft was detectable by MRI scans (Figure 4A). We were able to maintain one VS xenograft for 13 months until the animal was sacrificed for histopathological examination (see below). We also detected an increase in tumor volume in two of 15 VS xenografts over six months (Figure 4B and 4C). One showed a 60% increase in tumor volume while the other grew to 14 times its original volume.

Representative MR images from the mouse with the VS xenograft whose tumor volume diminished by about half over six months are shown in Figure 4A. Although the tumor was small and its size decreased over the study period, a persistent mass could be found at the surgical implant site (arrows) in all images obtained. Since this tumor was surrounded by fatty tissue, both T1 and T2-weighted images depicted the tumor. The post-contrast study at month six showed only weak marginal enhancement (Figure 4A, right column).

When similar MRI sequences were performed on the VS xenograft showing significant growth, changes in tumor growth could be easily seen from both the T1- and T2-weighted images (Figure 4B). Visual comparison of the images obtained at one and two months post implantation revealed that the xenograft became larger. By six months, the tumor grew so much that it created an obvious asymmetry in the left implanted thigh. T1-weighted, post-contrast images most clearly outlined the tumor and its growth into the adjacent muscle tissue. Together with the T2 scan, these images confirmed the growth of the VS xenograft.

Histopathological analysis was performed on the mouse with significant tumor growth in order to confirm that the mass seen on the MRI was in fact schwannoma tissue by phenotype.

Gross examination revealed a large globoid mass in the implanted thigh with no sign of metastasis. Histologically, the tumor was encapsulated and consisted of spindle-shaped cells. Alternating compact areas of elongated cells with occasional nuclear palisading (Antoni A pattern) and less cellular, loosely textured Antoni B areas were seen (Figure 5A). The tumor cells had relatively abundant cytoplasm with discernible cell margins. All of these characteristics were consistent with a primary benign human VS. **We also detected strong** immunoreactivity to S100, $p75^{NGFR}$, and MBP antigens in the area containing tumor cells (Figure 6A, B, and C).

Similarly, we performed a histopathological examination on the mouse with a VS implant present but without any growth for 13 months. The xenograft tissue could still be detected by MRI (data not shown) and macroscopic analysis confirmed the presence of a small tumor within the implanted region. Microscopically, the tumor was composed of both ovoid and spindle-shaped cells with foci of lipid laden tumor cells, characteristic of an aged vestibular schwannoma (Figure 5B). Similar to those detected in the VS tumor showing significant growth, strong immuno-reactivity to S100 and $p75^{NGFR}$ proteins were found in the area containing the tumor cells (Figures 6D and E)

Taken together, these results show that VS xenografts can persist or grow in SCID mice and are readily detectable and quantified by MRI. The tumors retained their original microscopic and immunohistochemical characteristics after prolonged implantation.

Discussion

Meaningful translational research in chemotherapy requires disease-specific, reproducible, quantifiable, and cost-effective animal models. Mice have been an attractive species for such models because they can be bred to have little genetic variability and are accessible to genetic manipulation. Over the past decade, most of the *in vivo* research with

schwannomas has focused on *Nf2* transgenic and knockout mice (16,17). While soft tissue, peripheral nerve, and CNS schwannomas have developed in these animals, no mouse to date has engendered a primary schwannoma on its 8th cranial nerve. Additionally, the conditional *Nf2* mutant mice with schwannomas were found at low frequency only in older mice. Both benign and malignant schwannomas have been found in these mice. This is in contrast to the clearly benign phenotype of VS frequently seen in patients with NF2. Although the reason for these differences is not known, basic schwannoma histology and perhaps, inter-species differences in normal vestibulocochlear nerve microanatomy may be considered. It should be mentioned that human vestibular bipolar ganglion cells are devoid of myelin sheaths while these cells in rodents are myelinated (16,17,19). Recently, Stemmer-Rachamimov et al. (20) thoroughly reviewed human and murine schwannomas in order to create a grading system for these tumors. The WHO describes benign human VS as composed of encapsulated, noninfiltrative tumors composed of mature Schwann cells in Antoni A and Antoni B patterns with Verocay bodies, which are rows of palisading Schwann cell nuclei separated from each other by stroma. The benign schwannomas seen in the *Nf2*-knockout mice were classified as murine genetic engineered mouse I or GEM I tumors since they were most closely related to human VS. Although these benign mouse schwannomas displayed primarily an Antoni A growth pattern with occasional Verocay bodies, they were not encapsulated and were far more infiltrative than human VS. The murine GEM II tumors, which refer to more malignant murine schwannomas, displayed nuclear pleomorphism, increased cellularity, and scattered mitotic figures. These histological differences between human and mouse schwannomas may make it difficult to directly translate research conclusions drawn from these models to the human disease. For this reason, an alternative model such as the reproducible, quantifiable VS xenograft model that we reported here will be important for translational VS research.

We have demonstrated the utility of MRI in assessing and quantifying schwannoma

xenografts in SCID mice. The technique offers investigators the ability to assess an individual xenograft over time without requiring serial surgery or animal sacrifice. We showed that MRI reliably visualized both human and rat malignant schwannoma xenografts and distinguished between the solid and cystic tumor phenotypes. **Immuno- and histopathological analyses confirmed the MRI findings. The RT4 xenograft is the first description of an animal model for cystic schwannomas in the literature. Human** cystic tumors are clinically aggressive, may grow rapidly, and have poorer outcomes. The unique RT4 xenograft may allow the investigation of the basic science behind cystic schwannomas.

MRI of human VS xenografts revealed that while most VS implants diminished slightly and two grew significantly over time, all of the tumors persisted and could be readily imaged. It is important to note that patients with VS *in situ* demonstrate a similar pattern of disease. Most individuals' tumors persist or grow slowly over time, approximately 5% diminish in size when imaged serially, and about 10% grow rapidly (1). Interestingly, the non-growing human VS xenografts persisted in SCID mice for 6 to 13 months. We were able to use the high-field MRI to monitor a xenograft for 13 **months. Histologically, the persistent xenograft** retained characteristics of an aged vestibular schwannoma. In most of the animals imaged over a six-month period, the variance in tumor volumes was limited. Defining the variance more precisely would require a larger cohort of animals imaged over a one-year time **period. Once established**, deviations from the expected variance could be used for evaluating growth-inhibiting effects of potential chemotherapeutic interventions.

The gold standard for evaluating human VS *in situ* is T1-weighted MRI with gadolinium enhancement (1). This technique provides sharp contrast between the tumor and surrounding fluid spaces and neural structures. Our MRI analysis of VS xenografts also suggests that T1 post-contrast images best delineate the tumor margins, and contrast can be adequately delivered to the mouse using tail vein catheter injections. However, this technique is not

without risk to the animal. The volume of gadolinium along with the flush of saline that follows can fluid-overload the animal and increase its mortality risk. We have found that T2-weighted RARE images may adequately delineate the xenografts margins and allow for volumetric measurements. Thus, the injection of contrast agent is used in those tumors that are difficult to differentiate from adjacent thigh musculature.

Most human VS tumors are slow growing, while only a few proliferate rapidly (1). Tumor genetics may play a role in the growth potential of these benign tumors. Mutations in the *NF2* gene have been detected in NF2-associated VS, sporadic VS, and cystic schwannomas (6). Several attempts have been made to correlate clinical expression and specific *NF2* mutations in VS and other NF2-associated tumors. Initially, mutations that cause truncation of the *NF2* protein were reported to cause a more severe phenotype, while missense mutations or small in-frame insertions correlated with a mild phenotype. However, there have been reports of severe phenotypes associated with missense mutations in the *NF2* gene, and likewise, large deletions have been reported to give rise to mild phenotypes. In addition, phenotypic variability within NF2 families carrying the same germline mutation has been reported. Given this heterogeneity of clinical response to various mutations, it remains vital to identify key regulatory factors involved in the growth of various types of schwannomas.

Research to better understand VS tumorigenesis has been hampered by the lack of a spontaneous VS cell line available for *in vitro* study. VS cells are difficult to culture and have a very limited life-span *in vitro*. A previous attempt to immortalize VS cells using the human papilloma virus E6-E7 oncogenes yielded the HEI193 cell line with altered growth properties such as morphological changes and independence of Schwann cell growth factors (21). The fact that some VS xenografts grow in SCID mice and may be transplantable suggests that they may be used as a means to enhance the growth potential of VS cells in culture. By transplanting the growing VS tissue repeatedly through mice, VS cells with

enhanced growth capability may be isolated and used to establish a **VS cell line.**

In summary, this study established a quantifiable human VS xenograft model in SCID mice that utilizes MRI to measure tumor volumes. VS xenografts demonstrate biologic variability in their growth potential, but while individual grafts may grow, persist, or regress over time, MRI successfully quantifies these tumors non-invasively. VS xenografts represent a model complimentary to *Nf2* transgenic and knockout mice for translational research and improved drug screening

Acknowledgements

We sincerely thank Dan Scoles for the RT4 cell line, Peter Wassenaar and Abdulkerim Eroglu for technical assistance, and Sarah S. Burns for critical reading of the manuscript. This study was supported by grants from the U.S. Department of Defense NF Research Program and National Institute of Deafness and Communication Disorders. Mark Lorenz was a recipient of the Young Investigator Award from the Children's Tumor Foundation.

References

1. Neff BA, Welling DB, Akhmametyeva E, Chang L-S. The Molecular Biology of Vestibular Schwannomas: Dissecting the Pathogenic Process at the Molecular Level. Otol Neurotol 2006;27:197-208.
2. **Rouleau GA, Merel P, Lutchman M, et al. Alteration in a new gene encoding a putative membrane-organising protein causes neurofibromatosis type 2. Nature 1993;363:515-21.**
3. **Trofatter JA, MacCollin MM, Rutter JL, et al. A novel Moesin-, Exrin-, Radixin-like gene is a candidate for the neurofibromatosis 2 tumor-suppressor. Cell 1993;72:791-800.**

4. **Charabi S, Klinken L, Tos M, Thomsen J. Histopathology and growth pattern of cystic acoustic neuromas. Laryngoscope 1994;104:1348-52.**
5. **Fundova P, Charabi S, Tos M, Thomsen J. Cystic vestibular schwannoma: surgical outcome. J Laryngol Otol 2000;114:935-9.**
6. **Welling DB, Lasak JM, Akhmametyeva EM, Chang L-S. cDNA microarray analysis of vestibular schwannomas. Otol Neurotol 2002;23:736-48.**
7. **Shin M, Ueki K, Kurita H, Kirino T. Malignant transformation of a vestibular schwannoma after gamma knife radiosurgery. Lancet 2002;360:309-10.**
8. **Niemczyk K, Vaneecloo FN, Lecomte MH, et al. Correlation between Ki-67 index and some clinical aspects of acoustic neuromas (vestibular schwannomas). Otolaryngol Head Neck Surg 2000;123:779-83.**
9. **Lee JK, Sobel RA, Chiocca EA, Kim TS, Martuza RL. Growth of human acoustic neuromas, neurofibromas and schwannomas in the subrenal capsule and sciatic nerve of the nude mouse. J Neurooncol 1992;14:101-12.**
10. **Charabi S, Rygaard J, Klinken L, Tos M, Thomsen J. Subcutaneous growth of human acoustic schwannomas in athymic nude mice. Acta Otolaryngol 1994;114:399-405.**
11. **Stidham KR, Roberson JB Jr. Human vestibular schwannoma growth in the nude mouse: evaluation of a modified subcutaneous implantation model. Am J Otol 1997;18:622-6.**
12. **Yamate J, Yasui H, Benn SJ, et al. Characterization of newly established tumor lines from a spontaneous malignant schwannoma in F344 rats: nerve growth factor production, growth inhibition by transforming growth factor-β1, and macrophage-like phenotype expression. Acta Neuropathol (Berlin) 2003;106:221-33.**
13. **Imada M, Sueoka N. Clonal sublines of rat neurotumor RT4 and cell differentiation.**

I. Isolation and characterization of cell lines and cell type conversion. Dev Biol 1978;66:97-108.

14. **John MR, Wickert H, Zaar K, et al. A case of neuroendocrine oncogenic osteomalacia associated with a PHEX and fibroblast growth factor-23 expressing sinusidal malignant schwannoma. Bone 2001;29:393-402.**
15. **Charabi S, Simonsen K, Charabi B, Jacobsen GK, Moos T, Rygaard J, Tos M, Thomsen J. Nerve growth factor receptor expression in heterotransplanted vestibular schwannoma in athymic nude mice. Acta Otolaryngol 1996;116:59-63.**
16. **Giovannini M, Robanus-Maandag E, Niwa-Kawakita M, et al. Schwann cell hyperplasia and tumors in transgenic mice expressing a naturally occurring mutant NF2 protein. Genes Dev 1999;13:978-86.**
17. **Giovannini M, Robanus-Maandag E, van der Valk M, et al. Conditional biallelic Nf2 mutation in the mouse promotes manifestations of human neurofibromatosis type 2. Genes Dev 2000;14:1617-30.**
18. **Hung G, Colton J, Fisher L, et al. Immunohistochemistry study of human vestibular nerve schwannoma differentiation. Glia 2002;38:363-70.**
19. **Ona A. The mammalian vestibular ganglion cells and the myelin sheath surrounding them. Acta Otolaryngol Suppl 1993;503:143-9.**
20. **Stemmer-Rachamimov AO, Louis DN, Nielsen GP, et al. Comparative pathology of nerve sheath tumors in mouse models and humans. Cancer Res. 2004;64:3718-24.**
21. **Hung G, Li X, Faudoa R, et al. Establishment and characterization of a schwannoma cell line from a patient with neurofibromatosis 2. Int J Oncol 2002 ;20:475-82.**

Figure Legends

Figure 1. MRI scans of malignant schwannoma xenografts. (A) Coronal (top) and axial (bottom) images of a rat KE-F11 schwannoma xenograft two weeks after implantation display the presence of solid tumor mass in the left thigh (arrow). The T2-weighted RARE images (left) and T1-weighted images without (middle) and with contrast agent (right) were obtained according to Methods. The tumor is seen hyperintense to muscle on T2 and isointense on T1 images, and enhances following the injection of contrast agent **(arrows). (B)** Coronal (top) and axial (bottom) images of a rat RT4 schwannoma xenograft two weeks after implantation show the presence of a cystic tumor. Blood appeared hypointense in signal intensity on both T1 and T2 images while the cyst was hyperintense on T2 images (left) and dark on T1 images (right). (C) MR images of a human HMS-97 schwannoma xenograft four weeks after implantation demonstrating a large tumor with solid architecture.

Figure 2. Histological analysis of malignant schwannoma xenografts. Malignant appearing cells with plump, pleomorphic nuclei and densely stained chromatin were present in both the KE-F11 (A) and RT4 (B) tumors. Numerous vascular channels in the RT4 tumor suggest significant tumor angiogenesis. Similarly, malignant appearing cells with multiple mitotic figures and a high nucleus to cytoplasm ratio were seen in the HMS-97 tumor (C).

Figure 3. Immunohistochemical analysis of the HMS-97 xenograft demonstrating continued Schwann cell lineage of tumor cells. Tissue sections containing tumor cells were **immunostained with anti-S100 (A), anti-MBP (B) and anti-p75^{NGFR} (C) antibodies. The positively stained tissue appeared** brown. All negative controls did not stain (not shown).

Figure 4. Quantification of human VS xenografts by MRI. (A) T2-weighted (left), pre- (middle) and post-contrast T1-weighted images (right) of a VS xenograft showed that the tumor persisted in the SCID mouse over the six-month study period. The first coronal and axial MRI scans were performed one month after surgery to ensure that the animals had

healed. Follow-up MR images were obtained at the two- and six-month time points. Note that the tumor is readily visible in a fatty tissue pocket between the thigh musculature on both T1 and T2 images (arrows). T1 post-contrast images obtained at six months show some enhancement at the tumor margins (arrowhead). (B) T2-weighted (left), pre- (middle) and post-contrast T1-weighted images (right) of a VS xenograft demonstrating significant growth over a six-month period. Note that the tumor (arrow) appears larger on the two-month images. T2-weighted imaging at six months showed that the tumor extended into the surrounding muscles. **Post-contrast T1-weighted images verified the presence of tumor within the thigh musculature. (C) Volumetric measurement of 15 VS xenografts over a six-month period. Note** that most tumors remained stable or regressed slightly, while two xenografts demonstrated significant growth.

Figure 5. Histological analysis of the human VS xenografts in SCID mice. (A) **A tissue section of a VS xenograft harvested six months after implantation demonstrated significant tumor growth. The** encapsulated tumor mass consisting of spindle cells with no significant atypia and palisading nuclei in Antoni A and Antoni B configurations, all of which are histological characteristics of benign human VS. (B) A tissue section of a VS xenograft 13 months post implantation confirmed the presence of tumor cells within the mass seen on MRI. Note the cells with bland-appearing homogeneous nuclei and some foci of lipid laden tumor cells in the specimen, characteristic of an aged schwannoma.

Figure 6. Immunostained human VS xenograft tissue sections. Tissue sections from the VS xenograft showing significant growth over a six-month period were stained with antibodies to S100 (A), MBP (B) and $p75^{NGFR}$ (C). Similarly, sections from a VS xenograft that did not grow but persisted in the mouse for six months were stained with anti-S100 (D) and anti- $p75^{NGFR}$ (E) antibodies. These VS xenografts retained positive immunoreactivity to these Schwann cell markers, while the adjacent non-tumor cells showed no staining.

Figure 1a

Click here to download high resolution image

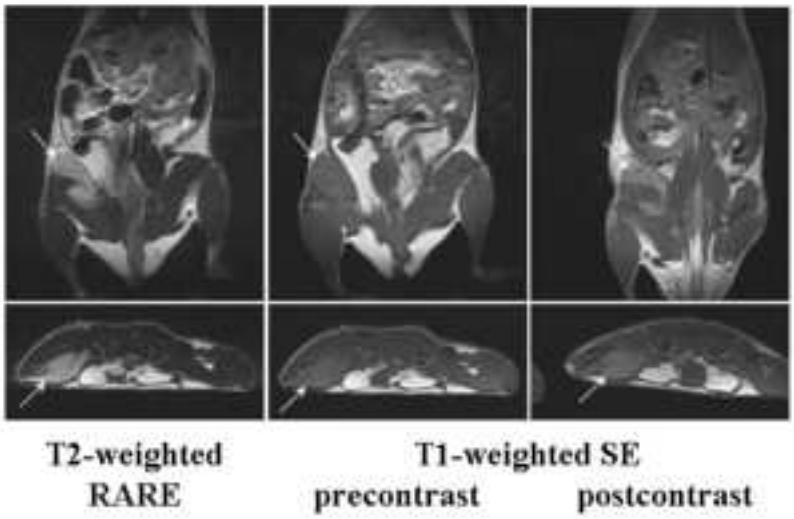

Figure 1A

Figure 1b

Click here to download high resolution image

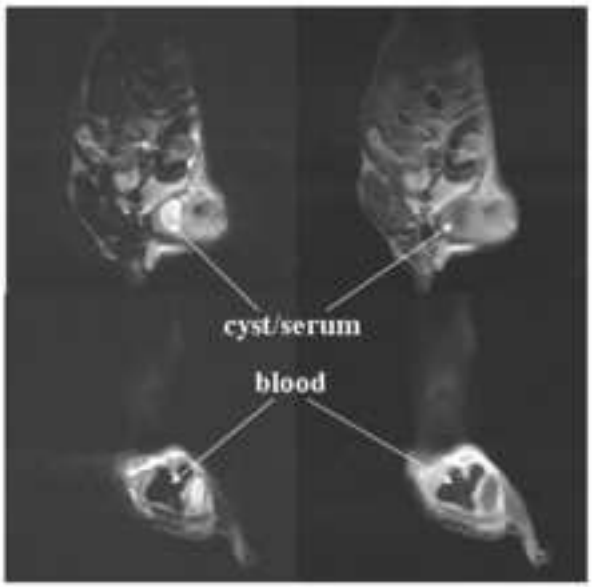

Figure 1B

Figure 1c

Click here to download high resolution image

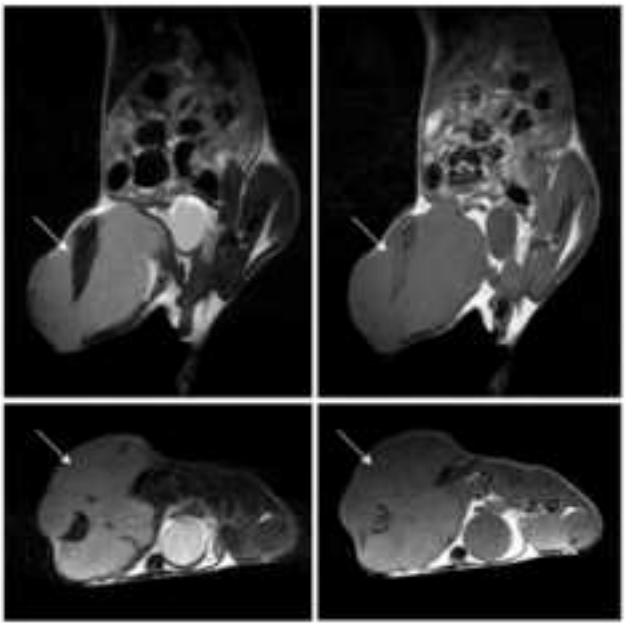

T2-weighted RARE T1-weighted SE

Figure 1C

Figure 2a/b

Click here to download high resolution image

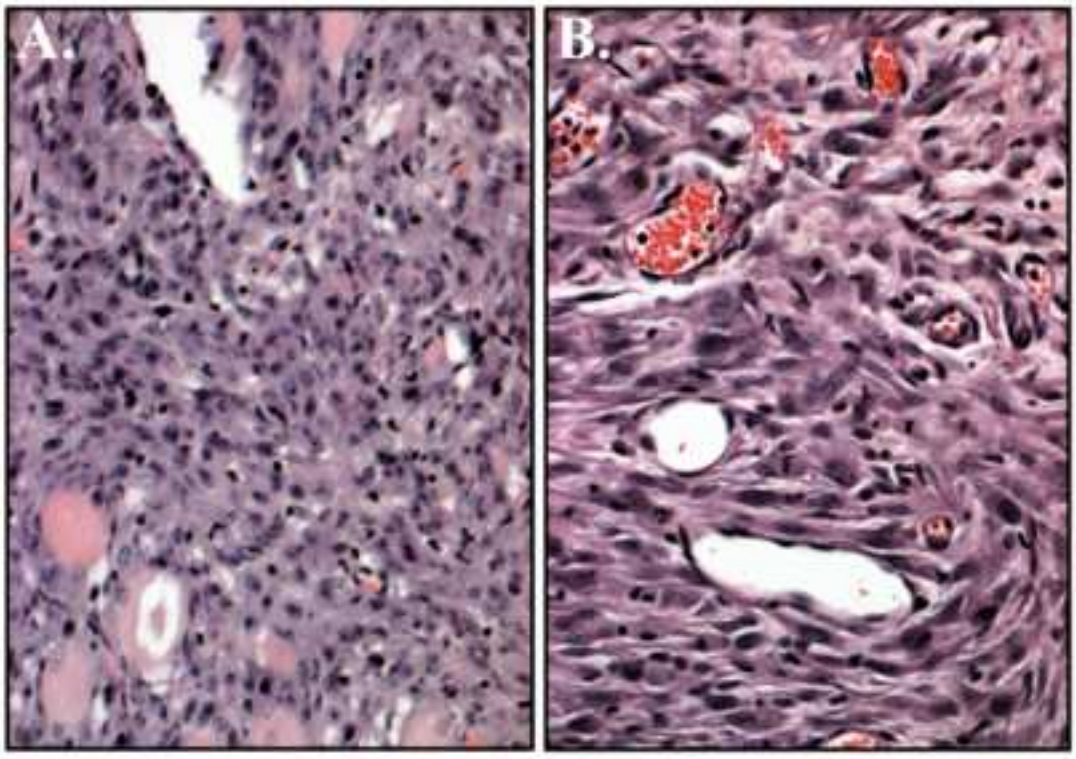

Figure 2AB

Figure 2c

Click here to download high resolution image

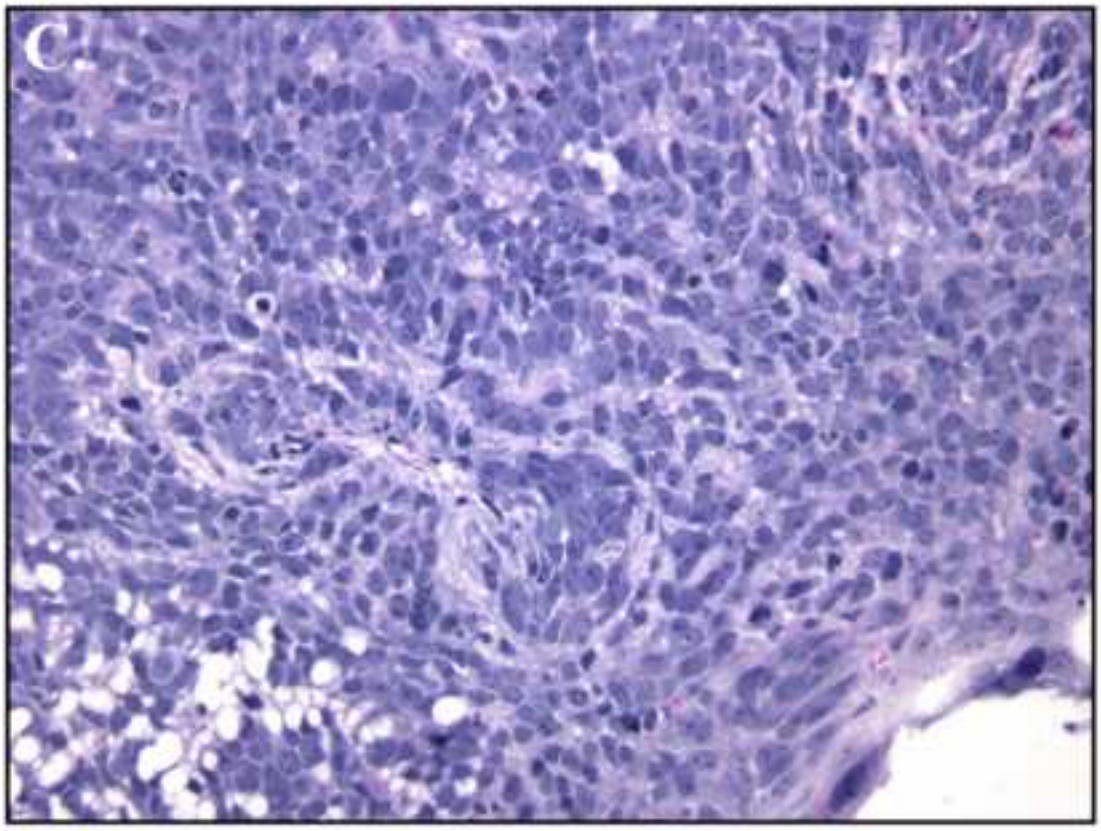

Figure 2C

Figure 3a

Click here to download high resolution image

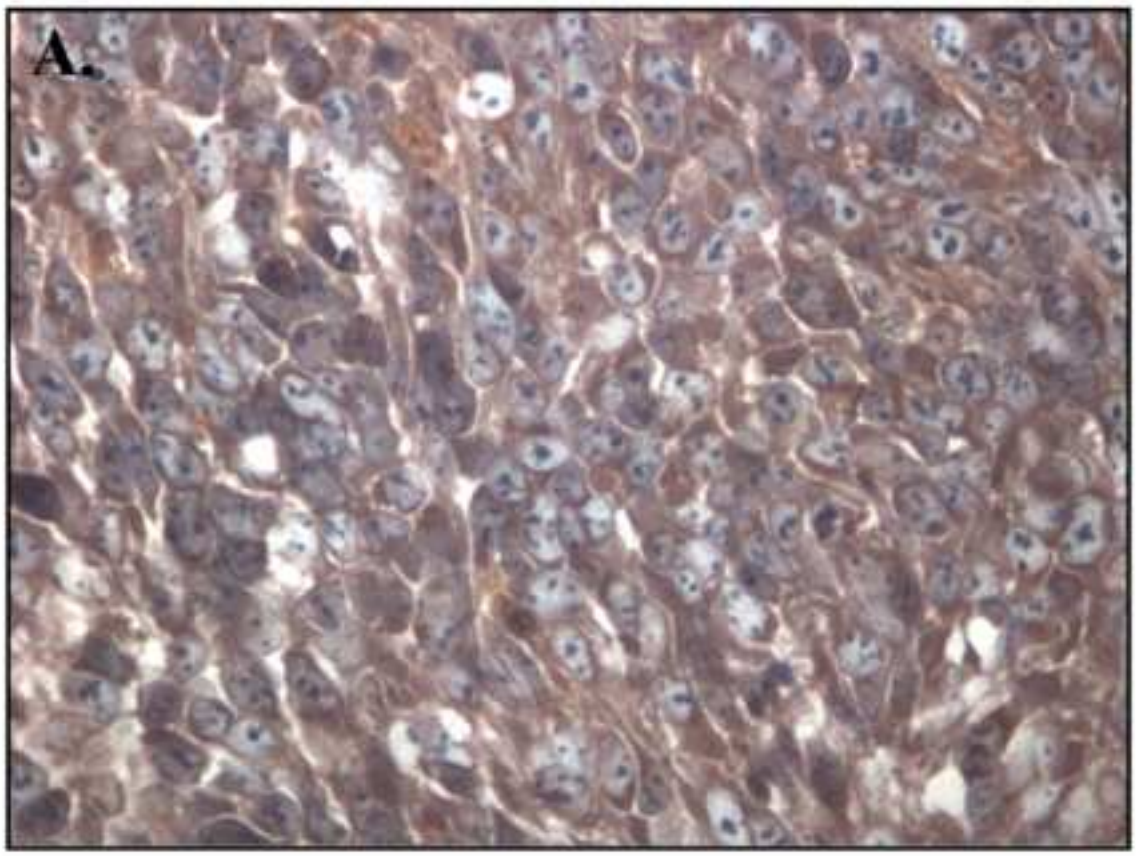

Figure 3A

Figure 3b

Click here to download high resolution image

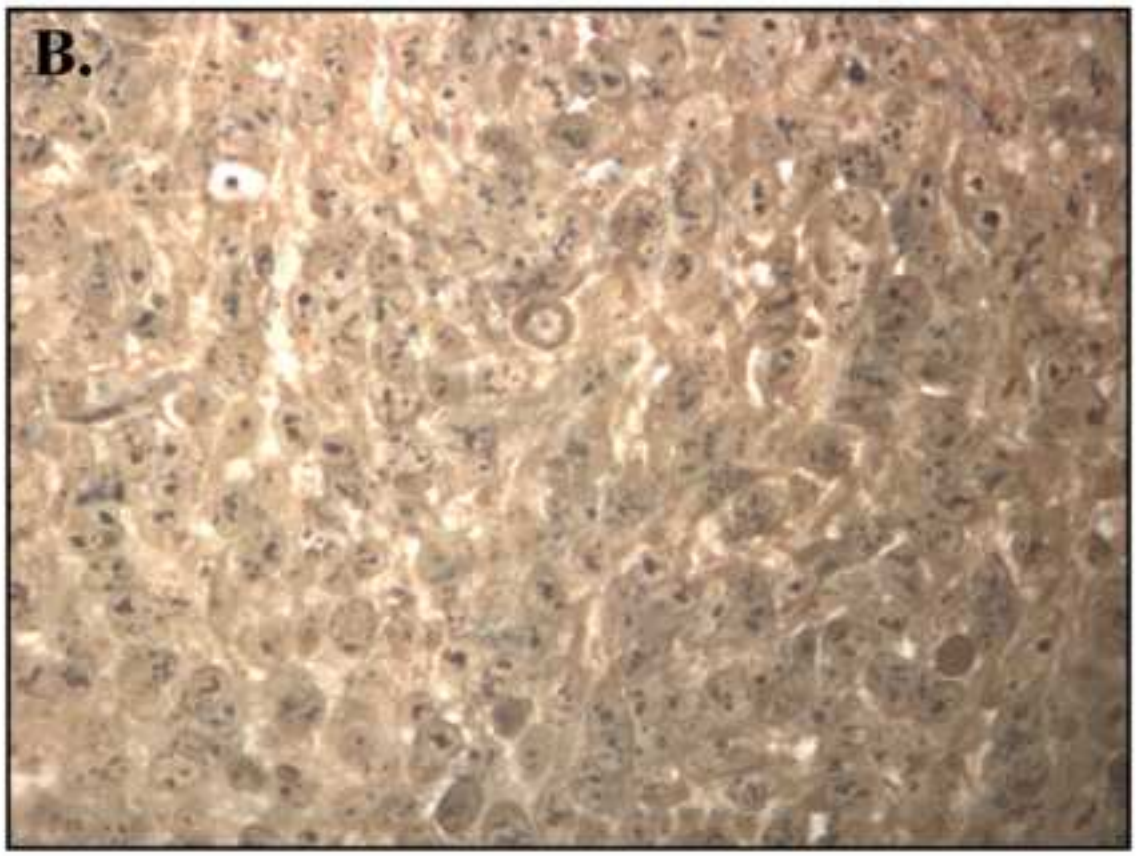

Figure 3B

Figure 3c

Click here to download high resolution image

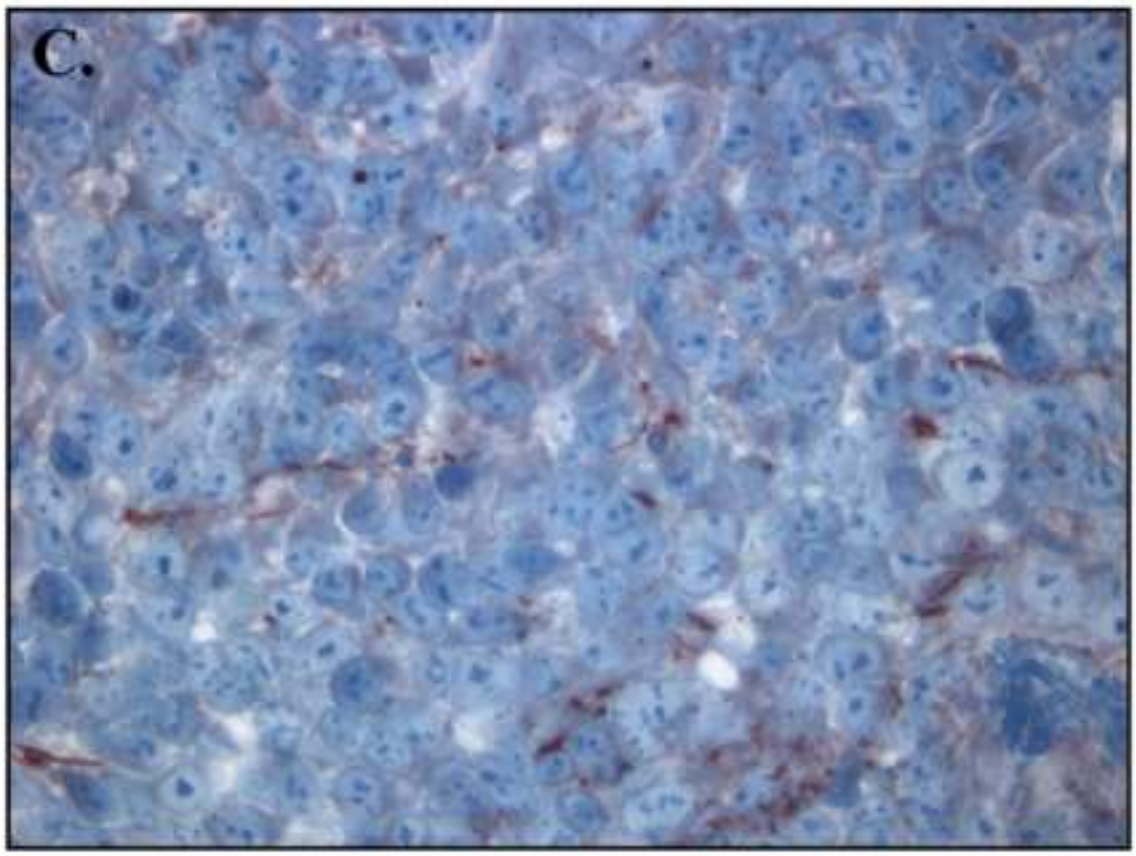

Figure 3C

Figure 4a

Click here to download high resolution image

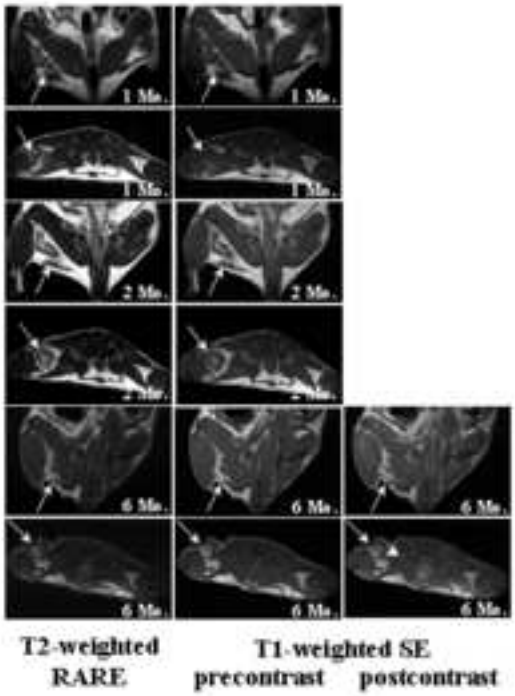

Figure 4A

Figure 4b

Click here to download high resolution image

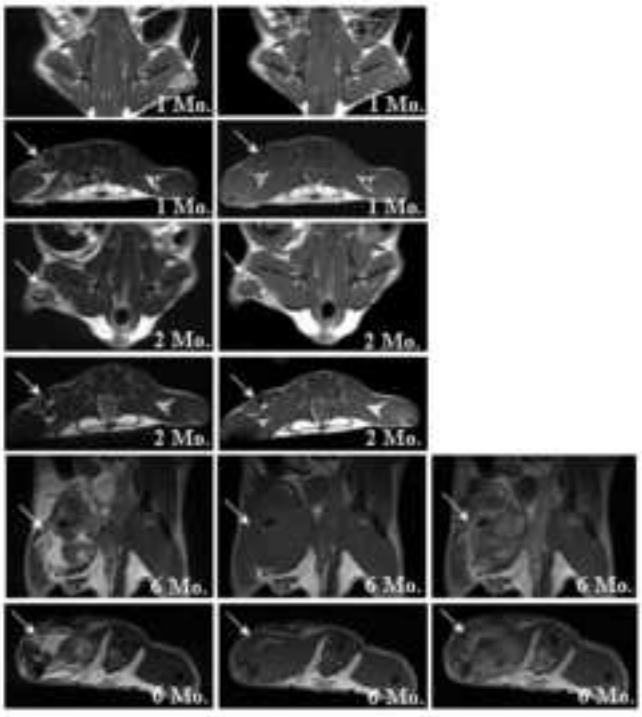

Figure 4B

Figure 4c

Click here to download high resolution image

Figure 4C

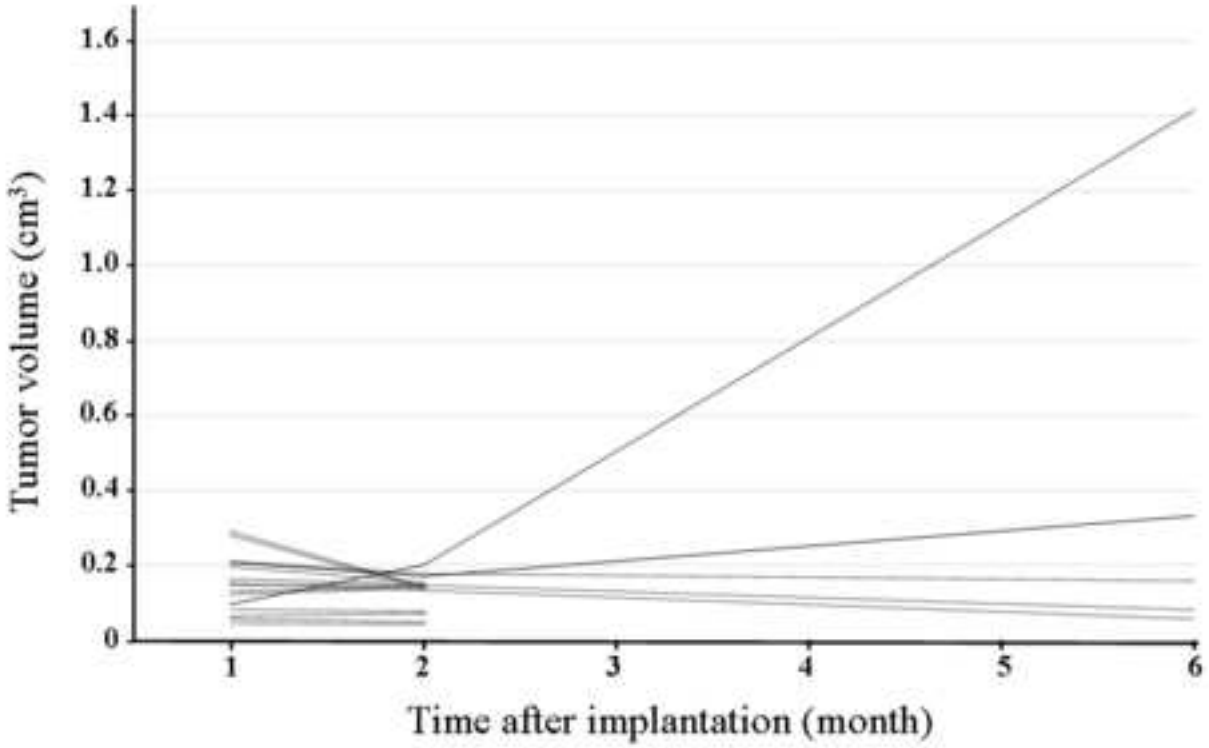

Figure 5a
Click here to download high resolution image

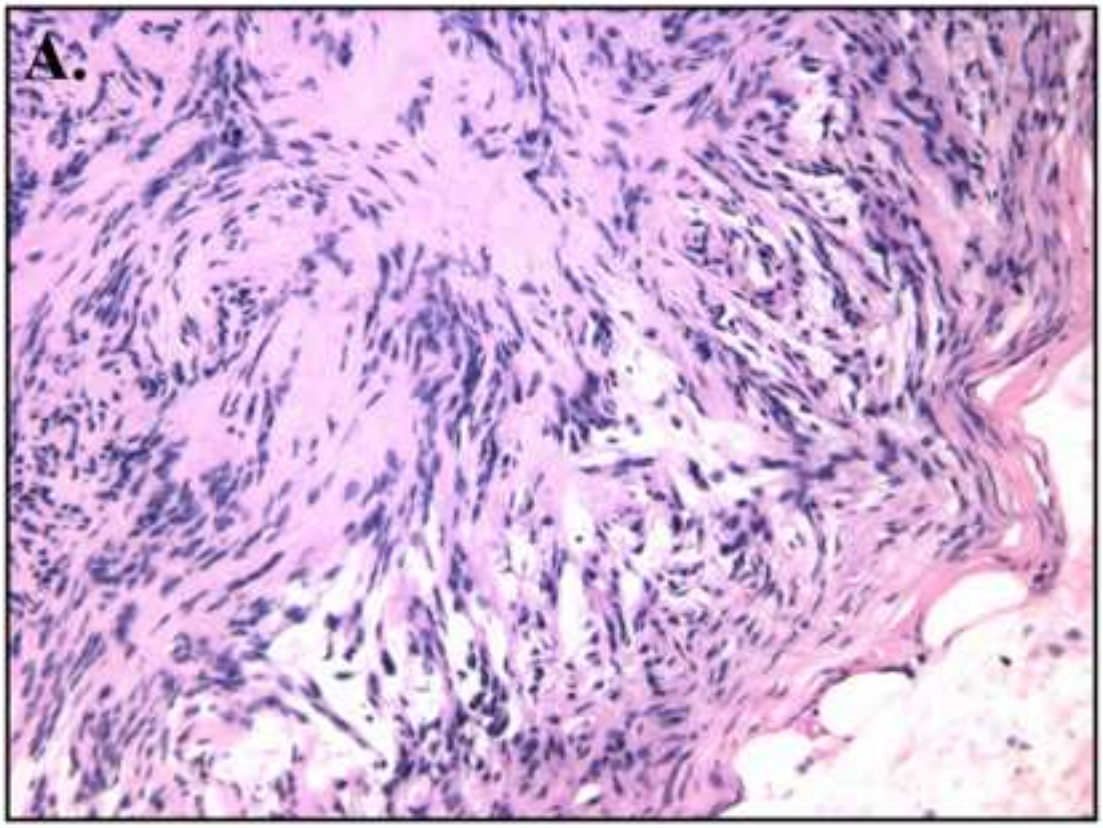

Figure 5A

Figure 5b

Click here to download high resolution image

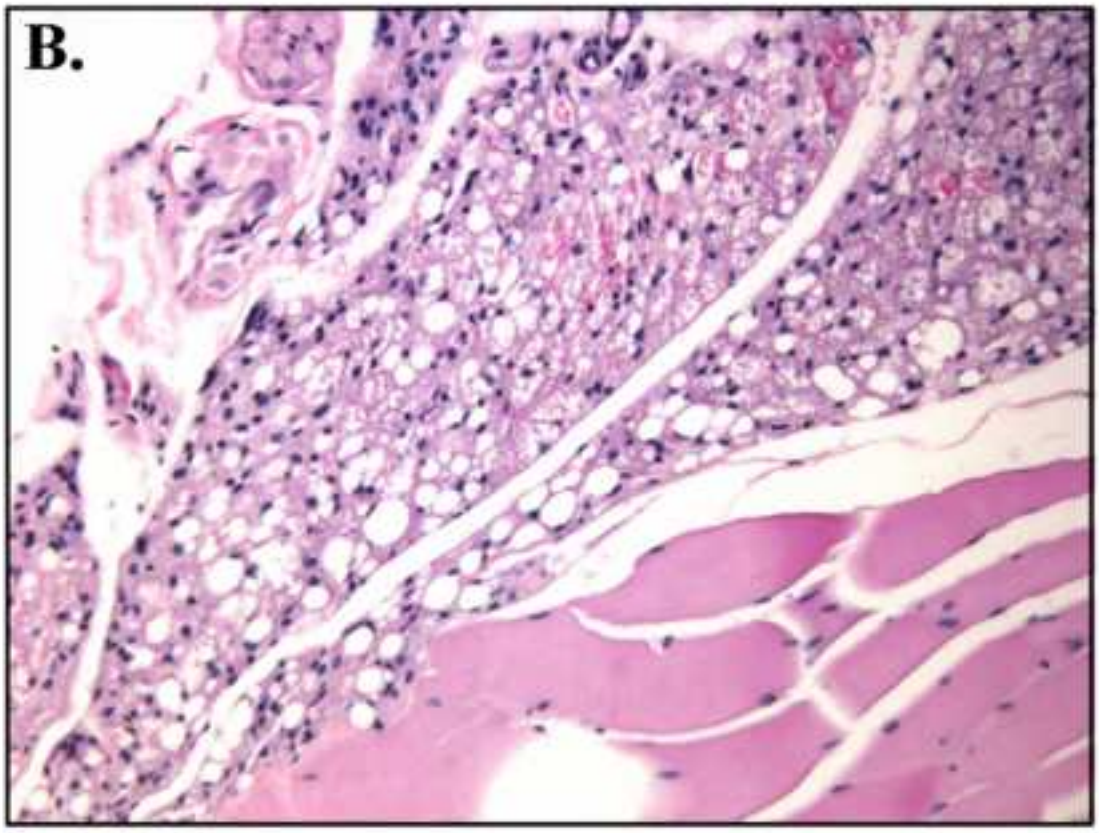

Figure 5B

Figure 6a
Click here to download high resolution image

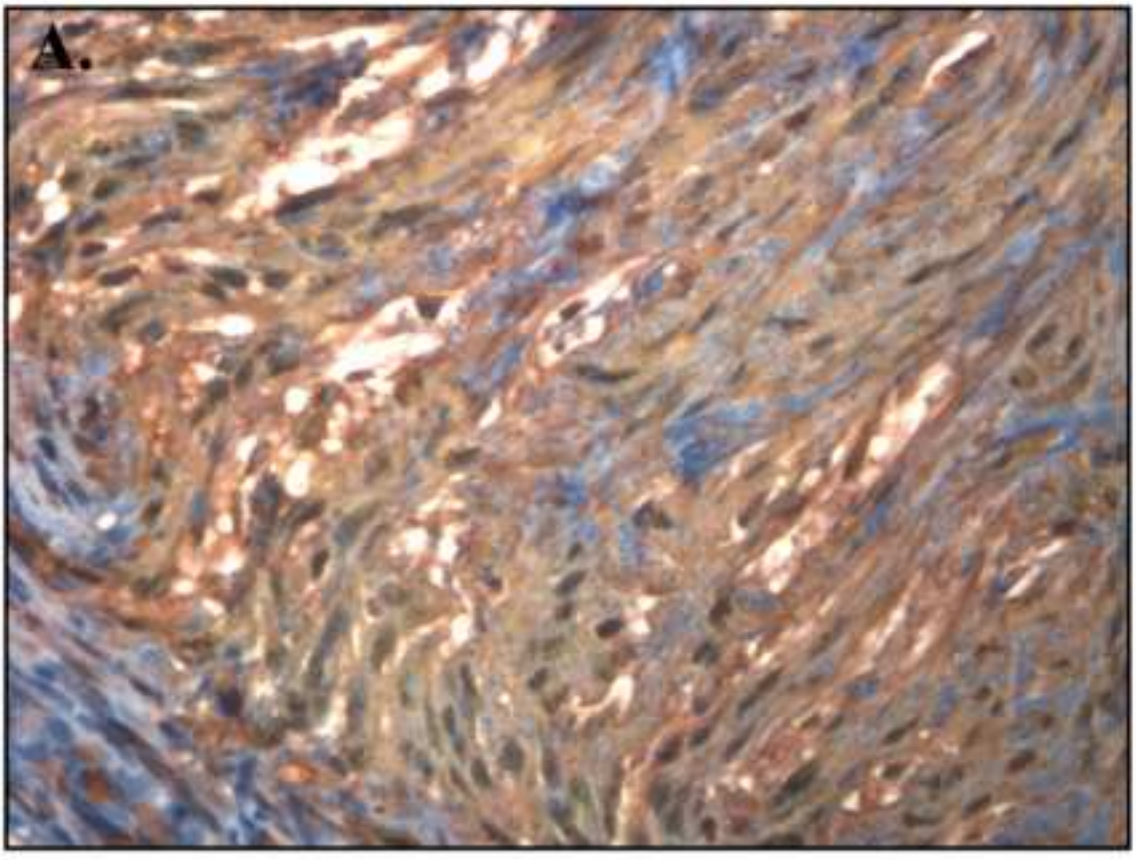

Figure 6A

Figure 6b

Click here to download high resolution image

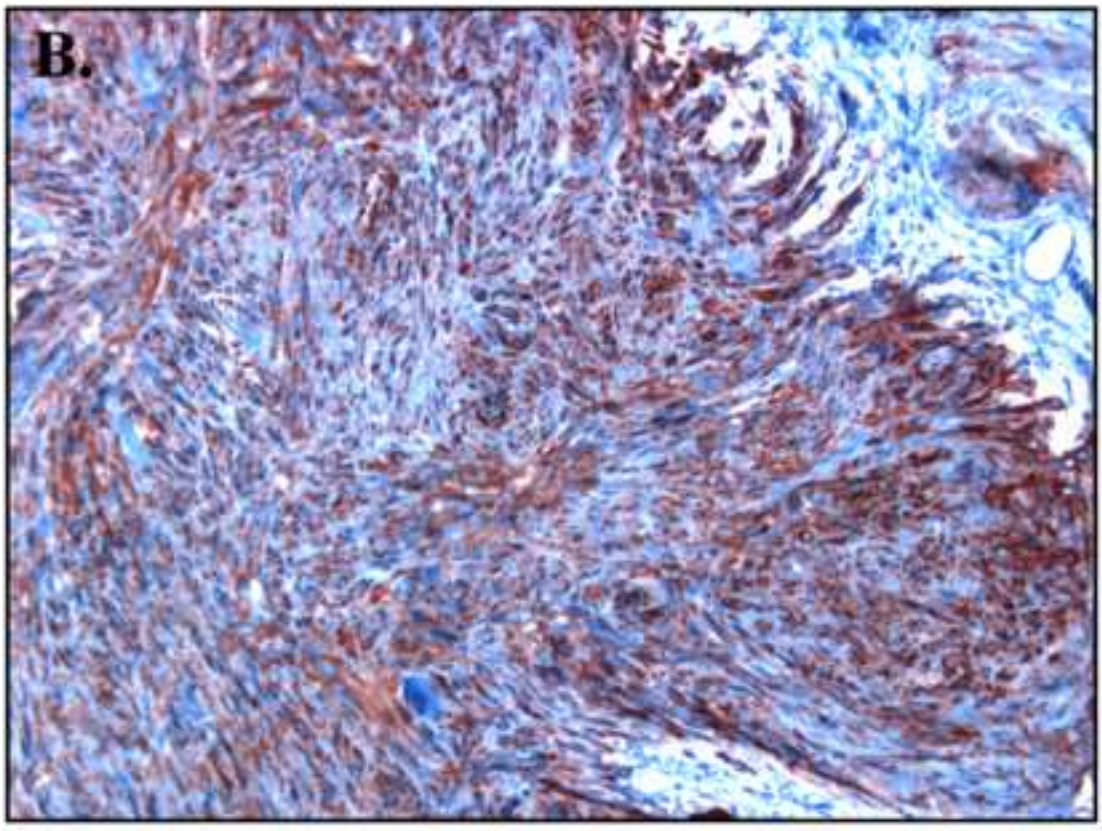

Figure 6B

Figure 6c

Click here to download high resolution image

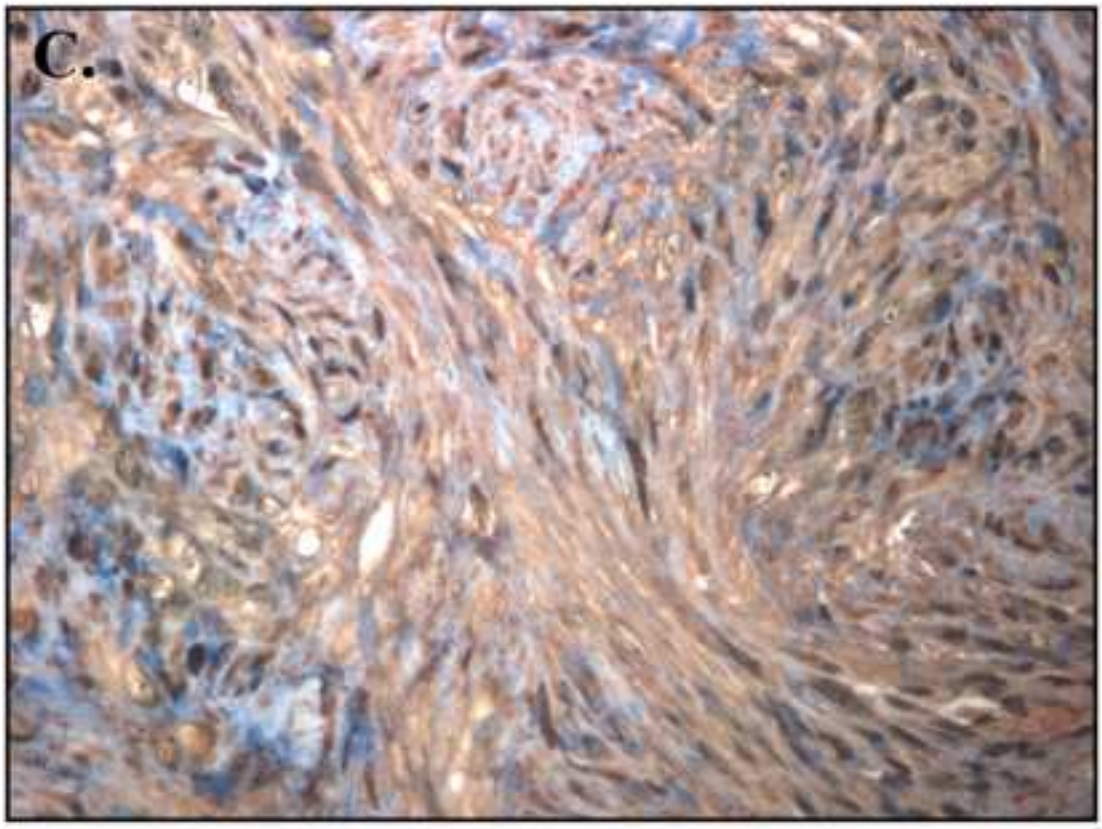

Figure 6C

Figure 6d

Click here to download high resolution image

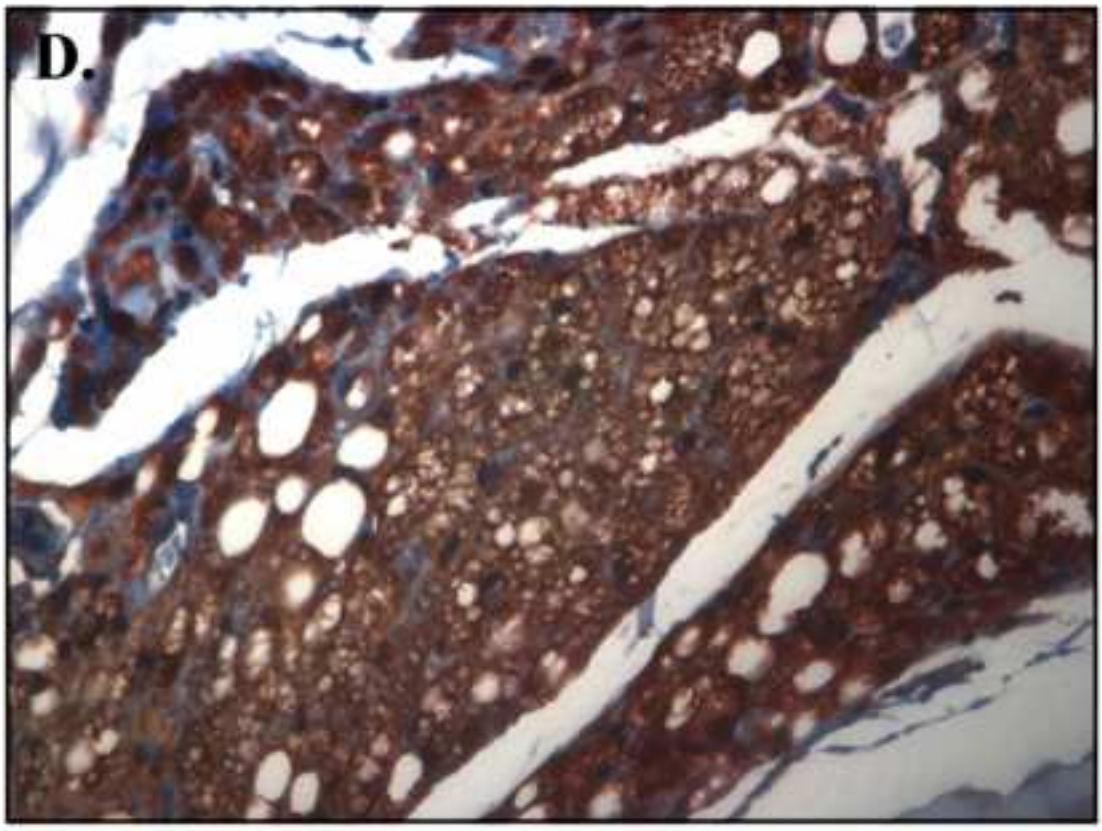

Figure 6D

Figure 6e

Click here to download high resolution image

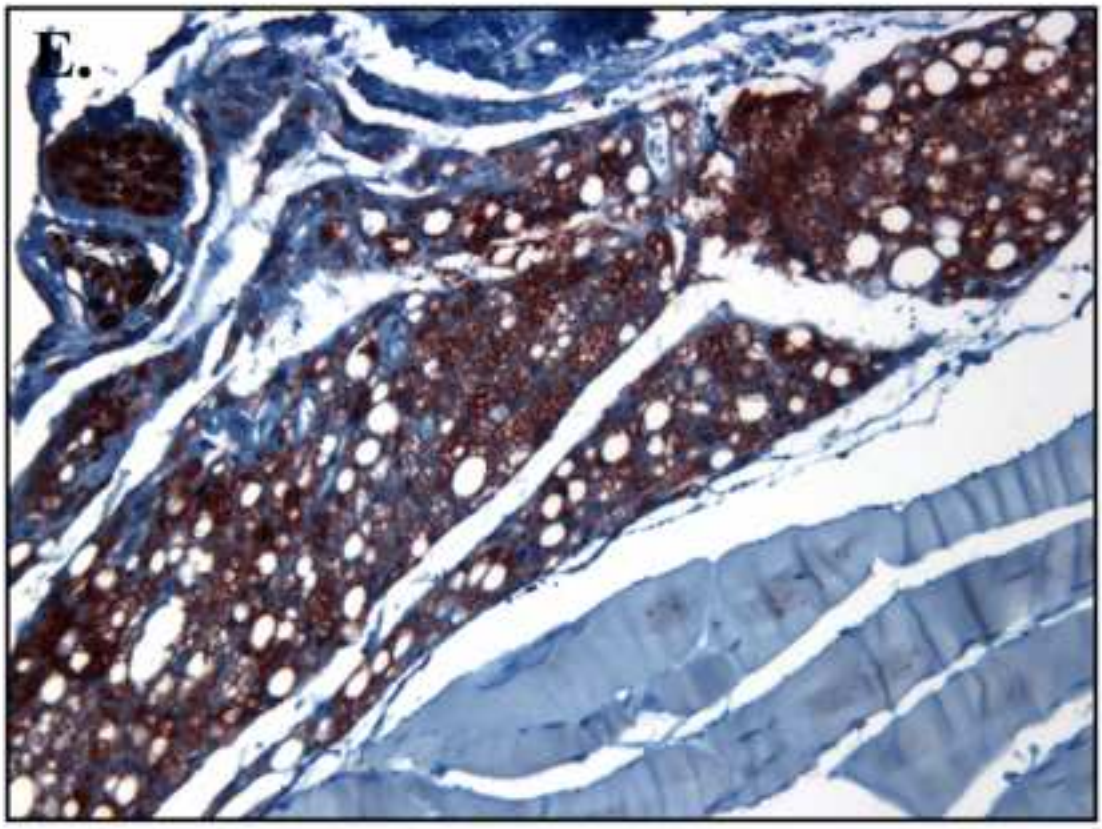

Figure 6E

Copyright Transfer

This piece of the submission is being sent via mail.

The Laryngoscope
Lippincott Williams & Wilkins, Inc.

Cyclin D_1 and D_3 Expression in Vestibular Schwannomas

Brian A. Neff, MD[1,4*]; Elly Oberstien, MS[4]; Mark Lorenz, MS[4]; Abhik R. Chaudhury, MD[2,4]; D. Bradley Welling, MD, PhD[1,4*]; Long-Sheng Chang, PhD[1,2,3,4,5*]

Objectives: **The G_1 regulators of the cell cycle, cyclin D_1 and D_3, have been implicated in the regulation of Schwann cell proliferation and differentiation. The purpose of this study is to evaluate cyclin D_1 and D_3 protein expression and the corresponding clinical characteristics of vestibular schwannomas.** ***Study Design and Methods:*** **Tissue sections of 15 sporadic vestibular schwannomas were prepared. Immunohistochemical analysis of the vestibular schwannomas was performed with anticyclin D_1 and anticyclin D_3 antibodies. The immunoreactivity was evaluated in comparison with adjacent vestibular nerves. Tissue sections of breast carcinoma and prostate carcinoma were used as positive controls for cyclin D_1 and D_3 staining, respectively. Patient demographics, tumor characteristics, and cyclin D expression were reviewed, and statistical analysis was performed.** ***Results:*** **While the breast carcinoma control expressed abundant cyclin D_1 protein, none of the 15 vestibular schwannomas showed detectable cyclin D_1 staining. In contrast, seven of 15 vestibular schwannomas stained positive for the cyclin D_3 protein. Cyclin D_3 staining was taken up in the nucleus of schwannoma tumor cells in greater proportion than Schwann cells of adjacent vestibular nerve. Although sample size was small, no significant difference in the average age of presentation, tumor size, and male to female ratios for the cyclin D_3+ or cyclin D_3− groups was found.** ***Conclusion:*** **The Cyclin D_1 protein does not appear to play a prominent role in promoting cell cycle progression in vestibular schwannomas. In contrast, cyclin D_3 expression was seen in nearly half of the tumors examined, suggesting that it may have a growth-promoting role in some schwannomas. Further studies are needed to define its cellular mechanism.** ***Key words:*** **Vestibular schwannoma, cyclin D_1 and D_3, neurofibromatosis type 2, *NF2* gene, and cell cycle.**
***Laryngoscope*, 116:423–426, 2006**

INTRODUCTION

Vestibular schwannomas are benign tumors originating from the vestibular divisions of the eighth cranial nerve.[1] Although advances have been made in the clinical treatment of these tumors, the morbidity associated with the current treatment modalities continues to be a problem. For this reason, it is important to find new methods to eradicate or control these tumors. The most promising approaches require a fundamental understanding of the molecular mechanisms underlying vestibular schwannoma tumorigenesis.

Although mutations inactivating both alleles of the neurofibromatosis type 2 gene (*NF2*) are responsible for the development of vestibular schwannomas, the mutation type and/or location of the mutation alone is insufficient to predict the clinical behavior of the tumors. In particular, predictors of growth rate are not yet known, but would be important clinically if such could be determined. Several genes or pathways including the retinoblastoma protein (pRb)-cyclin dependent kinase (CDK) pathway have been found to be frequently deregulated in these tumors.[2,3] Among the genes involved in the pRb-CDK pathway, which regulates G_1-to-S progression during the cell cycle,[4] CDK2 was substantially under expressed in most vestibular schwannomas examined. In addition, all schwannomas displayed deregulated expression of at least one of the genes involved in the pRb-CDK pathway.[2]

Recent studies suggest important roles for the D-type cyclins in the control of Schwann cell proliferation. Mice lacking cyclin D_1 display defects in the growth of mature Schwann cells.[5] Schwann cell proliferative responses to cAMP and platelet-derived growth factor appear to be mediated by cyclin D_1.[6] Finally, microarray analysis has revealed a strong correlation between Schwann cell proliferation and cyclin D_3 expression, and synergistic induction of cyclin D_3 expression may be critical to the stimu-

[1]From the Department of Otolaryngology Head and Neck Surgery (B.A.N., D.B.W., L.C.), [2]Pathology (A.R.C., L.C.), and [3]Pediatrics (L.C.), The Ohio State University, Columbus, Ohio, U.S.A. From [4]The Ohio State University College of Medicine (B.A.N., E.O., M.L., A.R.C., D.B.W., L.C.). From [5]the Center for Childhood Cancer (L.C.), Children's Research Institute, Children's Hospital, Columbus, Ohio, U.S.A.

This study was supported by the Department of Defense Neurofibromatosis Research Program and the National Institute of Deafness and Other Communication Disorders.

Send Correspondence to D. Bradley Welling, 456 W. 10th Avenue, Columbus, OH 43210; E-mail: welling.1@osu.edu; and Long-Sheng Chang, 700 Children's Drive, Columbus, OH 43205 U.S.A; E-mail: lchang@chi.osu.edu; Phone: 614-355-2658; Fax: 614-722-5895

[*]Department of Otolaryngology Head and Neck Surgery (B.A.N.), The Mayo Clinic, Rochester, Minnesota, U.S.A.

DOI: 10.1097/01.mlg.0000195076.05466.6c

lation of Schwann cell proliferation by heregulin and forskolin.[7–9]

Alterations in the expression of the cyclin D family of proteins have been demonstrated in a variety of benign and malignant tumors.[10–16] The cyclin D_1 gene is rearranged, amplified, and/or over-expressed in several human neoplasms. Also, over-expression and/or amplification of cyclin D_3 occur in some malignancies. In addition, expression of cyclin D_1 and D_3 may be of prognostic value in several of these pathologies.[17–18] However, the role of cyclin D_1 and D_3 in vestibular schwannomas has not been previously examined. Since cyclin D_1 and D_3 have been implicated in the regulation of Schwann cell proliferation and differentiation, we evaluated the protein expression of cyclin D_1 and D_3 in vestibular schwannomas.

METHODS

Tissue Procurement

Vestibular schwannomas were resected with informed patient consent and utilized per the Human Subjects Protocol for tissue procurement approved by the Institutional Review Board. Paraffin-embedded tissue sections were evaluated by a neuropathologist and histologically confirmed as vestibular schwannomas. Fifteen sporadic vestibular schwannoma specimens were obtained and used in the study. None of the 15 patients included in the study had undergone previous surgery or irradiation to treat their tumor.

Immunohistochemistry

Immunostaining of vestibular schwannoma tissue sections was performed as previously described.[2,3] Sections of cyclin D_1-positive breast carcinomas and cyclin D_3-positive prostate carcinomas were used as positive controls. Deparaffinized tissue sections were incubated overnight at 4°C with either the anticyclin D_1 (HD11, sc-246) or anticyclin D_3 (D-7, sc-6283) monoclonal antibody (Santa Cruz Biotechnology, Santa Cruz, CA) at a 1:40,000 or 1:1000 dilution, respectively. The antibody concentration was determined by serial dilution and staining of positive control tissues. The optimal concentration was chosen in which positive control tissues demonstrated the most discrete immunoreactivity with the least amount of background staining. After extensive washing, slides were sequentially treated with biotinylated secondary antibody for 20 min, conjugated streptovidin for 20 min, and AEC+ High Sensitivity substrate chromogen (Dako Corp., Carpinteria, CA) for 5 min. A hematoxylin counterstain was then applied and light microscopy used to visualize the stained tissues. Tissues expressing the cyclin D_1 or D_3 protein stained brown while the hematoxylin counterstain appeared blue. Immunostained slides were evaluated by a neuropathologist and the immunoreactivity was graded as 0 (negative), 1+ (faint), 2+ (distinct), 3+ (strong, focal), 4+ (strong, diffuse) according to a modification of a previously reported intensity grading scale.[19] The staining intensity in the tumor tissue was compared to the adjacent vestibular nerve to evaluate whether or not the expression of the cyclin D_1 or D_3 protein was increased or decreased in the tumor.

A review of patient demographics was done for the 15 patients whose tumor was immunostained for cyclin D_3. The average age at presentation, patient sex, and average tumor size at presentation were tabulated for the group of patients with cyclin D_3+ and cyclin D_3− tumors. The size of the tumor was measured as the largest tumor diameter in either the axial, coronal, or sagittal MRI view. The age and tumor size data for the two groups were compared using the Student t test with statistical significance being set at $P < .05$.

RESULTS

Aberrant nuclear overexpression and accumulation of the cyclin D_1 protein are frequently detected in breast carcinomas, and thus, breast carcinoma tissues were used as a positive control.[20] The anticyclin D_1 antibody gave rise to abundant, mostly nuclear immunoreactivity in the breast carcinoma tissue section (Fig. 1a). We detected no staining signal in either the nucleus or the cytoplasm of all 15 vestibular schwannoma specimens (Fig. 1b, Table I). Additionally, we also detected no cyclin D_1-staining signal in the adjacent vestibular nerve tissue (data not shown).

For cyclin D_3 staining, prostate carcinoma tissues were utilized as a positive control.[14,21] As expected, strong immunoreactivity for cyclin D_3 was detected in the prostate carcinoma tissue (Fig. 2a). Intriguingly, the cyclin D_3 staining signal was found mostly in the cytoplasm. Seven schwannoma specimens stained positive for cyclin D_3. Five tumors showed a 2+ distinct nuclear staining pattern (Table I), and the other two schwannoma specimens were graded 3+ with several foci of strong nuclear staining (Fig. 2b, Table I). Interestingly, when the adjacent vestibular nerve was examined for cyclin D_3 expression, only a few Schwann cells exhibited faint 1+ nuclear staining; furthermore, their staining intensity was much weaker than that seen in the schwannoma cells (compare Fig. 2b to Fig. 2c).

A review of patient demographics was done for the cyclin D_3+ and D_3− tumors. There was no significant difference ($P = .44$) in the average age at presentation which was 51 years for the cyclin D_3+ group compared to 58 years for the cyclin D_3− group. The average tumor size was 1.3 cm for the cyclin D_3+ tumors and 0.9 cm for the cyclin D_3− tumors, and again, the tumor size was not statistically different between the two groups ($P = .42$). Lastly, male to female ratios were the same for both groups.

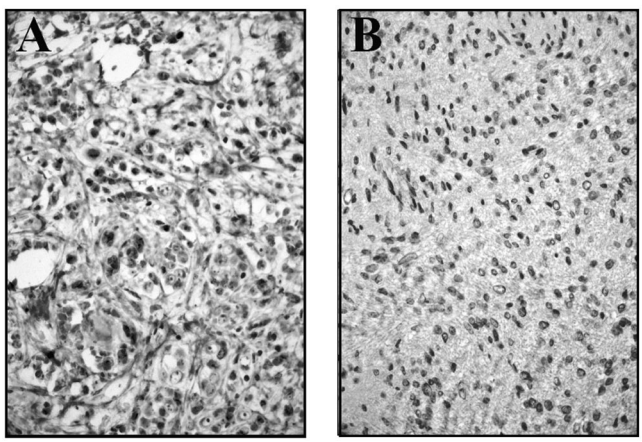

Fig. 1. Cyclin D_1 immunostaining. Tissue sections of a breast carcinoma (a) and a vestibular schwannoma (b) were stained with an anticyclin D_1 monoclonal antibody.

TABLE I.
Summary of Cyclin D_1 and D_3 Protein Expression in Vestibular Schwannomas.

Sample Number	Cyclin D_1	Cyclin D_3
17796 A1	Negative	2+ nuclear staining
17660 B1	Negative	Negative
1030012	Negative	2+ nuclear staining
1030069	Negative	Negative
0303C011	Negative	Negative
304577208	Negative	Negative
17607	Negative	3+ nuclear staining
17613	Negative	2+ nuclear staining
17644	Negative	Negative
17638	Negative	3+ nuclear staining
17579	Negative	Negative
17666	Negative	2+ nuclear staining
17661	Negative	2+ nuclear staining
17789	Negative	Negative
17696	Negative	Negative

DISCUSSION

The pRb-CDK pathway is frequently deregulated in human tumors including vestibular schwannomas.[2,3] Within this pathway, over expression of cyclin D_1 and/or D_3 has been detected in a variety of malignant tumors. In this study we showed that none of the 15 benign vestibular schwannomas examined displayed any cyclin D_1 staining signal, while 7 of 15 (47%) schwannomas over-expressed the cyclin D_3 protein, compared to the adjacent vestibular nerve.

The cyclin D proteins have been shown to contribute to oncogenic potential of tissues in a CDK-dependent and independent manner. In the CDK-dependent pathway, the D cyclins interact with CDK4 and CDK6, and through this interaction, phosphorylation of pRb occurs. In addition, the cyclin D-CDK 4/6 interaction sequesters the CIP/KIP (p21 and p27) and INK4 (p15, p16, p18, and p19) families of CDK inhibitors. This releases the cyclin E-CDK2 holoenzyme to further inactivate the pRb protein.

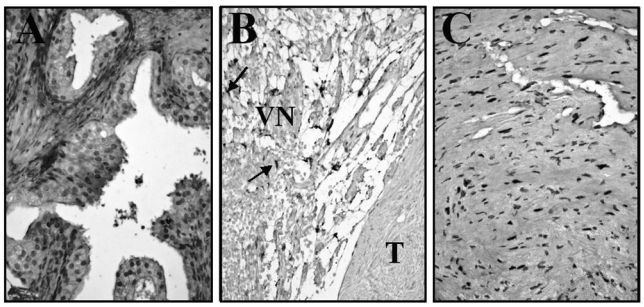

Fig. 2. Cyclin D_3 immunostaining. Tissue sections of a prostate carcinoma (a) and a vestibular schwannoma with (b) or without (c) adjacent vestibular nerve were stained with an anticyclin D_3 monoclonal antibody as described in Materials and Methods. Arrows indicate nuclear staining of some Schwann cells in the vestibular nerve (VN), adjacent to the vestibular schwannoma tumor (T).

Once pRb is hyperphosphorylated and inactivated, pRb dissociates from its pRb-E2F transcriptional repressor complex. The free E2F released from pRb inhibition binds and activates E2F target genes important for the cell to transit from G_1 to S phase.[22,23]

The cyclin D proteins can also affect the activity of several transcription factors including the cyclin D_1-interacting myb-like protein (DMP-1), the signal transducer and activator of transcription 3 (STAT 3), and the β-cell E-box transactivator 2 (BETA2/NeuroD) without the participation of CDK.[23] Furthermore, cyclin D_1 interacts with the transcription factor C/EBPβ and activating transcription factor 5 (ATF5) in a CDK-independent manner, and this may be a vital step in tumor formation.[22,23] Similar to cyclin D_1, cyclin D_3 may function in the CDK-independent pathway that involves C/EBPβ.[9]

In transgenic mice, cyclin D_3 over-expression in epithelial tissues results in epidermal hyperplasia.[24] Deregulated expression of cyclin D_3 and CDK6 could predispose cells to malignant transformation.[25] These results are consistent with the oncogenic role of cyclin D_3 activation in certain human malignancies. Our observation that cyclin D_3 is over-expressed in about half of vestibular schwannomas also suggests a role for cyclin D_3 in schwannoma formation. Given the fact that cyclin D_3 is important for Schwann cell proliferation,[7,8] vestibular schwannomas over-expressing cyclin D_3 may possess growth advantage. Due to the small sample size of tumors stained for cyclin D_3 expression, definitive clinical correlations between D_3+ expressing tumors and tumor size or age at presentation can not be made. However, a cursory review of patient data did not show any significant differences between D_3+ and D_3− patients. A larger clinical study will be needed to assess whether cyclin D_3 over-expression can act as a marker for increased vestibular schwannoma growth. This would require a study of patients who had an initial period of tumor observation and growth who subsequently underwent tumor resection and protein expression analysis of their schwannomas.

Similar to those found in human cancer cells,[19,26] we detected nuclear expression of the cyclin D_3 protein in Schwann cells and vestibular schwannomas. Intriguingly, intense cyclin D_3 immunoreactivity was detected in the cytoplasm of prostate carcinoma cells. Although the reason for this observation is presently not understood, it raises the question that cyclin D_3 may function in different cellular compartments. The subcellular localization of the cyclin D protein has been shown to play an important role in regulating Schwann cell proliferation.[27] Schwann cells in mature myelinating nerves expressed cyclin D_1 in the perinuclear region. After axon damage, cyclin D_1 expression is elevated in parallel with Schwann cell proliferation and translocates into Schwann cell nuclei. In contrast, cyclin D_1 expression is restricted to the perinuclear region of proliferating Schwann cells during normal development. These data indicate that there are different mechanisms regulating proliferation of Schwann cells during development or nerve injury.

CONCLUSION

The D-type cyclins are involved in cell-cycle progression from G_1 to S phase, and have been implicated in the oncogenesis of several human malignancies. Our study shows over expression of the cyclin D_3 protein in 7 of 15 vestibular schwannomas, and this suggests a role for cyclin D_3 in the growth of schwannoma cells.

BIBLIOGRAPHY

1. Welling DB. Clinical manifestations of mutations in the neurofibromatosis type 2 gene in vestibular schwannomas (acoustic neuromas). *Laryngoscope* 1998;108:178–189.
2. Lasak JM, Welling DB. Akhmametyeva EM, et al. Retinoblastoma-cyclin-dependent kinase pathway deregulation in vestibular schwannomas. *Laryngoscope* 2002;112: 1555–1561.
3. Welling DB, Lasak JM, Chang LS, et al. cDNA microarray analysis of vestibular schwannomas. *Otol Neurotol* 2002; 23:736–748.
4. Sherr CJ. Cell cycle control and cancer. *Harvey Lect* 2000-2001;96:73–92.
5. Kim HA, Pomeroy SL, Whoriskey W, et al. A developmentally regulated switch directs regenerative growth of Schwann cells through cyclin D1. *Neuron* 2000;26 (2):405–416.
6. Kim HA, Ratner N, Roberts TM, et al. Schwann cell proliferative responses to cAMP and *Nf1* are mediated by cyclin D1. *J Neurosci* 2001;21 (4):1110–1116.
7. Rahmatullah M, Schroering A, Rothblum K, et al. Synergistic regulation of Schwann cell proliferation by heregulin and forskolin. *Mol Cell Biol* 1998;18:6245–6252.
8. Schworer CM, Masker KK, Wood GC, et al. Microarray analysis of gene expression in proliferating Schwann cells: synergistic response of a specific subset of genes to the mitogenic action of heregulin plus forskolin. *J Neurosci Res* 2003;73:456–464.
9. Fuentealba L, Schworer C, Schroering A, et al. Heregulin and forskolin-induced cyclin D3 expression in Schwann cells: Role of a CCAAT promoter element and CCAAT enhancer binding protein. *Glia* 2004;45:238–248.
10. Seto M, Yamamoto K, Iida S, et al. Gene rearrangement and overexpression of PRAD1 in lymphoid malignancy with t(11;14)(q13;q32) translocation. *Oncogene* 1992;7: 1401–1406.
11. Leach FS, Elledge SJ, Sherr CJ, et al. Amplification of cyclin genes in colorectal carcinomas. *Cancer Res* 1993;53: 1986–1989.
12. Bartkova J, Lukas J, Strauss M, et al. Cyclin D1 oncoprotein aberrantly accumulates in malignancies of diverse histogenesis. *Oncogene* 1995;10:775–778.
13. Jares P, Fernandez PL, Campo E, et al. PRAD-1/cyclin D1 gene amplification correlates with messenger RNA overexpression and tumor progression in human laryngeal carcinomas. *Cancer Res* 1994;54:4813–4817.
14. Han EK, Lim JT, Arber N, et al. Cyclin D1 expression in human prostate carcinoma cell lines and primary tumors. *Prostate* 1998;35:95–101.
15. Oyama T, Kashiwabara K, Yoshimoto K, et al. Frequent overexpression of the cyclin D1 oncogene in invasive lobular carcinoma of the breast. *Cancer Res* 1998;58: 2876–2880.
16. Sonoki T, Harder L, Horsman DE, et al. Cyclin D3 is a target gene of t(6;14)(p21.1;q32.3) of mature B-cell malignancies. *Blood* 2001;98:2837–2844.
17. McIntosh GG, Anderson JJ, Milton I, et al. Determination of the prognostic value of cyclin D1 overexpression in breast cancer. *Oncogene* 1995;11:885–891.
18. Florenes VA, Faye RS, Maelandsmo GM, et al. Levels of cyclin D1 and D3 in malignant melanoma: deregulated cyclin D3 expression is associated with poor clinical outcome in superficial melanoma. *Clin Cancer Res* 2000;6: 3614–3620.
19. Doglioni C, Chiarelli C, Macri E, et al. Cyclin D3 expression in normal, reactive, and neoplastic tissues. *J Pathol* 1998; 185:159–166.
20. Bartkova J, Lukas J, Muller H, et al. Cyclin D1 protein expression and function in human breast cancer. *Int J Cancer* 1994;57:353–361.
21. Mukhopadhyay A, Banerjee S, Stafford LJ, et al. Curcumin-induced suppression of cell proliferation correlates with down-regulation of cyclin D1 expression and CDK4-mediated retinoblastoma protein phosphorylation. *Oncogene* 2002;21:8852–8861.
22. Lamb J, Ramaswamy S, Ford HL, et al. A mechanism of cyclin D1 action encoded in the patterns of gene expression in human cancer. *Cell* 2003;114:323–334.
23. Ewen ME, Lamb J. The activities of cyclin D1 that drive tumorigenesis. *Trends Mol Med* 2004;10:158–162.
24. Rodriguez-Puebla ML, LaCava M, Miliani DeMarval PL, et al. Cyclin D2 overexpression in transgenic mice induces thymic and epidermal hyperplasia whereas cyclin D3 expression results only in epidermal hyperplasia. *Am J Pathol* 2000;157:1039–1050.
25. Chen Q, Lin J, Jinno S, et al. Overexpression of Cdk6-cyclin D3 highly sensitizes cells to physical and chemical transformation. *Oncogene* 2003;22:992–1001.
26. Bartkova J, Zemanova M, Bartek J. Abundance and subcellular localization of cyclin D3 in human tumors. *Int J Cancer* 1996;65:323–327.
27. Atonasoski S, Shumas S, Dickson C, et al. Differential cyclin D1 requirements of proliferating Schwann cells during development and after injury. *Mol Cell Neurosci* 2001;18: 581–592.

tapraid5/z7h-devdyn/z7h-devdyn/z7h00906/z7h2000d06g | heckt | S=7 | 6/30/06 | 15:58 | Art: 050544R1

DEVELOPMENTAL DYNAMICS 00:000–000, 2006

RESEARCH ARTICLE

Regulation of the *Neurofibromatosis 2* Gene Promoter Expression During Embryonic Development

Elena M. Akhmametyeva,[1,2] Maria M. Mihaylova,[1,2] Huijun Luo,[1,2] Sadeq Kharzai,[1] D. Bradley Welling,[3] and Long-Sheng Chang[1–4]*

Mutations in the *Neurofibromatosis 2* (*NF2*) gene are associated with predisposition to vestibular schwannomas, spinal schwannomas, meningiomas, and ependymomas. Presently, how *NF2* is expressed during embryonic development and in the tissues affected by neurofibromatosis type 2 (NF2) has not been well defined. To examine *NF2* expression in vivo, we generated transgenic mice carrying a 2.4-kb *NF2* promoter driving β-galactosidase (β-gal) with a nuclear localization signal. Whole-mount embryo staining revealed that the *NF2* promoter directed β-gal expression as early as embryonic day E5.5. Strong expression was detected at E6.5 in the embryonic ectoderm containing many mitotic cells. β-gal staining was also found in parts of embryonic endoderm and mesoderm. The β-gal staining pattern in the embryonic tissues was corroborated by in situ hybridization analysis of endogenous *Nf2* RNA expression. Importantly, we observed strong *NF2* promoter activity in the developing brain and in sites containing migrating cells including the neural tube closure, branchial arches, dorsal aorta, and paraaortic splanchnopleura. Furthermore, we noted a transient change of *NF2* promoter activity during neural crest cell migration. While little β-gal activity was detected in premigratory neural crest cells at the dorsal ridge region of the neural fold, significant activity was seen in the neural crest cells already migrating away from the dorsal neural tube. In addition, we detected considerable *NF2* promoter activity in various NF2-affected tissues such as acoustic ganglion, trigeminal ganglion, spinal ganglia, optic chiasma, the ependymal cell-containing tela choroidea, and the pigmented epithelium of the retina. The *NF2* promoter expression pattern during embryogenesis suggests a specific regulation of the *NF2* gene during neural crest cell migration and further supports the role of merlin in cell adhesion, motility, and proliferation during development. *Developmental Dynamics 00:000–000, 2006.* © 2006 Wiley-Liss, Inc.

Key words: *Neurofibromatosis 2* (*NF2*) gene promoter; neurofibromatosis type 2 (NF2); neural tube closure; neural crest cell migration; pigmented epithelium of the retina; transgenic mouse

AQ: 1 Accepted 23 May 2006

INTRODUCTION

Neurofibromatosis type 2 (NF2) is an autosomal dominant disorder that predisposes affected individuals to bilateral vestibular schwannomas and the development of multiple meningiomas, intracranial tumors, ophthalmologic and skin abnormalities, and spinal schwannomas (NIH Consens. Statement, 1991). By positional cloning, the gene associated with NF2 has been identified and termed the *Neurofibromatosis 2* gene (*NF2*), which encodes a protein named "merlin" for moesin-

[1]Center for Childhood Cancer, Children's Research Institute, Children's Hospital, Columbus, Ohio
[2]Department of Pediatrics, The Ohio State University College of Medicine and Public Health, Columbus, Ohio
[3]Department of Otolaryngology, The Ohio State University College of Medicine and Public Health, Columbus, Ohio
[4]Department of Pathology, The Ohio State University College of Medicine and Public Health, Columbus, Ohio
Grant sponsor: US Department of Defense Neurofibromatosis Research Program; Grant number: DAMD17-02-1-0680; Grant sponsor: National Institute of Deafness and Other Communication Disorders; Grant number: DC5985; Grant sponsor: National Cancer Institute; Grant number: CA16058.
***Correspondence to: Dr. Long-Sheng Chang, Department of Pediatrics, Children's Hospital and The Ohio State University, WA-5104, 700 Children's Drive, Columbus, OH 43205-2696. E-mail: lchang@chi.osu.edu**

DOI 10.1002/dvdy.20883
Published online 00 Month 2006 in Wiley InterScience (www.interscience.wiley.com).

ezrin-radixin like protein (Trofatter et al., 1993), or "schwannomin," a word derived from schwannoma, the most prevalent tumor seen in NF2 (Rouleau et al., 1993). Mutations in the *NF2* gene have been found in NF2-associated vestibular schwannomas, sporadic vestibular schwannomas, and cystic schwannomas, as well as meningiomas (reviewed in Neff et al., 2005).

The *NF2* protein shares a high degree of homology to ezrin, radixin, and moesin (ERM), a family of membrane-cytoskeleton-associated proteins that are important for cell adhesion, motility, regulation of cell shape, and signal transduction (McClatchey, 2004; McClatchey and Giovannini, 2005). Like the ERM proteins, merlin is expressed in a variety of cell types where it localizes to areas of membrane remodeling, particularly membrane ruffles, although its precise distribution may differ from the ERM proteins expressed in the same cell (Gonzalez-Agosti et al., 1996). In addition, schwannoma cells from NF2-associated tumors have dramatic alterations in the actin cytoskeleton and display abnormalities in cell spreading (Pelton et al., 1998). These results suggest that merlin may play an important role in regulating both actin cytoskeleton-mediated processes and cell proliferation. However, unlike the ERM proteins, merlin exerts a growth suppression effect. Over-expression of merlin in mouse fibroblasts or rat schwannoma cells can limit cell growth (Lutchman and Rouleau, 1995; Sherman et al., 1997; Gutmann et al., 1998) and suppress transformation by a *ras* oncogene (Tikoo et al., 1994). Recent studies demonstrate that cells lacking *NF2* function exhibit characteristics of cells expressing activated alleles of the small GTPase Rac, and the p21-activated kinase 2, a downstream target of Rac1/Cdc42, which directly phosphorylates merlin, affecting merlin's localization and function (Shaw et al., 2001; Xiao et al., 2002; Kissil et al., 2002; Surace et al., 2004; Rong et al., 2004).

Studies of *Nf2* gene knockout in mice show that merlin function is essential during early embryonic development. Homozygous *Nf2* mutant mouse embryos fail in development at approximately day 7 of gestation and die immediately prior to gastrulation (McClatchey et al., 1997). Conditional homozygous deletion of *Nf2* in Schwann cells or arachnoid cells leads to hyperplasia and tumor development, which are characteristics of NF2 (Giovannini et al., 2000; Kalamarides et al., 2002). Although these results argue that loss of merlin is sufficient for schwannoma and meningioma formation in vivo, none of the lesions detected in these mice was found in the vestibular nerve. This observation contrasts with the vestibular schwannomas commonly found in patients with NF2.

To better understand merlin function during development, previous studies examined merlin expression using Northern blot, in situ hybridization, RT-PCR, or immunostaining; however, these studies have not yielded consistent results. An earlier report indicated that the *NF2* gene was only expressed in tissues of ectodermal origin (World Health Org., 1992). Subsequently, Bianchi et al. (1994) reported that merlin RNA was not detected in the adult human heart and liver, whereas Haase et al. (1994) noticed abundant merlin RNA expression in the adult mouse heart. Similarly, no merlin RNA was detected in the adult mouse lung, whereas abundant expression could be found in the adult human lung. Northern blot analysis, however, detected *Nf2* transcripts in the adult mouse brain, kidney, cardiac muscle, skin, and lung (Claudio et al., 1994). By in situ hybridization and reverse transcription-polymerase chain reaction (RT-PCR) analyses, Gutmann et al. (1994) reported that rat merlin was widely expressed during mid to late embryogenesis. High levels of merlin expression were seen in cerebral cortex, brainstem, spinal cord, and heart during embryonic days E12–16. Merlin RNA expression becomes restricted to the brainstem, cerebellum, dorsal root ganglia, spinal cord, adrenal gland, and testis in adult animals, while no appreciable levels of merlin RNA could be detected in kidney, lung, and skeletal muscle. On the contrary, by in situ hybridization and immunostaining, Huynh et al. (1996) showed that merlin was detected in most differentiated tissues but not in undifferentiated tissues. In particular, merlin was not detectable in mitotic neuroepithelial cells, the perichondrium, the liver, the neocortex, and the ventricular zone of the developing cerebral cortex. Furthermore, in contrast to the phenotype of early embryonic lethality in mice lacking *Nf2* function, Gronholm et al. (2005) did not detect merlin protein expression until E11 in mouse embryos. In light of these inconsistent results, a detailed analysis of *NF2* expression during embryonic development is needed.

Previously, we have defined the 5′ flanking sequence of the human *NF2* gene and showed that the 2.4-kb *NF2* promoter could direct strong expression in several cell lines including neuronal cells (Welling et al., 2000; Chang et al., 2002). However, whether the *NF2* promoter is sufficient for expression in a variety of tissues including Schwann cells and neurons in vivo has not been tested. The objective of this study was to define the *NF2* expression pattern during embryonic development using two approaches. First, we generated a construct containing the 2.4-kb *NF2* promoter-driven β-galactosidase (β-gal) with a nuclear localization signal and used it to produce transgenic mice. Whole-mount X-gal staining of transgenic embryos at various days post coitus (p.c.) was conducted and tissue sections were analyzed. Second, we performed whole-mount in situ hybridization using various *Nf2* cDNA fragments as probes to confirm the expression pattern. Our results show that the *NF2* promoter could direct β-gal expression as early as E5.5. β-gal expression was first detected in the embryonic ectoderm and, to a lesser extent, in some parts of endoderm and mesoderm. Subsequently, strong β-gal staining was seen in the developing neural tube, migrating neural crest cells, the heart, the dorsal aorta, and the paraaortic mesenchyme. As the embryos matured, significant levels of β-gal expression were found in the cranial ganglia V and VIII, spinal ganglia, pigmented epithelium of the retina, and skin.

RESULTS

The NF2 Promoter Directed Transgene Expression as Early as E5.5

To examine the *NF2* promoter expression pattern in vivo, we generated the

tapraid5/z7h-devdyn/z7h00906/z7h2000d06g | heckt | S=7 | 6/30/06 | 15:58 | Art: 050544R1

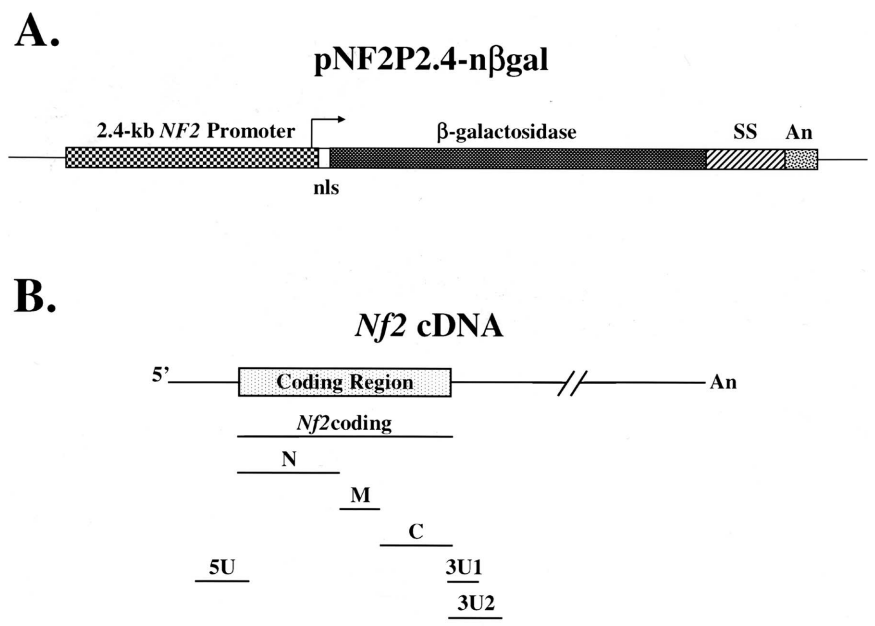

C.

Nf2 Primer	Sequence+	Position*
Coding-F	5'-ggtaccccgcgcc**atggccggagccatcgct**-3'	-13 ~ +18
Coding-R	5'-tcacctg**ctagagttcttcaaagaag**-3'	+1798 ~ +1773
5U-F	5'-acacgtgtgcgctcccaactactg-3'	-406 ~ -383
5U-R	5'-**cgatccgcaccgtgaatgtcttgg**-3'	+79 ~ +56
3U1-F	5'-**ggccttggacgtcctacacagcg**-3'	+1668 ~ +1690
3U1-R	5'-cggggccctcaactcaagagttcc-3'	+1913 ~ +1890
3U2-F	5'-**cagagcgccaagtcccgagtg**-3'	+1773 ~ +1798
3U2-R	5'-gcccatcccagaagcccagttg-3'	+2244 ~ +2223

Fig. 1. Schematic diagram of the pNF2P2.4-nβ-gal construct and various mouse cDNA fragments used in whole-mount RNA in situ hybridization. **A:** The pNF2P2.4-nβ-gal construct contains the 2.4-kb human *NF2* promoter fused with a nuclear localization signal (nls)-containing β-gal expression cassette. SS, SV40 splicing signal; An, SV40 polyadenylation sequence. **B:** Various mouse *Nf2* cDNA fragments were obtained by RT-PCR as described in the Experimental Procedures section and cloned into the pCRII-TOPO vector. The relative locations of the *Nf2* cDNA fragments are illustrated. **C:** Nucleotide sequences and locations of the mouse *Nf2*-specific primers. *Nucleotide position +1 is assigned to the A residue of the ATG translation start codon (GenBank accession No. L27090). +The ATG translation start codon is underlined. The primer sequence in the *Nf2* coding region is shown in bold letters while that in the 5′ or 3′ untranslated region is indicated in small letters.

pNF2P2.4-nβgal construct containing the β-gal reporter with a nuclear localization signal under the control of the 2.4-kb human *NF2* promoter (Fig. 1A), and used it to produce transgenic mice. Four lines of transgenic NF2P2.4-nβgal mice were generated. To detect the transgene-encoded β-gal, embryos were obtained from the mating of all four lines of transgenic mice at various days p.c. and whole-mount X-gal staining was performed. All four lines of the transgenic NF2P2.4-nβgal mice showed a similar β-gal staining pattern, eliminating the positional effect due to integration.

As shown in Figure 2A, β-gal staining could be seen in the transgenic embryo as early as E5.5. At this stage, β-gal expression was detected only in the embryonic tissue but not in the extraembryonic tissue. At E6.5, strong β-gal staining was found in the embryonic ectoderm. Cells in this embryonic tissue divided rapidly with visible mitotic figures, and were darkly stained (Fig. 2B). Significant β-gal expression was also seen in some parts of the proximal embryonic endoderm. Weak β-gal staining was detected in the mesoderm, while no staining was seen in the extraembryonic ectoderm (Fig. 2A). E7.5 is the stage when a portion of the dorsal embryonic ectoderm begins to specify into the neural ectoderm, a process important to the formation and shaping of the neural plate (Hogan et al., 1994; Rugh, 1994). High levels of β-gal expression continued to be observed in the embryonic ectoderm of the transgenic E7.5 embryo (Fig. 2A). Similar to that observed at E6.5, substantial β-gal staining was also detected in the embryonic endoderm. Intriguingly, the staining was not contiguous in this endoderm at E7.5; some regions were extensively labeled while others were not. In the mesoderm, only a few cells showed significant β-gal staining, while in the extraembryonic tissues, the ectoplacental cone and the chorionic ectoderm remained negative for β-gal expression.

The Transgene-Encoded β-gal Staining Pattern Coincided With the Endogenous Nf2 RNA Expression Pattern in the Embryonic Tissues

As mentioned earlier, previous studies examining merlin expression, particularly using in situ hybridization and immunostaining (Gutmann et al., 1994, 1996), did not yield consistent results. To examine whether the 2.4-kb *NF2* promoter could recapitulate the endogenous *Nf2* expression pattern, we performed whole-mount RNA in situ hybridization analysis. Various regions of the *Nf2* cDNA were cloned into the pCRII vector (Fig. 1B). Both sense and antisense riboprobes were synthesized from each plasmid by in vitro transcription and used in whole-mount embryo hybridization. We found that the antisense probe prepared from 3U1, containing the *Nf2* sequence immediately upstream of the translation termination codon to about 300 bp into the 3′ untranslated region (Fig. 1), consistently gave rise to a lower background when the

Developmental Dynamics

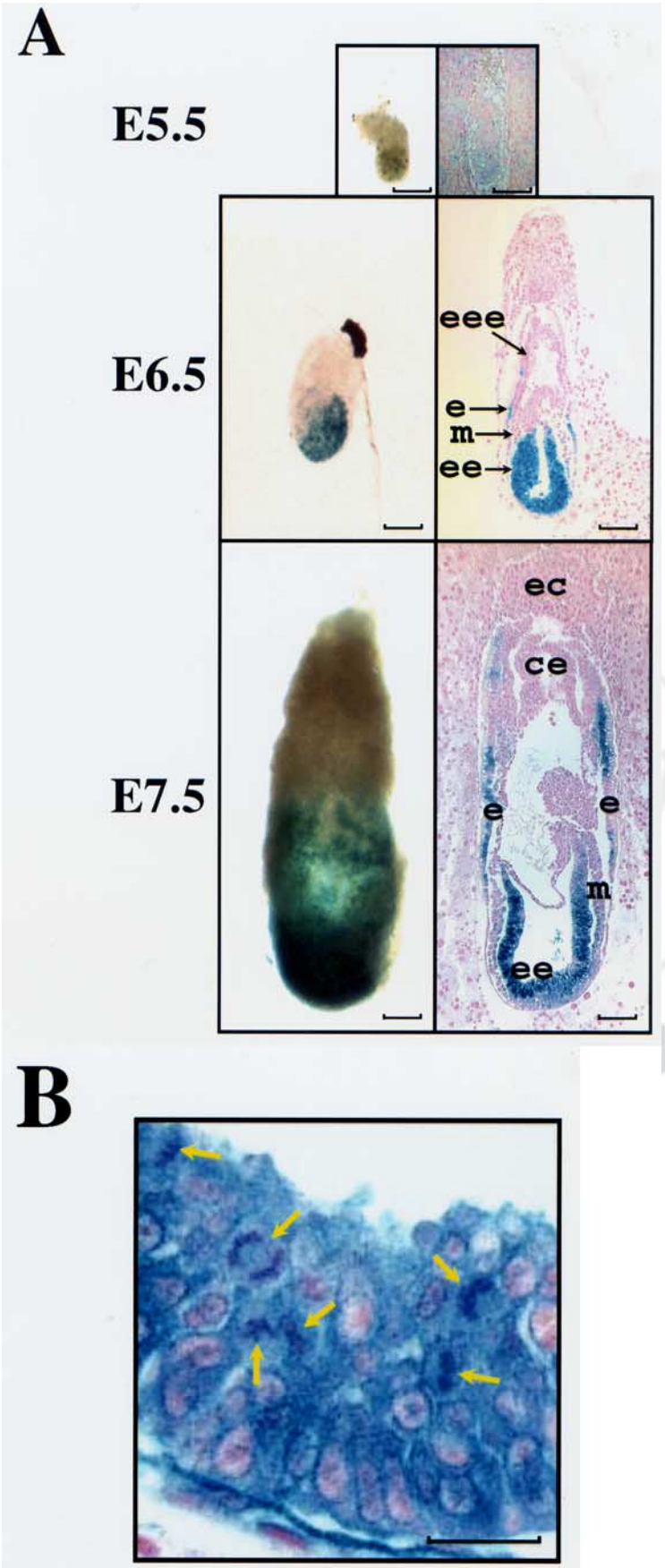

sense probe was compared with the antisense probe. The representative images of whole-mount RNA in situ hybridization of E7.5 embryos are shown in Figure 3. *Nf2* RNA expression was readily detected throughout the embedded embryo and its surrounding decidua, when the antisense probe, derived from 3U1, was used. In contrast, the sense probe yielded little hybridization (compare Fig. 3A with 3B). To visualize what embryonic tissues expressed *Nf2* RNA, dissected embryos were used in the in situ hybridization experiment. High levels of *Nf2* RNA expression were detected in the embryonic tissues, particularly in the developing neural ectoderm (Fig. 3C). For comparison, we performed whole-mount X-gal staining of transgenic E7.5 embryos. As shown in Figure 3D, the β-gal staining pattern in the embryonic tissue was similar to the endogenous *Nf2* RNA expression pattern, exhibiting the strongest staining in the neural ectoderm. F3

In addition, we performed whole-mount RNA in situ hybridization and β-gal staining of E8.5 and E9.5 embryos. Similar to that observed in the E7.5 embryo, *Nf2* RNA expression was detected throughout the E8.5 embryo with the strongest expression in the developing neural tube (compared Fig. 4A with 4B). Also, *Nf2* RNA expression was detected in the allantois and the yolk sac (Fig. 4A). Consistent with the RNA in situ hybridization result, strong β-gal staining was seen in the embryonic tissues of transgenic E8.5 embryo, particularly in the neural tube (Fig. 4C), while no β-gal staining was found in the wild-type E8.5 embryo (Fig. 4D). It should be noted that at this stage, β-gal expression was detected in the allantois and the yolk sac, but was not seen in the ectoplacental cone (Fig. 4C). As the F4

Fig. 2. Expression of β-gal in transgenic E5.5–7.5 embryos. **A:** Images of whole mount X-gal stained transgenic embryos at E5.5–7.5. eee, extraembryonic ectoderm; ee, embryonic ectoderm; m, mesoderm; e, endoderm; ec, ectoplacental cone; ce, chorionic ectoderm. Bar = 100 μm. **B:** Tissue section revealed strong β-gal staining in mitotic cells from embryonic ectoderm of the E6.5 embryo. Tissue section was photographed at 400× magnification. Arrows point to mitotic cells. Bar = 10 μm.

tapraid5/z7h-devdyn/z7h-devdyn/z7h00906/z7h2000d06g | heckt | S=7 | 6/30/06 | 15:58 | Art: 050544R1

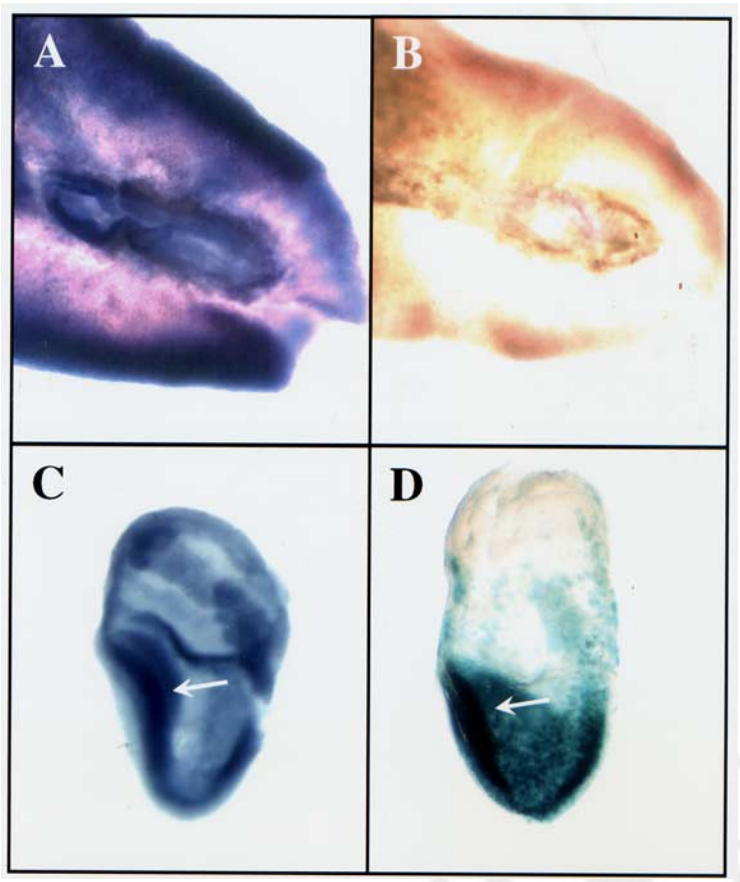

Fig. 3. Detection of endogenous *Nf2* RNA expression and β-gal staining in E7.5 embryos. Whole-mount RNA in situ hybridization of wild-type E7.5 embryos was performed using an antisense (**A,C**) or sense (**B**) *Nf2* 3U1 probe (Fig. 1) derived from the exon 17 region as described in the Experimental Procedures section. Compared to the results obtained from the sense probe control (B), strong *Nf2* RNA expression was detected in the embryo embedded in the decidua (A) or the dissected embryo (C), particularly in the developing neural ectoderm (arrow). Similarly, whole-mount X-gal staining showed strong β-gal expression in the developing neural ectoderm of the transgenic E7.5 embryo (**D**). The slight difference in the size and shape of the embryo shown in C and D was due to the procedures. The embryo processed for in situ hybridization was dehydrated with methanol, followed by proteinase K digestion and fixation. The embryo processed for β-gal was fixed in the fixation solution before X-gal staining. Nevertheless, the β-gal staining pattern in the embryonic tissue was similar to the endogenous *Nf2* RNA expression pattern.

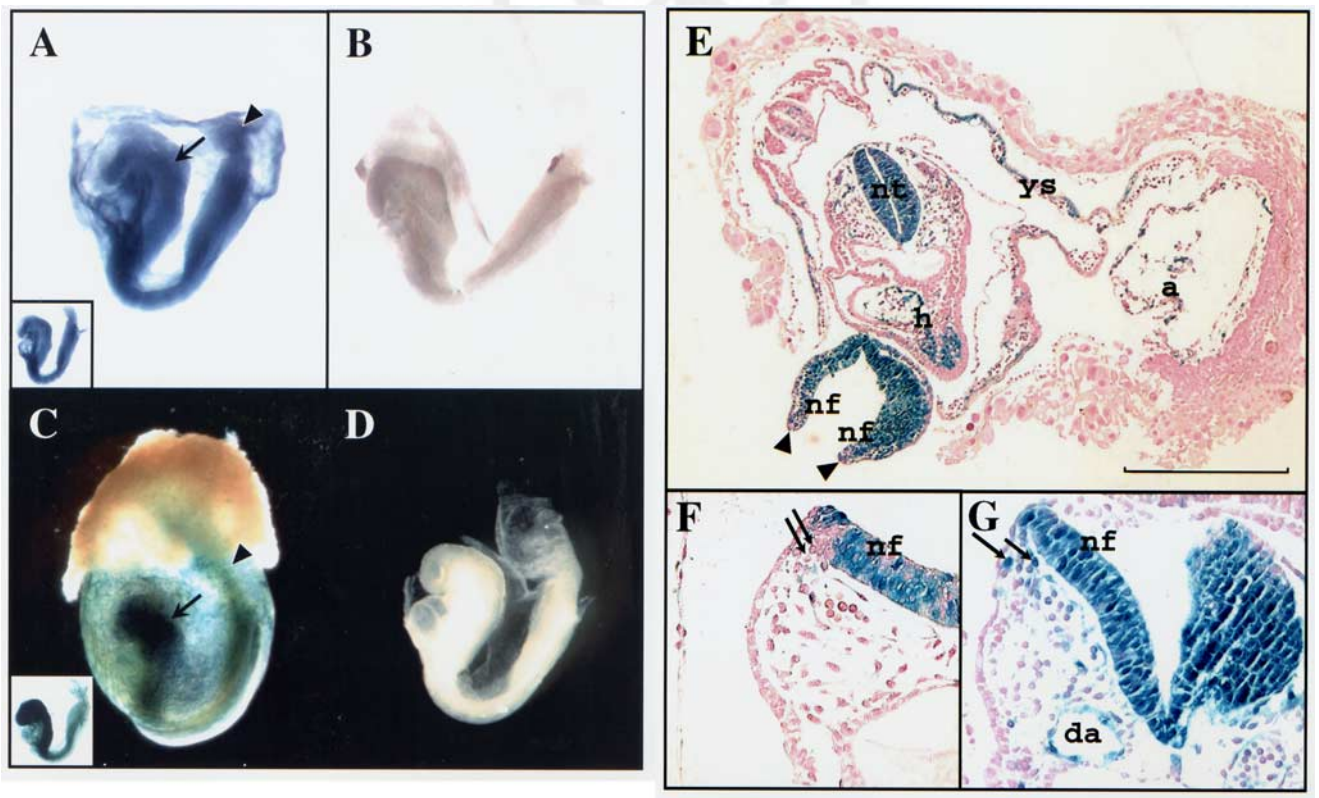

Fig. 4.

embryo matured to E9.5, *Nf2* RNA expression was consistently detected throughout the entire embryo with the strongest expression in the developing brain and spinal cord (compare Fig. 5A with 5B). The neural crest cell-populated branchial arches and the hematopoietic stem cell–containing paraaortic splanchnopleura also showed significant *Nf2* RNA expression (Fig. 5A). A similar β-gal staining pattern was detected in the transgenic E9.5 embryo (Fig. 5C). The tissues that gave rise to the strongest β-gal staining included the brain, spinal cord, and heart regions, the branchial arches, and the paraaortic splanchnopleura along with the dorsal aorta. Taken together, these results indicate that the β-gal staining pattern qualitatively matches most of the *Nf2* RNA distribution pattern, particularly in the embryonic tissues.

Changes in NF2 Promoter Activity During Neural Crest Cell Migration

Around E8.5, which is the early stage of organogenesis, the neural ectoderm-derived neural plate folds into the neural tube. Examination of β-gal-expressing cells in the E8.5 transgenic embryo section detected the highest level of expression in the neural tube, particularly in the rostral end, and the intensity of the β-gal staining gradually decreased toward the caudal extremity (Fig. 4E). Intriguingly, cells in the dorsal ridge of the neural folds in the cranial region and its adjacent non-neural ectoderm were only modestly stained (arrowheads pointed to this region in Fig. 4E). Previous studies have shown that the neural crest cells arise in the neural folds at the border between the neural and non-neural ectoderm (Hogan et al., 1994; LeDouarin and Kalcheim, 1999). Although initially contained within the central nervous system, the neural crest cells depart from the site of origin, migrate extensively throughout the embryo, and form many diverse derivatives including most of the peripheral nervous system, facial skeleton, and melanocytes of the skin. A detailed analysis of transversal sections of the anterior neural tube from transgenic embryos at around E8.5 revealed that while β-gal staining was detected in the neural folds, little staining was seen in the round-shaped neural crest cells that were in the process of delaminating from the dorsal ridge region of the neural fold (Fig. 4F). However, significant β-gal staining was detected in the neural crest cells already migrating away from the dorsal neural tube (Fig. 4G). Blue-stained cells were detected along the putative pathways of neural crest cell migration particularly in the dorsal trunk mesenchyme beneath the ectoderm and between the somite and neural tube (Fig. 4E and G; also see below). A number of markers on neural crest cells have been used to trace their migration. Among them, the Sox9 transcription factor is important for neural crest induction, survival, and delamination (Cheung and Briscoe, 2003; Mori-Akiyama et al., 2003). Interestingly, we observed abundant Sox9 protein expression in the migrating neural crest cells (Fig. 6A,B). Substantial β-gal expression was observed in the endocardium of the heart (Fig. 4E) and within the wall of the dorsal aorta (Fig. 4G). β-gal staining was also found in the yolk sac and allantois (Fig. 4E). At this embryonic stage, the yolk sac consists of an endodermal epithelium and underlying mesoderm within which blood islands and vessels develop. Significant β-gal expression was detected in the endodermal epithelium of the yolk sac and some labeled cells were seen within the blood island.

Upon examination of tissue sections of the transgenic E9.5 embryos, highly labeled cells continued to be detected in the neural tube. Within the neural tube, high levels of β-gal activity were found in the developing forebrain, midbrain, and hindbrain (Fig. 5C.D). As reported previously (LeDouarin and Kalcheim, 1999), the neural crest–derived cells from the posterior midbrain and hindbrain region migrate ventrolaterally and densely populate the first, second, and third branchial arches. Significant β-gal expression was seen in the cells of the craniofacial mesenchyme and the first branchial arch in the pharyngeal region (Fig. 5D). The entire mesenchymal component of the branchial arch, which was derived from the neural crest cells, was highly labeled, whereas the epithelium covering the branchial arch and the foregut endoderm were not labeled. Strong β-gal staining was also detected in the paraaortic splanchnopleura, and the heart region and the dorsal aorta were also positive for β-gal staining (Fig. 5D).

The Most Intense β-gal Staining Was Detected Along the Dorsal Midline of the Neural Tube

Whole-mount embryo staining showed that the *NF2* promoter-directed β-gal expression was predominantly observed in the anterior part of the transgenic embryo at E9.5 (Fig. 7A). The β-gal staining extended to the

Fig. 4. The *Nf2* RNA expression and β-gal staining pattern in E8.5 embryos. **A–D:**The pattern of strong *Nf2* RNA expression in the developing neural tube of the wild-type E8.5 embryo was confirmed by the β-gal staining of the E8.5 transgenic embryo. Whole-mount RNA in situ hybridization of wild-type E8.5 embryos was performed using an antisense (A) or sense (B) *Nf2* probe as described in Figure 3. Whole-mount X-gal staining was also performed on transgenic (C) or non-transgenic (D) E8.5 embryos. Note that the developing neural tube (arrow) showed strong *Nf2* RNA or β-gal expression. In addition, *Nf2* expression was also detected in the allantois (arrowhead). The small photograph inset in A and C displays the dissected embryo from in situ hybridization and β-gal staining analysis, respectively. **E–G:** Change of *NF2* promoter activity during neural crest cell migration. **E:** A transverse section of the transgenic E8.5 embryo showed significant β-gal expression in neural fold (nf) of the head region, the developing neural tube (nt) and heart (h), as well as yolk sac (ys) and allantois (a). Note that the tip (arrows) of the neural fold displayed weak β-gal staining compared to the rest of the neural fold, which exhibited strong β-gal activity. Bar = 100 μm. **F,G:** Detailed analysis of tissue sections containing the neural fold region revealed that while little β-gal staining was found in the round-shaped neural crest cells (arrows), which were at the moment of delaminating from the dorsal ridge region of the neural fold (F), significant β-gal expression was detected in the neural crest cells already migrating away from the dorsal neural tube (G). da, dorsal aorta.

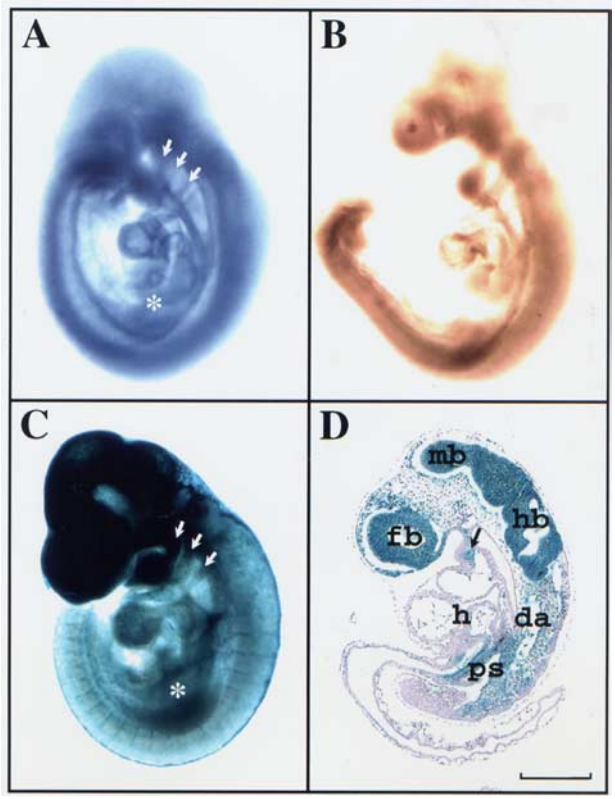

Fig. 5.

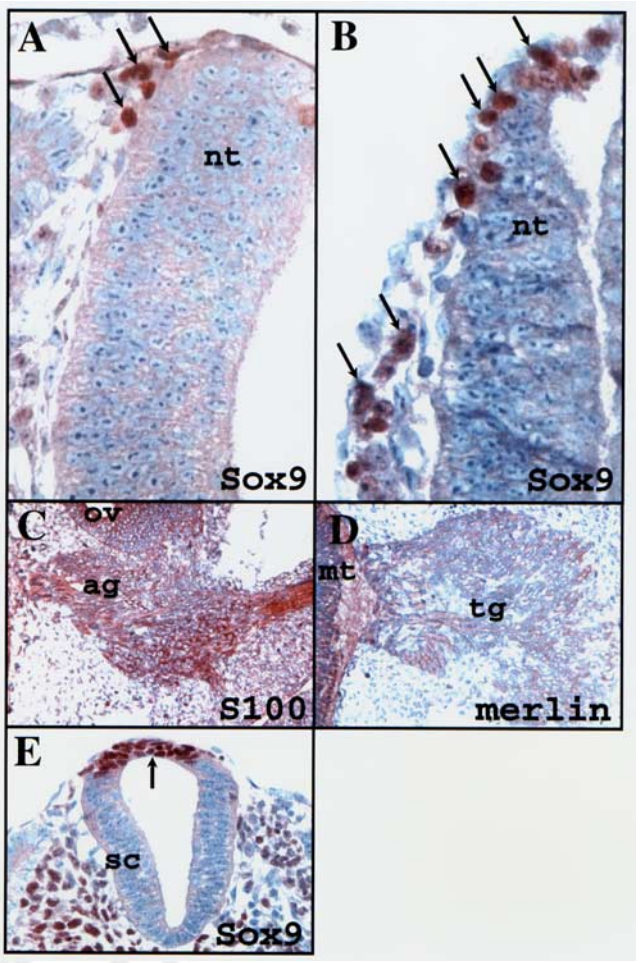

Fig. 6.

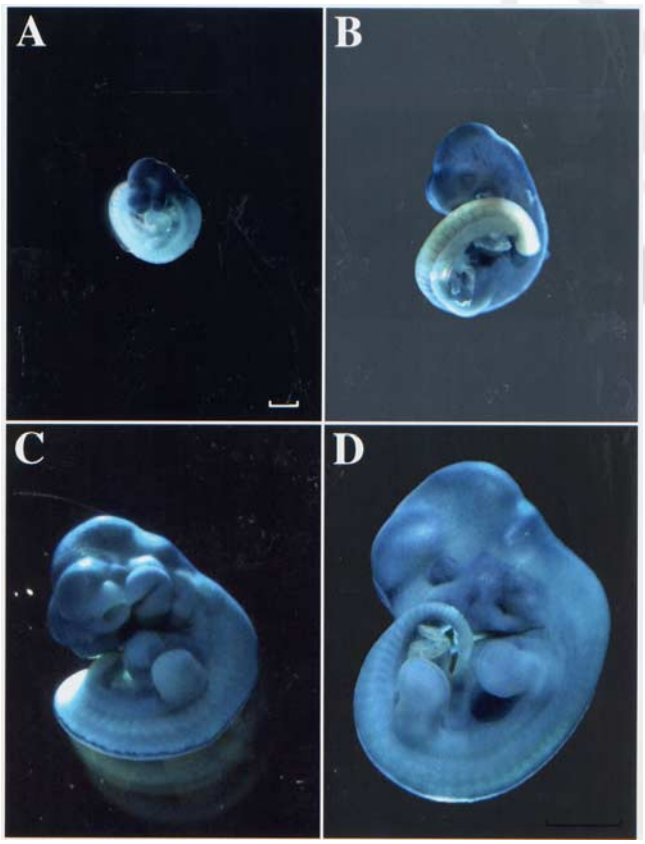

Fig. 7.

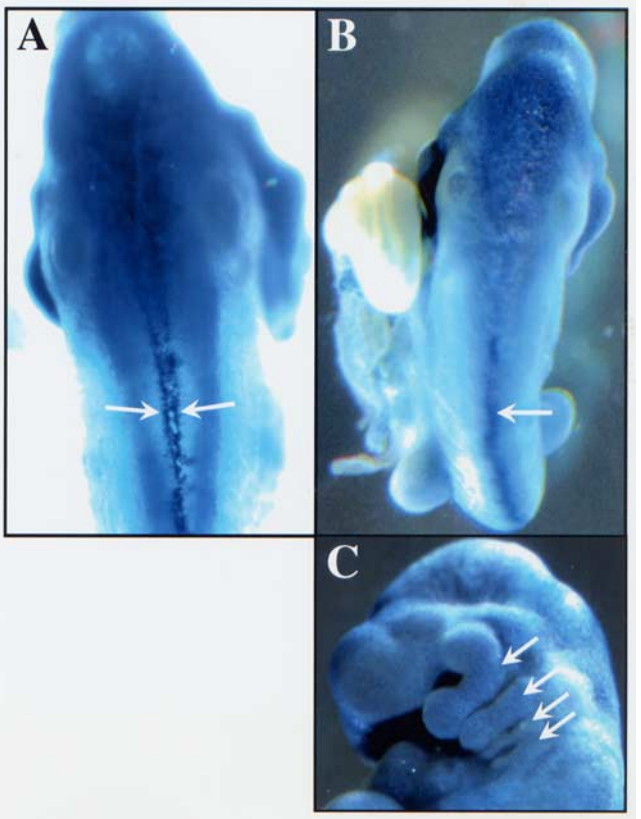

Fig. 8.

posterior extremity as the embryo matured from E10.5 to E14.5 (Fig. 7B–D). By E14.5, extensive β-gal expression was detected throughout the embryo (Fig. 7D).

Previous studies (Rugh, 1994; Wallingord, 2005) indicate that the neural tube begins to close at E8.5 from multiple sites in the middle portion of the embryo and extends toward the anterior and posterior ends in a zipper-like fashion. By E9.5, most parts of the neural tube have already closed, and only small openings, called neural pores, are left in both the anterior and posterior ends of the embryo. We found that the most intense β-gal staining was located along the dorsal midline, the line of the neural tube closure, in the E9.5 embryo (Fig. 8A). Deep staining was observed particularly in the area of the anterior neuropore, forming the fourth brain ventricle, also known as myelocoel. By E10.5, the anterior neuropore is completely closed (Rugh, 1994; Wallingord, 2005). Intense β-gal staining was still observed at the site of the thin roof of the fourth ventricle and along the dorsal midline of the neural tube (Fig. 8B). Consistent with those observed at the earlier stages of development, strong β-gal expression was detected in the branchial arches I–IV of the E10.5 embryo (Fig. 8C).

Strong β-gal Expression in the Embryonic Ectoderm-Derived Tissues

In tissue sections of the E10.5 embryo, very intense β-gal labeling was noted in the tela choroidea, which is the thin roof of the fourth ventricle (Fig. 9A). This roof plate consists of a single layer of ependymal cells, which is later covered by the pia mater, the inner layer of the meninges (Rugh, 1994). Significant β-gal expression was detected in the metencephalon and the myelencephalon. In addition, strong β-gal staining was found in the forebrain, including the telencephalon and the diencephalon, the optic chiasma, the tuberculum posterius, and the infundibulum (Fig. 9B). However, only some parts of the mesencephalon were darkly stained while others were lightly stained. In the head region, the epidermal layer, which contains presumptive melanocytes, was also labeled (Fig. 9A).

The retina is the innermost layer of the eye and is derived embryologically from the outgrowth of the developing brain (Martinez-Morales et al., 2004). It is comprised of two major layers, the inner layer (prospective neural layer of the retina) and the outer layer (prospective pigmented epithelium). In the E10.5 transgenic embryo, intense β-gal staining was readily detected in the pigmented epithelium layer of the retina, whereas the neural layer of the retina and the lens show very little expression (Fig. 9C).

As noted above, strong β-gal activity was detected in the mesenchyme of the mandible prominence of the first branchial arch in the E10.5 transgenic embryo (Fig. 9D). The adjacent neural crest cells populating the truncus arteriosus also showed intense labeling. In addition, significant β-gal expression was found in the paraaortic mesenchyme and the heart region. Furthermore, the dorsal aspect of the forming spinal cord and its flanking primordial spinal ganglia were strongly labeled. Together, these results indicate that the *NF2* promoter is strongly expressed in various embryonic ectoderm-derived tissues.

NF2 Promoter-Directed β-gal Expression to the Trigeminal Ganglion and Acoustic Ganglion

At E11.5, the forebrain is separated into a paired telencephalic vesicles and the diencephalon. We observed high levels of β-gal activity in both lobes of the telencephaon and in the diencephalon of the E11.5 transgenic embryo (Fig. 10A). However, the midbrain mesencephalon was only lightly stained with the exception of the dorsal midline closure, which consistently displayed intense staining similar to those seen at earlier stages. Interestingly, we detected a striped pattern of β-gal staining in the hindbrain-derived myelencephalon (Fig. 10B) and the metencephalon (also see below). β-gal expression can also be found in the cranial ganglion VIII, derived from the hindbrain and also known as the acoustic ganglion, and its extending nerve. The β-gal staining was particularly notable in the cells surrounding the acoustic ganglion and extending nerve (Fig. 10B). It should be mentioned that the extending nerve expressed a higher level of S100 immunoreactivity than the ganglion (Fig. 6C). Some of the cells inside the ganglion also expressed β-gal (Fig. 10B). In addition, strong β-gal staining was detected in the cranial ganglion V, which is also called the trigeminal ganglion; both the trigemi-

Fig. 5. Strong *Nf2* RNA expression and β-gal staining were detected in the developing brain, the branchial arches, and the paraaortic splanchnopleura of E9.5 embryos. In situ hybridization of wild-type E9.5 embryos was performed using an antisense (**A**) or sense (**B**) *Nf2* probe as described before. Whole-mount X-gal staining was also performed on transgenic E9.5 embryos (**C**). Sagittal section of the β-gal stained embryo was obtained (**D**). Arrows point to neural crest cell populated branchial arches and the asterisk marks the location of the paraaortic splanchnopleura. fb, forebrain; mb, midbrain; hb, hindbrain; h, heart; da, dorsal aorta; ps, paraaortic splanchnopleura. Bar = 200 μm.

Fig. 6. Immunohistochemical analysis of tissue sections from E9 (**A,B**) and E11.5 embryos (**C–E**). Tissue sections were stained with anti-Sox9 (A,B,D), anti-S100 (C), and anti-merlin (E) antibodies according to the Experimental Procedures section. A hematoxylin was used as a counterstain. The positively stained tissue appeared brown. Arrows point to migrating neural crest cells (A,B) or dorsal midline of the neural tube closure (D). nt, neural tube; sc; spinal cord, ag, acoustic ganglion; ov, otic vesicle; mt, metencephalon; tg, trigeminal ganglion.

Fig. 7. Lateral views of whole-mount X-gal-stained transgenic mouse embryos at various days p.c. (**A**) E 9.5, (**B**) E10.5, (**C**) E12.5, and (**D**) E14.5. Bar = 400 μm.

Fig. 8. The most intense β-gal expression was detected along the dorsal closure (arrows) of neural tube in E9.5 (**A**) and E10.5 (**B**) transgenic embryos. Strong β-gal expression was also seen in the Branchial arches I–IV (arrows) of the E10.5 embryo (**C**).

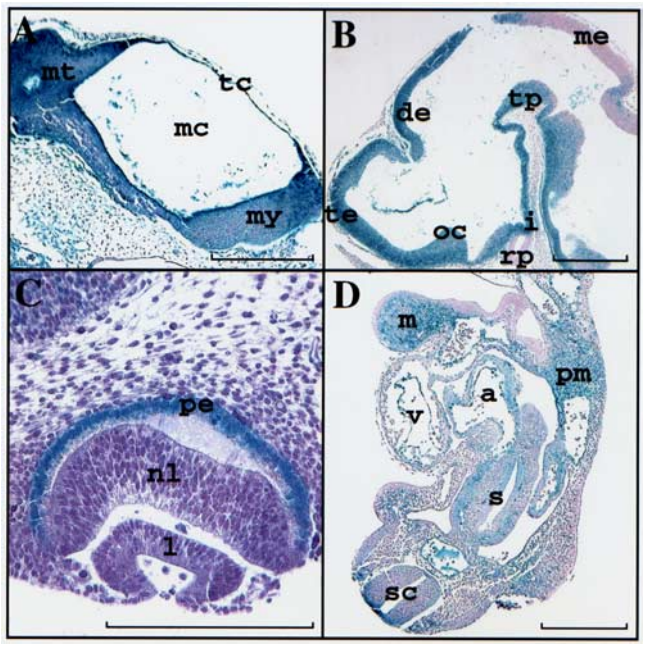

Fig. 9.

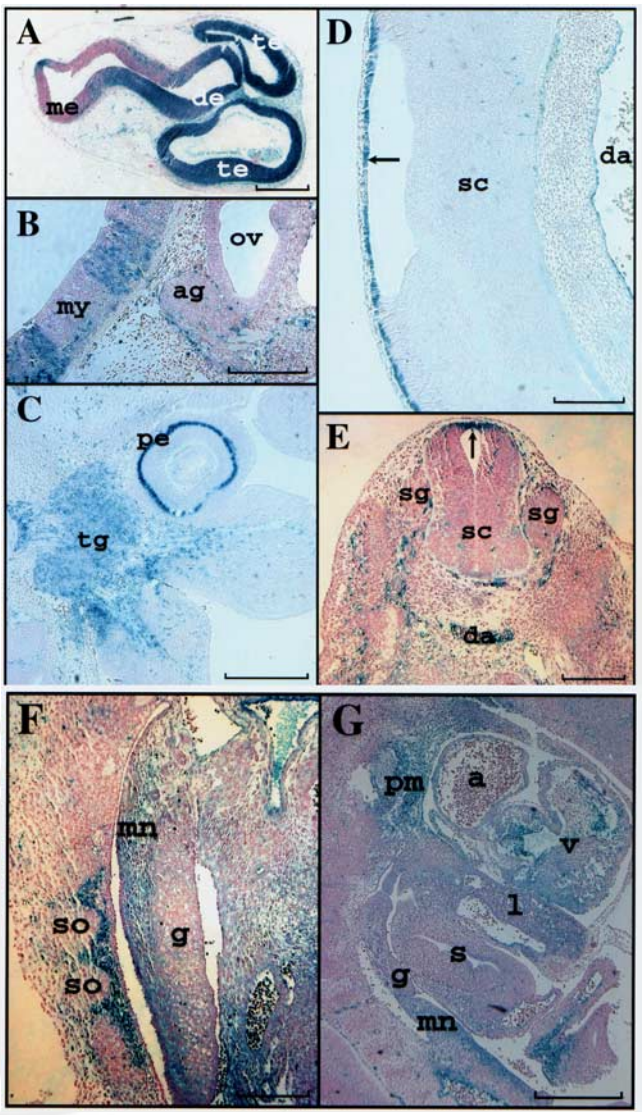

Fig. 10.

Fig. 9. Strong β-gal staining in the neural ectoderm-derived tissues of E10.5 transgenic embryos. **A:** Intense β-gal staining was detected in the metencephalon (mt), the tela choroidea (tc), and the myelencephalon (my). mc, myelocoel. Bar = 400 μm. **B:** Sagittal section of the head region revealed strong β-gal expression in the telencephalon (te), the diencephalon (de), the optic chiasma (oc), the tuberculum posterius (tp), and the infundibulum (i). Striped pattern of β-gal staining was seen in the mesencephalon (me), while little or no expression was detected in the Rathke's pocket (rp). Bar = 200 μm. B,D: Parasagittal sections. **C:** Sagittal section of the eye showed that the prospective pigmented epithelium (pe) of retina displayed robust β-gal staining, while the neural layer (nl) of the retina and the lens (l) exhibited very little expression. Bar = 100 μm. **D:** Significant β-gal expression was detected in the mandible prominence of the first branchial arch (m), the paraaortic mesenchyme (pm), the atrium (a) and the ventricle (v) of the heart, and the dorsal aspect of the spinal cord (sc). Some β-gal expression was seen in the stomach region (s). Bar = 400 μm.

Fig. 10. Significant *NF2* promoter activity was detected in various NF2-affected tissues such as the acoustic ganglion, the trigeminal ganglion, the spinal ganglia, and the pigmented epithelium of the retina in transgenic E11.5 embryos. A,E,F: Transverse sections. B–D,G: Sagittal sections. **A:** Strong β-gal expression was detected in the telencephalon (te) and the diencephalon (de). me, mesencephalon. Bar = 500 μm. **B:** The myelencephalon (my) showed a striped pattern of β-gal expression. The peripheral region of the acoustic ganglion (ag; cranial ganglion VIII) and its extending nerve also stained positive for β-gal expression. ov, otic vesicle. Bar = 250 μm. **C:** Intense β-gal expression was found in the pigmented epithelium (pe) of the retina. Also, strong β-gal expression was seen in the trigeminal ganglion (tg; cranial ganglion V) and its nerve branches. Bar = 250 μm. **D:** Robust β-gal staining continued to be seen along the dorsal midline (arrow) of the spinal cord (sc). Positive β-gal staining was also detected in the wall of the dorsal aorta (da). Bar = 200 μm. **E:** Strong β-gal expression was found in the dorsal aspect (arrow) of the spinal cord (sc). Positive β-gal staining was also detected along the dorsolateral and late ventral pathways of neural crest cell migration surrounding the spinal ganglion (sg). da, dorsal aorta. Bar = 300 μm. **F:** The sclerotome of somites showed strong β-gal expression. While the mesonephros (mn) exhibited positive β-gal staining, the gonad (g) showed little expression. Bar = 200 μm. **G:** Significant β-gal expression was observed in the paraaotic mesenchyme (pm), the heart, particularly the endocardium including the valves, the liver (l), and the mesonephros (mn). a, atrium; v, ventricle; pn, pronephros; s, stomach; g, gonad. Bar = 500 μm.

nal ganglion and its three nerve divisions were robustly labeled (Fig. 10C). Consistent with the β-gal staining, immunostaining revealed that merlin was expressed throughout the trigeminal ganglion (Fig. 6D). Similar to that seen at E10.5, very intense β-gal staining was seen in the pigmented epithelium of the retina (Fig. 10C).

As noted before, the dorsal midline of the spinal cord from the E11.5 embryo was darkly stained for β-gal expression; however, only a few cells inside the spinal cord were labeled (Fig. 10D,E). Interestingly, we noted that the cells in the dorsal midline of neural tube closure expressed a high level of Sox9, a neural crest determinant marker (Fig. 6E). β-gal staining was detected in the cells surrounding the spinal ganglia and in some, but few, cells inside the spinal ganglia. It appeared that the cells along the ventral and dorsolateral pathways of neural crest cell migration were labeled (Fig. 10E). The sclerotome of somites has been shown to play an essential role in neural crest migration of the early ventral pathway (Hogan et al., 1994; Chen et al., 2004; Hay 2005; Honjo and Eisen, 2005). Significantly, we also detected deep β-gal staining in the sclerotome (Fig. 10F).

In addition to intense β-gal staining in the dorsal aorta as seen in earlier stages, the paraaortic mesenchyme were strongly labeled at E11.5 (Fig. 10G). Within the four-chambered heart, the endometrial tissue, including the valves, showed the highest β-gal activity. Intervertebral arteries were also labeled. While some β-gal was expressed in the liver and mesonephros, only weak staining was detected in the gonad (Fig. 10F,G).

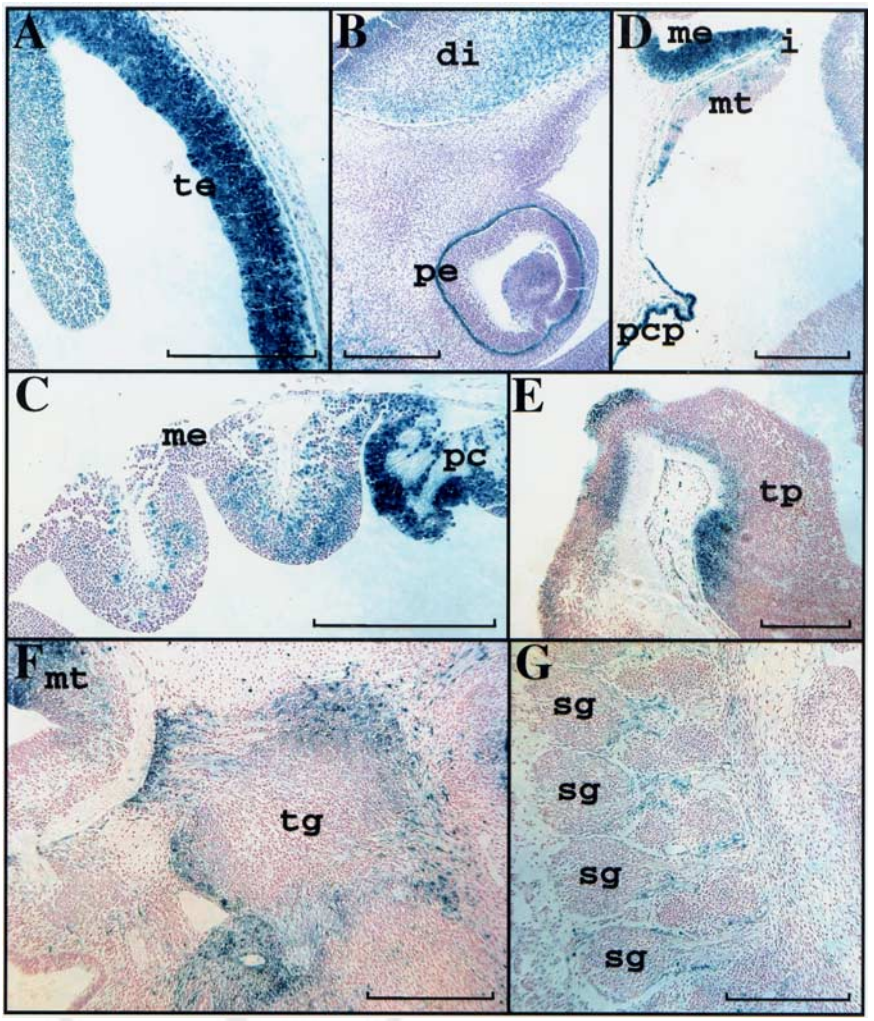

Fig. 11. The β-gal staining pattern in various neural tissue sections from transgenic E12.5 embryos. Whole-mount X-gal stained embryos were prepared and sagittal sections were obtained as described before. **A:** Intense β-gal expression was found in the telencephalon (te). **B:** Deep β-gal staining continued to be detected in the pigmented epithelium of the retina (pe). di, diencephalon. **C:** Strong β-gal staining was observed in the posterior commissure (pc) compared to that in the mesencephalon (me), which showed patchy expression. **D:** The tela choroidea-derived posterior choroid plexus (pcp) in the 4th ventricle area was deeply labeled. me, mesencephalon; i, isthmus; mt, metencephalon. **E:** Only certain areas in the tuberculum posterius (tp) were positive for β-gal staining. **F:** Significant β-gal expression was also observed in the trigeminal ganglion (tg) and its nerve divisions. mt, metencephalon. **G:** Cells surrounding the spinal ganglia (sg) and their extending nerves continued to show β-gal staining. Bar = 300 μm.

Broad β-gal Expression Pattern in Various Neural Tissues During Mid-Embryogenesis

At E12.5, the anterior portion of the telencephalon continued to express high levels of β-gal, while the staining in the posterior part was less saturated (Fig. 11A). Similarly, some portions of the diencephalon expressed significant levels of β-gal, whereas other regions were weakly stained (Fig. 11B). Curiously, the pigmented epithelium of the retina continued to be intensely labeled at this stage. The lens epithelium and some cells in the lens also expressed moderate levels of β-gal.

The posterior commissure is the roof of the brain between the anterior limit of the mesencephalon and the posterior portion of the diencephalon. Saturated β-gal staining was observed in the posterior commissure, while only patchy staining was seen in the rest of the mesencephalon (Fig. 11C). However, it appeared that more labeled cells were present in the mesencephalon proximal to the posterior commissure. The isthmus or mesencephalon-metencephalon junction tissue is an organizing center that plays an important role in the midbrain-hindbrain patterning (Wassef and Joyner, 1997). Intriguingly, intense β-gal staining was found in the isthmic tissue of the mesencephalic part (Fig. 11D). In contrast, the metencephalic portion of this junction tissue showed a striped β-gal staining pattern, similar to that of the rest of the metencephalon. Consistent with robust β-gal expression in the tela choroidea observed at earlier stages, the tela choroidea-derived posterior choroid plexus was strongly labeled in the E12.5 embryo. The tuberculum posterius is a thickening in the floor of the brain at the region of the anterior end of the notochord. It represents the posterior margin of the diencephalon and

develops into a part of the hypothalamus. We noted that some discrete regions of the tuberculum posterius showed high levels of β-gal activity, while some other parts expressed notably smaller amounts of β-gal (Fig. 11E). At this stage, significant β-gal staining was still seen in the trigeminal ganglion and its nerve divisions; however, unlike the strong labeling throughout the entire ganglion observed at E11.5, the central part of the trigeminal ganglion from the E12.5 embryo appeared to show little β-gal staining (Fig. 11F). Interestingly, the synaptic junction area between the trigeminal ganglion and the hindbrain remained strongly labeled (Figs. 10C and 11F). In addition, similar to that noted at E11.5, cells surrounding spinal ganglia and their extending nerves continued to show significant β-gal expression in the E12.5 embryo (Fig. 11G). Taken together, these results indicate that the *NF2* promoter is widely expressed in neural tissues during embryogenesis.

DISCUSSION

The development of schwannomas on or around the vestibular branch of both eighth cranial nerves has been considered as the hallmark of NF2, but other tumors and ocular abnormalities are observed as well (Neff et al., 2005). Most NF2 patients go on to develop multiple schwannomas that are associated with other cranial nerves, such as the trigeminal nerve and the spinal nerve roots. In addition, cranial and spinal meningiomas and, less frequently, ependymomas occur. Such restricted symptoms and phenotypes associated with NF2 are unusual, given the fact that the *NF2* tumor suppressor protein is widely expressed in many cell types. In this report, we showed that the *NF2* promoter was active at early embryogenesis. *NF2* promoter–directed β-gal expression was detected as early as E5.5 and intense β-gal staining was observed at E6.5 in the embryonic ectoderm containing many mitotic cells. In addition, *NF2* promoter activity was detected in parts of the embryonic endoderm and mesoderm. *NF2* promoter continued to be actively expressed in the neural ectoderm and its derived neural tissues throughout mid-embryogenesis. These results are consistent with earlier findings (Gutmann et al., 1994; McClatchey et al., 1997; Stemmer-Rachamimov et al., 1997) and further indicate that *NF2* is an early expression marker.

Currently, limited information is known about the role of merlin during embryonic development and tissue differentiation. In mice, homozygous *Nf2* inactivation is embryonically lethal (McClatchey et al., 1997). Although these results suggest an essential role for *NF2* during early embryogenesis, the function of merlin in these processes is not understood. Merlin has been shown to regulate cell motility and cell adhesion. In cultured mammalian cells, merlin is concentrated in the membrane ruffle and adherens junction (Gonzalez-Agosti et al., 1996; Shaw et al., 1998; Maeda et al., 1999; Lallemand et al., 2003). In cultured polarized neurons, merlin localizes to synaptic junctions (Gronholm et al. 2005). Merlin can associate with the actin cytoskeleton directly (Xu and Gutmann, 1998) or indirectly by interacting with actin-binding proteins (Scoles et al., 1998; Fernandez-Valle et al., 2002). Re-expression of merlin in *Nf2*-deficient cells attenuates actin cytoskeleton-associated processes, including motility (Gutmann et al., 1999). In addition, overexpression of merlin mutants alters cell adhesion, causing fibroblasts to detach from the substratum (Stokowski and Cox, 2000). Also, *Nf2* deficiency results in an inability of mouse fibroblasts or keratinocytes to undergo contact-dependent growth arrest and to form stable cadherin-containing cell:cell junctions (Lallemand et al., 2003). Merlin may stabilize adherens junctions by inhibiting Rac/Pak signaling and stabilizing the actin cytoskeleton (Shaw et al. 2001; Kissil et al., 2002; Xiao et al., 2002; McClatchey and Giovannini, 2005). Moreover, *Nf2*-deficient mouse tumor cells are highly motile and metastatic in vivo (McClatchey et al., 1998). Together, these results suggest that merlin may participate in fundamental processes involving the regulation of cell migration, cell adhesion, and cell proliferation during embryonic development.

It has been well documented that during embryogenesis, many cells and tissues undergo complex morphogenetic movements, such as neural crest and progenitor germ cell migration, migration of hematopoietic progenitors into the embryonic hematopoietic rudiments, and neural tube closure (Graham, 2003; Bertrand et al., 2005; Wallingford, 2005); however, the underlying cellular and molecular mechanisms are poorly understood. Studies have shown that cell migration is highly regulated and involves the extension of leading processes, where continuous remodeling of actin and adhesive contacts is required (Li et al., 2005). Interestingly, we observed strong *NF2* promoter activity in sites where migrating cells were located including the neural tube closure, the branchial arches, the dorsal aorta, and the paraaortic splanchnopleura. The most intense activity was detected along the dorsal midline during neural tube closure, the location where the adhesion and fusion of two opposing neural folds and epithelial sheets occur. Similarly, high levels of *NF2* promoter activity were seen at the site of the anterior neuropore closure in the head region. Notably, McLaughlin et al. (2004) recently generated conditional *Nf2* knockout mice in which *Nf2* was deleted throughout the developing central nervous system by using nestin promoter-driving *Cre* recombinase. These mice displayed defects in neural tube closure and tissue fusion. It is known that cell adhesion during dorsal closure relies on the activities of the dynamic actin-based protrusions (Jacinto et al., 2002; Woolner et al., 2005). Since merlin localizes to membrane ruffles and adherens junctions (Gonzalez-Agosti et al., 1996; Shaw et al., 1998; Maeda et al., 1999) and plays critical roles in cell motility and cell adhesion (Gutmann et al., 1999; Stokowski and Cox, 2000; Lallemand et al., 2003), the most intense *NF2* promoter activity along the dorsal midline and at the site of anterior neuropore closure that we detected suggests that merlin may be necessary for cytoskeletal machinery driving cell adhesion and movement during neural tube closure.

In addition, it is tempting to speculate that merlin may participate in neural crest cell migration. The neural crest comprises a group of highly motile cells, which are the precursors of peripheral neurons, Schwann cells,

pigment and facial cartilage cells (LeDouarin and Kalcheim, 1999; Jessen and Mirsky. 2005). Intriguingly, we detected little *NF2* promoter activity in premigratory neural crest cells and the round-shaped neural crest cells, which had just delaminated from the dorsal ridge region of the neural fold. On the contrary, significant *NF2* promoter activity was found in the neural crest cells already migrating away from the dorsal neural tube. Such a transient change of *NF2* promoter activity implies a transcriptional regulation during neural crest cell migration and further corroborates with the role of merlin in cell motility and cell adhesion (McClatchey, 2004; McClatchey and Giovannini, 2005). It is possible that down-regulation of *NF2* promoter expression may allow premigratory neural crest cells to delaminate from the dorsal neural tube. Once migrating away, the neural crest cells turn on the *NF2* gene to ensure cell migration and cell adhesion in order to colonize different parts of the embryo. Recently, several developmentally regulated transcription factors have been implicated in the control of neural crest induction and delamination (Cheung et al., 2005). Thus, it will be important to see whether these transcription factors regulate *NF2* promoter expression during neural crest cell migration.

Analogously, the *NF2* promoter was highly expressed in hematopoietic stem cell–producing tissues such as the yolk sac and the paraaortic mesenchyme. This mesodermally derived intraembryonic region, known as the aorta-gonad-mesonephros region or, at a slightly earlier developmental stage, the paraaortic splanchnopleura, produces, respectively, potent hematopoietic stem cells and multipotent progenitor cells in addition to the yolk sac (Bertrand et al., 2005). The strong *NF2* promoter activity in these hematopoietic stem cell–producing tissues suggest that merlin may also play a role in the migration of hematopoietic progenitors into these embryonic hematopoietic rudiments including fetal liver, thymus, spleen, and bone marrow during embryonic development.

As mentioned above, in addition to vestibular schwannomas, most NF2 patients develop multiple schwannomas that are associated with trigeminal nerve and spinal nerve roots, and less commonly, meningiomas and ependymomas (McClatchey, 2004; McClatchey and Giovannini, 2005; Neff et al., 2005). We detected significant *NF2* promoter activity in all these affected tissues during embryonic development. In particular, very intense promoter activity was noted in the tela choroidea, which consists of a layer of ependymal cells covered by the meninges.

Significant *NF2* promoter activity was also seen in the acoustic ganglion, trigeminal ganglion, spinal ganglia, and their extending nerves. Furthermore, NF2 patients frequently suffer from juvenile lens opacities and a variety of retinal and optic nerve lesions including defects of the pigment epithelium and pigment epithelial retinal hamartomas (Evans et al., 1992; Parry et al., 1994; Meyers et al., 1995; Hazim et al., 1998; Levine and Slattery, 2003). Consistent with previous observations (Claudio et al., 1995; Huynh et al., 1996), we detected some *NF2* promoter activity in the lens. Strong promoter activity was also seen in the optic chiasma. In the retina, *NF2* promoter is highly expressed in the pigmented epithelium. The fact that the *NF2* promoter is very active in the tissues affected by NF2 during embryonic development further supports the role of merlin in the pathogenesis of this genetic disorder.

It should be noted that the 2.4-kb *NF2* promoter appeared to be sufficient to recapitulate most of the endogenous *Nf2* RNA expression pattern in the embryonic tissues during embryogenesis, as we compared the β-gal staining pattern with the results from the RNA in situ hybridization (Figs. 3–5; McClatchey et al., 1997; McLaughlin et al., 2004). A detailed comparison with embryo sections from in situ hybridization analysis will strengthen this conclusion. However, while the 2.4-kb *NF2* promoter could direct β-gal expression to some extraembryonic tissues such as allantois and yolk sac, no expression was detected in the ectoplacental cone and chorionic ectoderm in transgenic embryos at E6.5–7.5, the time when *Nf2* knockout mice show defects in extraembryonic tissues. We hypothesize that additional elements located in the upstream or downstream region of the *NF2* promoter are required for proper expression in these extraembryonic tissues.

Previously, we (Welling et al., 2000; Chang et al., 2002) showed that while multiple elements are required for full *NF2* promoter activity in transfected cells, a GC-rich sequence, which was located in the promoter proximal region and could be bound by transcription factor Sp1, served as a positive *cis*-acting regulatory element. We are presently conducting experiments to test whether the GC-rich sequence and other *cis*-acting regulatory elements are important for the spatial and temporal expression pattern of the *NF2* promoter. Understanding of the regulation of the *NF2* gene in vivo may provide us new clues regarding merlin's participation in cell migration and cell adhesion during embryonic development.

EXPERIMENTAL PROCEDURES

Transgene Construct and Transgenic Production

The pNF2P(-2092)-Luc plasmid containing the 2.4-kb human *NF2* promoter was described previously (Chang et al., 2002). The MFG-S-nlsLacZ retroviral vector was kindly provided by Dr. Bruce Bunnell (Imbert et al., 1998). To generate the pNF2P(-2092)-nlsLacZ construct, the luciferase expression unit was removed from pNF2P(-2092)-Luc and substituted with the LacZ gene, which contained a nuclear localization signal (nlsLacZ) and was excised from MFG-S-nlsLacZ vector. Subsequently, the splicing signal and the polyadenylation signal sequences isolated from pSV2-βG (Chang et al., 1989) were inserted downstream of the nlsLacZ sequence (Fig. 1A).

The *NF2* promoter-driven nls-*LacZ* expression cassette was excised from the pNF2P2.4-nls-LacZ plasmid by double digestions with *Not*I and *Sal*I enzymes. The *NF2* promoter-nls-LacZ DNA fragment was purified through a Qiaquick Gel Extraction kit (Qiagen, Chatsworth, CA) and microinjected into male pronuclei of fertilized one-cell mouse eggs obtained from superovulated FVB/N female mice (Hogan

et al., 1994). Injected embryos were transferred into the oviduct of pseudopregnant female foster mice to allow complete development to term.

To identify transgenic mice, mouse-tail DNA was prepared using the Puregene kit (Gentra) and used in Southern blot analysis. High-molecular-weight mouse-tail DNA was digested with *Bam*HI enzyme, which cut once between the *NF2* promoter and nls-*Lac*Z DNA of the transgene. Digested DNA was electrophoresed onto a 0.7% agarose gel and then transferred to a GeneScreen Plus® hybridization transfer membrane (NEN Life Science). For the probe, the *Lac*Z DNA was labeled with biotinylated dNTP mixture by the random primed method using the NEBlot™ Phototope™ kit (New England Biolabs). Filter membranes containing mouse-tail DNAs were prehybridized in hybridization buffer for one hour, and then hybridized with the biotin-labeled *Lac*Z probe overnight. After hybridization, filters were washed twice in 0.1× SSC and 0.1% SDS at 65°C for 30 min each time. For detecting hybridization signal, the Phototope™-Star Detection Kit for Nucleic Acids (New England Biolabs) was used, and chemiluminescence was captured by the ChemiGenius^2 Image Acquisition System (Syngene) or by exposure to X-ray films. Once identified, transgenic mice were mated with FVB/N mice to generate offspring.

Whole-Mount X-Gal Staining

Transgenic mice were mated with each other. The day when the vaginal plug was found, the embryo was aged as 0.5 day p.c. (E0.5). On the following day, the embryo was aged as E1.5 and so on. Embryos at various days p.c. were harvested and fixed in the fixative solution containing 1% formaldehyde, 0.2% glutaraldehyde, and 0.02% NP-40 in phosphate-buffered saline (PBS) for 40 min on ice. After fixation, embryos were incubated overnight in the X-gal staining solution, containing 5 mM $K_3Fe(CN)_6$, 5 mM $K_4Fe(CN)_6$, 2 mM $MgCl_2$, and 1 mg/ml of 5-bromo-4-chloro-3-indolyl-β-galactoside, at 37°C with gentle shaking. Stained embryos were rinsed with PBS and photographed under a Leica MZ16FA stereoscope. Embryos were further fixed overnight in 4% paraformaldehyde in PBS at 4°C and then embedded in paraffin. Five-micron tissue sections were obtained using a rotary microtome. Sections were deparaffinized, counter-stained with nuclear fast red, mounted with a coverslip, and then photographed under a Leica DM4000B microscope.

Cloning of Mouse *Nf2* cDNAs

Total RNA was isolated from adult mouse brain using the TRIzol reagent (Invitrogen) and used in RT-PCR to isolate *Nf2* cDNAs (Fig. 1B) as described previously (Chang et al., 2002). The mouse *Nf2* cDNA containing the entire coding region was obtained by RT-PCR using the primers Coding-F and Coding-R (Fig. 1C). The resulting *Nf2* cDNA was cloned into pCRII-TOPO vector (Invitrogen) to generate the pCRII-*Nf2*coding plasmid (Fig. 1B). The *Nf2* cDNA was digested with *Hind*III enzyme to yield the N-terminal 0.9-kb, middle 0.3-kb, and C-terminal 0.6-kb fragments. Each cDNA fragment was subcloned into pCRII-TOPO to generate the pCRII-N, pCRII-M, or pCRII-C subclone, respectively. To obtain the *Nf2* cDNA containing the 5′ untranslated region, RT-PCR was performed using the 5U-F and 5U-R primers (Fig. 1C). The resulting cDNA product was cloned into pCRII-TOPO to generate the pCRII-5U construct (Fig. 1B). Similarly, cDNAs containing the sequences immediately upstream of the translation termination codon and extending into the 3′ untranslated region were obtained using the primer pairs 3U1-F and 3U1-R, or 3U2-F and 3U2-R (Fig. 1C). The resulting cDNAs containing the 3′ untranslated region were also cloned into pCRII-TOPO to generate pCRII-3U1 and pCRII-3U2, respectively (Fig. 1B). All *Nf2* cDNA sequences obtained were confirmed by DNA sequencing.

Whole-Mount RNA In Situ Hybridization

Mouse embryos (E7.5, E8.5, and E9.5) were harvested and fixed in 4% paraformaldehyde in PBS overnight at 4°C. Fixed embryos were rinsed with PBT (PBS plus 0.1% Tween) three times, placed in 100% methanol, and then bleached at room temperature for 5 hr by adding hydrogen peroxide to 6%. After rinsing with 100% methanol three times, embryos were stored in 100% methanol at −20°C.

In situ hybridization was performed as previously described (Wilkinson, 1992) with minor modifications (Correia and Conlon, 2001). Following hydration through a 75, 50, and 25% methanol/PBT series, embryos were treated with 10 mg/ml proteinase K in PBT at room temperature (5 min for E7.5 embryos, 7 min for E8.5 embryos, and 8 min for E9.5 embryos). Treated embryos were washed twice for 5 min with 2 mg/ml glycine in PBT, rinsed three times with PBT, and then refixed with freshly prepared 4% paraformaldehyde/0.2% glutaraldehyde in PBT for 20 min at room temperature. AQ: 1

For riboprobe preparation, transcription plasmids carrying a different portion of the *Nf2* cDNA (pCRII-5U, N, M, C, 3U1, and 3U2) were linearized with an appropriate restriction enzyme, which cuts at the junction between the cDNA and vector sequences. In vitro transcription that produced riboprobes, which incorporate digoxygenin-labeled nucleotides from each linearized plasmid with T7 or SP6 polymerase, was performed using the DIG RNA Labeling Kit (Roche). Both the sense and antisense riboprobes from each transcription plasmid were produced.

For hybridization, embryos were briefly rinsed with hybridization buffer (5× SSC, pH 5, 1% SDS, 50 μg/ml yeast tRNA, 50 μg/ml heparin, and 50% formamide) and then incubated in hybridization buffer for 1 hr at 65°C with gentle shaking. After removing the pre-hybridization buffer, each riboprobe was diluted in hybridization buffer to about 1 μg/ml and then added to the embryos. Hybridization was carried out at 65°C with gentle shaking overnight.

Hybridized embryos were sequentially washed with Wash Solution 1, a 1:1 solution of Wash Solutions 1 and 2, and Wash Solution 2, followed by digestion with 100 μg/ml RNase A and washing with Wash Solution 2 and 3 (Wilkinson, 1992). To detect the hybridization signal, the DIG Nucleic Acid Detection Kit (Roche) was used. Embryos were pre-blocked with 10% sheep serum and then incubated overnight at 4°C with alkaline phospha-

tase-conjugated anti-digoxigenin antibody, which had been pre-absorbed with embryo powder (Wilkinson, 1992). After extensive washing, embryos were incubated in 1 ml of freshly prepared NTMT (100 mM NaCl, 100 mM Tris-HCl, pH 9.5, 50 mM MgCl2, and 0.1% Tween 20) containing 4.5 μl/ml NBT stock and 3.5 μl/ml BCIP stock (Correia and Conlon, 2001). Incubation was performed in the dark with gentle shaking. When color was developed to the desired extent, embryos were rinsed several times with PBT, stored in a 50/50 mix of glycerol and PBT, and photographed under a Leica MZ16FA stereoscope.

Immunohistochemical Analysis

Embryos at various days p.c. were harvested, fixed in 4% paraformaldehyde, and then embedded in paraffin. Tissue sections were obtained, deparaffinized, and processed for immunostaining with antibodies against Sox 9 (sc-20095; Santa Cruz Biotechnology), S100 (z 0311; Dako), and merlin (sc-331; Santa Cruz Biotechnology) according to previously described procedures (Welling et al., 2002). Negative controls were treated with the same immunostaining procedure except without the primary antibody. Hematoxylin was used as a counterstain.

ACKNOWLEDGMENTS

We sincerely thank Sarah Burns for a critical reading of the manuscript and members of the Chang lab for helpful discussion throughout the work. Part of the work described in this report was presented at the 2004 and 2005 NNFF Int. Consortium for the Mol. Biol. of NF1 and NF2 in Aspen, CO.

REFERENCES

Bertrand JY, Giroux S, Cumano A, Godin, I. 2005. Hematopoietic stem cell development during mouse embryogenesis. Methods Mol Med 105:273–288.

AQ: 2 Bianchi AB, Hara T, Ramesh V, Gao J, Klein-Szanto AJ, Morin F, Menon AG, Trofatter JA, Gusella JF, Seizinger BR, et al. 1994. Mutations in transcript isoforms of the neurofibromatosis 2 gene in multiple human tumour types. Nat Genet 6:185–192.

Chang L-S, Yang S, Shenk T. 1989. Adeno-associated virus P5 promoter contains an adenovirus E1A-inducible element and a binding site for the major late transcription factor. J Virol 63:3470–3488.

Chang L-S, Akhmametyeva EM, Wu Y, Zhu L, Welling DB. 2002. Multiple transcription initiation sites, alternative splicing, and differential polyadenylation contribute to the complexity of human neurofibromatosis 2 transcripts. Genomics 79:63–76.

Chen Y, Gutmann DH, Haipek CA, Martinsen BJ, Bronner-Fraser M, Krull CE. 2004. Characterization of chicken Nf2/merlin indicates regulatory roles in cell proliferation and migration. Dev Dyn 229: 541–554.

Cheung M, Briscoe J. 2003. Neural crest development is regulated by the transcription factor Sox9. Development 130: 5681–5693.

Cheung M, Chaboissier MC, Mynett A, Hirst E, Shedl A, Briscoe J. 2005. The transcriptional control of trunk neural crest induction, survival, and delamination. Dev Cell 8:179–192.

Claudio JO, Marineau C, Rouleau GA. 1994. The mouse homologue of the neurofibromatosis type 2 gene is highly conserved. Hum Mol Genet 3:185–190.

Claudio JO, Lutchman M, Rouleau, GA. 1995. Widespread but cell type-specific expression of the mouse neurofibromatosis type 2 gene. Neuroreport 6:1942–1946.

Correia KM, Conlon RA. 2001. Whole-mount in situ hybridization to mouse embryos. Methods 23:335–338.

Evans DG, Huson SM, Donnai D, Neary W, Blair V, Newton V, Strachan T, Harris R. 1992. A genetic study of type 2 neurofibromatosis in the United Kingdom. II. Guidelines for genetic counseling. J Med Genet 29:847–852.

Fernandez-Valle C, Tang Y, Ricard J, Rodenas-Ruano A, Taylor A, Hackler E, Biggerstaff J, Iacovelli J. 2002. Paxillin binds schwannomin and regulates its density-dependent localization and effect on cell morphology. Nat Genet 31:354–362.

Giovannini M, Robanus-Maandag E, van der Valk M, Niwa-Kawakita M, Abramowski V, Goutebroze L, Woodruff JM, Berns A, Thomas G. 2000. Conditional biallelic Nf2 mutation in the mouse promotes manifestations of human neurofibromatosis type 2. Genes Dev 14:1617–1630.

Godin I, Cumano A. 2005. Of birds and mice: hematopoietic stem cell development. Int J Dev Biol 49:251–257.

Gonzalez-Agosti C, Xu L, Pinney D, Beauchamp R, Hobbs W, Gusella J, Ramesh V. 1996. The merlin tumor suppressor localizes preferentially in membrane ruffles. Oncogene 13:1239–1247.

Graham A. 2003. The neural crest. Curr Biol 13:R381–384.

Gronholm M, Teesalu T, Tyynela J, Piltti K, Bohling T, Wartiovaara K, Vaheri A, Carpen O. 2005. Characterization of the NF2 protein merlin and the ERM protein ezrin in human, rat, and mouse central nervous system. Mol Cell Neurosci 28: 683–693.

Gutmann DH, Wright DE, Geist RT, Snider WD. 1994. Expression of the neurofibromatosis 2 (*NF2*) gene isoforms during rat embryonic development. Hum Mol Genet 4:471–478.

Gutmann DH, Geist RT, Xu HM, Kim JS, Saporito-Irwin S. 1998. Defects in neurofibromatosis 2 protein function can arise at multiple levels. Hum Mol Genet 7:335–345

Gutmann DH, Sherman L, Seftor L, Haipek C, Hoang Lu K, Hendrix M. 1999. Increased expression of the NF2 tumor suppressor gene product, merlin, impairs cell motility, adhesion and spreading. Hum Mol Genet 8:267–275.

Haase VH, Trofatter JA, MacCollin M, Tarttelin E, Gusella JF, Ramesh V. 1994. The murine NF2 homologue encodes a highly conserved merlin protein with alternative forms. Neuroreport 8: 2025–2030.

Hay ED. 2005. The mesenchymal cell, its role in the embryo, and the remarkable signaling mechanisms that create it. Dev Dyn 233:706–720.

Hazim W, Mautner VF, Christiani B, Hasse W. 1998. Fluorescein angiography of retinal changes in patients with neurofibromatosis 2. Ophthalmologe 95:687–690.

Hogan B, Beddington R, Costantini F, Lacy E. 1994. Manipulating the mouse embryo, a laboratory manual. Plainview, NY: Cold Spring Harbor Laboratory Press.

Honjo Y, Eisen JS. 2005. Slow muscle regulates the pattern of trunk neural crest migration in zebrafish. Development 132: 4461–4470.

Huynh DP, Tran TM, Nechiporuk T, Pulst SM. 1996. Expression of neurofibromatosis 2 transcript and gene product during mouse fetal development. Cell Growth Differ 7:1551–1561.

Imbert AM, Bagnis C, Galindo R, Chabannon C, Mannoni P. 1998. A neutralizing anti-TGF-β1 antibody promotes proliferation of CD34+Thy-1+ peripheral blood progenitors and increases the number of transduced progenitors. Exp Hematol 26: 374–381.

Jacinto A, Wood W, Woolner S, Hiley C, Turner L, Wilson C, Martinez-Arias A, Martin P. 2002. Dynamic analysis of actin cable function during Drosophila dorsal closure. Curr Biol 12:1245–1250.

Jessen KR, Mirsky R. 2005. The origin and development of glial cells in peripheral nerves. Nat Rev Neurosci 6:671–682. AQ: 3

Kalamarides M, Niwa-Kawakita M, Leblois H, Abramowski V, Perricaudet M, Janin A, Thomas G, Gutmann DH, Giovannini M. 2002. Nf2 gene inactivation in arachnoidal cells is rate-limiting for meningioma development in the mouse. Genes Dev 16:1060–1065.

Kissil JL, Johnson KC, Eckman MS, Jacks T. 2002. Merlin phosphorylation by p21-activated kinase 2 and effects of phosphorylation on merlin localization. J Biol Chem 277:10394–10399.

Lallemand D, Curto M, Saotome I, Giovannini M, McClatchey AI. 2003. NF2 de-

ficiency promotes tumorigenesis and metastasis by destabilizing adherens junctions. Genes Dev 17:1090–1100.

LeDouarin N, Kalcheim C. 1999. The neural crest. Cambridge, UK: Cambridge University Press.

Levine RE, Slattery WH III. 2003. Documenting changes in the pre-retinal membrane using the Optical Coherence Tomography 3. Abstract presented to the 2003 NNFF Int. Consortium for the Mol Biol of NF1 and NF2, Aspen, CO.

Li S, Guan J-L, Chien S. 2005. Biochemistry and biomechanics of cell motility. Annu Rev Biomed Eng 7:105–150.

Lutchman M, Rouleau GA. 1995. The neurofibromatosis type 2 gene product, schwannomin, suppresses growth of NIH 3T3 cells. Cancer Res 55:2270–2274.

Maeda M, Matsui T, Imamura M, Tsukita S, Tsukita S. 1999. Expression level, subcellular distribution and rho-GDI binding affinity of merlin in comparison with Ezrin/Radixin/Moesin proteins. Oncogene 18:4788–4797.

Martinez-Morales JR, Rodrigo I, Bovolenta P. 2004. Eye development: a view from the retina pigmented epithelium. BioEssays 26:766–777.

McClatchey AI. 2004. Merlin and ERM proteins: unappreciated roles in cancer development. Nat Rev Cancer 3:877–883.

McClatchey AI, Giovannini M. 2005. Membrane organization and tumorigenesis: the NF2 tumor suppressor, Merlin. Genes Dev 19:2265–2277.

McClatchey AI, Saotome I, Ramesh V, Gusella JF, Jacks T. 1997. The NF2 tumor suppressor gene product is essential for extraembryonic development immediately prior to gastrulation. Genes Dev 11:1253–1265.

McClatchey AI, Saotome I, Mercer K, Crowley D, Gusella JF, Bronson RT, Jacks T. 1998. Mice heterozygous for a mutation at the NF2 tumor suppressor locus develop a range of highly metastatic tumors. Genes Dev 12:1121–1133.

McLaughlin ME, Slocum K, Jacks T. 2004. The NF2 tumor suppressor, merlin, is required for tissue fusion during mouse embryonic development. Abstract presented to the 2004 NNFF Int. Consortium for the Mol Biol of NF1 and NF2, Aspen, CO.

Meyers SM, Gutman FA, Kaye LD, Rothner AD. 1995. Retinal changes associated with neurofibromatosis 2. Trans Am Ophthalmol Soc 93:245–252; discussion 252–257.

Mori-Akiyama Y, Akiyama H, Rowitch DH, de Crombrugghe B. 2003. Sox9 is required for determination of the chondrogenic cell lineage in the cranial neural crest. Proc Natl Acad Sci USA 100:9360–9365.

Neff B, Welling DB, Akhmametyeva E, Chang L-S. 2005. The molecular biology of vestibular schwannomas: dissecting the pathogenic process at the molecular level. Otol Neurotol 27:197–208.

NIH Consens. Statement. 1991. Acoustic neuroma. Consens. Statement 9:1–24.

Parry DM, Eldridge R, Kaiser-Kupfer MI, Bouzas EA, Pikus A, Patronas, N. 1994. Neurofibromatosis 2 (NF2): clinical characteristics of 63 affected individuals and clinical evidence for heterogeneity. Am J Med Genet 52:450–461.

Pelton PD, Sherman LS, Rizvi TA, Marchionni MA, Wood P, Friedman RA, Ratner N. 1998. Ruffling membrane, stress fiber, cell spreading and proliferation abnormalities in human Schwannoma cells. Oncogene 17:2195–2209.

Rong R, Surace EI, Haipek CA, Gutmann DH, Ye K. 2004. Serine 518 phosphorylation modulates merlin intramolecular association and binding to critical effectors important for NF2 growth suppression. Oncogene 23:8447–8454.

Rouleau GA, Merel P, Lutchman M, Sanson M, Zucman J, Marineau C, Hoang-Xuan K, Demezuk S, Desmaze C, Plougastel B, Pulst SM, Lenoir G, Bijlsma E, Fashold R, Dumanshki J, de Jong P, Parry D, Eldridge R, Aurias A, Delattre O, Thomas G. 1993. Alteration in a new gene encoding a putative membrane-organising protein causes neurofibromatosis type 2. Nature 363:515–521

Rugh R. 1994. The mouse: its reproduction and development. Oxford: Oxford University Press.

Scoles DR, Huynh DP, Morcos PA, Coulsell ER, Robinson NG, Tamanoi F, Pulst, SM. 1998. Neurofibromatosis 2 tumor suppressor schwannomin interacts with βII-spectrin. Nat Genet 18:354–359.

Shaw RJ, McClatchey AI, Jacks T. 1998. Localization and functional domains of the neurofibromatosis type II tumor suppressor, Merlin Cell Growth Diff 9:287–296.

Shaw RJ, Paez JG, Curto M, Yaktine A, Pruitt WM, Saotome I, O'Bryan JP, Gupta V, Ratner N, Der CJ, Jacks T, McClatchey, AI. 2001. The Nf2 tumor suppressor, merlin, functions in Rac-dependent signaling. Dev Cell 1:63–72.

Sherman L, Xu HM, Geist RT, Saporito-Irwin S, Howells N, Ponta H, Herrlich P, Gutmann DH. 1997. Interdomain binding mediates tumor growth suppression by the NF2 gene product. Oncogene 15: 2505–2509.

Stemmer-Rachamimov AO, Gonzalez-Agosti C, Xu L, Burwick JA, Beauchamp R, Pinney D, Louis DN, Ramesh V. 1997. Expression of NF2-encoded merlin and related ERM family proteins in the human central nervous system. J Neuropathol Exp Neurol 56:735–742.

Stokowski RP, Cox DR. 2000. Functional analysis of the neurofibromatosis type 2 protein by means of disease-causing point mutations. Am J Hum Genet 66: 873–891.

Surace EI, Haipek CA, Gutmann DH. 2004. Effect of merlin phosphorylation on neurofibromatosis 2 (NF2) gene function. Oncogene 23:580–587.

Tikoo A, Varga M, Ramesh V, Gusella J, Maruta H. 1994. An anti-Ras function of neurofibromatosis type 2 gene product (NF2/Merlin). J Biol Chem 269:23387–23390

Trofatter JA, MacCollin MM, Rutter JL, Murrell JR, Duyao MP, Parry DM, Eldridge R, Kley N, Menon AG, Pulaski K, Haase VH, Ambrose CM, Munroe D, Bove C, Haines JL, Martuza RL, MacDonald ME, Seizinger BJ, Short MP, Buckler AL, Gusella JF. 1993. A novel Moesin-, Exrin-, Radixin-like gene is a candidate for the neurofibromatosis 2 tumor-suppressor. Cell 72:791–800.

Wallingford JB. 2005. Neural tube closure and neural tube defects: studies in animal models reveal known knowns and known unknowns. Am J Med Genet Part C Semin Med Genet 135:59–68.

Wassef M, Joyner AL. 1997. Early mesencephalon/metencephalon patterning and development of the cerebellum. Perspect Dev Neurobiol 5:3–16.

Welling DB, Akhmametyeva EM, Daniels RL, Lasak JM, Zhu L, Miles-Markley BA, Chang L-S. 2000. Analysis of the human neurofibromatosis type 2 gene promoter and its expression. Otolaryngol Head Neck Surg 123:413–418.

Welling DB, Lasak JM, Akhmametyeva E, Ghehari B, Chang L-S. 2002. cDNA microarray analysis of vestibular schwannomas. Otol Neurol 23:736–748.

Wilkinson DG. 1992. In situ hybridization, a practical approach. Oxford: IRL Press. p 75–83.

Woolner S, Jacinto A, Martin P. 2005. The small GTPase Rac plays multiple roles in epithelial sheet fusion: dynamic studies of Drosophila dorsal closure. Dev Biol 282:163–173.

World Health Org. 1992. Prevention and control of neurofibromatosis: Memorandum from a joint WHO/NNFF meeting. Bull. World Health Org 70:173–182.

Xiao GH, Beeser A, Chernoff J, Testa JR. 2002. p21-activated kinase links Rac/Cdc42 signaling to merlin. J Biol Chem 277:883–886.

Xu HM, Gutmann DH. 1998. Merlin differentially associates with the microtubule and actin cytoskeleton. J Neurosci Res 51:403–415.

Transworld Research Network
37/661 (2), Fort P.O., Trivandrum-695 023, Kerala, India

Recent Res. Devel. Genes & Genomes, 1(2005): ISBN: 81-7895-166-5

Dissecting the molecular pathways in vestibular schwannoma tumorigenesis

Long-Sheng Chang[1,2,3], Elena M. Akhmametyeva[1,2], Maria Mihaylova[1] Huijun Luo[1], Sookil Tae[4], Brain Neff[3], Abraham Jacob[3] and D. Bradley Welling[3]

[1]Center for Childhood Cancer, Children's Research Institute, Children's Hospital and Departments of [2]Pediatrics and [3]Otolaryngology and [4]Ohio State Biochemistry Program, The Ohio State University, Columbus, Ohio, USA

Abstract

Human vestibular schwannomas, which are benign Schwann cell tumors originating from the eighth nerve in the posterior cranial fossa, continue to cause morbidity associated with hearing loss, balance dysfunction, facial paralysis and paresthesias, and occasionally life-threatening brainstem compression. Vestibular schwannomas can be divided into three general categories including unilateral spontaneous vestibular schwannomas, neurofibromatosis type 2 (NF2)-associated vestibular schwannomas, and cystic type schwannomas. Recent advances in molecular oncology have led to the discovery of the neurofibro-

Correspondence/Reprint request: Dr. Long-Sheng Chang, 700 Children's Drive, Columbus, Ohio 43205, USA
E-mail: lchang@chi.osu.edu

matosis type 2 gene (NF2), whose mutation has been found in all three types of vestibular schwannomas. Expression of the NF2 gene is regulated at the transcriptional and post-transcriptional level, and its expression is essential during early embryonic development. The NF2 gene encodes a protein termed merlin/schwannomin, which shares a high degree of homology with the ezrin, radixin, and moesin (ERM) proteins. Genetic knockout experiments have shown that the NF2 gene product is a tumor suppressor for Schwann cell and meningeal cells. Analysis of cDNA microarray has revealed potential underlying molecular differences among the types of vestibular schwannomas. Avenues for the development of potential future therapies have begun to emerge.

Introduction

Vestibular schwannomas are histologically benign tumors of the neural sheath that originate from the superior or inferior vestibular branches of cranial nerve VIII. The term "vestibular schwannoma" is preferred over the more commonly used term "acoustic neuroma" because these tumors are neither neuromas, nor do they arise from the acoustic (cochlear) nerve (170). The tumors can lead to profound hearing loss, balance dysfunction, facial nerve paralysis, brainstem compression, hydrocephalus, and if left untreated, death. In a silent, off-balance world with impaired facial expression, these patients are directly affected in their ability to communicate and interact with others. Currently there are no known medical treatments for these tumors. Sensitive diagnostic techniques such as magnetic resonance imaging (MRI) are diagnosing these tumors at early stages. Surgical excision through a craniotomy or stereotactic radiation are the current treatments of choice. This review aims to address the types of vestibular schwannomas and molecular mechanisms underlying schwannoma tumorigenesis. Potential sources of phenotypic variation among schwannoma tumor types have been investigated and potenial deregulated signaling pathways identified will be discussed with respect to the future development of novel pharmaco-therapeutics.

Vestibular schwannoma types

Three types of vestibular schwannomas, which have distinct clinical features, are encountered in clinical practice including unilateral sporadic vestibular schwannomas, bilateral or NF2-associated schwannomas, and cystic schwannomas (238). Vestibular schwannomas, typically slow growing and non-malignant, most commonly occur as sporadic unilateral solid tumors with an annual incidence of about 1 in 20,000 population. Patients with vestibular schwannomas usually present with unilateral tinnitus, hearing loss and imbalance. These tumors can lead to deafness, facial nerve paralysis, brainstem

compression, hydrocephalus, and death, if left untreated. The mean age at onset in our series is 49 years of age and there is a slight female predominance without ethnic predilection (238). NF2-associated vestibular schwannomas and cystic schwannomas are both distinctly less common, each occurring at approximately 4% of the rate of unilateral schwannomas (30-32). NF2-associated and cystic tumors are more likely to be multi-lobulated than unilateral sporadic tumors.

NF2 is a highly penetrant, autosomal dominant disorder (26). The hallmark of NF2 is the development of bilateral vestibular schwannomas. Other disease features include cranial meningiomas, ependymomas, spinal schwannomas and presenile lens opacities (61,109,111,148). NF2 is an extremely debilitating disease, leading to a decreased life expectancy in those afflicted. It has a prevalence estimated at approximately 1 in 40,000 (10,53). There is no known ethnic predilection. Affected individuals often show eighth-nerve dysfunction beginning in early adulthood including tinnitus, bilateral profound hearing loss, and ataxia. Bilateral facial nerve paralysis is an additional debilitating event. The mean age at presentation for NF2-associated vestibular schwannomas is 20 to 21 years of age (54,174). Occasionally the onset will be delayed into the 5th or 6th decade of life, but it may also present in early childhood (150). Patients who inherit an abnormal copy of the neurofibromatosis 2 gene (*NF2*) on chromosome 22q12 (245) have a 95% chance of developing bilateral vestibular schwannomas. However, about one half of the cases have no family history of NF2 and thus represent new germline mutations. NF2 is now recognized as a disease that is distinctly different from neurofibromatosis type 1 (NF1) or von Recklinghausen's disease. NF1, which is associated with multiple peripheral neuromas, is caused by a mutation in the neurofibromatosis 1 gene (NF1) located on the long arm of chromosome 17 (for recent reviews, see 9,40,142).

Cystic vestibular schwannomas are a particularly aggressive group of unilateral schwannomas, which invade the surrounding cranial nerves, splaying them throughout the tumor. Cystic vestibular schwannomas are associated with either intra-tumoral or extra-tumoral cysts, which develop in the loosely organized Antoni B tissues. In addition, a higher degree of nuclear atypia is seen in cystic tumors (33,110). Careful distinction must be drawn between truly cystic schwannomas and the more common heterogeneous schwannomas, which are not as aggressive in their clinical behavior. Cystic tumors may grow rapidly and are very difficult to manage, because of the high rate of hearing loss and facial nerve paralysis that occurs subsequent to their removal. When cystic tumors are removed surgically, only 35% of patients maintain a House-Brackmann grade I or II (normal or mild dysfunction) facial function postoperatively (30-32). These results are unfavorable when compared to surgical excision of NF2-associated vestibular schwannomas and sporadic

unilateral vestibular schwannomas which result in House-Brackmann grade I or II facial function in 66% and 90% of patients, respectively (238). In addition, surgical removal of cystic tumors resulted in a 41% rate of complete facial nerve paralysis (House-Brackmann grade VI) as compared to solid unilateral schwannomas of a similar size in which complete paralysis only occurred 27% of the time (62). The results from stereotactic radiation have been similarly disappointing for cystic tumors. These tumors are also much more likely to have continued growth and facial nerve paralysis with stereotactic radiation treatments than either unilateral spontaneous or NF2-associated schwannomas (177,200,214).

MRI distinguishes clearly among the three types of vestibular schwannomas (Figure 1). Cystic regions within cystic schwannomas are signal intense on T2-weighted images without contrast enhancement, while non-cystic components of the tumors enhance on T1 images with gadolinium, in a

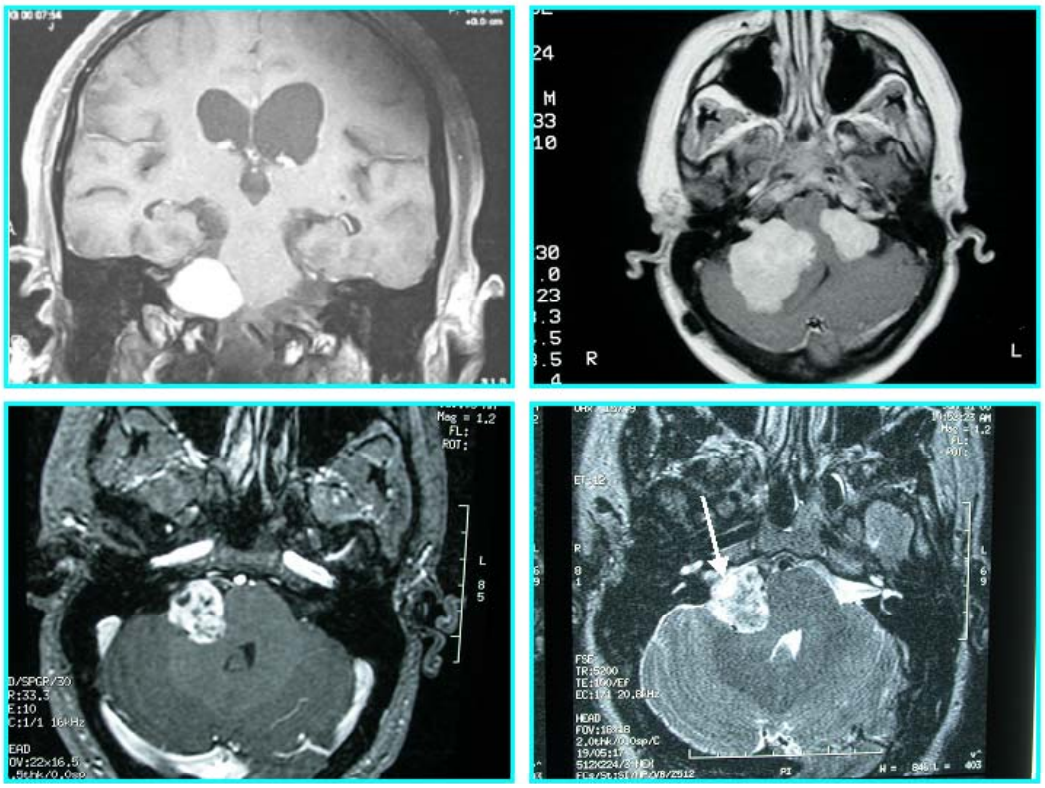

Figure 1. MRI images of vestibular schwannomas. (A) Coronal T1-weighted image with gadolinium enhancement demonstrating a right-sided sporadic vestibular schwannoma. (B) Axial T1-weighted image with gadolinium enhancement illustrating bilateral NF2-associated vestibular schwannomas. (C) Axial T1-weighted image with gadolinium enhancement showing a right-sided vestibular schwannoma with areas of central low intensity corresponding to cysts within the tumor. (D) Axial T2-weighted image displaying a right-sided cystic vestibular schwannoma with focal areas of increased signal intensity that correspond to intra-tumoral cysts (arrow).

similar manner to those seen in unilateral and NF2-associated schwannomas. The irregular appearance of heterogeneous tumors on contrast enhanced MRI can be accounted for by hemosiderin deposits, which correlates with increasing tumor size (169).

Although quite distinct clinically and radiographically, the underlying molecular differences among the types of vestibular schwannomas are not understood. Furthermore, the optimal treatment regimens are not known because of a lack of understanding of fundamental tumor biology and a lack of rigorous clinical outcomes studies.

NF2 gene, gene product, and mutation in vestibular schwannomas

The gene associated with *NF2* was cloned by positional cloning and named the *NF2* gene, which encodes a protein named 'schwannomin' (a word derived from schwannoma, the most prevalent tumor seen in NF2) by Rouleau et al. (190) or 'merlin' (for moesin-ezrin-radixin like protein) by Trofatter et al. (229). To honor both groups, to retain the significance associated with each name, and to unify the nomenclature in the literature, we recommended that the *Nf2* gene product be called 'schwannomerlin' (240). However, for simplicity, we refer to the *NF2* gene product as merlin in this review.

Merlin shares a high degree of homology with the ezrin, radixin, and moesin (ERM) proteins (190,229). The ERM proteins are members of the erythrocyte protein 4.1-related superfamily, linking the actin cytoskeleton to the plasma membrane (2). The proteins belonging to this family all have similar designs with an N-terminal globular FERM domain (F for 4.1 protein) (35), followed by an α-helical stretch and then by a charged C-terminus. The overall structure of merlin is similar to that of the ERM proteins. Biochemical and biological analysis indicates that the highly conserved FERM domain and the unique C-terminus of the merlin protein are important for its function. However, unlike the ERM proteins, which seem to facilitate growth, merlin exerts a growth suppression effect (78).

The isolation of the *NF2* gene facilitates the identification of mutations within the *NF2* gene, the relative frequency of mutations in each exon, and the specific clinical expression associated with specific *NF2* mutations in vestibular schwannomas and other NF2-associated tumors. *NF2* mutations have been identified in NF2-associated vestibular schwannomas, sporadic unilateral schwannomas, and cystic schwannomas (6,14,16-19,43-44,55-56, 75,77,82,96,98-103,112,119-122,135-136, 143-145, 155-156,158,165,176,190, 192,194,196-198,220-221,229-230,238,242,243,255). Additionally, mutations within the *NF2* gene have been frequently identified in meningiomas and

occasionally identified in other tumor types such as mesotheliomas (14,15,41,44,127,136,155,193,207).

Attempts have been made to correlate clinical expression with specific *NF2* mutations in vestibular schwannomas and other NF2-associated tumors. A number of somatic mutations and their specific clinical expression in sporadic unilateral tumors and NF2 tumors have been characterized (14, 18, 19,44,55,75, 100-103, 119-122, 140, 143-144, 149, 155,175,192,196-198, 204, 221,230,242). In tumors from NF2 patients, point mutations accounted for the majority of mutations, whereas small deletions accounted for the majority of mutations in the unilateral tumors. Initially, mutations, which cause truncation of the NF2 protein, were reported to cause a more severe phenotype (99,103,175), while missense mutations or small in-frame insertions had been reported to associate with a mild phenotype (19,75,156,192,242). However, phenotypic variability within NF2 families carrying the same germline mutation has also been reported (149). Although some missense mutations of the *NF2* gene have been associated with a milder phenotype, severe phenotypes have also been identified. Missense mutations within the α-helical domain of merlin appear to be associated with a less severe phenotype than mutations within the conserved FERM domains (75). Likewise, large deletions may give rise to mild phenotypes as well (24). Given the heterogeneity of clinical response to various mutations, other yet unknown regulatory factors likely play a key role in the clinical manifestations in the various types of schwannomas.

It should be noted that not all vestibular schwannomas examined carry an identifiable *NF2* mutation. By performing an exhaustive alteration screening, including large deletions for the *NF2* gene, Zucman-Rossi et al. (255) reported the efficiency of mutation detection in NF2 patients to be 84%. Thus, additional mechanisms for inactivation of the *NF2* gene in some NF2 patients exist. The possibility of a modifier gene has been suggested (22-23). Also, the possibility of methylation or mutation in the *NF2* regulatory region has been postulated (29,116). In addition, the complexity of *NF2* transcripts generated by post-transcriptional alternative splicing and differential polyadenylation may be considered as possible means of inactivating the *NF2* gene (29).

Of clinical importance is the ability to completely identify a specific mutation in the *NF2* gene in a given family member because it allows the performance of direct DNA diagnostic testing on other family members, leading to an early, even presymptomatic diagnosis of affected patients. Early detection makes a distinct difference in the ability to successfully treat the patients (67). Decreased morbidity and mortality are associated with early intervention. Ultimately, facial nerve function and hearing preservation are directly correlated with smaller tumor size and early detection. NF2 patients now often suffer profound bilateral deafness (241). Early detection however,

may allow hearing preservation by early surgical intervention. Additionally hearing restoration by cochlear implantation is only possible in NF2 patients diagnosed early enough to allow surgical sparing of the cochlear nerve. Cochlear implantation, if possible, is likely to achieve superior hearing results when compared to auditory brainstem implants (75,90). Individuals who have not inherited the abnormal *NF2* gene will be spared repeated medical evaluations and expensive imaging studies (125). All of these factors suggest that further refinement in the diagnosis and treatment of NF2 is necessary.

Merlin: A tumor suppressor in schwann cells

Over-expression of the *NF2* gene in mouse NIH3T3 fibroblasts or rat RT-4 schwannoma cells can limit cell growth (75,78,141,210) and suppress transformation by a ras oncogene (228). The growth control of certain Schwann cells and meningeal cells is abrogated by the loss of *NF2* function, suggesting that *NF2* deficiency disrupts some aspect of intracellular signaling that leads to a signal for cell proliferation. Like the ERM proteins, merlin is expressed in a variety of cell types where it localizes to areas of membrane remodeling (21), particularly membrane ruffles (70). Schwannoma cells from NF2 tumors have dramatic alterations in the actin cytoskeleton and display abnormalities in cell spreading (178). These results suggest that merlin may play an important role in regulating both actin cytoskeleton-mediated processes and cell proliferation.

A few merlin-interacting proteins have been identified. These include the ERM proteins, F-actin, microtubules, βII-spectrin, hyalurin receptor CD44, β1-integrin, paxillin, β-fodrin, syntenin, the regulatory cofactor of Na^+-H^+ exchanger (NHE-RF), SCHIP-1, hepatocyte growth factor-regulated tyrosine kinase substrate (HRS), p21-activated kinase 1 and 2 (Pak1and Pak2), Rac1, and RIβ subunit of protein kinase A (1,58,70,72,74,86,94,106,117-118,162,164,167,173,195,205-206,209-211,227,249-250). Presently, how these protein-protein interactions relate to the tumor suppressor activity of merlin is largely not understood. The association of merlin with the CD44 hyaluronic acid receptor and β1-integrin raises the possibility that merlin might function as a molecular switch through signals from the extracellular matrix (86,162,212). Intriguingly, we have found that several extracellular matrix proteins are differentially regulated in vestibular schwannomas (243).

Mice carrying a deletion of the *Nf2* allele have been produced. Heterozygous *Nf2*-knockout mice develop a variety of malignant metastatic tumors with osteosarcomas at a high frequency, and fibrosarcoma and hepatocellular carcinoma at an increased, but lower frequency (152). Almost all of the tumors exhibit loss of the wild-type *Nf2* allele, indicating that merlin has a classical tumor suppressor function. However, none of the heterozygous

Nf2 mice develop vestibular schwannomas or other non-tumoral manifestations of human NF2. Homozygous *Nf2* mutant mouse embryos fail in development at day 6.5~7 of gestation and die immediately prior to gastrulation, displaying poorly organized extra-embryonic ectoderm (153). These results suggest that merlin is essential during embryonic development. By using Cre-mediated excision of exon 2 in Schwann cells targeted by a myelin basic protein P0 promoter, conditional *Nf2*-knockout mice have been produced and display characteristics of NF2, including schwannomas, Schwann cell hyperplasia, cataracts, and osseous metaplasia (66). Although these results argue that loss of merlin is sufficient for schwannoma formation *in vivo*, none of the lesions observed in these mice involve the vestibular nerve. This is in contrast to those vestibular schwannomas commonly found in patients with NF2. In addition, meningiomas, a frequent manifestation of the human NF2 disease, were not observed in the conditional homozygous *Nf2* knockout mice suggesting that meningioma progenitor cells may not be permissive to the P0 promoter. The use of the *NF2* gene promoter to direct proper temporal and spatial expression of the Cre recombinase to Schwann cells and other cell lineages to generate additional conditional knockout mice may allow validation of this hypothesis.

Transcriptional and post-transcriptional regulation of the NF2 gene

The human *NF2* gene spans over 90-kb DNA on chromosome 22 (239,255). To better understand *NF2* gene expression and regulation, we previously mapped the 5' and 3' ends of the *NF2* transcript (29). The human *NF2* transcripts initiate at multiple positions, with the major transcription initiation site mapped at position –423, relative to the A residue of the ATG translation start codon designated as +1. The proximal 5' flanking region of the human *NF2* gene is G+C rich and no consensus TATA sequence is present in the region 30 bp upstream of the major transcription initiation site. However, several potential binding sites for transcription factors AP2, CTF, E2F, EKLF, GCF, HIP1, LEF/TCF-1, NF-S, peroxisome proliferator-activating receptor (PPAR), *c-Sis*/PDGF, and Sp1 are present in the 5' flanking region (29).

The NF2 protein is expressed in a variety of cell types (29,79,97,153,190,229). Consistently, our promoter analysis shows that a 2.4-kb 5' flanking DNA of the human *NF2* gene directs the efficient expression of a reporter enzyme in several human cell types (29,239). Deletion analysis reveals a core promoter region extending 400 bp from the major transcription initiation site. Multiple positive and negative elements within the 5' flanking region appear to be important for *NF2* promoter expression. In particular, a G/C-rich sequence located at position –58 to -46, which can be bound by the Sp1 transcription factor, serves as a positive regulatory element. Co-

transfection experiments in *Drosophila* SL2 cells demonstrate that Sp1 can activate the *NF2* promoter through the G/C-rich sequence (29).

To examine if the *NF2* promoter is sufficient to direct expression to Schwann cells and other cell types, we have produced transgenic mice carrying a 2.4-kb *NF2* promoter-driven β-galactosidase (β-gal) construct. Whole mount *X-gal* staining of transgenic embryos detected β-gal expression at early embryonic development (Akhmametyeva, E., M. Mihaylova, and L.-S. Chang, unpublished data). At 10.5 days post coitus (p.c.), strong β-gal staining was detected in the developing neural tissues, including those developing into the brain and the cells surrounding the spinal nerves. A broad β-gal staining pattern was seen in transgenic embryos at 12.5 days p.c. and older. This early embryonic expression pattern of the *NF2* promoter is consistent with the phenotype of embryonic lethality seen in *Nf2*-knockout mice (153). Together, these results suggest that *NF2* may have a broad role during early development.

We have also found that the promoter region of the human *Nf2* gene could function bi-directionally (Chang, L.-S. and E. Akhmametyeva, unpublished data). When a *NF2* promoter-luciferase construct containing the 600-bp *NF2* promoter DNA placed in the antisense orientation with respect to the luciferase expression cassette, was used in transfection, it gave rise to very strong promoter activity, which was higher than that of the 600-bp *NF2* promoter in the sense configuration. Further analysis on the bi-directional transcription architecture of the NF2 locus should allow us to better understand the regulatory mechanism interplayed between two closely spaced promoters and possibly transcription units.

The *NF2* coding region encompasses 17 exons (190,229,239,255). Northern blot analysis detects multiple *NF2* RNA species of 6.1, 3.9, and 2.7 kb in various human tissues and cell lines (29). We have shown that the complexity of *NF2* transcripts is be attributed to multiple levels of regulation including multiple transcription initiation sites, alternative splicing, and differential usage of multiple poly(A) signal sequences (29). Various lengths of *NF2* cDNAs have also been isolated. The longest human *NF2* cDNA, containing all 17 exons, consists of 6,067 nucleotides (nt), which is consistent with the size of the major RNA species hybridized to the *NF2* probe. The cDNA has a 425-nt 5' untranslated (UT) region upstream from the ATG start codon, and a long 3' UT region of 3,869 nt.

NF2 transcripts undergo alternative splicing in the coding exons (7,14,29,88,123,171,182,202) and possibly in the 3' UT region (Wu, Y., E. Akhmametyeva, and L.-S. Chang, unpublished data). So far, more than 10 alternatively spliced cDNA isoforms have been identified in various human cells and tissues. The most common isoforms expressed in these cells are the so-called "isoform II", containing all 17 exons, and "isoform I", which is

missing exon 16. Isoform I is a 595 amino-acid protein. Isoform II differs from isoform I only at the C-terminus. Due to the inclusion of exon 16 in the mRNA providing a new stop codon, isoform II encodes a 590 amino-acid protein that is identical to isoform I over the first 579 residues. Other alternatively splice *NF2* isoforms include those missing exon 2, 3, 8, 10, or 15, or multiple exons and those with insertion of sequences from intron 2 or 16 (7,14,29,88,123,171,182,202; Akhmametyeva, E. and L.-S. Chang, unpublished data).

We have also examined the expression of alternatively spliced *NF2* mRNA isoforms in NF2-associated schwannomas, sporadic unilateral schwannomas, and cystic schwannomas. While the expression pattern and relative frequency of alternatively spliced *NF2* transcripts were similar among the three types of schwannoma; however, some differences were found when the *NF2* transcripts from schwannomas were compared to those isolated in other human cell types. For example, in addition to isoforms I and II, the schwannomas expressed a high percentage of the *NF2* mRNA isoform lacking exons 15 and 16 (Akhmametyeva, E., D.B. Welling, and L.-S. Chang, unpublished data).

Presently, the role of alternative splicing of *NF2* mRNA is not well understood. It is important to note that these alternatively spliced *NF2* isoforms could potentially encode different sizes of merlin protein. Intriguingly, among all isoforms tested, only isoform I possesses growth inhibitory activity when assayed *in vitro* (Yao, S., E. Akhmametyeva, and L.-S. Chang, unpublished data). However, transgenic mice expressing the *NF2* isoform lacking exon 2 showed high prevalence of Schwann cell-derived tumors and Schwann cell hyperplasia (65). Also, it is not known why schwannomas preferentially express certain *NF2* isoforms. It is possible that the functional contribution of the *NF2* tumor suppressor may require a balanced expression of various isoform proteins in Schwann cells and/or other cell lineages (29,65). Alternatively, it is tempting to speculate that alternative splicing may be another mechanism for Schwann cells to inactivate merlin function and/or to generate isoforms that have additional properties conducive to tumor formation. We are presently conducting experiments to test these possibilities.

In addition to the longest full-length 6.1-kb *NF2* cDNA, we have also isolated two shorter *NF2* cDNAs that were terminated by different polyadenylation signal sequences within intron 16 (29). These results indicate that differential usage of multiple polyadenylation sites also contributes to the complexity of human *NF2* transcripts. Presently, the functional significance for the differential polyadenylation of *NF2* transcripts is not understood. The structural difference among these *NF2* transcripts argues that they may play some role in the regulation of *NF2* expression. Nevertheless, in conjunction

with tissue-specific alternative splicing (29,202), differential polyadenylation may further provide functional diversity of the *NF2* protein.

cDNA microarray analysis of vestibular schwannomas

Carcinogenesis is a multi-stage phenomenon including both genetic and epigenetic alterations (for recent reviews, see 81,113,219,237). In addition to mutations in oncogenes and tumor suppressor genes, deregulated expression of genes involved in specific signaling pathways, damage surveillance, DNA repair or mitotic apparatus frequently occurs in human cancer. In recent years, large-scale gene expression analysis using cDNA microarray has been successfully utilized in evaluating a number of solid tumors and leukemias (4,5,20,36,39,45,46,48,51,57,59,68,76,80,85,87,89,92,93,95,105,107,114,128, 129,133,134,137,138,146,154,161,165,166,172,179,186,199,201,208,215,216, 222,226,243,244,246). Analysis of gene expression profiles using a variety of statistical algorithms to arrange tissues according to similarity in pattern of gene expression (64) has revealed differences among tumors, which are not distinguishable histologically. Molecular classification, rather than histological classification, has been shown to predict the response of specific tumor types to specific therapies (12,25,147,168,189,236,248). This genomic scale approach has helped to identify sub-classes of colon carcinoma, breast carcinoma, melanoma, leukemia and lymphomas (3,8,37,49,63,84,139,157, 163,191,203,217,218,225,251). In several instances, microarray analysis has already identified genes that appear to be useful for predicting clinical behavior (11,13,27,34,52,69,71,91,108,115,180,185,188,213,232-235,247).

Vestibular schwannoma characteristics cannot be explained by the current understanding of gene mutation types alone. Investigating inter-tumor variability of gene expression profiles shows promise to help unravel the clinical differences among subtypes of vestibular schwannomas. Three complementary approaches can be used to evaluate the gene expression profile of vestibular schwannomas. The first is to identify pathways of tumorigenesis common to schwannomas regardless of clinical variation in tumor manifestations. The second is to find pathways and/or genes, which are differentially expressed in tumors of the same type, and the third is to compare normal tissue expression profiles with tumor tissues' profiles.

To better understand the pathways leading to schwannoma formation, we have utilized cDNA microarray analysis to evaluate gene expression profiles of vestibular schwannomas (129,243). Three sporadic vestibular schwannomas, two NF2-associated schwannomas, and three cystic schwannomas were compared to a normal vestibular nerve from a patient with a sporadic schwannoma. Of 25,920 genes or expressed sequence tags screened, 42 genes were significantly up-regulated by a factor of three or more in 6 of the 8

tumors examined. Additionally, multiple genes were found to be significantly down-regulated in the majority of vestibular schwannomas examined. Of these genes, eight genes involved with cell signaling and division were down-regulated. These include an apoptosis-related, putative tumor suppressor gene LUCA-15, which was down-regulated in seven of eight schwannomas, studied (243). The LUCA-15 gene maps to the lung cancer tumour suppressor locus 3p21.3 and encodes an RNA binding nuclear protein (47,50). A number of alternative LUCA-15 RNA splice variants have been isolated and display different abilities to either enhance or suppress apoptosis (159,160,185,223, 224). The LUCA-15 protein contains zinc fingers and possesses transcription-activation function (Luo, H. and L.-S. Chang, unpublished data).

Among the up-regulated genes, two mediators of angiogenesis, endoglin and osteonectin, were highly elevated in most, if not all, vestibular schwannomas examined (243). Endoglin, also called CD105, is a cell membrane glycoprotein, which is frequently over-expressed on tumor-associated vascular endothelium (60). Endoglin functions as an accessory component of the transforming growth factor-β receptor complex and has been suggested to have prognostic significance in selected neoplasia. In addition, the potential usefulness of endoglin in tumor imaging and anti-angiogenic therapy has been well documented (60). Endoglin was found to be significantly up-regulated in all of the solid vestibular schwannomas but not in any of the cystic schwannomas examined (243). The difference in endoglin gene expression may be a key to unlocking why some schwannomas develop into the aggressive cystic phenotype. Osteonectin is a secreted glycoprotein that interacts with extracellular matrix proteins to decrease adhesion of cells from the matrix, thereby inducing a biological state conducive to cell migration. Osteonectin was elevated in all of the tumors studied and may be a target for potential therapies including angiogenesis inhibitors (243).

An example of a deregulated signaling pathway suggested by the microarray data is the retinoblastoma protein (pRb)-cyclin dependent kinase (CDK) pathway, which regulates G_1-S progression (129). All schwannomas examined displayed deregulated expression of at least one of the genes involved in this pRb-CDK pathway. In addition, CDK2 was found to be down-regulated in 7 of 8 tumors.

We also found up-regulation of transforming factor RhoB all of the schwannomas examined (243). The Rho GTPase proteins share about 30% homology with Ras and are crucial regulators of the actin cytoskeleton, cell adhesion, and motility (reviewed in 28,38,151,184). Rho-family members play a critical role in Ras transformation (100,181,183,254), making them potential anticancer therapeutic targets. Unlike most members of the Rho family, RhoB is a growth factor- and oncogenic-induced immediate early gene product that is regulated during the cell cycle (104,252). RhoB, by itself, is weakly

oncogenic, but is required for the initiation and maintenance of transformation by the oncogenic Ras protein (131,181). In addition, RhoB is a critical target of farnesyltransferase inhibitors, a novel class of anti-tumor chemotherapeutics (124,131-132,253). The fact that RhoB expression is elevated in all schwannomas examined suggests that RhoB may be a downstream target of merlin in Schwann cells (243).

One important consideration in our cDNA microarray analysis is the use of the paired normal vestibular nerve as the control (129,243). Experiments using cultured Schwann cells may yield data for direct comparison with schwannoma tissue. However, the drawback of using a cell culture is that culture conditions could alter gene expression patterns. Also, limited division has been commonly observed with cultured Schwann cells and vestibular schwannoma cells. Nevertheless, a direct comparison of protein expression for CDK2, RhoB, osteonectin, and merlin in tissue sections together with quantitative real-time PCR analysis for CDK2 and LUCA-15 yielded results consistent with our cDNA microarray data when schwannoma tumors were compared with the normal vestibular nerve (129,243). For confirmation, we are presently conducting additional cDNA microarray analysis comparing multiple pairs of vestibular nerves, vestibular schwannomas, and cultured Schwann cells.

Microarray analysis of vestibular schwannomas has opened many new potential avenues of investigation. A more complete understanding of why *NF2* mutations lead to tumor formation is dependent upon understanding other interacting genes whose expression are deregulated during tumorigenesis. Investigating inter-tumor variability and comparing normal Schwann cells to schwannoma cells via gene expression profiles shows promise to help unravel the clinical differences among the types of vestibular schwannomas.

Summary

Recent advances in molecular oncology have identified the *NF2* tumor suppressor gene, which is frequently mutated in all three types of vestibular schwannomas. Analysis of *NF2* function and regulation has provided the first step toward the better understanding of the molecular mechanism of schwnnoma tumorigenesis. Functional genomics and proteonomics studies have generated vast amounts of information for translational approaches. It is anticipated that further analysis of the information will lead to the development of novel pharmaco-therapeutics, offering alternatives to the current options of untreated observation of tumor growth, stereotactic radiation, or surgical removal.

Acknowledgement

We thank members of the Chang laboratory for contributing to the work. This study was supported by the US Department of Defense Neurofibromatosis Research Program.

References

1. Alfthan, K., Heiska, L., Gronholm, M., Renkema, G.H., and Carpen, O. 2004. Cyclic AMP-dependent protein kinase phosphorylates merlin at serine 518 independently of p21-activated kinase and promotes merlin-ezrin heterodimerization. J. Biol. Chem. 279:18559-18566.
2. Algrain, M., Arpin, M., and Louvard, D. 1993. Wizardry at the cell cortex. Current Biol. 3:451-454.
3. Alizadeh, A.A., Eisen, M.B., Davis, R.E., Ma, C., Lossos, I.S., Rosenwald, A., Boldrick, J.C., Sabet, H., Tran, T., Yu, X., Powell, J.I., Yang, L., Marti, G.E., Moore, T., Hudson, J. Jr., Lu, L., Lewis, D.B., Tibshirani, R., Sherlock, G., Chan, W.C., Greiner, T.C., Weisenburger, D.D., Armitage, J.O., Warnke, R., Levy, R., Wilson, W., Grever, M.R., Byrd, J.C., Botstein, D., Brown, P.O., and Staudt, L.M. 2000. Distinct types of diffuse large B-cell lymphoma identified by gene expression profiling. Nature 403:503-511.
4. Almstrup, K., Hoei-Hansen, C.E., Wirkner, U., Blake, J., Schwager, C., Ansorge, W., Nielsen, J.E., Skakkebaek, N.E., Rajpert-De Meyts, E., and Leffers, H. 2004. Embryonic stem cell-like features of testicular carcinoma in situ revealed by genome-wide gene expression profiling. Cancer Res. 64:4736-4743.
5. Alon, U., Barkai, N., Notterman, D.A., Gish, K., Ybarra, S., Mack, D., and Levine, A.J. 1999. Broad patterns of gene expression revealed by clustering analysis of tumor and normal colon tissues probed by oligonucleotide arrays. Proc. Natl. Acad. Sci. USA 96:6745-6750.
6. Antinheimo, J., Sallinen, S.L., Sallinen, P., Haapasalo, H., Helin, H., Horelli-Kuitunen, N., Wessman, M., Sainio, M., Jaaskelainen, J., and Carpen, O. 2000. Genetic aberrations in sporadic and neurofibromatosis 2 (NF2)-associated schwannomas studied by comparative genomic hybridization (CGH). Acta Neurochir. (Wien) 142:1099-1104; discussion 1104-1105.
7. Arakawa, H., Hayashi, N., Nagase, H., Ogawa, M., and Nakamura, Y. 1994. Alternative splicing of the NF2 gene and its mutation analysis of breast and colorectal cancers. Hum. Mol. Genet. **3**: 565-568.
8. Armstrong, S.A., Staunton, J.E., Silverman, L.B., Pieters, R., den Boer, M.L., Minden, M.D., Sallan, S.E., Lander, E.S., Golub, T.R., and Korsmeyer, S.J. 2002. MLL translocations specify a distinct gene expression profile that distinguishes a unique leukemia. Nat. Genet. 30:41-47.
9. Arun, D. and Gutmann, D.H. 2004. Recent advances in neurofibromatosis type 1. Curr. Opin. Neurol. 17:101-105.
10. Baser, M.E., Evans, R., and Gutmann, D.H. 2003. Neurofibromatosis 2. Curr. Opin. Neurol. 16:27-33.
11. Beer, D.G., Kardia, S.L., Huang, C.C., Giordano, T.J., Levin, A.M., Misek, D.E., Lin, L., Chen, G., Gharib, T.G., Thomas, D.G., Lizyness, M.L., Kuick, R.,

Hayasaka, S., Taylor, J.M., Iannettoni, M.D., Orringer, M.B., and Hanash, S. 2002. Gene-expression profiles predict survival of patients with lung adenocarcinoma. Nat. Med. 8:816-824.

12. Belbin, T.J., Singh, B., Barber, I., Socci, N., Wenig, B., Smith, R., Prystowsky, M.B., and Childs, G. 2002. Molecular classification of head and neck squamous cell carcinoma using cDNA microarrays. Cancer Res. 62:1184-1190.
13. Bertucci, F., Salas, S., Eysteries, S., Nasser, V., Finetti, P., Ginestier, C., Charafe-Jauffret, E., Loriod, B., Bachelart, L., Montfort, J., Victorero, G., Viret, F., Ollendorff, V., Fert, V., Giovaninni, M., Delpero, J.R., Nguyen, C., Viens, P., Monges, G., Birnbaum, D., and Houlgatte, R. 2004. Gene expression profiling of colon cancer by DNA microarrays and correlation with histoclinical parameters. Oncogene 23:1377-1391.
14. Bianchi, A.B., Hara, T., Ramesh, V., Gao, J., Klein-Azanto, A.J., Morin, F., Menon, A.G., Trofatter, J.A., Gusella, J.F., Seizinger, B.R., et al. 1994. Mutations in transcript isoforms of the neurofibromatosis 2 gene in multiple human tumour types. Nat. Genet. 6:185-192.
15. Bianchi, A.B., Mitsunnaga, S.I., Cheng, J.Q., Klein, W.M., Jhanwar, S.C., Seizinger, B., Kley, N., Klein-Szanto, A.J., and Testa, J.R. 1995. High frequency of inactivating mutations in the neurofibromatosis type 2 gene (NF2) in primary malignant mesotheliomas. Proc. Natl. Acad. Sci. USA 92:10854-10858.
16. Bijlsma, E.K., Merel, P., Fleury, P., van Asperen, C.J., Westerveld, A., Delattre, O., Thomas, G., and Hulsebos, T.J. 1995. Family with neurofibromatosis type 2 and autosomal dominant hearing loss: identification of carriers of the mutated NF2 gene. Hum. Genet. 96:1-5.
17. Bikhazi, P.H., Lalwani, A.K., Kim, E.J., Bikhazi, N., Attaie, A., Slattery, W.H., Jackler, R.K., and Brackmann, D.E. 1998. Germline screening of the NF-2 gene in families with unilateral vestibular schwannoma. Otolaryngol. Head Neck Surg. 119:1-6.
18. Bourn, D., Carter, S.A., Mason, S., Gareth, D., Evans, R., and Strachan, T. 1994. Germline mutations in the neurofibromatosis type 2 tumour suppressor gene. Hum. Mol. Genet. 3:813-816.
19. Bourn, D., Evans, G., Mason, S., Tekes, S., Trueman, L., and Strachan, T. 1995. Eleven novel mutations in the NF2 tumour suppressor gene. Hum. Genet. 95:572-574.
20. Boussioutas, A., Li, H., Liu, J., Waring, P., Lade, S., Holloway, A.J., Taupin, D., Gorringe, K., Haviv, I., Desmond, P.V., and Bowtell, D.D. 2003. Distinctive patterns of gene expression in premalignant gastric mucosa and gastric cancer. Cancer Res. 63:2569-2577.
21. Bretscher, A., Chambers, D., Nguyen, R., and Reczek, D. 2000. ERM-Merlin and EBP50 protein families in plasma membrane organization and function. Annu. Rev. Cell. Dev. Biol. 16:113-143.
22. Bruder, C.E., Ichimura, K., Blennow, E., Ikeuchi, T., Yamaguchi, T., Yuasa, Y., Collins, V.P., and Dumanski, J.P. 1999. Severe phenotype of neurofibromatosis type 2 in a patient with a 7.4-MB constitutional deletion on chromosome 22: possible localization of a neurofibromatosis type 2 modifier gene? Genes Chrom. Cancer 25:184-190.

23. Bruder, C.E., Ichimura, K., Tingby, O., Hirakawa, K., Komatsuzaki, A., Tamura, A., Yuasa, Y., Collins, V.P., and Dumanski, J.P. 1999. A group of schwannomas with interstitial deletions on 22q located outside the NF2 locus shows no detectable mutations in the NF2 gene. Hum. Genet. 104:418-424.
24. Bruder, C.E., Hirvela, C., Tapia-Paez, I., Fransson, I., Segraves, R., Hamilton, G., Zhang, X.X., Evans, D.G., Wallace, A.J., Baser, M.E., Zucman-Rossi, J., Hergersberg, M., Boltshauser, E., Papi, L., Rouleau, G.A., Poptodorov, G., Jordanova, A., Rask-Andersen, H., Kluwe, L., Mautner, V., Sainio, M., Hung, G., Mathiesen, T., Moller, C., Pulst, S.M., Harder, H., Heiberg, A., Honda, M., Niimura, M., Sahlen, S., Blennow, E., Albertson, D.G., Pinkel, D., and Dumanski, J.P. 2001. High resolution deletion analysis of constitutional DNA from neurofibromatosis type 2 (NF2) patients using microarray-CGH. Hum. Mol. Genet. 10: 271-282.
25. Bubendorf, L., Kolmer, M., Kononen, J., Koivisto, P., Mousses, S., Chen, Y., Mahlamaki, E., Schraml, P., Moch, H., Willi, N., Elkahloun, A.G., Pretlow, T.G., Gasser, T.C., Mihatsch, M.J., Sauter, G., and Kallioniemi, O.P. 1999. Hormone therapy failure in human prostate cancer: analysis by complementary DNA and tissue microarrays. J. Natl. Cancer Inst. 91:1758-1764.
26. Bull. World Health Org. 1992. Prevention and control of neurofibromatosis: Memorandum from a joint WHO/NNFF meeting. 70:173-182.
27. Bullinger, L., Dohner, K., Bair, E., Frohling, S., Schlenk, R.F., Tibshirani, R., Dohner, H., and Pollack, J.R. 2004. Use of gene-expression profiling to identify prognostic subclasses in adult acute myeloid leukemia. N. Engl. J. Med. 350:1605-1616.
28. Burridge, K. and Wennerberg, K. 2004. Rho and Rac take center stage. Cell 116:167-179.
29. Chang, L.-S., Akhmametyeva, E.M., Wu, Y., Zhu, L., and Welling, D.B. 2002. Multiple transcription initiation sites, alternative splicing, and differential polyadenylation contribute to the complexity of human neurofibromatosis 2 transcripts. Genomics 79:63-76.
30. Charabi, S., Klinken, L., Tos, M., and Thomsen, J. 1994. Histopathology and growth pattern of cystic acoustic neuromas. Laryngoscope 104:1348-1352.
31. Charabi, S., Mantoni, M., Tos, M., and Thomsen, J. 1994. Cystic vestibular schwannomas: neuroimaging and growth rate. J. Laryngol. Otol. 108:375-379.
32. Charabi, S., Tos, M., Borgesen, S.E., and Thomsen, J. 1994. Cystic acoustic neuromas. Results of translabyrinthine surgery. Arch. Otolaryngol. H.N. Surg. 120:1333-1338.
33. Charabi, S., Tos, M., Thomsen, J., Rygaard, J., Fundova, P., and Charabi, B. 2000. Cystic vestibular schwannoma - clinical and experimental studies. Acta Otolaryngol. Suppl. 543:11-13.
34. Cheok, M.H., Yang, W., Pui, C.H., Downing, J.R., Cheng, C., Naeve, C.W., Relling, M.V., and Evans, W.E. 2003. Treatment-specific changes in gene expression discriminate in vivo drug response in human leukemia cells. Nat. Genet. 34:85-90.
35. Chishti, A.H., Kim, A.C., Marfatia, S.M., Lutchman, M., Hanspal, M., Jindal, H., Liu, S.C., Low, P.S., Rouleau, G.A., Mohandas, N., Chasis, J.A., Conboy, J.G., Gascard, P., Takakuwa, Y., Huang, S.C., Benz, E.J., Jr, Bretscher, A., Fehon, R.G.,

Gusella, J.F. et al. 1998. The FERM domain: a unique module involved in the linkage of cytoplasmic proteins to the membrane. TIBS 23:281-282.
36. Chuaqui, R.F., Cole, K.A., Emmert-Buck, M.R., and Merino, M.J. 1998. Histopathology and molecular biology of ovarian epithelial tumors. Ann. Diagn. Pathol. 2:195-207.
37. Chung, C.H., Parker, J.S., Karaca, G., Wu, J., Funkhouser, W.K., Moore, D., Butterfoss, D., Xiang, D., Zanation, A., Yin, X., Shockley, W.W., Weissler, M.C., Dressler, L.G., Shores, C.G., Yarbrough, W.G., and Perou, C.M. 2004. Molecular classification of head and neck squamous cell carcinomas using patterns of gene expression. Cancer Cell. 5:489-500.
38. Coleman, M.L., Marshall, C.J., and Olson, M.F. 2004. RAS and RHO GTPases in G1-phase cell-cycle regulation. Nat Rev Mol. Cell. Biol. 5:355-366.
39. Cromer, A., Carles, A., Millon, R., Ganguli, G., Chalmel, F., Lemaire, F., Young, J., Dembele, D., Thibault, C., Muller, D., Poch, O., Abecassis, J., and Wasylyk, B. 2004. Identification of genes associated with tumorigenesis and metastatic potential of hypopharyngeal cancer by microarray analysis. Oncogene 23:2484-2498.
40. Dasgupta, B. and Gutmann, D.H. 2003. Neurofibromatosis 1: closing the GAP between mice and men. Curr. Opin. Genet. Dev. 13:20-27.
41. Deguen, B., Goutebroze, L., Giovannini, M., Boisson, C., van der Neut, R., Jaurand, M.C., and Thomas, G. 1998. Heterogeneity of mesothelioma cell lines as defined by altered genomic structure and expression of the NF2 gene. Int. J. Cancer 77:554-560.
42. Deguen, B., Merel, P., Goutebroze, L., Giovannini, M., Reggio, H., Arpin, M., and Thomas, G. 1998. Impaired interaction of naturally occurring mutant NF2 protein with actin-based cytoskeleton and membrane. Hum. Mol. Genet. 7:217-226
43. De Klein, A., Riegman, P.H., Bijlsma, E.K., Heldoorn, A., Muijtjens, M., den Bakker, M.A., Avezaat, C.J., and Zwarthoff, E.C. 1998. A G→A transition creates a branch point sequence and activation of a cryptic exon, resulting in the hereditary disorder neurofibromatosis 2. Hum Mol Genet. 7:393-398.
44. Deperez, R.H.L., Bianchi, A.B., Groen, N.A., Seizinger, B.R., Hagemeijer, A., van Drunen. E., Bootsma, D., Kiper, J.W., Avezaat, C.J.J., Kley, N., and Zwarthoff, E.C. 1994. Frequent NF2 Gene Transcript Mutations in Sporadic Meningiomas and Vestibular Schwannomas. Am. J. Hum. Genet. 54:1022-1029.
45. DeRisi, J., Penland, L., Brown, P.O., Bittner, M.L., Meltzer, P.S., Ray, M., Chen, Y., Su, Y.A., and Trent, J.M. 1996. Use of a cDNA microarray to analyse gene expression patterns in human cancer. Nat. Genet. 14:457-460.
46. Dhanasekaran, S.M., Barrette, T.R., Ghosh, D., Shah, R., Varambally, S., Kurachi, K., Pienta, K.J., Rubin, M.A., and Chinnaiyan, A.M. 2001. Delineation of prognostic biomarkers in prostate cancer. Nature 412:822-826.
47. Drabkin, H.A., West, J.D., Hotfilder, M., Heng, Y.M., Erickson, P., Calvo, R., Dalmau, J., Gemmill, R.M., and Sablitzky, F. 1999. DEF-3(g16/NY-LU-12), an RNA binding protein from the 3p21.3 homozygous deletion region in SCLC. Oncogene 18:2589-2597.
48. Dyrskjot, L., Kruhoffer, M., Thykjaer, T., Marcussen, N., Jensen, J.L., Moller, K., and Orntoft, T.F. 2004. Gene expression in the urinary bladder: a common

carcinoma in situ gene expression signature exists disregarding histopathological classification. Cancer Res. 64:4040-4048.
49. Dyrskjot, L., Thykjaer, T., Kruhoffer, M., Jensen, J.L., Marcussen, N., Hamilton-Dutoit, S., Wolf, H., and Orntoft, T.F. 2003. Identifying distinct classes of bladder carcinoma using microarrays. Nat. Genet. 33:90-96.
50. Edamatsu, H., Kaziro, Y., and Itoh, H. 2000. LUCA15, a putative tumour suppressor gene encoding an RNA-binding nuclear protein, is down-regulated in ras-transformed Rat-1 cells. Genes Cells 5:849-858.
51. Elek, J., Park, K.H., and Narayanan, R. 2000. Microarray-based expression profiling in prostate tumors. In Vivo 14:173-182.
52. Eisen, M.B., Spellman, P.T., Brown, P.O., and Botstein, D. 1998. Cluster analysis and display of genome-wide expression patt. Proc. Natl. Acad. Sci. USA 95:14863-14868.
53. Evans, D.G.R., Huson, S.M., Donnai, D., Neary, W., Blair, V., Newton, V., and Harris, R. 1992. A clinical study of type 2 neurofibromatosis. Q. J. Med. 84:603-618.
54. Evans, D.G.R., Huson, S.M., Donnai, D., Neary, W., Blair, V., Teare, D., Newton, V., Strachan, T., Ramsden, R., and Harris, R. 1992. A genetic study of type 2 neurofibromatosis in the United Kingdom. I. Prevalence, mutation rate, fitness, and confirmation of maternal transmission effect on severity. J. Med. Genet. 29:841-846.
55. Evans, D.G., Trueman, L., Wallace, A., Collins, S., and Strachan, T. 1998. Genotype/phenotype correlations in type 2 neurofibromatosis (NF2): evidence for more severe disease associated with truncating mutations. J. Med. Genet. 35:450-455.
56. Evans, D.G., Wallace, A.J., Wu, C.L., Trueman, L., Ramsden, R.T., and Strachan, T. 1998. Somatic mosaicism: a common cause of classic disease in tumor-prone syndromes? Lessons from type 2 neurofibromatosis. Am. J. Hum. Genet. 63:727-736.
57. Fernandez-Teijeiro, A., Betensky, R.A., Sturla, L.M., Kim, J.Y., Tamayo, P., and Pomeroy, S.L. 2004. Combining gene expression profiles and clinical parameters for risk stratification in medulloblastomas. J. Clin. Oncol. 22:994-998.
58. Fernandez-Valle, C., Tang, Y., Ricard, J., Rodenas-Ruano, A., Taylor, A., Hackler, E., Biggerstaff, J., and Iacovelli, J. 2000. Paxillin binds schwannomin and regulates its density-dependent localization and effect on cell morphology. Nat. Genet. 31:354-362.
59. Ferrando, A.A., Neuberg, D.S., Staunton, J., Loh, M.L., Huard, C., Raimondi, S.C., Behm, F.G., Pui, C.H., Downing, J.R., Gilliland, D.G., Lander, E.S., Golub, T.R., and Look, A.T. 2002. Gene expression signatures define novel oncogenic pathways in T cell acute lymphoblastic leukemia. Cancer Cell 1:75-87.
60. Fonsatti, E., Jekunen, A.P., Kairemo, K.J., Coral, S., Snellman, M., Nicotra, M.R., Natali, P.G., Altomonte, M., Maio, M. 2000. Endoglin is a suitable target for efficient imaging of solid tumors: in vivo evidence in a canine mammary carcinoma model. Clin Cancer Res. 6:2037-2043.
61. Fontaine, B., Rouleau, G.A., Seizinger, B.R., Menon, A.G., Jewell, A.F., Martuza, R.L., and Gusella, J.F. 1991. Molecular genetics of neurofibromatosis 2 and related tumors (Acoustic neuroma and meningioma). Ann. NY Acad. Sci. 615:338-343.

62. Fundova, P., Charabi, S,. Tos, M., and Thomsen, J. 2000. Cystic vestibular schwannoma: surgical outcome. J. Laryngol. Otol. 114:935-939.
63. Furge, K.A., Lucas, K.A., Takahashi, M., Sugimura, J., Kort, E.J., Kanayama, H.O., Kagawa, S., Hoekstra, P., Curry, J., Yang, X.J., and The, B.T. 2004. Robust classification of renal cell carcinoma based on gene expression data and predicted cytogenetic profiles. Cancer Res. 64:4117-4121.
64. Getz, G., Levine, E., and Domany, E. 2000. Coupled two-way clustering analysis of gene microarray data. Proc. Natl. Acad. Sci. USA 97:12079-12084.
65. Giovannini, M., Robanus-Maandag, E., Niwa-Kawakita, M., van der Valk, M., Woodruff. J.M., Goutebroze, L., Merel, P., Berns, A., and Thomas, G. 1999. Schwann cell hyperplasia and tumors in transgenic mice expressing a naturally occurring mutant NF2 protein. Genes Dev. 13:978-986.
66. Giovannini, M., Robanus-Maandag, E., van der Valk, M., Niwa-Kawakita, M., Abramowski, V., Goutebroze, L., Woodruff, J.M., Berns, A., and Thomas, G. 2000. Conditional biallelic *Nf2* mutation in the mouse promotes manifestations of human neurofibromatosis type 2. Genes Dev. 14:1617-1630.
67. Glasscock, M.E., Woods, C.I., Jackson, C.G., and Welling, D.B. 1989. Management of bilateral acoustic tumors. Laryngoscope 99:475-484.
68. Godard, S., Getz, G., Delorenzi, M., Farmer, P., Kobayashi, H., Desbaillets, I., Nozaki, M., Diserens, A.C., Hamou, M.F., Dietrich, P.Y., Regli, L., Janzer, R.C., Bucher, P., Stupp, R., de Tribolet, N., Domany, E., and Hegi, M.E. 2003. Classification of human astrocytic gliomas on the basis of gene expression: a correlated group of genes with angiogenic activity emerges as a strong predictor of subtypes. Cancer Res. 63:6613-6625.
69. Golub, T.R., Slonim, D.K., Tamayo, P., Huard, C., Gaasenbeek, M., Mesirov, J.P., Coller, H., Loh, M.L., Downing, J.R., Caligiuri, M.A., Bloomfield, C.D., and Lander, E.S. 1999. Molecular classification of cancer: class discovery and class prediction by gene expression monitoring. Science 286:531-537.
70. Gonzalez-Agosti, C., Xu, L., Pinney, D., Beauchamp, R., Hobbs, W., Gusella, J., and Ramesh, V. 1996. The merlin tumor suppressor localizes preferentially in membrane ruffles. Oncogene 13:1239-1247.
71. Gordon, G.J., Jensen, R.V., Hsiao, L.L., Gullans, S.R., Blumenstock, J.E., Richards, W.G., Jaklitsch, M.T., Sugarbaker, D.J., and Bueno, R. 2003. Using gene expression ratios to predict outcome among patients with mesotheliomas. J. Natl. Cancer Inst. 95:598-605.
72. Goutebroze, L., Brault, E., Muchardt, C., Camonis, J., and Thomas, G. 2000. Cloning and characterization of SCHIP-1, a novel protein interacting specifically with spliced isoforms and naturally occurring mutant NF2 proteins. Mol. Cell. Biol. 20:1699-1712.
73. Grant, I.L., Hall, B.E. and Welling, D.B. 2000. Cochlear Implantation in Neurofibromatosis Type 2 in Cochlear Implants. Eds: Waltzman S and Cohen N. Thieme Medical Publishers, New York.
74. Gronholm, M., Vossebein, L., Carlson, C.R., Kuja-Panula, J., Teesalu, T., Alfthan, K., Vaheri, A., Rauvala, H., Herberg, F.W., Tasken, K., and Carpen, O. 2003. Merlin links to the cAMP neuronal signaling pathway by anchoring the RIβ subunit of protein kinase A. J. Biol Chem 278:41167-41172.

75. Gutmann, D.H., Geist, R.T., Xu, H., Kim, J.S., and Saporito-Irwin, S. 1998. Defects in neurofibromatosis 2 protein function can arise at multiple levels. Hum. Mol. Genet. 7:335-345.
76. Gutmann, D.H., Hedrick, N.M., Li, J., Nagarajan, R., Perry, A., and Watson, M.A. 2002. Comparative Gene Expression Profile Analysis of Neurofibromatosis 1-associated and sporadic pilocytic astrocytomas. Cancer Res. 62:2085-2091.
77. Gutmann, D.H., Hirbe, A.C., and Haipek, C.A. 2001. Functional analysis of neurofibromatosis 2 (NF2) missense mutations. Hum Mol Genet. 10:1519-1529.
78. Gutmann, D.H., Sherman, L., Seftor, L., Haipek, C., Hoang Lu, K., and Hendrix, M. 1999. Increased expression of the NF2 tumor suppressor gene product, merlin, impairs cell motility, adhesion and spreading. Hum. Mol. Genet. 8:267-275.
79. Gutmann, D.H., Wright, D.E., Geist, R.T., and Snider, W.D. 1995. Expression of the neurofibromatosis 2 (NF2) gene isoforms during rat embryonic development. Hum. Mol. Genet. **4**: 471-478.
80. Ha, P.K., Benoit, N.E., Yochem, R., Sciubba, J., Zahurak, M., Sidransky, D., Pevsner, J., Westra, W.H., and Califano, J. 2003. A transcriptional progression model for head and neck cancer. Clin. Cancer Res. 9:3058-3064.
81. Hahn, W.C. and Weinberg, R.A. 2002. Rules for making human tumor cells. N. Engl. J. Med. 347:1593-1603.
82. Harada, H., Kumon, Y., Hatta, N., Sakaki, S., and Ohta, S. 1999. Neurofibromatosis type 2 with multiple primary brain tumors in monozygotic twins. Surg. Neurol. 51:528-535.
83. Hedenfalk, I., Duggan, D., Chen, Y., Radmacher, M., Bittner, M., Simon, R., Meltzer, P., Gusterson, B., Esteller, M., Kallioniemi, O.P., Wilfond, B., Borg, A., and Trent, J. 2001. Gene-expression profiles in hereditary breast cancer. N. Engl. J. Med. 344:539-548.
84. Hedenfalk, I., Ringner, M., Ben-Dor, A., Yakhini, Z., Chen, Y., Chebil, G., Ach, R., Loman, N., Olsson, H., Meltzer, P., Borg, A., and Trent, J. 2003. Molecular classification of familial non-BRCA1/BRCA2 breast cancer. Proc. Natl. Acad. Sci. USA 100:2532-2537.
85. Heighway, J., Knapp, T., Boyce, L., Brennand, S., Field, J.K., Betticher, D.C., Ratschiller, D., Gugger, M., Donovan, M., Lasek, A., and Rickert, P. 2002. Expression profiling of primary non-small cell lung cancer for target identification. Oncogene 21:7749-7763.
86. Herrlich, P., Morrison, H., Sleeman, J., Orian-Rousseau, V., Konig, H., Weg-Remers, S., and Ponta, H. 2000. CD44 acts both as a growth- and invasiveness-promoting molecule and as a tumor-suppressing cofactor. Ann. NY Acad. Sci. 910:106-118.
87. Hibbs, K., Skubitz, K.M., Pambuccian, S.E., Casey, R.C., Burleson, K.M., Oegema, T.R., Jr., Thiele, J.J., Grindle, S.M., Bliss, R.L., and Skubitz, A.P. 2004. Differential gene expression in ovarian carcinoma: identification of potential biomarkers. Am. J. Pathol. 165:397-414.
88. Hitotsumatsu, T., Kitamoto, T., Iwaki, T., Fukui, M., and Tateishi, J. 1994. An exon 8-spliced out transcript of neurofibromatosis 2 gene is constitutively expressed in various human tissues. J. Biochem. (Tokyo) **116**: 1205-1207.
89. Hoek, K., Rimm, D.L., Williams, K.R., Zhao, H., Ariyan, S., Lin, A., Kluger, H.M., Berger, A.J., Cheng, E., Trombetta, E.S., Wu, T., Niinobe, M., Yoshikawa,

K., Hannigan, G.E., and Halaban, R. 2004. Expression profiling reveals novel pathways in the transformation of melanocytes to melanomas. Cancer Res. 64:5270-5282.

90. Hoffman, R.A., Kohan, D., and Cohen, N.L. 1992. Cochlear implants in the management of bilateral acoustic neuromas. Am. J. Otol. 13:525-528.
91. Huang, E., Cheng, S.H., Dressman, H., Pittman, J., Tsou, M.H., Horng, C.F., Bild, A., Iversen, E.S., Liao, M., Chen, C.M., West, M., Nevins, J.R., and Huang, A.T. 2003. Gene expression predictors of breast cancer outcomes. Lancet 361:1590-1596.
92. Huang, H., Colella, S., Kurrer, M., Yonekawa, Y., Kleihues, P., and Ohgaki, H. 2000. Gene expression profiling of low-grade diffuse astrocytomas by cDNA arrays. Cancer Res. 60:6868-6874.
93. Huang, H., Okamoto, Y., Yokoo, H., Heppner, F.L., Vital, A., Fevre-Montange, M., Jouvet, A., Yonekawa, Y., Lazaridis, E.N., Kleihues, P., and Ohgaki, H. 2004. Gene expression profiling and subgroup identification of oligodendrogliomas. Oncogene 23:6012-22.
94. Huang, L., Ichimaru, E., Pestonjamasp, K., Cui, X., Nakamura, H., Lo, G.Y., Lin, F.I., Luna, E.J., and Furthmayr, H. 1998. Merlin differ from moesin in binding to F-actin and in its intra- and intermolecular interactions. Biochim. Biophys. Res. Comm. 248:548-553.
95. Huang, Y., Prasad, M., Lemon, W.J., Hampel, H., Wright, F.A., Kornacker, K., LiVolsi, V., Frankel, W., Kloos, R.T., Eng, C., Pellegata, N.S., and de la Chapelle, A. 2001. Gene expression in papillary thyroid carcinoma reveals highly consistent profiles. Proc. Natl. Acad. Sci. USA 98:15044-15049.
96. Hung, G., Faudoa, R., Baser, M.E., Xue, Z., Kluwe, L., Slattery, W., Brackman, D., and Lim, D. 2000. Neurofibromatosis 2 phenotypes and germ-line NF2 mutations determined by an RNA mismatch method and loss of heterozygosity analysis in NF2 schwannomas. Cancer Genet. Cytogenet. 118:167-168.
97. Huynh, D.P., Tran, T.M., Nechiporuk, T., and Pulst, S.M. 1996. Expression of neurofibromatosis 2 transcript and gene product during mouse fetal development. Cell Growth Differ. 7: 1551-1561.
98. Irving, R.M., Harada, T., Moffat, D.A., Hardy, D.G., Whittaker, J.L., Xuereb, J.H., and Maher, E.R. 1997. Somatic neurofibromatosis type 2 gene mutations and growth characteristics in vestibular schwannoma. Am. J. Otol. 18:754-760.
99. Irving, R.M., Moffat, D.A., Hardy, D.G., Barton, D.E., Xuereb, J.H., and Maher, E.R. 1994. Somatic NF2 gene mutations in familial and non-familial vestibular schwannoma. Hum. Mol. Genet. 3:347-350.
100. Izawa, I., Amano, M., Chihara, K., Yamamoto, T., and Kaibuchi, K. 1998. Possible involvement of the inactivation of the Rho-Rho-kinase pathway in oncogenic Ras-induced transformation. Oncogene 17:2863-2871.
101 Jacoby, L.B., Jones, D., Davis, K., Kronn, D., Short, M.P., Gusella, J.F., and MacCollin, M. 1997. Molecular analysis of the NF2 tumor-suppressor gene in schwannomatosis. Am J Hum. Genet. 61:1293-1302.
102. Jacoby, L.B., MacCollin, M., Barone, R., Ramesh, V., and Gusella, J.F. 1996. Frequency and distribution of NF2 mutations in schwannomas. Genes Chrom. Cancer 17:45-55.

103. Jacoby, L.B., MacCollin, M., Louis, D.N., Mohney, T., Rubio, M.P., Pulaski, K., Trofatter, J.A., Kley, N., Seizinger, B., Ramesh, V., et al. 1994. Exon scanning for mutation of the NF2 gene in schwannomas. Hum. Mol. Genet. 3:413-419.
104. Jahner, D. and Hunter, T. 1991. The ras-related gene rhoB is an immediate-early gene inducible by v-Fps, epidermal growth factor, and platelet-derived growth factor in rat fibroblasts. Mol. Cell. Biol. 11:3682-3690.
105. Jain, S., Watson, M.A., DeBenedetti, M.K., Hiraki, Y., Moley, J.F., and Milbrandt, J. 2004. Expression profiles provide insights into early malignant potential and skeletal abnormalities in multiple endocrine neoplasia type 2B syndrome tumors. Cancer Res. 64:3907-3913.
106. Jannatipour, M., Dion, P., Khan, S., Jindal, H., Fan, X., Laganiere, J., Chishti, A.H., and Rouleau, G.A. 2001. Schwannomin isoform-1 interacts with syntenin via PDZ domains. J. Biol. Chem. 276:33093-33100.
107. Jinawath, N., Furukawa, Y., Hasegawa, S., Li, M., Tsunoda, T., Satoh, S., Yamaguchi, T., Imamura, H., Inoue, M., Shiozaki, H., and Nakamura, Y. 2004. Comparison of gene-expression profiles between diffuse- and intestinal-type gastric cancers using a genome-wide cDNA microarray. Oncogene 23:6830-6844.
108. Jones, M.H., Virtanen, C., Honjoh, D., Miyoshi, T., Satoh, Y., Okumura, S., Nakagawa, K., Nomura, H., and Ishikawa, Y. 2004. Two prognostically significant subtypes of high-grade lung neuroendocrine tumours independent of small-cell and large-cell neuroendocrine carcinomas identified by gene expression profiles. Lancet 363:775-781.
109. Kaiser-Kupfer, M., Freidlin, V., Datiles, M.B., Edwards, P.A., Sherman, J.L., Parry, D., McCain, L.M., and Eldridge, R. 1989. The association of posterior capsular lens opacities with bilateral acoustic neuromas in patients with neurofibromatosis type 2. Arch Ophthalmol. 107:541-544.
110. Kameyama, S., Tanaka, R., Kawaguchi, T., Fukuda, M., and Oyanagi, K. 1996. Cystic acoustic neurinomas: studies of 14 cases. Acta Neurochir. 138:695-699.
111. Kanter, W.R., Eldridge, R., Fabricant, R., Allen, J.C., and Koerber, T. 1980. Central neurofibromatosis with bilateral acoustic neuroma: Genetic, clinical and biochemical distinctions from peripheral neurofibromatosis. Neurology 30:851-859.
112. Kehrer-Sawatzki, H., Udart, M., Krone, W., Baden, R., Fahsold, R., Thomas, G., Schmucker, B., and Assum, G. 1997. Mutational analysis and expression studies of the neurofibromatosis type 2 (NF2) gene in a patient with a ring chromosome 22 and NF2. Hum. Genet. 100:67-74.
113. Khanna, C. and Hunter, K. 2004. Modeling metastasis in vivo. Carcinogenesis 25: 1787-1793.
114. Kim, B., Bang, S., Lee, S., Kim, S., Jung, Y., Lee, C., Choi, K., Lee, S.G., Lee, K., Lee, Y., Kim, S.S., Yeom, Y.I., Kim, Y.S., Yoo, H.S., Song, K., and Lee, I. 2003. Expression profiling and subtype-specific expression of stomach cancer. Cancer Res. 63:8248-8255.
115. Kim, J.H., Skates, S.J., Uede, T., Wong, K.K., Schorge, J.O., Feltmate, C.M., Berkowitz, R.S., Cramer, D.W., and Mok, S.C. 2002. Osteopontin as a potential diagnostic biomarker for ovarian cancer. JAMA 287:1671-1679.
116. Kino, T., Takeshima, H., Nakao, M., Nishi, T., Yamamoto, K., Kimura, T., Saito, Y., Kochi, M., Kuratsu, J., Saya, H., and Ushio, Y. 2001. Identification of the cis-

acting region in the NF2 gene promoter as a potential target for mutation and methylation-dependent silencing in schwannoma. Genes Cells 6:441-454.
117. Kissil, J.L., Johnson, K.C., Eckman, M.S., and Jacks, T. 2002. Merlin phosphorylation by p21-activated kinase 2 and effects of phosphorylation on merlin localization. J. Biol. Chem. 277:10394-10399.
118. Kissil, J.L., Wilker, E.W., Johnson, K.C., Eckman, M.S., Yaffe, M.B., and Jacks, T. 2003. Merlin, the product of the Nf2 tumor suppressor gene, is an inhibitor of the p21-activated kinase, Pak1. Mol. Cell. 12:841-849.
119. Kluwe, L., Bayer, S., Baser, M.E., Hazim, W., Haase, W., Funsterer, C., and Mautner, V.F. 1996. Identification of NF2 germ-line mutations and comparison with neurofibromatosis 2 phenotypes. Hum. Genet. 98:534-538.
120. Kluwe, L., MacCollin, M., Tatagiba, M., Thomas, S., Hazim, W., Haase, W., and Mautner, V.F. 1998. Phenotypic variability associated with 14 splice-site mutations in the NF2 gene. Am. J. Med. Genet. 77:228-33.
121. Kluwe, L., Mautner, V., Parry, D.M., Jacoby, L.B., Baser, M., Gusella, J., Davis, K., Stavrou, D., and MacCollin, M. 2000. The parental origin of new mutations in neurofibromatosis 2. Neurogenetics 3:17-24.
122. Kluwe, L. and Mautner, V.F. 1996. A missense mutation in the NF2 gene results in moderate and mild clinical phenotypes of neurofibromatosis type 2. Hum. Genet. 97:224-227.
123. Koga, H., Araki, N., Takeshima, H., Nishi, T., Hirota, T., Kimura, Y., Nakao, M., and Saya, H. 1998. Impairment of cell adhesion by expression of the mutant neurofibromatosis type 2 (NF2) genes which lack exons in the ERM-homology domain. Oncogene 17:801-810.
124. Kohl, N.E. 1999. Farnesyltransferase inhibitors. Preclinical development. Ann. NY Acad. Sci. 886:91-102.
125. Koizuka, I., Seo, R., Sano, M., Matsunaga, T., Murakami, M., Seo, Y., and Watari, H. 1991. High-resolution magnetic resonance imaging of the human temporal bone. ORL J. Otorhinolaryngo.l Relat. Spec. 53:357-361.
126. Laird, A.D., Vajkoczy, P., Shawver, L.K., Thurnher, A., Liang, C., Mohammadi, M., Schlessinger, J., Ullrich, A., Hubbard, S.R., Blake, R.A., Fong, T.A., Strawn, L.M., Sun, L., Tang, C., Hawtin, R., Tang, F., Shenoy, N., Hirth, K.P., McMahon, G., and Cherrington. 2000. SU6668 is a potent antiangiogenic and antitumor agent that induces regression of established tumors. Cancer Res. 60:4152-4160.
127. Lamszus, K., Vahldiek, F., Mautner, V.F., Schichor, C., Tonn, J., Stavrou, D., Fillbrandt, R., Westphal, M., and Kluwe, L. 2000. Allelic losses in neurofibromatosis 2-associated meningiomas. J. Neuropathol. Exp. Neurol. 59:504-512.
128. Lapointe, J., Li, C., Higgins, J.P., van de Rijn, M., Bair, E., Montgomery, K., Ferrari, M., Egevad, L., Rayford, W., Bergerheim, U., Ekman, P., DeMarzo, A.M., Tibshirani, R., Botstein, D., Brown, P.O., Brooks, J.D., and Pollack, J.R. 2004. Gene expression profiling identifies clinically relevant subtypes of prostate cancer. Proc. Natl. Acad. Sci. USA 101:811-816.
129. Lasak, J.M., Welling, D.B., Salloum, M., Akhmametyeva, E.M., and Chang, L.-S. 2002. Deregulation of the pRb-CDK pathway in vestibular schwannomas. Laryngoscope 112:1555-1561.

130. Lasota, J., Fetsch, J.F., Wozniak, A., Wasag, B., Sciot, R., and Miettinen, M. 2001. The neurofibromatosis type 2 gene is mutated in perineurial cell tumors: a molecular genetic study of eight cases. Am. J. Pathol. 158:1223-1229.
131. Lebowitz, P.F., Davide, J.P., and Prendergast, G.C. 1995. Evidence that farnesyltransferase inhibitors suppress Ras transformation by interfering with Rho activity. Mol. Cell. Biol. 15:6613-6622.
132. Lebowitz, P.F., Du, W., and Prendergast, G.C. 1997. Prenylation of RhoB is required for its cell transforming function but not its ability to activate serum response element-dependent transcription. J. Biol. Chem. 272:16093-16095.
133. Lee, B.C., Cha, K., Avraham, S., and Avraham, H.K. 2004. Microarray analysis of differentially expressed genes associated with human ovarian cancer. Int. J. Oncol. 24:847-851.
134. Leethanakul, C., Patel, V., Gillespie, J., Pallente, M., Ensley, J.F., Koontongkaew, S., Liotta, L.A., Emmert-Buck, M., and Gutkind, J.S. 2000. Distinct pattern of expression of differentiation and growth-related genes in squamous cell carcinomas of the head and neck revealed by the use of laser capture microdissection and cDNA arrays. Oncogene 19:3220-3224.
135. Legoix, P., Sarkissian, H.D., Cazes, L., Giraud, S., Sor, F., Rouleau, G.A., Lenoir, G., Thomas, G., and Zucman-Rossi, J. 2000. Molecular characterization of germline NF2 gene rearrangements. Genomics 65:62-66.
136. Lekanne Deprez, R.H., Bianchi, A.B., Groen, N.A., Seizinger, B.R., Hagemeijer, A., van Drunen, E., Bootsma, D., Koper, J.W., Avezaat, C.J., and Kley, N. 1994. Frequent NF2 gene transcript mutations in sporadic meningiomas and vestibular schwannomas. Am. J. Hum. Genet. 54:1022-1029.
137. Leonard, P., Sharp, T., Henderson, S., Hewitt, D., Pringle, J., Sandison, A., Goodship, A., Whelan, J., and Boshoff, C. 2003. Gene expression array profile of human osteosarcoma. Br. J. Cancer 89:2284-2288.
138. Lipshutz, R.J., Fodor, S.P., Gingeras, T.R., and Lockhar, D.J. 1999. High density synthetic olgonucleotide arrays. Nat. Genet. 21:20-24.
139. Logsdon, C.D., Simeone, D.M., Binkley, C., Arumugam, T., Greenson, J.K., Giordano, T.J., Misek, D.E., Kuick, R., and Hanash, S. 2003. Molecular profiling of pancreatic adenocarcinoma and chronic pancreatitis identifies multiple genes differentially regulated in pancreatic cancer. Cancer Res. 63:2649-2657.
140. Lopez-Correa, C., Zucman-Rossi, J., Brems, H., Thomas, G., and Legius, E. 2000. NF2 gene deletion in a family with a mild phenotype. J. Med. Genet. 37:75-77.
141. Lutchman, M. and Rouleau, G.A. 1995. The neurofibromatosis type 2 gene product, schwannomin, suppresses growth of NIH 3T3 cells. Cancer Res. 55:2270-2274.
142. Lynch, T.M. and Gutmann, D.H. 2002. Neurofibromatosis 1. Neurol. Clin. 20:841-865.
143. MacCollin, M., Braverman, N., Viskochil, D., Ruttledge, M., Davis, K., Ojemann, R., Gusella, J., and Parry, D.M. 1996. A point mutation associated with a severe phenotype of neurofibromatosis 2. Ann. Neurol. 40:440-445.
144. MacCollin, M., Mohney, T., Trofatter, J., Wertelecki, W., Ramesh, V., and Gusella, J. 1993. DNA diagnosis of neurofibromatosis 2. JAMA, 270:2316-2320.

145. MacCollin, M., Ramesh, V., Jacoby, L.B., Louis, D.N., Rubio, M.P., Pulaski, K., Trofatter, J.A., Short, M.P., Bove, C., Eldridge, R., et al. 1994. Mutational analysis of patients with neurofibromatosis 2. Am. J. Hum. Genet. 55:314-320.
146. Magrangeas, F., Nasser, V., Avet-Loiseau, H., Loriod, B., Decaux, O., Granjeaud, S., Bertucci, F., Birnbaum, D., Nguyen, C., Harousseau, J.L., Bataille, R., Houlgatte, R., and Minvielle, S. 2003. Gene expression profiling of multiple myeloma reveals molecular portraits in relation to the pathogenesis of the disease. Blood 101:4998-5006.
147. Martin, K.J., Kritzman, B.M., Price, L.M., Koh, B., Kwan, C.P., Zhang, X., Mackay, A., O'Hare, M.J., Kaelin, C.M., Mutter, G.L., Pardee, A.B., and Sager, R. 2000. Linking gene expression patterns to therapeutic groups in breast cancer. Cancer Res. 60:2232-2238.
148. Martuza, R.L. and Eldridge, R. 1988. Neurofibromatosis 2 (Bilateral acoustic neurofibromatosis). New Engl. J. Med. 318:684-688.
149. Mautner, V.F., Baser, M.E., and Kluwe, L. 1996. Phenotypic variability in two families with novel splice-site and frameshift NF2 mutations. Hum. Genet. 98:203-206.
150. Mautner, V.F., Tatagiba, M., Guthoff, R., Samii, M., and Pulst, S.M. 1993. Neurofibromatosis 2 in the pediatric age group. Neurosurgery 33:92-96.
151. McClatchey, A.I. 2003. Merlin and ERM proteins: unappreciated roles in cancer development? Nat. Rev. Cancer 3:877-883.
152. McClatchey, A.I., Saotome, I., Mercer, K., Crowley, D., Gusella, J.F., Bronson, R.T., and Jacks, T. 1998. Mice heterozygous for a mutation at the NF2 tumor suppressor locus develop a range of highly metastatic tumors. Genes Dev. 12:1121-1133.
153. McClatchey, A.I., Saotome, I., Ramesh, V., Gusella, J.F., and Jacks, T. 1997. The NF2 tumor suppressor gene product is essential for extraembryonic development immediately prior to gastrulation. Genes Dev. 11:1253-1265.
154. Mendez, E., Cheng, C., Farwell, D.G., Ricks, S., Agoff, S.N., Futran, N.D., Weymuller, E.A., Jr., Maronian, N.C., Zhao, L.P., and Chen, C. 2002. Transcriptional expression profiles of oral squamous cell carcinomas. Cancer 95:1482-1494.
155. Merel, P., Hoang-Xuan, K., Sanson, M., Moreau-Aubry, A., Bijlsma, E.K., Lazaro, C., Moisan, J.P., Resche, F., Nishisho, I., Estivill, X., Delattre, J.Y., Poisson, M., Theillet, C., Hulsebos, T., Delattre, O., and Thomas, G. 1995. Predominant occurrence of somatic mutations of the NF2 gene in meningiomas and schwannomas. Genes Chrom. Cancer 13:1211-1216.
156. Merel, P., Hoang-Xuan, K., Sanson, M., Bijlsma, E., Rouleau, G., Laurent-Puig, P., Pulst, S., Baser, M., Lenoir, G., Sterkers, J.M., et al. 1995. Screening for germ-line mutations in the NF2 gene. Genes Chromosomes Cancer 12:117-127.
157. Miura, K., Bowman, E.D., Simon, R., Peng, A.C., Robles, A.I., Jones, R.T., Katagiri, T., He, P., Mizukami, H., Charboneau, L., Kikuchi, T., Liotta, L.A., Nakamura, Y., and Harris, C.C. 2002. Laser capture microdissection and microarray expression analysis of lung adenocarcinoma reveals tobacco smoking- and prognosis-related molecular profiles. Cancer Res. 62:3244-3250.
158. Mohyuddin, A., Neary, W.J., Wallace, A., Wu, C.L., Purcell, S., Reid, H., Ramsden, R.T., Read, A., Black, G., and Evans, D.G. 2002. Molecular genetic

analysis of the NF2 gene in young patients with unilateral vestibular schwannomas. J. Med. Genet. 39:315-322.
159. Mourtada-Maarabouni, M., Sutherland, L.C., Meredith, J.M., and Williams, G.T. 2003. Simultaneous acceleration of the cell cycle and suppression of apoptosis by splice variant delta-6 of the candidate tumour suppressor LUCA-15/RBM5. Genes Cells 8:109-119.
160. Mourtada-Maarabouni, M., Sutherland, L.C., and Williams, G.T. 2002. Candidate tumour suppressor LUCA-15 can regulate multiple apoptotic pathways. Apoptosis 7:421-32.
161. Morrison, C., Farrar, W., Kneile, J., Williams, N., Liu-Stratton, Y., Bakaletz, A., Aldred, M.A., and Eng, C. 2004. Molecular classification of parathyroid neoplasia by gene expression profiling. Am. J. Pathol. 165:565-576.
162. Morrison, H., Sherman, L.S., Legg, J., Banine, F., Isacke, C., Haipek, C.A., Gutmann, D.H., Ponta, H., and Herrlich, P. 2001. The NF2 tumor suppressor gene product, merlin, mediates contact inhibition of growth through interactions with CD44. Genes Dev. 15:968-980.
163. Mukasa, A., Ueki, K., Matsumoto, S., Tsutsumi, S., Nishikawa, R., Fujimaki, T., Asai, A., Kirino, T., and Aburatani, H. 2002. Distinction in gene expression profiles of oligodendrogliomas with and without allelic loss of 1p. Oncogene 21:3961-3968.
164. Murthy, A., Gonzalez-Agosti, C., Cordero, E., Pinney, D., Candia, C., Soloman, F., Gusella, J., and Ramesh, V. 1998. NHE-RF, a regulatory cofactor for Na(+)-H+ exchange, is a common interactor for merlin and ERM (MERM) proteins. J. Biol. Chem. 273:1273-1276.
165. Nagayama, S., Katagiri, T., Tsunoda, T., Hosaka, T., Nakashima, Y., Araki, N., Kusuzaki, K., Nakayama, T., Tsuboyama, T., Nakamura, T., Imamura, M., Nakamura, Y., and Toguchida, J. 2002. Genome-wide analysis of gene expression in synovial sarcomas using a cDNA microarray. Cancer Res. 62:5859-5866.
166. Neben, K., Korshunov, A., Benner, A., Wrobel, G., Hahn, M., Kokocinski, F., Golanov, A., Joos, S., and Lichter, P. 2004. Microarray-based screening for molecular markers in medulloblastoma revealed STK15 as independent predictor for survival. Cancer Res. 64:3103-3111.
167. Neill, G.W. and Crompton, M.R. 2001. Binding of the merlin-I product of the neurofibromatosis type 2 tumour suppressor gene to a novel site in β-fodrin is regulated by association between merlin domains. Biochem. J. 358(Pt 3):727-735.
168. Nielsen, T.O., West, R.B., Linn, S.C., Alter, O., Knowling, M.A., O'Connell, J.X., Zhu, S., Fero, M., Sherlock, G., Pollack, J.R., Brown, P.O., Botstein, D., and van de Rijn, M. 2002. Molecular characterisation of soft tissue tumours: a gene expression study. Lancet 359:1301-1307.
169. Niemczyk, K., Vaneecloo, F.N., Lecomte, M.H., Lejeune, J.P., Lemaitre, L., Skarzynski, H., Vincent, C., and Dubrulle, F. 2000. Correlation between Ki-67 index and some clinical aspects of acoustic neuromas (vestibular schwannomas). Otolaryngol. Head Neck Surg. 123:779-783.
170. NIH Consensus Statement on Acoustic Neuroma, 1992. Neurofibromatosis Res. Newsletter 8:1-7.
171. Nishi, T., Takeshima, H., Hamada, K., Yoshizato, K., Koga, H., Sato, K., Yamamoto, K., Kitamura, I., Kochi, M., Kuratsu, J.I., Saya, H., and Ushio, Y.

1997. Neurofibromatosis 2 gene has novel alternative splicing which control intracellular protein binding. Int. J. Oncol. 10:1025-1029.
172. Nowicki, M.O., Pawlowski, P., Fischer, T., Hess, G., Pawlowski, T., and Skorski, T. 2003. Chronic myelogenous leukemia molecular signature. Oncogene 22:3952-3963.
173. Obremski, V.J., Hall, A.M., and Fernandez-Valle, C. 1998. Merlin, the neurofibromatosis type 2 gene product, and β1 integrin associate in isolated and differentiating Schwann cells. J. Neurobiol. 37:487-501.
174. Parry, D.M., Eldridge, R., Kaiser-Kupfer, M.I., Bouzas, E.A., Pikus, A., and Patronas, N. 1994. Neurofibromatosis 2 (NF2): clinical characteristics of 53 affected individuals and clinical evidence for heterogeneity. Am. J. Med. Genet. 52:450-61.
175. Parry, D.M., MacCollin, M.M., Kaiser-Kupfer, M.I., Pulaski, K., Nicholson, H.S., Bolesta, M., Eldridge, R., Gusella, J.F. 1996. Germ-line mutations in the neurofibromatosis 2 gene: correlation with disease severity and retinal abnormalities. Am. J. Hum. Genet. 59:529-539.
176. Paz-y-Mino, C. and Leone, P.E. 2000. Three novel somatic mutations in the NF2 tumor suppressor gene [g816T>A; g1159A>G; gIVS11-1G>T]. Hum. Mutat. 15:487.
177. Pendl, G., Ganz, J.C., Kitz, K., and Eustacchio, S. 1996. Acoustic neurinomas with macrocysts treated with Gamma Knife radiosurgery. Stereotact. Funct. Neurosurg. 66(Suppl. 1):103-111.
178. Pelton, P.D., Sherman, L.S., Rizvi, T.A., Marchionni, M.A., Wood, P., Friedman, R.A., and Ratner, N. 1998. Ruffling membrane, stress fiber, cell spreading and proliferation abnormalities in human Schwannoma cells. Oncogene 17:2195-2209.
179. Perou, C.M., Sorlie, T., Eisen, M.B., van de Rijn, M., Jeffrey, S.S., Rees, C.A., Pollack, J.R., Ross, D.T., Johnsen, H., Akslen, L.A., Fluge, O., Pergamenschikov, A., Williams, C., Zhu, S.X., Lonning, P.E., Borresen-Dale, A.L., Brown. P.O., and Botstein, D. 2000. Molecular portraits of human breast tumours. Nature 406:747-752.
180. Pomeroy, S.L., Tamayo, P., Gaasenbeek, M., Sturla, L.M., Angelo, M., McLaughlin, M.E., Kim, J.Y., Goumnerova, L.C., Black, P.M., Lau, C., Allen, J.C., Zagzag, D., Olson, J.M., Curran, T., Wetmore, C., Biegel, J.A., Poggio, T., Mukherjee, S., Rifkin, R., Califano, A., Stolovitzky, G., Louis, D.N., Mesirov, J.P., Lander, E.S., and Golub, T.R. 2002. Prediction of central nervous system embryonal tumour outcome based on gene expression. Nature 415:436-442.
181. Prendergast, G.C., Khosravi-Far, R., Solski, P.A., Kurzawa, H., Lebowitz, P.F., and Der, C.J. 1995. Critical role of Rho in cell transformation by oncogenic Ras. Oncogene 10:2289-2296.
182. Pykett, M.J., Murphy, M., Harnish, P.R., and George, D.L. 1994. The neurofibromatosis 2 (NF2) tumor suppressor gene encodes multiple alternatively spliced transcripts. Hum. Mol. Genet. 3: 559-564.
183. Qiu, R.G., Chen, J., McCormick, F., and Symons, M. 1995. A role for Rho in Ras transformation. Proc. Natl. Acad. Sci. USA 92:11781-11785.
184. Raftopoulou, M. and Hall, A. 2004. Cell migration: Rho GTPases lead the way. Dev. Biol. 265:23-32.

185. Ramaswamy, S., Ross, K.N., Lander, E.S., and Golub, T.R. 2003. A molecular signature of metastasis in primary solid tumors. Nat. Genet. 33:49-54.
186. Rhodes, D.R., Yu, J., Shanker, K., Deshpande, N., Varambally, R., Ghosh, D., Barrette, T., Pandey, A., and Chinnaiyan, A.M. 2004. Large-scale meta-analysis of cancer microarray data identifies common transcriptional profiles of neoplastic transformation and progression. Proc. Natl. Acad. Sci. USA 101:9309-9314.
187. Rintala-Maki, N.D. and Sutherland, L.C. 2004. LUCA-15/RBM5, a putative tumour suppressor, enhances multiple receptor-initiated death signals. Apoptosis 9:475-484.
188. Rosenwald, A., Wright, G., Wiestner, A., Chan, W.C., Connors, J.M., Campo, E., Gascoyne, R.D., Grogan, T.M., Muller-Hermelink, H.K., Smeland, E.B., Chiorazzi, M., Giltnane, J.M., Hurt, E.M., Zhao, H., Averett, L., Henrickson, S., Yang, L., Powell, J., Wilson, W.H., Jaffe, E.S., Simon, R., Klausner, R.D., Montserrat, E., Bosch, F., Greiner, T.C., Weisenburger, D.D., Sanger, W.G., Dave, B.J., Lynch, J.C., Vose, J., Armitage, J.O., Fisher, R.I., Miller, T.P., LeBlanc, M., Ott, G., Kvaloy, S., Holte, H., Delabie, J., Staudt, L.M. 2003. The proliferation gene expression signature is a quantitative integrator of oncogenic events that predicts survival in mantle cell lymphoma. Cancer Cell 3:185-197.
189. Rosenwald, A., Wright, G., Chan, W.C., Connors, J.M., Campo, E., Fisher, R.I., Gascoyne, R.D., Muller-Hermelink, H.K., Smeland, E.B., Giltnane, J.M., Hurt, E.M., Zhao, H., Averett, L., Yang, L., Wilson, W.H., Jaffe, E.S., Simon, R., Klausner, R.D., Powell, J., Duffey, P.L., Longo, D.L., Greiner, T.C., Weisenburger, D.D., Sanger, W.G., Dave, B.J., Lynch, J.C., Vose, J., Armitage, J.O., Montserrat, E., Lopez-Guillermo, A., Grogan, T.M., Miller, T.P., LeBlanc, M., Ott, G., Kvaloy, S., Delabie, J., Holte, H., Krajci, P., Stokke, T., Staudt, L.M.; Lymphoma/Leukemia Molecular Profiling Project. 2002. The use of molecular profiling to predict survival after chemotherapy for diffuse large-B-cell lymphoma. N. Engl. J. Med. 346:1937-1947.
190. Rouleau, G.A., Merel, P., Lutchman, M., Sanson, M., Zucman, J., Marineau, C., Hoang-Xuan, K., Demezuk, S., Desmaze, C., Plougastel, B., Pulst, S.M., Lenoir, G., Bijlsma, E., Fashold, R., Dumanshki, J., de Jong, P., Parry, D., Eldrige, R., Aurias, A., Delattre, O., and Thomas, G. 1993. Alteration in a new gene encoding a putative membrane-organising protein causes neurofibromatosis type 2. Nature 363:515-521.
191. Ross, M.E., Zhou, X., Song, G., Shurtleff, S.A., Girtman, K., Williams, W.K., Liu, H.C., Mahfouz, R., Raimondi, S.C., Lenny, N., Patel, A., and Downing, J.R. 2003. Classification of pediatric acute lymphoblastic leukemia by gene expression profiling. Blood 102:2951-2959.
192. Ruttledge, M.H., Andermann, A.A., Phelan, C.M., Claudio, J.O., Han, F.Y., Chretien, N., Rangaratnam, S., MacCollin, M., Short, P., Parry, D., Michels, V., Riccardi, V.M., Weksberg, R., Kitamura, K., Bradburn, J.M., Hall, B.D., Propping, P., and Rouleau, G.A. 1996. Type of mutation in the neurofibromatosis type 2 gene (NF2) frequently determines severity of disease. Am. J. Hum. Genet. 59:331-342.
193. Ruttledge, M.H., Sarrazin, J., Rangaratnam, S., Phelan, C.M., Twist, E., Merel, P., Delattre, O., Thomas, G., Nordenskjoid, M., Collins, V.P., Dumanski, J.P., and Rouleau, G.A. 1994. Evidence for the complete inactivation of the NF2 gene in the majority of sporadic meningiomas. Nat. Genet. 6:180-184.

194. Sainio, M., Jaaskelainen, J., Pihlaja, H., and Carpen, O. 2000. Mild familial neurofibromatosis 2 associates with expression of merlin with altered COOH-terminus. Neurology 54:1132-1138.
195. Sainio, M., Zhao, F., Heiska, L., Turunen, O., ver M, Zwarthoff, E., Lutchman, M,, Rouleau, G.A., Jaaskelainen, J., Vaheri, A., and Carpen, O. 1997. Neurofibromatosis 2 tumor suppressor protein colocalizes with ezrin and CD44 and associates with actin-containing cytoskeleton. J. Cell Sci. 110:2249-2260.
196. Sainz, J., Figueroa, K., Baser, M.E., Mautner, V.F., and Pulst, S.M. 1995. High frequency of nonsense mutations in the NF2 gene caused by C to T transitions in five CGA codons. Hum. Mol. Genet. 4:137-139.
197. Sainz, J., Figueroa, K., Baser, M.E., and Pulst, S.M. 1996. Identification of three neurofibromatosis type 2 (NF2) gene mutations in vestibular schwannomas. Hum. Genet. 97:121-123.
198. Sainz, J., Huynh, D.P., Figueroa, K., Ragge, N.K., Baser, M.E., and Pulst, S.M. 1994. Mutations of the neurofibromatosis type 2 gene and lack of the gene product in vestibular schwannomas. Hum. Mol. Genet. 3:885-891.
199. Sallinen, S.L., Sallinen, P.K., Haapasalo, H.K., Helin, H.J., Helen, P.T., Schraml, P., Kallioniemi, O.P., and Kononen, J. 2000. Identification of differentially expressed genes in human gliomas by DNA microarray and tissue chip techniques. Cancer Res. 60:6617-6622.
200. Sawamura, Y., Shirato, H., Sakamoto, T., Aoyama, H., Suzuki, K., Onimaru, R., Isu, T., Fukuda, S., and Miyasaka, K. 2003. Management of vestibular schwannoma by fractionated stereotactic radiotherapy and associated cerebrospinal fluid malabsorption. J. Neurosurg. 99:685-692.
201. Schaner, M.E., Ross, D.T., Ciaravino, G., Sorlie, T., Troyanskaya, O., Diehn, M., Wang, Y.C., Duran, G.E., Sikic, T.L., Caldeira, S., Skomedal, H., Tu, I.P., Hernandez-Boussard, T., Johnson, S.W., O'Dwyer, P.J., Fero, M.J., Kristensen, G.B., Borresen-Dale, A.L., Hastie, T., Tibshirani, R., van de Rijn, M., Teng, N.N., Longacre, T.A., Botstein, D., Brown, P.O., and Sikic, B.I. 2003. Gene expression patterns in ovarian carcinomas. Mol. Biol. Cell. 14:4376-4386.
202. Schmucker, B., Tang, Y., and Kressel, M. (1999). Novel alternatively spliced isoforms of the neurofibromatosis type 2 tumor suppressor are targeted to the nucleus and cytoplasmic granules. Hum. Mol. Genet. 8: 1561-1570
203. Schwartz, D.R., Kardia, S.L., Shedden, K.A., Kuick, R., Michailidis, G., Taylor, J.M., Misek, D.E., Wu, R., Zhai, Y., Darrah, D.M., Reed, H., Ellenson, L.H., Giordano, T.J., Fearon, E.R., Hanash, S.M., Cho, K.R. 2002. Gene expression in ovarian cancer reflects both morphology and biological behavior, distinguishing clear cell from other poor-prognosis ovarian carcinomas. Cancer Res. 62:4722-4729.
204. Scoles, D.R., Baser, M.E., and Pulst, S.M. 1996. A missense mutation in the neurofibromatosis 2 gene occurs in patients with mild and severe phenotypes. Neurology 47:544-546.
205. Scoles, D.R., Huynh, D.P., Morcos, P.A., Coulsell, E.R., Robinson, N.G., Tamanoi, F., and Pulst, S.M. 1998. Neurofibromatosis 2 tumor suppressor schwannomin interacts with bII-spectrin. Nat. Genet. 18:354-359.
206. Scoles, D.R., Huynh, D.P., Chen, M.S., Burke, S.P., Gutmann, D.H., and Pulst, S.M. 2000. The neurofibromatosis 2 tumor suppressor protein interacts with

hepatocyte growth factor-regulated tyrosine kinase substrate. Hum. Mol. Genet. 9:1567-1574.
207. Sekido, Y., Pass, H.I., Bader, S., Mew, D.J., Christman, M.F., Gazdar, A.F., and Minna, J.D. 1995. Neurofibromatosis type 2 (NF2) gene is somatically mutated in mesothelioma but not in lung cancer. Cancer Res. 55:1227-1231.
208. Shai, R., Shi, T., Kremen, T.J., Horvath, S., Liau, L.M., Cloughesy, T.F., Mischel, P.S., and Nelson, S.F. 2003. Gene expression profiling identifies molecular subtypes of gliomas. Oncogene 22:4918-4923.
209. Shaw, R.J., Paez, J.G., Curto, M., Yaktine, A., Pruitt, W.M., Saotome, I., O'Bryan, J.P., Gupta, V., Ratner, N., Der, C.J., Jacks, T., and McClatchey, A.I. The NF2 tumor suppressor, merlin, functions in Rac-dependent signaling. Dev. Cell 1:63-72.
210. Sherman, L., Xu, H.M., Geist, R.T., Saporito-Irwin, S., Howells, N., Ponta, H., Herrlich, P., and Gutmann, D.H. 1997. Interdomain binding mediates tumor growth suppression by the NF2 gene product. Oncogene 15:2505-2509.
211. Sherman, L.S., Rizvi, T.A., Karyala, S., and Ratner, N. 2000. CD44 enhances neuregulin signaling by Schwann cells. J. Cell. Biol. 150:1071-1084.
212. Sherman, L., Sleeman, J., Herrlich, P., and Ponta, H. 1994. Hyaluronate receptors: key players in growth, differentiation, migration and tumor progression. Curr. Opin. Cell Biol. 6:726-733.
213. Shipp, M.A., Ross, K.N., Tamayo, P., Weng, A.P., Kutok, J.L., Aguiar, R.C., Gaasenbeek, M., Angelo, M., Reich, M., Pinkus, G.S., Ray, T.S., Koval, M.A., Last, K.W., Norton, A., Lister, T.A., Mesirov, J., Neuberg, D.S., Lander, E.S., Aster, J.C., and Golub, T.R. 2002. Diffuse large B-cell lymphoma outcome prediction by gene-expression profiling and supervised machine learning. Nat. Med. 8:68-74.
214. Shirato, H., Sakamoto, T., Takeichi, N., Aoyama, H., Suzuki, K., Kagei, K., Nishioka, T., Fukuda, S., Sawamura, Y., and Miyasaka, K. 2000. Fractionated stereotactic radiotherapy for vestibular schwannoma (VS): comparison between cystic-type and solid-type VS. Int. J. Radiat. Oncol. Biol. Phys. 48:1395-1401.
215. Singhal, S., Wiewrodt, R., Malden, L.D., Amin, K.M., Matzie, K., Friedberg, J., Kucharczuk, J.C., Litzky, L.A., Johnson, S.W., Kaiser, L.R., and Albelda, S.M. 2003. Gene expression profiling of malignant mesotheliomas. Clin. Cancer Res. 9:3080-3097.
216. Skubitz, K.M. and Skubitz, A.P. 2003. Differential gene expression in leiomyosarcoma. Cancer 98:1029-1038.
217. Sorlie, T., Tibshirani, R., Parker, J., Hastie, T., Marron, J.S., Nobel, A., Deng, S., Johnsen, H., Pesich, R., Geisler, S., Demeter, J., Perou, C.M., Lonning, P.E., Brown, P.O., Borresen-Dale, A.L., and Botstein, D. 2003. Repeated observation of breast tumor subtypes in independent gene expression data sets. Proc. Natl. Acad. Sci. USA 100:8418-8423.
218. Sorlie, T., Perou, C.M., Tibshirani, R., Aas, T., Geisler, S., Johnsen, H., Hastie, T., Eisen, M.B., van de Rijn, M., Jeffrey, S.S., Thorsen, T., Quist, H., Matese, J.C., Brown, P.O., Botstein, D., Eystein Lonning, P., and Borresen-Dale, A.L. 2001. Gene expression patterns of breast carcinomas distinguish tumor subclasses with clinical implications. Proc. Natl. Acad. Sci. USA 98:10869-10874.

219. Soto, A.M. and Sonnenschein, C. 2004. The somatic mutation theory of cancer: growing problems with the paradigm? Bioessays 26:1097-1107.
220. Stemmer-Rachamimov, A.O., Ino, Y., Lim, Z.Y., Jacoby, L.B., MacCollin, M., Gusella, J.F., Ramesh, V., and Louis, D.N. 1998. Loss of the NF2 gene and merlin occur by the tumorlet stage of schwannoma development in neurofibromatosis 2. J. Neuropathol. Exp. Neurol. 57:1164-1167.
221. Stokowski, R.P. and Cox, D.R. 2000. Functional analysis of the neurofibromatosis type 2 protein by means of disease-causing point mutations. Am. J. Hum. Genet. 66:873-891.
222. Su, H., Hu, N., Shih, J., Hu, Y., Wang, Q.H., Chuang, E.Y., Roth, M.J., Wang, C., Goldstein, A.M., Ding, T., Dawsey, S.M., Giffen, C., Emmert-Buck, M.R., and Taylor, P.R. 2003. Gene expression analysis of esophageal squamous cell carcinoma reveals consistent molecular profiles related to a family history of upper gastrointestinal cancer. Cancer Res. 63:3872-3876.
223. Sutherland, L.C., Lerman, M., Williams, G.T., and Miller, B.A. 2001. LUCA-15 suppresses CD95-mediated apoptosis in Jurkat T cells. Oncogene 20:2713-2719.
224. Sutherland, L.C., Edwards, S.E., Cable, H.C., Poirier, G.G., Miller, B.A., Cooper, C.S., and Williams, G.T. 2000. LUCA-15-encoded sequence variants regulate CD95-mediated apoptosis. Oncogene 19:3774-81.
225. Takahashi, M., Rhodes, D.R., Furge, K.A., Kanayama, H., Kagawa, S., Haab, B.B., and The, B.T. 2001. Gene expression profiling of clear cell renal cell carcinoma: gene identification and prognostic classification. Proc. Natl. Acad. Sci. USA 98:9754-9759.
226. Takahashi, M., Yang, X.J., Lavery, T.T., Furge, K.A., Williams, B.O., Tretiakova, M., Montag, A., Vogelzang, N.J., Re, G.G., Garvin, A.J., Soderhall, S., Kagawa, S., Hazel-Martin, D., Nordenskjold, A., and The, B.T. 2002. Gene expression profiling of favorable histology Wilms tumors and its correlation with clinical features. Cancer Res. 62:6598-6605.
227. Takeshima, H., Izawa, I., Lee, P.S., Safdar, N., Levin, V.A., and Saya, H. 1994. Detection of cellular proteins that interact with the NF2 tumor suppressor gene product. Oncogene 9:2135-2144.
228. Tikoo, A., Varga, M., Ramesh, V., Gusella, J., and Maruta, H. 1994. An anti-Ras function of neurofibromatosis type 2 gene product (NF2/Merlin). J. Biol. Chem. 269:23387-23390.
229. Trofatter, J.A., MacCollin, M.M., Rutter, J.L., Murrell, J.R., Duyao, M.P., Parry, D.M., Eldridge, R., Kley, N., Menon, A.G., Pulaski, K., Haase, V.H., Ambrose, C.M., Munroe, D., Bove, C., Haines, J.L., Martuza, R.L., MacDonald, M.E., Seizinger, B.R., Short, M.P., Buckler, A.L., and Gusella, J.F. 1993. A novel Moesin-, Exrin-, Radixin-like gene is a candidate for the neurofibromatosis 2 tumor-suppressor. Cell 72:791-800.
230. Twist, E.C., Ruttledge, M.H., Rousseau, M., Sanson, M., Papi, L., Merel, P., Delattre, O., Thomas, G., and Rouleau, G.A. 1994. The neurofibromatosis type 2 gene is inactivated in schwannomas. Hum. Mol. Genet. 3:147-151.
231. Vajkoczy, P., Menger, M.D., Vollmar, B., Schilling, L., Schmiedek, P., Hirth, K.P., Ullrich, A., and Fong, T.A. 1999. Inhibition of tumor growth, angiogenesis, and microcirculation by the novel Flk-1 inhibitor SU-5416 as assessed by intravital multi-fluorescence videomicroscopy. Neoplasia 1:31-41

232. Valk, P.J., Verhaak, R.G., Beijen, M.A., Erpelinck, C.A., Barjesteh van Waalwijk van Doorn-Khosrovani, S., Boer, J.M., Beverloo, H.B., Moorhouse, M.J., van der Spek, P.J., Lowenberg, B., and Delwel, R. 2004. Prognostically useful gene-expression profiles in acute myeloid leukemia. N. Engl. J. Med. 350:1617-1628.
233. van de Vijver, M.J., He, Y.D., van't Veer, L.J., Dai, H., Hart, A.A., Voskuil, D.W., Schreiber, G.J., Peterse, J.L., Roberts, C., Marton, M.J., Parrish, M., Atsma, D., Witteveen, A., Glas, A., Delahaye, L., van der Velde, T., Bartelink, H., Rodenhuis, S., Rutgers, E.T., Friend, S.H., and Bernards, R. 2002. A gene-expression signature as a predictor of survival in breast cancer. N. Engl. J. Med. 347:1999-2009.
234. van 't Veer, L.J., Dai, H., van de Vijver, M.J., He, Y.D., Hart, A.A., Mao, M., Peterse, H.L., van der Kooy, K., Marton, M.J., Witteveen, A.T., Schreiber, G.J., Kerkhoven, R.M., Roberts, C., Linsley, P.S., Bernards, R., and Friend, S.H. 2002. Gene expression profiling predicts clinical outcome of breast cancer. Nature 415:530-536.
235. Vasselli, J.R., Shih, J.H., Iyengar, S.R., Maranchie, J., Riss, J., Worrell, R., Torres-Cabala, C., Tabios, R., Mariotti, A., Stearman, R., Merino, M., Walther, M.M., Simon, R., Klausner, R.D., and Linehan, W.M. 2003. Predicting survival in patients with metastatic kidney cancer by gene-expression profiling in the primary tumor. Proc. Natl. Acad. Sci. USA 100:6958-6963.
236. Virtaneva, K., Wright, F.A., Tanner, S.M., Yuan, B., Lemon, W.J., Caligiuri, M.A., Bloomfield, C.D., de La Chapelle, A., and Krahe, R. 2001. Expression profiling reveals fundamental biological differences in acute myeloid leukemia with isolated trisomy 8 and normal cytogenetics. Proc. Natl. Acad. Sci. USA 98:1124-1129.
237. Vogelstein, B. and Kinzler, K.W. 2004. Cancer genes and the pathways they control. Nat. Med. 10:789-799.
238. Welling, D.B. 1998. Clinical manisfestations of mutations in the neurofibromatosis type 2 gene in vestibular schwannomas (acoustic neuromas). Laryngoscope 108:178-189.
239. Welling, D.B., Akhmametyeva, E.M., Daniels, R.L., Lasak, J.M., Zhu, L., Miles-Markley, B.A., and Chang, L.-S. 2000. Analysis of the human neurofibromatosis Type 2 gene promoter and its expression. Otolaryngol. Head Neck Surg. 123:413-418.
240. Welling, D.B. and Chang, L.-S. 2000. All in a name: Schwannomin versus Merlin. Am. J. Otol. 21:289.
241. Welling, D.B., Glasscock, M.E., Woods, C.I., and Jackson, C.G. 1990. Acoustic neuroma: A cost-effective approach. Otolaryngol. Head Neck Surg. 103:364-370.
242. Welling, D.B., Guida, M., Goll, F., Pearl, D.K., Glasscock, M.E., Pappas, D.G., Linthicum, F.H., Rogers, D., and Prior, T.W. 1996. Mutational spectrums in the neurofibromatosis type 2 gene in sporadic and familial schwannomas. Hum. Genet. 98:189-193.
243. Welling, D.B., Lasak, J.M., Akhmametyeva, E.M., and Chang, L.-S. 2002. cDNA microarray analysis of vestibular schwannomas. Otol. Neurotol. 23:736-748.
244. Welsh, J.B., Zarrinkar, P.P., Sapinoso, L.M., Kern, S.G., Behling, C.A., Monk, B.J., Lockhart, D.J., Burger, R.A., and Hampton, G.M. 2001. Analysis of gene expression profiles in normal and neoplastic ovarian tissue samples identifies

candidate molecular markers of epithelial ovarian cancer. Proc. Natl. Acad. Sci. USA 98:1176-1181.

245. Wertelecki, W., Rouleau, G.A., Superneau, D.W., Forehand, L.W., Williams, J.P., Haines, J.L., and Gusella, J.F. 1988. Neurofibromatosis 2: Clinical and DNA linkage studies of a larger kindred. New Engl. J. Med. 319:278-283.
246. Whipple, M.E., Mendez, E., Farwell, D.G., Agoff, S.N., and Chen, C. 2004. A genomic predictor of oral squamous cell carcinoma. Laryngoscope 114:1346-1354.
247. Wigle, D.A., Jurisica, I., Radulovich, N., Pintilie, M., Rossant, J., Liu, N., Lu, C., Woodgett, J., Seiden, I., Johnston, M., Keshavjee, S., Darling, G., Winton, T., Breitkreutz, B.J., Jorgenson, P., Tyers, M., Shepherd, F.A., and Tsao, M.S. 2002. Molecular profiling of non-small cell lung cancer and correlation with disease-free survival. Cancer Res. 62:3005-3008.
248. Willenbrock, H., Juncker, A.S., Schmiegelow, K., Knudsen, S., and Ryder, L.P. 2004. Prediction of immunophenotype, treatment response, and relapse in childhood acute lymphoblastic leukemia using DNA microarrays. Leukemia 18:1270-1277.
249. Xiao, G.H., Beeser, A., Chernoff, J., and Testa, J.R. 2002. P21-activated Kinase links Rac/Cdc42 signaling to merlin. J. Biol. Chem. 277:883-886.
250. Xu, H.M. and Gutmann, D.H. 1998. Merlin differentially associates with the microtubule and actin cytoskeleton. J. Neurosci. Res. 51:403-415.
251. Yeoh, E.J., Ross, M.E., Shurtleff, S.A., Williams, W.K., Patel, D., Mahfouz, R., Behm, F.G., Raimondi, S.C., Relling, M.V., Patel, A., Cheng, C., Campana, D., Wilkins, D., Zhou, X., Li, J., Liu, H., Pui, C.H., Evans, W.E., Naeve, C., Wong, L., and Downing, J.R. 2002. Classification, subtype discovery, and prediction of outcome in pediatric acute lymphoblastic leukemia by gene expression profiling. Cancer Cell 1:133-143.
252. Zalcman, G., Closson, V., Linares-Cruz, G., Lerebours, F., Honore, N., Tavitian, A., and Olofsson, B. 1995. Regulation of Ras-related RhoB protein expression during the cell cycle. Oncogene 10:1935-1945.
253. Zeng, P.Y., Rane, N., Du, W., Chintapalli, J., and Prendergast, G.C. 2003. Role for RhoB and PRK in the suppression of epithelial cell transformation by farnesyltransferase inhibitors. Oncogene 22:1124-1134.
254. Zhong, C., Kinch, M.S., and Burridge, K. 1997. Rho-stimulated contractility contributes to the fibroblastic phenotype of Ras-transformed epithelial cells. Mol. Biol. Cell. 8:2329-2344.
255. Zucman-Rossi, J., Legoix, P., Der Sarkissian, H., Cheret, G., Sor, F., Bernardi, A., Cazes, L., Giraud, S., Ollagnon, E., Lenoir, G., and Thomas, G. 1998. NF2 gene in neurofibromatosis type 2 patients. Hum. Mol. Genet. 7:2095-2101.